

Electronic Thesis and Dissertation Repository

6-12-2018 10:30 AM

The Role of p66Shc in Mouse Blastocyst Development

Nicole A. Edwards

The University of Western Ontario

Supervisor

Betts, Dean H.

The University of Western Ontario Co-Supervisor

Watson, Andrew J.

The University of Western Ontario

Graduate Program in Physiology and Pharmacology

A thesis submitted in partial fulfillment of the requirements for the degree in Doctor of
Philosophy

© Nicole A. Edwards 2018

Follow this and additional works at: <https://ir.lib.uwo.ca/etd>



Part of the [Developmental Biology Commons](#)

Recommended Citation

Edwards, Nicole A., "The Role of p66Shc in Mouse Blastocyst Development" (2018). *Electronic Thesis and Dissertation Repository*. 5403.

<https://ir.lib.uwo.ca/etd/5403>

This Dissertation/Thesis is brought to you for free and open access by Scholarship@Western. It has been accepted for inclusion in Electronic Thesis and Dissertation Repository by an authorized administrator of Scholarship@Western. For more information, please contact wlsadmin@uwo.ca.

Abstract

The earliest cell fate specification events during mammalian development occur in the blastocyst-stage preimplantation embryo, during which a pluripotent cell population is established. These cells form the basis of the developing fetus and must be correctly specified in order for successful development to occur. Cell signalling in response to environmental cues has a critical role in cell differentiation. The signalling adaptor protein p66Shc is expressed in mammalian embryos and promotes apoptosis and permanent embryo arrest in response to stress-inducing conditions. However, loss-of-function studies suggest that p66Shc may be important for embryonic development to the blastocyst stage. In this thesis, I aimed to determine the role of p66Shc in mouse blastocyst development and mouse embryonic stem cell function. Through a combination of environmental modulation of p66Shc expression, experimental knockdown, and genetic knockout of p66Shc in mouse preimplantation embryos and mouse embryonic stem cells, I demonstrated that p66Shc is required for normal embryo physiology, and correct cell lineage-associated marker expression in the blastocyst inner cell mass and mouse embryonic stem cells. First, I observed that p66Shc is normally upregulated at the blastocyst stage *in vivo*, and oxygen-induced increases in p66Shc expression are associated with altered embryo metabolism *in vitro*. Secondly, I demonstrated that knockdown of p66Shc transcript abundance significantly alters the timing and proportion of cells expressing lineage-associated transcription factors in the blastocyst inner cell mass. Lastly, I observed that knockout of p66Shc in mouse embryonic stem cells alters the expression of the core pluripotency marker NANOG and causes an upregulation of mesoderm-associated markers during stem cell differentiation. Collectively, my work provides insight into a novel role for p66Shc during preimplantation embryo development, expanding the diversity of cellular functions attributed to p66Shc in mammalian development.

Keywords

Blastocyst, preimplantation embryo, p66Shc, embryonic stem cells, cell fate, pluripotency, epiblast, primitive endoderm, inner cell mass

Co-Authorship Statement

Chapter two is adapted from Edwards, N.A., Watson, A.J., Betts, D.H. (2016) P66Shc, a key regulator of metabolism and mitochondrial ROS production, is dysregulated by mouse embryo culture. *Molecular Human Reproduction*. 22(9): 634-647. Text and figures are reproduced here with permission from Oxford University Press. NA Edwards designed all experiments with the assistance of Drs. Andrew J. Watson and Dean H. Betts. All data was generated by NA Edwards in the laboratories of AJ Watson and DH Betts. All figures were prepared by NA Edwards. The manuscript was written by NA Edwards with the assistance of AJ Watson and DH Betts.

Chapter three is adapted from a manuscript submitted for publication entitled “Loss of p66Shc promotes primitive endoderm identity in the inner cell mass of mouse blastocysts”. NA Edwards designed all experiments with the assistance of AJ Watson and DH Betts. NA Edwards generated all data and prepared all figures. The manuscript was written by NA Edwards with the assistance of AJ Watson and DH Betts.

Chapter four is entitled “P66Shc maintains pluripotency in mouse embryonic stem cells”. The CRISPR-Cas9 gene targeting strategy, guide RNA design, synthesis and cloning, and transfection of mouse embryonic stem cells was performed by Dr. Jonathan H. Teichroeb. Courtney R. Brooks performed selection of cells, generation of clonal lines, culture of mouse embryonic stem cell lines, and formation of embryoid bodies. Genomic DNA isolation and screening of clones was performed by JH Teichroeb and NA Edwards. All other data presented was generated by NA Edwards. All figures were prepared by NA Edwards. The manuscript was written by NA Edwards with the assistance of AJ Watson and DH Betts.

Data regarding the transgenic p66Shc-loxP mouse presented in Chapter Five was generated by NA Edwards with the assistance of Linsay A. Drysdale, Dr. Daniel A. Passos and Dr. Frederick A. Dick, generated in the laboratory of FA Dick and the London Regional Transgenic and Gene Targeting Facility. All figures were prepared by NA Edwards.

Acknowledgments

I have had the wonderful opportunity to participate in and bridge research from embryology and stem cell biology by working in two labs. Thank you to all the past and current members of the Betts and Watson labs for your friendship, advice, and guidance over the past four and a half years. Even small things like injecting mice or feeding cells when I was away made a huge difference. Thank you particularly to Jonathan Teichroeb, who offered to create a knockout mouse embryonic stem cell line of my project's gene after I presented at a lab meeting, and to Courtney Brooks, who helped turn what I thought would be an interesting side project into a major chapter of my thesis.

Thank you to past and present members of the Regnault and Hardy labs, and to the close friends I made in Physiology and Pharmacology, Biology, the Developmental Biology program, and the Western Stem Cell Group. Grad school was fun largely due to my interactions with you on a daily basis.

Thank you to Dr. Fred Dick and the members of his lab who helped me work in their space for weeks, especially Dr. Daniel Passos, for helping me achieve the once thought impossible Southern blot screening of my targeted clonal lines.

Thank you to my thesis committee members – Drs. Lina Dagnino, Rob Cumming, and John DiGuglielmo – for providing equipment, reagents, and outstanding feedback and guidance on my thesis throughout my degree.

Thank you to my close friends Kayla, Karl, Stephany, and Omar, for your support and time spent together. Time spent away from school during holidays, birthdays, and weddings was time well spent in your company.

Thank you to my family, especially my sister and mother, for supporting and encouraging me during my degree.

Thank you to my M.Sc. supervisor, Dr. Hugh Clarke, for your support during scholarship applications, which no doubt contributed to my success in receiving them.

Lastly, thank you to my supervisors, Dr. Dean Betts and Dr. Andrew Watson. I have become a better scientist and person with your mentorship and guidance. I don't think I would have experienced the same degree of support and freedom to explore my research interests as a graduate student with anyone else. Thank you for all that you have done to lead me to where I am now.

Table of Contents

Abstract.....	i
Co-Authorship Statement	iii
Acknowledgments.....	iv
Table of Contents	vi
List of Tables	xi
List of Figures.....	xii
List of Appendices.....	xvi
List of Abbreviations.....	xvii
Chapter 1.....	1
1 Introduction	1
1.1 Overview.....	1
1.1.1 Embryonic development and cell fate decisions.....	1
1.2 Preimplantation embryo development.....	2
1.2.1 Overview of mouse preimplantation development.....	2
1.2.2 The first embryonic fate decision: inner cell mass vs. trophoctoderm.....	5
1.2.3 The second embryonic fate decision: epiblast vs. primitive endoderm	8
1.3 Mouse embryonic stem cells.....	11
1.3.1 From epiblast to embryonic stem cells.....	11
1.3.2 Characteristics of pluripotency	12
1.3.3 Embryonic stem cell differentiation.....	14
1.4 The role of p66Shc in preimplantation embryos and embryonic stem cells.....	16
1.4.1 Receptor tyrosine kinase signalling.....	16
1.4.2 Shc isoforms and functions.....	17

1.4.3	P66Shc in bovine preimplantation embryos	23
1.4.4	P66Shc in mouse preimplantation embryos	25
1.4.5	P66Shc in embryonic stem cells	26
1.5	Rationale and study aims	27
1.6	References	28
Chapter 2.....		40
2	P66Shc is expressed in mouse preimplantation embryos and is dysregulated by mouse embryo culture.....	40
2.1	Introduction	41
2.2	Materials and Methods.....	42
2.2.1	Animal Source and Ethical Approval.....	42
2.2.2	Embryo Collection and Culture	43
2.2.3	Real time RT-qPCR.....	43
2.2.4	Western Blot Analysis.....	44
2.2.5	HT-22 culture and transfection	46
2.2.6	Immunofluorescence and Confocal Microscopy	46
2.2.7	ATP content assay.....	47
2.2.8	MitoSOX superoxide staining.....	47
2.2.9	Blastocyst Cell Counts	47
2.2.10	Statistical Analyses	47
2.3	Results.....	48
2.3.1	P66Shc expression increases in blastocysts during mouse preimplantation development.....	48
2.3.2	Validation of NT-Shc antibody specificity.....	48
2.3.3	P66Shc expression is sensitive to oxygen tension, but not glucose concentration, during embryo culture	52

2.3.4	Changes to p66Shc expression in culture correlate with altered embryo metabolism.....	64
2.4	Discussion	69
2.5	References	74
Chapter 3	78
3	Loss of p66Shc accelerates primitive endoderm identity in the inner cell mass of mouse blastocysts	78
3.1	Introduction	79
3.2	Materials and Methods.....	81
3.2.1	Animal source and ethical approval.....	81
3.2.2	Mouse zygote collection and culture.....	81
3.2.3	Cytoplasmic microinjection of siRNA	82
3.2.4	Mouse embryonic stem cell transfection.....	82
3.2.5	Quantitative real time RT-PCR.....	84
3.2.6	Immunoblotting.....	84
3.2.7	Immunofluorescence and confocal microscopy.....	86
3.2.8	BrdU incorporation assay	86
3.2.9	Statistical Analyses	87
3.3	Results.....	87
3.3.1	Specific knockdown of p66Shc in mouse preimplantation embryos.....	87
3.3.2	P66Shc knockdown embryos form blastocysts containing more cells than controls.....	91
3.3.3	P66Shc knockdown accelerates the onset of primitive endoderm identity in mouse blastocysts	97
3.3.4	P66Shc knockdown increases the number of DUSP4-positive cells in the blastocyst.....	104
3.4	Discussion	108

3.5	References	111
Chapter 4.....		115
4	Knockout of p66Shc alters pluripotency-associated transcription factor expression in mouse embryonic stem cells.....	115
4.1	Introduction	116
4.2	Materials and Methods.....	118
4.2.1	Generation of p66Shc knockout mESCs with CRISPR-Cas9	118
4.2.2	Embryonic stem cell culture	121
4.2.3	Immunofluorescence and confocal microscopy.....	121
4.2.4	Immunoblotting.....	124
4.2.5	Embryoid body formation and differentiation	124
4.2.6	RNA extraction, RT ² Profiler PCR array and quantitative real time (qRT)-PCR.....	125
4.2.7	Statistical analyses.....	125
4.3	Results.....	126
4.3.1	Generation of p66Shc-specific knockout mESCs.....	126
4.3.2	Altered pluripotency marker expression in p66Shc knockout mESCs ...	126
4.3.3	p66Shc knockout upregulates markers of mesoderm-derivatives during spontaneous embryoid body differentiation	128
4.4	Discussion	139
4.5	References	143
Chapter 5.....		146
5	General Discussion and Conclusions.....	146
5.1	Discussion and Significance of Research	146
5.1.1	P66Shc expression likely needs to be maintained at a level which promotes normal blastocyst development	148
5.1.2	P66Shc promotes the expression of pluripotency-associated markers....	151

5.2 Future studies: generation of p66Shc-loxP mice.....	156
5.3 Summary	160
5.4 References	160
Appendix A: Materials and Methods for generation of p66Shc-loxP mice	164
Construction of mShc1 targeting vector	164
Southern blotting	164
Chromosome Counting	168
Appendix B: Copyright Agreement	169
Appendix C: Ethics Approval.....	170
Curriculum Vitae.....	172

List of Tables

Table 2-1. Oligonucleotide primer sequences.....	45
Table 3-1. siRNA sequences.....	83
Table 3-2. Oligonucleotide primer sequences.....	85
Table 4-1. Oligonucleotide primer sequences.....	119
Table 4-2. Summary of predicted Cas9-gRNA off-target effects.....	122
Table 4-3. Primary antibody information.....	123
Table A-1. Sequences of DNA probes used for Southern blotting.....	167

List of Figures

Figure 1-1. Overview of mouse preimplantation development.	3
Figure 1-2. Protein and genetic structures of Shc1.	18
Figure 2-1. p66Shc expression increases during mouse preimplantation development <i>in vivo</i>	49
Figure 2-2. Full Western blots for anti-NT-Shc, anti-pSer36-p66Shc, and anti-pY239/Y240-Shc.	50
Figure 2-3. p66Shc progressively localizes to the cell periphery during mouse preimplantation development.	51
Figure 2-4. NT-Shc and phosphorylated S36 p66Shc antibody validation for immunofluorescence and confocal microscopy.	53
Figure 2-5. Developmental outcomes of embryos cultured in KSOMaa Evolve under low and high oxygen tensions.	54
Figure 2-6. Culture and high oxygen tension increases the relative p66Shc mRNA abundance in mouse blastocysts.	55
Figure 2-7. Culture and high oxygen tension increases the relative p66Shc protein abundance in mouse blastocysts.	58
Figure 2-8. Relative p66Shc mRNA and protein abundance in cultured 2-cell and 8-cell embryos.	59
Figure 2-9. Total p66Shc becomes detectable in the inner cells of mouse blastocysts cultured under atmospheric oxygen tension.	60
Figure 2-10. Phosphorylated S36 p66Shc localization does not change in cultured mouse blastocysts.	62

Figure 2-11. High glucose media concentrations reversibly inhibit mouse embryo cavitation.....	63
Figure 2-12. High glucose media concentrations do not significantly change relative p66Shc mRNA and protein abundance in mouse blastocysts.....	66
Figure 2-13. Increased p66Shc expression correlates with decreased ATP and increased superoxide in cultured mouse blastocysts.....	68
Figure 3-1. p66Shc siRNA reduces p66Shc transcript and protein abundance in mouse preimplantation embryos.	89
Figure 3-2. Efficiency of p66Shc knockdown by siRNA.....	90
Figure 3-3. P66Shc protein knockdown confirmed post siRNA injection in mouse embryos.....	93
Figure 3-4. p66Shc knockdown embryos form blastocysts containing more cells than controls.	94
Figure 3-5. Altered proliferation in p66Shc knockdown blastocysts.....	96
Figure 3-6. Earlier restriction of OCT3/4 to the inner cells in p66Shc knockdown blastocysts.	98
Figure 3-7. P66Shc knockdown increases percent GATA4-positive cells of total cells in blastocysts but does not affect expression of TE markers.....	99
Figure 3-8. Loss of p66Shc promotes primitive endoderm fate in the inner cell mass at E3.5.....	101
Figure 3-9. Loss of p66Shc accelerates sorting of the primitive endoderm in 64-128 cell blastocysts.	103
Figure 3-10. High background after immunofluorescent staining of total and phosphorylated ERK1/2.....	105

Figure 3-11. p66Shc knockdown blastocysts displayed altered ERK1/2 activity.	107
Figure 4-1. CRISPR-Cas9 knockout of p66Shc in mESCs.	127
Figure 4-2. p66Shc knockout does not change morphology of mESCs cultured on MEFs in serum/LIF conditions.	129
Figure 4-3. Reduced SOX2 and NANOG expression in p66Shc knockout mESCs.	130
Figure 4-4. Reintroduction of p66Shc expression rescues NANOG fluorescence intensity in 4D p66Shc knockout mESCs.	131
Figure 4-5. Altered expression of naïve and primed pluripotent markers in p66Shc knockout mESCs.	132
Figure 4-6. Embryoid bodies derived from p66Shc knockout mESCs upregulate markers of mesoderm derivatives and downregulate markers of neuroectoderm after 14 days of spontaneous differentiation.	134
Figure 4-7. Embryoid bodies derived from p66Shc knockout mESCs upregulate <i>Fgf2</i> and downregulate neuroectoderm markers at day 7 of spontaneous differentiation.	135
Figure 4-8. PAX6/Brachyury-positive projections emerge from wild type EBs and are absent in p66Shc knockout EBs after 14 days of spontaneous differentiation.	136
Figure 4-9. Brachyury and OTX2 is detectable in wild type and p66Shc knockout EBs after 7 days of spontaneous differentiation.	137
Figure 4-10. PAX6/SOX2-positive cells present in wild type and p66Shc knockout EBs after 7 days of spontaneous differentiation.	138
Figure 4-11. Reduced OTX2 fluorescence in p66Shc knockout EBs after 24 hours (Day 0) of spontaneous differentiation.	140
Figure 5-1. Summary of p66Shc functions and potential mechanisms in the mouse preimplantation embryo and mouse embryonic stem cells.	147

Figure 5-2. P66Shc likely needs to be expressed at a certain level to promote normal mouse preimplantation development..... 149

Figure 5-3. p66Shc knockout mESCs are likely in the formative pluripotent state..... 154

Figure 5-4. Targeting strategy by homologous recombination to generate p66Shc-loxP transgenic mice..... 158

Figure 5-5. Distribution of chromosome counts, and chimeras generated from targeted clones. 159

Figure A-1. Shc1 targeting vector..... 165

Figure A-2. Southern blot strategy for genotyping targeted clones. 166

List of Appendices

Appendix A: Materials and Methods for generation of p66Shc-loxP mice	164
Construction of mShc1 targeting vector	164
Southern blotting	164
Chromosome Counting	168
Appendix B: Copyright Agreement	169
Appendix C: Ethics Approval	170
Curriculum Vitae.....	172

List of Abbreviations

Amot	Angiomotin
ANOVA	Analysis of variance
aPKC	Atypical protein kinase C
ART	Assisted reproductive technologies
ATP	Adenosine triphosphate
BMP	Bone morphogenetic protein
BrdU	Bromodeoxyuridine
cDNA	Complementary deoxyribonucleic acid
CDX2	Caudal type homeobox 2
CH1/2	Collagen homology domain 1/2
CRISPR	Clustered regulatory interspaced short palindromic repeats
DUSP4	Dual specificity phosphatase 4
EB	Embryoid body
EGF	Epidermal growth factor
EGFR	Epidermal growth factor receptor
EOMES	Eomesodermin
EPI	Epiblast
ERK1/2	Extracellular signal-related kinase 1/2

ESC	Embryonic stem cell
FGF	Fibroblast growth factor
FGFR	Fibroblast growth factor receptor
GATA3	GATA binding protein 3
GATA4	GATA binding protein 4
GATA6	GATA binding protein 6
gDNA	Genomic deoxyribonucleic acid
GFP	Green fluorescent protein
gRNA	Guide ribonucleic acid
GSK3 β	Glycogen synthase kinase 3 beta
GV	Germinal vesicle
hCG	Human chorionic gonadotropin
ICM	Inner cell mass
iPSC	Induced pluripotent stem cell
IVF	In vitro fertilization
KSOMaa	Potassium simplex optimized medium with amino acids
LATS	Large tumour suppressor kinase
LIF	Leukemia inhibitory factor
MAPK	Mitogen activated protein kinase
MEF	Mouse embryonic fibroblast

MEK1/2	Mitogen activated protein kinase kinase 1/2
mEpiSC	Mouse epiblast stem cell
mESC	Mouse embryonic stem cell
mRNA	Messenger ribonucleic acid
mTOR	Mammalian target of rapamycin
OTX2	Orthodenticle homeobox 2
PAX6	Paired box 6
PDGFR α	Platelet derived growth factor receptor alpha
PrE	Primitive endoderm
PKC β	Protein kinase C beta
PMSG	Pregnant mare serum gonadotropin
PTB	Phosphotyrosine binding domain
qRT-PCR	Quantitative real time polymerase chain reaction
RIPA	Radioimmunoprecipitation assay
RNAi	Ribonucleic acid interference
ROS	Reactive oxygen species
RT-PCR	Reverse transcription polymerase chain reaction
RTK	Receptor tyrosine kinase
SD	Standard deviation
SEM	Standard error of the mean

SH2	Src homology 2
Shc	Src homology 2 domain-containing
shRNA	Short hairpin ribonucleic acid
siRNA	Short interfering ribonucleic acid
SOX17	Sex determining region Y box 17
SOX2	Sex determining region Y box 2
STAT3	Signal transducer and activator of transcription 3
TEAD4	TEA domain transcription factor 4
UTR	Untranslated region
XEN	Extraembryonic endoderm
YAP	Yes associated protein

Chapter 1

1 Introduction

1.1 Overview

1.1.1 Embryonic development and cell fate decisions

Development describes the process of how the structure of an organism changes with time, with embryonic development referring to how a single fertilized egg grows and forms an entire organism. Embryonic development has conserved mechanisms across the Animal Kingdom (Slack, 2006). These encompass four main themes: morphogenesis, growth, regional specification, and cell differentiation. Morphogenesis is the mechanism behind cell and tissue movement that provides the organism with a three-dimensional structure. Growth is an increase in organismal size and the control of body part proportions. Regional specification describes how a pattern appears in an originally similar population of cells. Lastly, cell differentiation characterizes how different types of cells emerge from an originating population (Slack, 2006). Cell differentiation and cell fate decisions form the foundation of how a single cell (fertilized egg or zygote) can lead to the generation of all cells of the adult body.

Ongoing research in cell differentiation and cell fate regulation has shown that control of gene expression is critical to ensuring the normal development of an organism.

Observations from cellular cloning and reprogramming of mature cells to de-differentiated induced pluripotent stem cells (iPSCs) demonstrate that, with a few exceptions, every cell in the adult organism has identical genomes (Lokken and Ralston, 2016; Slack, 2006; Takahashi and Yamanaka, 2006). However, there are over two hundred cell types with distinct functions in the adult body. To reconcile this, the genome must be differentially regulated/expressed in each specialized cell type. This happens through differential transcription, translation, post-transcriptional and post-translational modification of gene products, ultimately leading to the cell acquiring a certain morphology and function. Understanding how cells acquire their specialized fate requires determining which genes are necessary for embryonic development, determining how

spatiotemporal regulation of gene expression occurs, and understanding how the expression of certain proteins cause cells to differentiate into certain cell types (Lokken and Ralston, 2016). Understanding these aspects of cell fate decisions will help us understand how normal development occurs and how alterations in cell fate and cell differentiation lead to disease and cancer (Lokken and Ralston, 2016).

Cell fate decisions during development typically undergo sequential phases of commitment. Cells are first specified to a fate, meaning that when isolated from a developing embryo they can form the specified cell type, but their fate is plastic and can be altered, for example, by the type of environment into which they are placed (Slack, 2006). After specification, cells are determined. Cell determination is defined as irreversible development into the specified cell type regardless of the environment post-transplantation. Some progenitor, or precursor, cells may be restricted to a range of possible cell types that they can develop to – a property known as potency (Slack, 2006). The first observable cell fate decision in mammalian embryonic development is to determine which cells of the embryo will contribute to embryonic tissues or extraembryonic tissues after implantation. This is determined during preimplantation embryo development, and proper specification and determination of these two cell fates is essential to establish a successful pregnancy and support fetal development (Lokken and Ralston, 2016).

1.2 Preimplantation embryo development

1.2.1 Overview of mouse preimplantation development

Preimplantation development is defined as the period of mammalian embryonic development between fertilization of the egg and implantation of the blastocyst in the uterus (summarized in Figure 1-1). This process takes approximately 3-4 days in the mouse and up to 7 days in humans. After fertilization, the one cell zygote undergoes a series of mitotic divisions (cleavage) during which there is an increase in the number of cells (blastomeres), but no net increase in embryo size (Cockburn and Rossant, 2010). The maternal to zygotic transition in transcriptional control occurs during the first cleavage division in the mouse, when oocyte-stored transcripts and proteins that are

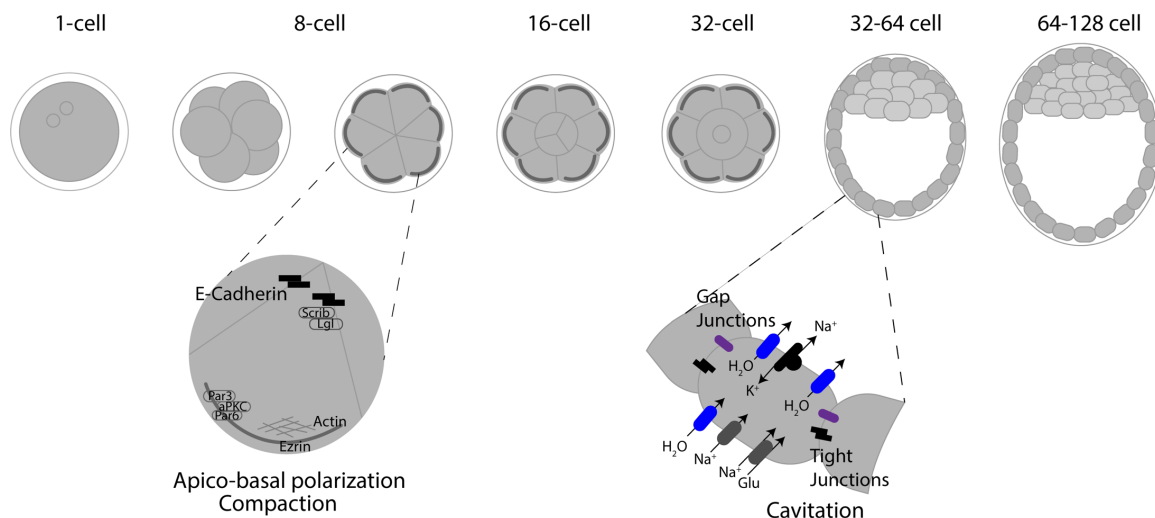


Figure 1-1. Overview of mouse preimplantation development.

Two key events occur during the developmental progression to the blastocyst stage. Apico-basal polarization and compaction occur at the 8-cell stage. Compaction results in an increase in cell-cell adhesion and surface contact, while intracellular polarity components segregate to form apical and basolateral domains in each blastomere. Following specification of the trophectoderm the embryo undergoes cavitation to form a fluid-filled cavity. Cavitation is mediated by the formation of intercellular tight junctions (black rectangles), expression of basolateral Na⁺/K⁺-ATPases (black) and trophectoderm-specific expression of aquaporins (blue).

essential for supporting oocyte maturation and fertilization are progressively degraded and the embryonic genome begins transcription. In mouse embryos, embryonic genome activation is initiated in the male pronucleus with a minor wave of gene activation, followed by a major wave during the one to the two-cell stage transition once syngamy and pronuclear fusion have occurred (Hamatani et al., 2004).

Up to the uncompact eight-cell stage, blastomeres remain totipotent, as they can equally contribute to either the inner cell mass (embryonic) or trophoctoderm (extraembryonic) lineages. Developmental biases in blastomere contribution to the inner cell mass or trophoctoderm have been identified as early as the four-cell stage (Piotrowska-Nitsche et al., 2005; Tabansky et al., 2013; Torres-Padilla et al., 2007). However, blastomeres are not yet committed to their fate, as at this developmental time point embryos can adapt to the addition, repositioning, or removal of blastomeres (Cockburn and Rossant, 2010). This property is the basis of preimplantation genetic diagnosis, an assisted reproductive technology (ART) during which one or a few blastomere(s) is/are removed from the embryo and genotyped to avoid the transfer of embryos carrying a heritable genetic disease (Handyside et al., 1992; Hardy et al., 1990). Totipotency is lost as the embryo further develops and as the lineages of the blastocyst are subsequently specified (Suwinska et al., 2008; Tarkowski et al., 2010).

At the late eight-cell stage, mouse preimplantation embryos undergo compaction, a process during which there is an increase in intracellular adhesion resulting in blastomeres flattening, and morphological distinction between individual blastomeres is lost (White et al., 2016). Adherens and tight junctions subsequently form. The onset of compaction is independent of cell number, and it can be artificially induced in four-cell embryos if the nuclear to cytoplasmic ratio is increased, if protein synthesis is inhibited, or if protein kinase C is activated (Kidder and McLachlin, 1985; Lee et al., 2001; Winkel et al., 1990). The initiation signal for compaction is not well understood. However, calcium-dependent adhesion mediated by E-Cadherin is required, as chelating Ca^{2+} ions causes the embryo to decompact and ultimately fail to develop to the blastocyst stage (Pey et al., 1998). Basolateral E-Cadherin mediates adhesion between blastomeres by ligating its extracellular domain to cadherins on neighbouring cells (White et al., 2016).

Cell polarization along the inside-outside axis of the embryo occurs simultaneously with compaction as apical-basal polarity is established (Cockburn and Rossant, 2010; Leung et al., 2016). Actin, microvilli, and apical complexes including Ezrin, the Par proteins Par3 and Par6, and atypical protein kinase C localize to the apical domain, while E-Cadherin, Scribble, and Lgl localize to the basolateral domain (Leung et al., 2016). Functionally, the polarization of cell components is linked to the first fate decision in the embryo and eventual blastocyst formation. Polarization is not fully dependent on cell-cell contact, as blastomeres isolated from embryos can polarize, as well as blastomeres in embryos that are inhibited from compacting, but at a lower frequency than in intact embryos (Houliston et al., 1989). Together, compaction and polarization are required to ensure proper development to the blastocyst stage.

After specification of the trophectoderm, the blastocyst forms a fluid-filled cavity during a process known as cavitation. Formation of a cavity is dependent on ion transport by the trophectoderm. Expression of Na^+/K^+ -ATPases in trophectoderm cells causes an osmotic gradient to form as Na^+ ions accumulate at the basolateral side of the cells (Baltz et al., 1997; Madan et al., 2007). Water then enters the blastocyst through aquaporins expressed in trophectoderm cells (Barcroft et al., 2003; Offenberg et al., 2000). Tight junctions composed of occludins, claudins, and junction adhesion molecules form in the trophectoderm and act as a permeability seal against paracellular transport, facilitating expansion of the cavity (Fleming et al., 2001). The first three cell types – the epiblast, primitive endoderm, and trophectoderm – are then specified in the blastocyst and uterine implantation occurs at E4.5 in the mouse (Cockburn and Rossant, 2010).

1.2.2 The first embryonic fate decision: inner cell mass vs. trophectoderm

Cell polarization and cell fate are closely linked and are described by two experimental models known as the “inside-outside” and the “cell polarity” models. In the “inside-outside” model, the cells on the inside and outside of the 8-16 cell morula experience different degrees of cell-to-cell contact and this positional information is translated into

differences in cell fate, with the outer cells becoming trophectoderm and the inner cells becoming the inner cell mass. In the “cell polarity” model, the presence or absence of an apical domain and its inheritance determines cell fate. During symmetric blastomere divisions, the daughter cells will inherit the apical domain and remain on the outside of the embryo, while asymmetric divisions result in one polar and one apolar cell. The apolar cell lacking an apical domain will internalize or remain on the inside of the embryo. Increasing evidence suggests that polarity, rather than position, drives cell fate specification at this stage of development with research focusing on discovering the driving signalling mechanisms that regulate and stabilize cell fate (Anani et al., 2014; Yamanaka et al., 2006). Ultimately, cell fate in the blastocyst is determined by differential expression of transcription factors in the trophectoderm and inner cell mass. CDX2, EOMES, and GATA3 are specific to the trophectoderm lineage, while OCT4, NANOG, and SOX2 regulate the inner cell mass. The importance of these transcription factors has been outlined in genetic knockout studies. *Cdx2* knockout embryos form blastocysts, but the trophectoderm expresses ectopic NANOG and OCT4 and cannot implant, suggesting that CDX2 is important for maintaining trophectoderm identity in the embryo (Strumpf et al., 2005). *Oct4* knockout embryos also form blastocysts; however, their inner cell masses are not pluripotent and ectopically express trophectoderm markers (Nichols et al., 1998).

More recent work has focused on how these transcription factors are restricted to their respective lineages, which has led to the finding that differential cell signalling emerges during compaction and polarization. TEAD4, a transcriptional effector of the Hippo signalling pathway, was identified as a regulator of *Cdx2*, and its knockout in mice results in a preimplantation lethal defect. *Tead4*^{-/-} embryos do not form blastocyst cavities despite the normal expression of components of adherens junctions and polarity complexes. Instead these embryos fail to upregulate trophectoderm markers (*Cdx2*, *Eomes*, *Fgfr2*) and fail to specify the trophectoderm (Nishioka et al., 2008; Yagi et al., 2007). TEAD4 is localized to the nucleus in all cells of the 8-16 cell embryo and thus the presence of the transcriptional co-activator YAP in the nucleus and binding to TEAD4 is required for *Tead4*-mediated expression of *Cdx2* (Hirate et al., 2012). YAP is nuclear in the outer cells of the embryo, while YAP is cytoplasmic in the inner cells of the embryo

(Nishioka et al., 2009). Overexpressing LATS, a kinase mediating phosphorylation of YAP, in mouse embryos significantly reduced nuclear accumulation of YAP, suggesting that LATS regulates YAP localization in the embryo through phosphorylation (Nishioka et al., 2009). By experimentally manipulating the position of blastomeres inside the embryo, outside cells re-establish polarity and nuclear YAP became detectable, while YAP remained cytoplasmic in inner cells, linking cell position to YAP localization (Nishioka et al., 2009). TEAD4 also restricts SOX2 to the inner cells of the preimplantation embryo, as *Tead4*^{-/-} embryos and overexpression of *Lats2* in the outer cells had ectopic SOX2 expression. Therefore, differential Hippo signalling is not only required for trophectoderm patterning, but also for proper ICM patterning (Wicklow et al., 2014).

As TEAD4, YAP, and LATS are members of the Hippo signalling pathway, research has been focused on identifying known upstream regulators important for signal transduction in the preimplantation embryo, and how they could integrate cell position and/or cell polarity signals. Disrupting cell polarity by *Pard6b* short hairpin (sh)RNA knockdown reduced nuclear YAP, increased cytoplasmic phosphorylated YAP, and reduced *Cdx2* expression, suggesting that an intact apical domain is required for inhibiting Hippo pathway activation (Hirate et al., 2013). Similarly, transplantation of the apical domain from a polar to apolar blastomere was sufficient to induce trophectoderm specification in the daughter cell inheriting the apical domain after asymmetrical division (Korotkevich et al., 2017). Angiomotin (Amot) is a Hippo pathway member that binds tight junctions, and thus may mediate the link between cell-cell contact and activation of Hippo signalling in the embryo. Amot is localized to the apical membrane in outer cells of the embryo while in inner cells, it is detectable across the entire plasma membrane (Hirate et al., 2013; Leung and Zernicka-Goetz, 2013). The nuclei of inner cells of *Amot*^{-/-} embryos do not robustly activate Hippo signalling, do not exclude YAP from the nucleus until the 32-cell stage, and at E4.5, all cells express CDX2. Thus, these results suggest that polarized Amot localization prevents Hippo signalling activation in outer cells, leading to nuclear YAP and *Cdx2* expression, while in inner cells, Amot activates Hippo signalling, phosphorylating and excluding YAP from the nucleus (Hirate et al., 2013).

Nf2 (Merlin) is another upstream Hippo component required for activating Hippo signalling in the mouse preimplantation embryo. Embryos expressing dominant negative Nf2 had localization of YAP to the nucleus in the inner cells, and maternal-zygotic Nf2 knockout embryos had ectopic trophectoderm gene expression in the inner cells (Cockburn et al., 2013). These results suggest that like Amot, Nf2 expression is required for activation of Hippo signalling in the inner cells of the embryo. Through co-immunoprecipitation experiments in NIH 3T3 and HEK293 cells, Nf2 was found to associate indirectly with Amot, potentially linking Amot to the E-Cadherin complex in preimplantation embryos. It was then found that this interaction mediated LATS-dependent phosphorylation of Amot, leading to Hippo activation (Hirate et al., 2013). Binding sites for RPBJ in the trophectoderm-specific enhancer of *Cdx2*, and NOTCH1 localization to the nucleus of only outer cells in the embryo led to the finding that Notch signalling also regulates *Cdx2* expression concomitant with Hippo signalling (Rayon et al., 2014). Thus, a combination of differential Hippo signalling activation mediated by the apical domain and Notch signalling regulates the trophectoderm-inner cell mass fate decision.

1.2.3 The second embryonic fate decision: epiblast vs. primitive endoderm

Following specification of the trophectoderm and inner cell mass, a second differentiation event establishes the epiblast and primitive endoderm within the inner cell mass. At E3.5, the inner cell mass is a mixed population of epiblast and primitive endoderm cell progenitors that are identified by mutually-exclusive expression of NANOG (epiblast) and GATA6 (primitive endoderm) (Lokken and Ralston, 2016). How these initial differences arise in the inner cell mass cell population has been represented by two developmental models: the cleavage history-dependent model and the stochastic gene activation model (Lokken and Ralston, 2016). The cleavage history-dependent model suggests that inner cell mass cell specification depends on the origin of the parental cell, e.g. if cells originated from the outer or inner cells. To test this, cell lineage tracing was performed in the 8-cell embryo. Inner cell mass cells can be generated during multiple rounds of division and thus primary (generated from 8 to 16 cell divisions) and secondary

(generated from 16 to 32 cell divisions) inner cells were classified and their cell fate mapped. In contrast to previous studies (Morris et al., 2013; Morris et al., 2010), no bias was found in restriction of inner cells towards epiblast or primitive endoderm fates (Chazaud et al., 2006; Yamanaka et al., 2010). Furthermore, plasticity in primitive endoderm specification is maintained until the late blastocyst stage, suggesting that the cleavage history of inner cells does not definitively restrict cell fate in the inner cell mass (Grabarek et al., 2012). In the stochastic gene activation model, random differences in the expression of FGF4 or FGFR2 arise as early as the 32-cell stage, leading to cell fate specification to the epiblast (FGF4-expressing cells) or primitive endoderm (FGFR2-expressing cells) (Guo et al., 2010; Kang et al., 2017; Lokken and Ralston, 2016; Molotkov et al., 2017). Strong evidence supporting this model has led it to become the predominant model in describing the epiblast versus primitive endoderm cell fate decision.

FGF4/MAPK signalling is thus the predominant signalling pathway mediating the epiblast vs. primitive endoderm cell fate decision in the blastocyst inner cell mass. GRB2, a receptor tyrosine kinase adaptor protein, was identified as a possible candidate in the regulation of epiblast vs. primitive endoderm differentiation as its knockout results in the failure to form endoderm lineages *in vivo* and *in vitro* (Cheng et al., 1998). *Grb2*^{-/-} blastocysts do not express GATA6 but instead express NANOG in all cells of the inner cell mass (Chazaud et al., 2006). Treatment with inhibitors of the FGF receptor and MEK recapitulated the *Grb2* knockout phenotype, and high doses of FGF4 treatment during embryo development resulted in all inner cell mass cells expressing GATA6, suggesting that the FGF4/FGFR2/*Grb2*/MAPK pathway regulates primitive endoderm cell fate (Yamanaka et al., 2010). Accordingly, knockout of *Fgf4* results in no primitive endoderm cells in the inner cell mass despite *Gata6* and *Nanog* expression (Kang et al., 2013; Krawchuk et al., 2013). The balance of epiblast and primitive endoderm in the inner cell mass therefore relies on the relative levels of FGF4, NANOG, and GATA6 in each cell (Schrode et al., 2014). Interestingly, pluripotency-associated transcription factors appear to be required for correct primitive endoderm specification, likely through maintaining an epiblast fate and production of the FGF4 ligand. *Sox2*^{-/-} embryos have lower GATA6 expression in the blastocyst and delayed SOX17 expression, a mature primitive endoderm

marker (Wicklow et al., 2014). OCT4 is required for FGF4 expression in epiblast cells and operates downstream of FGF4 signalling to regulate primitive endoderm gene expression (Frum et al., 2013; Le Bin et al., 2014). These studies suggest that successful specification of the primitive endoderm requires a correctly specified epiblast. Following specification, primitive endoderm cells upregulate GATA4, SOX17, and PDGFR α (Chazaud and Yamanaka, 2016).

Before implantation, the mixed inner cell mass population of epiblast and primitive endoderm cells sort into morphologically distinct layers with the primitive endoderm forming an epithelial layer between the layers of epiblast and the blastocyst cavity (Chazaud and Yamanaka, 2016). This process occurs through a combination of the polarization of primitive endoderm cells, actin-dependent cell movement, and selective apoptosis (Meilhac et al., 2009; Plusa et al., 2008; Saiz et al., 2013). Using a H2B:GFP-Pdgfra reporter, primitive endoderm cell movements were tracked to determine their timing and positional changes (Plusa et al., 2008). Cell movements begin in blastocysts containing 80 cells, and cells are almost all sorted in embryos with over 100 cells. If GFP-positive cells originated in the inner cell mass in the layer of cells bordering the cavity, they tended to keep their position, while GFP-positive cells originating in the inner layers changed position. If inner cells did not move, they either downregulated GFP expression or underwent apoptosis (Plusa et al., 2008). Thus, primitive endoderm cells must have some positional-sensing mechanism to determine if movement to the primitive endoderm layer is required, and if this mechanism fails, cells can adopt an epiblast fate or undergo apoptosis. Cell polarization is thought to drive this position-sensing mechanism in the primitive endoderm mediated by atypical protein kinase C (aPKC). LRP2, DAB2, and aPKC are localized to the apical side of primitive endoderm cells (Gerbe et al., 2008; Saiz et al., 2013). Polarization of aPKC is dependent on FGF/ERK signalling, as its inhibition results in diffuse aPKC localization. Furthermore, siRNA knockdown of aPKC prevents primitive endoderm cells from sorting, and inhibiting aPKC causes cells to fail to maintain their final position in contact with the blastocyst cavity (Saiz et al., 2013).

Under the appropriate conditions, stem cells can be derived from all three lineages of the mouse blastocyst and studied *in vitro* (Garg et al., 2016). Epiblast cells give rise to mouse

embryonic stem cells (mESCs) and mouse epiblast stem cells (mEpiSCs) (Brons et al., 2007; Martin and Evans, 1975; Tesar et al., 2007), trophoctoderm forms trophoblast stem cells (Tanaka et al., 1998), and primitive endoderm cells form extraembryonic endoderm cells (XEN) (Garg et al., 2016; Kunath et al., 2005; Niakan et al., 2013). Each lineage-derived stem cell is representative of their developmental origin from the blastocyst or peri-implantation embryo, and thus their potency is restricted to their associated embryonic or extraembryonic fates.

1.3 Mouse embryonic stem cells

1.3.1 From epiblast to embryonic stem cells

The epiblast cell population in the mammalian inner cell mass is considered pluripotent as these cells have the potential to differentiate into cell types of the three embryonic germ layers (endoderm, ectoderm, mesoderm). Pluripotency in the epiblast is transient *in vivo* as these cells subsequently differentiate along their developmental program.

However, if the preimplantation epiblast is isolated from the embryo and maintained in culture, embryonic stem cells (ESCs) can be propagated. ESCs retain the pluripotency of the preimplantation epiblast with differentiation potential into the three germ layers and the ability to self-renew indefinitely (Nichols and Smith, 2009). Mouse ESCs were first derived by culturing intact blastocysts on mitotically inactivated mouse embryonic fibroblasts (MEFs) in medium used to culture embryonal carcinoma cells (Evans and Kaufman, 1981; Martin, 1981). It was then found that MEFs produce leukemia inhibitory factor (LIF), and STAT3 activation downstream of LIF inhibits differentiation and promotes viability of ESCs. The mouse preimplantation epiblast was identified as the source of mESCs, as microsurgical separation of the epiblast from the trophoctoderm and primitive endoderm prior to culture resulted in ESC derivation (Brook and Gardner, 1997). ESC lines were subsequently derived from human blastocysts by culturing isolated inner cell masses (Thomson et al., 1998). Human ESCs are pluripotent as they form derivatives of all three germ layers *in vitro* and *in vivo* but have differences in cell surface marker staining and colony morphology compared to mouse ESCs, suggesting species-specific differences between mouse and human development (Thomson et al., 1998). Subsequently, it was discovered that ESCs could also be isolated from the post-

implantation mouse epiblast with distinct characteristics and culture conditions from cells derived from the preimplantation epiblast, known as epiblast stem cells (EpiSC) (Brons et al., 2007; Tesar et al., 2007). Interestingly, these cells have properties similar to human ESCs (Tesar et al., 2007). Derivation of EpiSCs then suggested that there may be more than one pluripotent state that exists in embryonic stem cells, likely corresponding to the developmental origins of the cell lines. Two terms for pluripotency were subsequently established: “naïve”, corresponding to cells resembling the preimplantation epiblast (e.g. mouse ESCs), and “primed”, corresponding to cells resembling the post-implantation epiblast (e.g. human ESCs, mouse EpiSCs).

1.3.2 Characteristics of pluripotency

Naïve and primed pluripotency represent two metastable pluripotent states of ESCs that are morphologically, molecularly, and functionally distinguishable. Naïve ESC pluripotency is reliant on LIF/STAT3 signalling, while primed ESCs self-renew in FGF/Activin culture conditions (Nichols and Smith, 2009). Morphologically, naïve ESCs appear in round, domed-like colonies that can be passaged as single cells that proliferate rapidly, while primed ESCs are more flattened and compact, cannot be single cell passaged, and proliferate more slowly. In female lines, naïve ESCs have both X chromosomes active, while primed ESCs have epigenetic inactivation of one X chromosome. Naïve ESCs represent the ground state of pluripotency, e.g., they are unrestricted in their developmental potential, and can reincorporate into the inner cell mass of the blastocyst and contribute to all embryonic lineages (Nichols and Smith, 2009). Primed ESCs, however, cannot contribute to chimeras if introduced into the blastocyst, but can form derivatives of endoderm, ectoderm, and mesoderm when induced to form a teratocarcinoma (teratoma). While both naïve and primed ESCs express the core pluripotency factors OCT4, SOX2, and NANOG, they differ in the expression of other markers such as *Rex1*, *Dppa3* (naïve), *Fgf5*, Brachyury/*T*, and *Lefty* (primed) (Chen and Lai, 2015).

Naïve and primed pluripotent states can be interconverted by manipulating the culture conditions or genetically overexpressing pluripotency markers. Mouse EpiSCs can be converted to naïve ESCs by culturing in LIF and inhibitors of GSK3 β (CIHR99021) and

MEK1/2 (PD0325901) (a combination known as 2i), or at a higher efficiency by overexpressing *Nanog*, *Klf4*, *Stat3*, *Klf2*, *Nr5a*, *c-Myc* and *Tfcp2l1* (Hassani et al., 2014). Conversely, naïve mouse ESCs can be converted to primed EpiSCs by culture in basic FGF/Activin (Guo et al., 2009). Efforts have been made to convert primed human ESCs to the naïve state by overexpression of the pluripotency markers OCT4, KLF4, and KLF2, and culture in 2i/LIF (Hanna et al., 2010). These cells show similarity to mouse ESCs with reactivation of the silenced X chromosome and dependence on LIF signalling for self-renewal (Hanna et al., 2010). Further work includes identifying small molecules supporting self-renewal and pluripotency to make reversion to the naïve state transgene-free (Chan et al., 2013; Theunissen et al., 2014). Since the standard test for pluripotency, blastocyst chimerism, is not ethically feasible to perform with human ESCs, confirmation of *bona fide* naïve human ESCs has not yet been attained (Hassani et al., 2014).

The difficulty in deriving or obtaining naïve human ESCs suggests that either the derivation conditions have not been fully optimized for human-specific ESCs, or that there is a species-specific difference between human and mouse embryonic development that precludes the capture of the human naïve state. There is mounting evidence suggesting that the role of lineage-specific transcription factors and cell signalling pathways differs for human blastocyst development compared to in the mouse. For example, the FGF-MAPK pathway is not critical for establishing primitive endoderm versus epiblast identity in the inner cell mass of the human blastocyst (Kuijk et al., 2012). In addition, lineage-specific transcription factors such as CDX2, OCT4, and SOX17 have a different spatiotemporal expression pattern in the human than in mouse (Niakan and Eggan, 2013), and with the use of genome editing, functions of these transcription factors in human development are now being elucidated (Fogarty et al., 2017). A major developmental difference between humans and mice is the formation of the rodent egg cylinder, in contrast to human embryos developmentally proceeding to the embryonic disc stage. The organization of the egg cylinder into an epithelium likely results in a longer time frame for ESCs to remain in the naïve state, thus allowing for a large time window for the derivation of naïve mouse ESCs. Furthermore, rodents are capable of embryonic diapause, a hormonally-regulated state of delayed implantation, which may permit the derivation of naïve ESCs in these species in contrast to those that cannot

undergo diapause (Nichols and Smith, 2009). Thus, while the mouse is an important model for studying early mammalian development, it is becoming increasingly evident that observations made in the mouse cannot be directly translated to human development.

1.3.3 Embryonic stem cell differentiation

When removed from factors maintaining pluripotency, ESCs can differentiate into derivatives of mesoderm, endoderm, and ectoderm lineages *in vitro*. ESC differentiation into specific lineages is typically achieved using three established methods (Murry and Keller, 2008). Firstly, under low adherence culture conditions, mESCs aggregate and form three-dimensional embryoid bodies (EBs) which mimic early post-implantation mouse development (Doetschman et al., 1985; Martin and Evans, 1975). If EBs remain in suspension, they form cystic structures and spontaneously generate endoderm, blood islands, and myocardium (Doetschman et al., 1985). If EBs adhere to a substrate (e.g. gelatin), differentiated cells emerge from the EB and form morphologically identifiable derivatives of the three germ layers (e.g. myocardial cells, neural cells, glandular cells, skeletal/smooth muscle cells, etc.) (Doetschman et al., 1985; Martin and Evans, 1975). The three-dimensional aspect of EB formation allows for cell-cell interactions, promoting the differentiation of certain lineages. However, the signalling factors and cytokines generated in these structures are complex and may confound investigation into the role of certain signalling pathways in ESC differentiation. Another disadvantage of forming large EB aggregates is the disorganization of differentiating cells that emerge, which does not fully recapitulate early mouse postimplantation development or gastrulation. To overcome this, it was recently discovered that smaller aggregates of mESCs (approximately 300 cells) form structures known as gastruloids, which self-organize and behave developmentally similar to gastrulating mouse embryos (van den Brink et al., 2014). Similarly, human ESCs can be spatially confined in culture to form structures with organized germ layers in response to BMP4 (Warmflash et al., 2014). As a second method of differentiation, ESCs can be co-cultured on stromal cells or cultured in stromal cell conditioned medium, particularly to generate hematopoietic lineages (Nakano et al., 1994; Vodyanik et al., 2005). However, stromal cells produce undefined factors and are difficult to separate from ESCs for downstream applications. Lastly, ESCs can be

cultured in a monolayer on defined extracellular matrix proteins to promote differentiation of certain lineages. This method is the simplest and allows for selection of lineage commitment depending on the type of extracellular matrix protein used. For example, neural differentiation is promoted by culture on gelatin (Ying et al., 2003), hematopoietic differentiation by culture on type IV collagen (Nishikawa et al., 1998), and cardiac differentiation by culture on Matrigel (Laflamme et al., 2007). Ultimately, the goal of ESC differentiation strategies is to recapitulate the *in vivo* developmental program as closely as possible to have the most potential for regenerative medicine applications (Keller, 2005).

In vivo, gastrulation is the process by which the three germ layers of the embryo are formed. Gastrulation begins with the formation of the primitive streak, which defines the posterior end of the embryo. Uncommitted cells of the epiblast then sequentially migrate through the primitive streak and adopt either mesoderm or endoderm fates. Cells that migrate through the posterior parts of the primitive streak become mesoderm, while cells that migrate through the most anterior parts become definitive endoderm. Cells that remain in the anterior region of the epiblast and do not migrate through the primitive streak become ectoderm. This process is not random but is spatially and temporally regulated, likely through different signalling environments generated in the primitive streak that induce specific lineages. It is now known that cell fate regulation during gastrulation is dependent on the relative balance of BMP, Wnt, and Nodal signalling, which can be used for *in vitro* applications to direct ESC differentiation to the three germ layers. Ectoderm differentiation is inhibited by BMP, Wnt, and Nodal signalling, which underlies why ESCs appear to default to the neural differentiation program when removed from culture conditions promoting pluripotency. However, this process is dependent on FGF signalling produced by the differentiating ESCs and thus cannot be defined as a true default pathway (e.g. a pathway that requires no input signals) (Ying et al., 2003). High levels of Nodal/Activin signalling promote differentiation to definitive endoderm. Interestingly, it is thought that ESCs pass through a mesendoderm intermediate progenitor stage characterized by the expression of *Gsc* and *Cdh1* before forming definitive endoderm, as both endoderm and mesoderm cells are observed at the primitive streak stage in culture (Tada et al., 2005). Mesoderm differentiation is

dependent on BMP and Wnt signalling initially, but subsequent inhibition of Wnt/ β -Catenin signalling is required to generate cardiac mesoderm (Naito et al., 2006). Once cells have passed through their initial germ layer specification, lineage-specific protocols can be used to generate more committed, progenitor cell populations of organs such as the pancreas, liver, heart, brain, and the hematopoietic lineages (reviewed in (Murry and Keller, 2008). Thus, differential activation of cell signalling pathways and their subsequent regulation of gene expression is critical to the specification and commitment of cells as they follow their developmental program.

1.4 The role of p66Shc in preimplantation embryos and embryonic stem cells

1.4.1 Receptor tyrosine kinase signalling

As a critical and recurring cell signalling pathway during development, fibroblast growth factor (FGF) is an example of a ligand that signals through receptor tyrosine kinases (RTK) to mediate its effects. RTK signalling is a mechanism for cells to respond to external stimuli and to communicate signals for proliferation, differentiation, cell survival, metabolism, cell migration, and cell cycle control (Lemmon and Schlessinger, 2010). Mechanisms of RTK activation across family members of receptors is generally conserved. Growth factor ligand binding to a receptor induces receptor dimerization or oligomerization, followed by autophosphorylation of tyrosines on the intracellular domain of the receptor. Tyrosine phosphorylation then serves as a site for the recruitment and activation of signalling proteins leading to the assembly of signalling complexes. Proteins with Src homology 2 (SH2) and/or phosphotyrosine binding (PTB) domains either directly bind phosphorylated RTKs or interact indirectly with the receptor through docking proteins phosphorylated by the receptor (Lemmon and Schlessinger, 2010). Assembly of these complexes then link activated RTK to intracellular signalling pathways such as the Ras/MAPK and PI3K/Akt pathways. RTK pathway activation and regulation is critical to ensure proper preimplantation embryo development and ESC function, including signalling by the epidermal growth factor receptor (EGFR) and fibroblast growth factor receptor (FGFR). Embryos are capable of producing autocrine growth factors as they can be cultured in simple medium without the addition of any

exogenous factors. EGF and transforming growth factor alpha both signal through the EGFR to promote trophectoderm differentiation and, to a lesser extent, mitogenic signalling (Brice et al., 1993). As previously outlined, regulation of the FGF4/FGFR2/MAPK signalling mediates epiblast and primitive endoderm differentiation in the inner cell mass, while inhibition of ERK1/2 signalling in ESCs maintains naïve pluripotency (Nichols et al., 2009; Yamanaka et al., 2010). RTK signalling is regulated at multiple levels including dephosphorylation of signalling pathway components, cross-talk between signalling pathways, and regulation at the level of the receptor (Lemmon and Schlessinger, 2010).

1.4.2 Shc isoforms and functions

Src homology 2 domain-containing transforming proteins (Shc) are RTK signalling adaptor proteins expressed in mammalian cells with four identified genes: ShcA (also known as Shc1), ShcB, ShcC, and ShcD (Wills and Jones, 2012). These adaptor proteins transduce external stimuli within cells by identifying changes in phosphorylation residues via the SH2 domain. Shc proteins all have a common N-terminal PTB, C-terminal SH2 domain, and CH1 region (Figure 1-2). Unlike other SH2-containing proteins like Src and PLC γ , Shc proteins have no catalytic function but instead recruit downstream signalling components of RTK pathways (Wills and Jones, 2012). ShcA is composed of three isoforms transcribed from the same genetic locus and defined by their molecular weight: p46Shc, p52Shc, and p66Shc. P46Shc/p52Shc are ubiquitously expressed, while p66Shc is absent from mature cells of the central nervous system and hematopoietic cells (Wills and Jones, 2012). Differential regulation of Shc1 isoform expression is due to the regulation of a p66Shc-specific promoter, which can be epigenetically modified through acetylation or methylation (Ventura et al., 2002). Treatment with histone deacetylase inhibitors (Trichostatin A) or demethylating agents (5-Aza-dC) results in increased p66Shc expression in bone marrow cells, and p66Shc expression levels in different tissues and cell lines are correlated with the degree of methylation in its promoter (Ventura et al., 2002). ShcB and ShcC are thought to mainly act in neural derived cells, as knockout mice are viable but have lower numbers of specific neural cells. ShcD is the

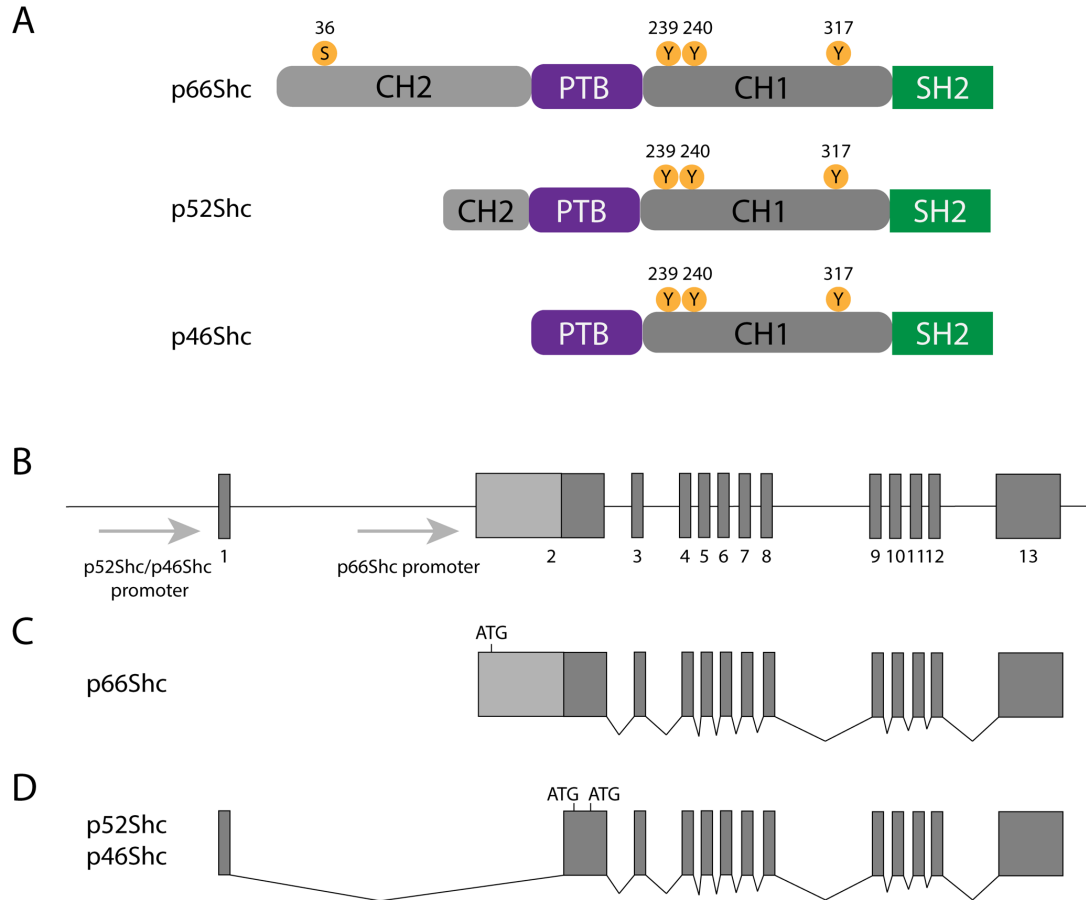


Figure 1-2. Protein and genetic structures of Shc1.

(A) Protein structure of p66Shc, p52Shc, and p46Shc. Phosphorylation sites are indicated in orange (S = serine, Y = tyrosine) with the amino acid number above. CH2 = collagen homology domain 2, PTB = phosphotyrosine binding domain, CH1 = collagen homology domain 1, SH2 = Src homology 2 domain. (B) Shc1 genetic locus. P66Shc transcription is under the control of a unique promoter located in the intronic region of exon 1 and exon 2, while the p52Shc/p46Shc promoter is located upstream of exon 1. (C) Structure of the p66Shc transcript and translational start site (ATG). (D) Structure of the p52Shc/p46Shc and translational start sites (ATG).

most recently identified Shc family member, and shares the highest identity with ShcA (Jones et al., 2007).

All Shc1 family members have conserved tyrosine 239/240 and 317 motifs that when phosphorylated act as recognition motifs for GRB2 (Lai and Pawson, 2000). GRB2 is constitutively associated with Son of Sevenless (SOS) a guanine nucleotide exchange factor, and recruitment to Shc proteins results in SOS localization to the membrane, which activates Ras. Ras then activates Raf, which then phosphorylates MEK1/2, which then phosphorylates and activates ERK1/2. ERK1/2 then has many potential downstream effects including transcription factor regulation of c-Myc and c-Fos. Shc1 participation is not an absolute requirement in the EGFR-MAPK pathway as Grb2 can directly bind phosphotyrosines on the EGFR. However, Shc1 adaptors are required to sensitize the cellular response to low concentrations of growth factors present in the extracellular environment (Lai and Pawson, 2000; Wills and Jones, 2012).

Unlike p52Shc, p66Shc does not result in MAPK phosphorylation downstream of EGFR activation. Treatment with EGF following the overexpression of p52Shc cDNA in COS-1 cells (monkey kidney fibroblasts) increases MAPK phosphorylation by 14 to 16-fold, while overexpression of p66Shc cDNA results in no significant increase in MAPK phosphorylation (Migliaccio et al., 1997). In a separate study, overexpression of p52Shc increases p52Shc co-immunoprecipitation with GRB2, while overexpression of p66Shc decreases p52Shc co-immunoprecipitation with GRB2 and concomitantly increases p66Shc co-immunoprecipitation with GRB2. P66Shc overexpression also decreases EGFR co-immunoprecipitation with GRB2, suggesting reduced EGFR-GRB2 interactions under these conditions (Okada et al., 1997). These observations have led to a model that p66Shc competes with p52Shc for GRB2 binding, then sequesters GRB2 away from the EGFR, inhibiting subsequent Ras/MAPK activation. The most updated model outlines that upon EGF stimulation, p66Shc is recruited to the EGFR, phosphorylated on Tyr239/240, Tyr317, and Ser/Thr residues of CH2 domain by MEK. Phosphorylated p66Shc recruits GRB2-SOS, but due to the additional Ser/Thr phosphorylation, the EGFR-p66Shc interaction is destabilized, which sequesters GRB2-SOS away from Ras (Okada et al., 1997; Wills and Jones, 2012). This may lead to

accelerated inactivation of ERK1/2, leading to reduced downstream c-Fos transcription (Migliaccio et al., 1997; Okada et al., 1997).

A number of genetically modified mice have been generated to investigate the role of the Shc1 proteins and p66Shc-specific biochemical and biological functions. Deletion of all three Shc1 proteins results in embryonic lethality at E12 with major cardiovascular developmental defects, predominantly in vascular morphogenesis. The cardiac vasculature in Shc1^{-/-} embryos is less complex, dilated, and immature, leading to outflow tracts becoming congested with blood and abnormal cardiac contractions (Lai and Pawson, 2000). This suggests that Shc1 proteins are required to sensitize blood vessel progenitor cells to stimuli required for angiogenic remodelling, particularly in areas of low growth factor concentration (Lai and Pawson, 2000). To overcome embryonic lethality, a Shc1-loxP transgenic mouse was generated for tissue-specific conditional knockout using Cre-loxP recombination (Zhang et al., 2002). Lymphocyte-specific deletion of Shc1 led to reduced numbers of mature thymocytes, pointing to a role in T-cell maturation, and Shc1 has since been identified as mediating its effects through MAPK signalling in T-cells (Tramont et al., 2006; Zhang et al., 2002). However, because these knockout strategies target exons common to all three Shc1 isoforms, these knockout models prevent investigation into the specific functions of p66Shc.

The first p66Shc-specific, body-wide knockout mouse was generated around the same time as the Shc1 knockout mice (Migliaccio et al., 1999). A novel role for p66Shc in mediating the cellular response to oxidative stress was identified in experiments demonstrating that cell death was reduced in p66Shc^{-/-} MEFs after treatment with H₂O₂ (Migliaccio et al., 1999). When p66Shc^{-/-} mice were injected with paraquat (a chemical that generates superoxide anions), 3 of 5 mice had lengthened survival (72 hours to weeks after injection) compared to wild type mice that died within the first 48 hours of injection, indicating that p66Shc^{-/-} mice have increased resistance to oxidative stress. When basal lifespan was assessed, all wild type animals died after 28 months, while 73% of p66Shc^{-/-} mice lived another 8 months, an approximate 30% increase in lifespan (Migliaccio et al., 1999). These results implicated p66Shc as one of the first aging-related proteins identified whose deletion resulted in a prolonged lifespan. However, when the

same group repeated the study several years later with a larger population of mice at two separate research centres, there was no significant difference in lifespan between p66Shc^{-/-} and wild type mice raised on three different strain backgrounds (Ramsey et al., 2014). Furthermore, p66Shc deletion is detrimental to mice raised in natural conditions, e.g., not in traditional laboratory animal housing (Giorgio et al., 2012). When p66Shc^{-/-} mice were exposed to cold and food competition, there was an increase in mortality compared to wild type mice with only 10 of 62 p66Shc^{-/-} mice surviving 8 months after exposure to natural conditions (Giorgio et al., 2012). P66Shc^{-/-} mice were found to have reduction in body fat deposits and reduced fertility with repeated breeding cycles (Giorgio et al., 2012). Thus, benefits of p66Shc deletion appear to be selective to preventing diseases associated with metabolism, and p66Shc deletion instead is detrimental under conditions requiring body fat storage and thermoregulation. Fertility was reported to be normal in p66Shc^{-/-} mice, however, it is unclear if homozygote mice were mated for the longevity studies, as mating heterozygote mice could result in a maternal rescue effect due to p66Shc expression in the oocyte (Migliaccio et al., 1999). Furthermore, the neomycin resistance gene used as a selectable marker in the targeting vector is retained in p66Shc^{-/-} mice, which may affect the expression of the other Shc isoforms, leading to a confounding phenotype (Tomilov et al., 2011). In fact, p52Shc decreases and p46Shc increases in certain tissues in this mouse, while their expression is unaffected in another genetic knockout with the selectable marker removed (Tomilov et al., 2011).

The oxidative stress response function unique to p66Shc is attributed to its N-terminal extension containing serine/threonine sites that are phosphorylated when cells are treated with UV or H₂O₂ (Migliaccio et al., 1999). Mutation of the serine-36 site to alanine does not restore the oxidative stress response when expressed in p66Shc^{-/-} MEFs, suggesting that phosphorylation of this site is critical to the oxidative stress response function of p66Shc (Migliaccio et al., 1999). Work has since been done to characterize the downstream response of p66Shc occurring in the mitochondria. Under basal conditions, a fraction of cellular p66Shc is localized to the mitochondria based on co-localization with Mitotracker, which increases slightly after treatment with UV or H₂O₂ (from approximately 6% to 12% of total cellular p66Shc) (Orsini et al., 2004). Subcellular fractionation of purified mitochondria confirms p66Shc localization to the inner

mitochondrial membrane (Orsini et al., 2004). Mitochondrial p66Shc appears to form a complex with Hsp70, translocase of the outer membrane (TOM), and translocase of the inner membrane (TIM), while oxidative stress promotes dissociation of p66Shc from the complex (Orsini et al., 2004). Phosphorylation of p66Shc at serine-36 is thought to be predominantly through PKC β activation in response to oxidative stress, as treatment with hispidin, a PKC β inhibitor, inhibits p66Shc phosphorylation *in vitro*. The prolyl isomerase Pin-1 binds to p66Shc at the Ser36/Pro37 binding site, which then mediates its translocation to the mitochondria (Pinton et al., 2007). Experiments performed on purified liver mitochondria then demonstrated that p66Shc mediates electron transfer between itself and cytochrome C, which could lead to generation of H₂O₂, cleaved caspase-3 activation, and apoptosis (Giorgio et al., 2005). Work leading to the generation of this model of p66Shc activation and function during oxidative stress, however, has been performed mostly *in vitro* or in purified mitochondrial preparations, and should be confirmed in a physiological context (Galimov, 2010).

Other groups speculated that results from the oxidative stress studies in p66Shc^{-/-} mice may be due to p66Shc directly regulating reactive oxygen species (ROS) production through regulating mitochondrial metabolism. Oxidative phosphorylation metabolism generates ROS as a by-product, which could accelerate cellular aging. Supporting this, *C. elegans* mutants with extended lifespan are associated with decreased mitochondrial metabolism (Rea and Johnson, 2003). P66Shc^{-/-} MEFs had a reduction in basal oxygen consumption by 30-50% compared to wild type MEFs, and a reduction in oxygen consumption when treated with a mitochondrial uncoupler (Nemoto et al., 2006). P66Shc^{-/-} MEFs increase lactate production, suggesting that their metabolic profile switches to become more glycolytic to compensate for the lack of ATP production by oxidative phosphorylation (Nemoto et al., 2006). Similarly, short-hairpin mediated knockdown of p66Shc in HeLa cells increases the abundance of glycolytic and anabolic intermediates such as lactate and citrate (Soliman et al., 2014). There are multiple suggested models of how p66Shc regulates metabolism which are cell signalling context-dependent (Acin-Perez et al., 2010; Nemoto et al., 2006; Soliman et al., 2014). P66Shc appears to negatively regulate mTOR signalling downstream of IGF-1 or insulin binding, but not EGF binding, inhibiting anabolic metabolism and favouring oxidative phosphorylation

(Soliman et al., 2014). Another model suggests that p66Shc acts as an adaptor in the inner mitochondrial membrane to relay PKC δ signalling to cytochrome c downstream of retinoic acid, which ultimately regulates pyruvate dehydrogenase activity and influx of acetyl CoA into the TCA cycle (Acin-Perez et al., 2010). Direct regulation of metabolism is an alternative explanation for the increased lifespan in p66Shc^{-/-} mice. If tissues in these mice use alternative metabolic pathways such as glycolysis, overall, they generate less ROS in their tissues, which could slow aging (Hoyos et al., 2012).

Interestingly, expression of p66Shc has been identified during preimplantation development (Favetta et al., 2007b; Ren et al., 2014). Its role in the oxidative stress response suggests that p66Shc is present in early embryos in order to prevent developmentally compromised embryos from proceeding to the blastocyst stage (Betts and Madan, 2008). However, knockdown of p66Shc in bovine embryos reduces blastocyst development, and p66Shc overexpression in mESCs promotes a pluripotent colony morphology, suggesting that p66Shc may have an important physiological role during early development (Favetta et al., 2007a; Papadimou et al., 2009). The following section summarizes research into the role of p66Shc in preimplantation embryos and embryonic stem cells to date.

1.4.3 P66Shc in bovine preimplantation embryos

Studies thus far regarding the role of p66Shc during bovine preimplantation development have shown a link between its expression and the promotion of permanent embryo arrest, a senescence-like state, or apoptosis. In bovine embryos produced by *in vitro* fertilization, p66Shc exhibits a steadily decreasing expression pattern during which its expression is highest in the GV oocyte and lowest in the blastocyst (Favetta et al., 2004). This pattern is different than the pattern which most transcripts follow during mammalian preimplantation development, as transcript levels typically increase after embryonic genome activation up to the blastocyst stage (Hamatani et al., 2004). Favetta *et al.* further hypothesized that bovine embryos arrested at the 2-4 cell stage would have increased levels of both p66Shc and p53, characteristic of senescence in other cell types. However, 2-4 cell arrested bovine embryos had significant increases only in p66Shc transcript levels compared to embryos that continued to cleave. Furthermore, late cleaving

embryos, associated with poor embryo quality and a reduced likelihood to develop to the blastocyst stage, also contained higher p66Shc mRNA abundance and higher p66Shc immunofluorescence intensity compared to early cleaving embryos (Favetta et al., 2004). Conditions that promote embryo arrest and decrease blastocyst development, such as culture under 20% oxygen, result in a significant increase in p66Shc mRNA levels in bovine embryos (Favetta et al., 2007b). These initial studies suggest that p66Shc expression levels predict bovine embryo developmental competence, and that the elevation in p66Shc mRNA in late cleaving embryos may precede and functionally promote embryo arrest at the 2-4 cell stage.

To understand the functional role of p66Shc in early embryo arrest, RNA interference using both shRNA and short interfering (si)RNA was employed in two separate studies. When GV oocytes were injected with p66Shc shRNA, then fertilized by IVF, embryos were less likely to undergo the first division (cleavage) and were less likely to develop into blastocysts. However, if p66Shc injected oocytes did cleave, fewer of them were arrested at the 2-4 cell stage (Favetta et al., 2007a). In contrast, when bovine zygotes were injected with p66Shc siRNA, embryo development to the blastocyst stage improved compared to non-injected and siRNA controls (Betts et al., 2014). The difference in developmental phenotypes could be attributed to the timing of siRNA introduction, as p66Shc may be critical for events involved in oocyte maturation and fertilization. Knockdown at the zygote stage may bypass these requirements and instead improve baseline embryo development by conferring protection to exogenous stress present in the culture system. These studies together suggest that p66Shc has more than one function during preimplantation development, and these functions are temporally and environmentally context-dependent.

Additional studies have linked p66Shc levels with redox imbalance in the bovine embryo. Treatment with 50 μ M H₂O₂ significantly increases p66Shc transcript levels and increases histone γ -H2AX immunostaining, a marker of DNA damage, while treatment with PEG-conjugated catalase significantly decreases p66Shc transcript abundance and γ -H2AX immunostaining compared to non-treated controls (Bain et al., 2013). Furthermore, p66Shc siRNA-injected zygotes produce less ROS, have decreased

detectable γ -H2AX immunostaining, have improved development to the blastocyst stage, and reduced permanent embryo arrest and apoptosis when treated with 50 μ M H₂O₂ (Betts et al., 2014). This suggests that the embryo's response to conditions promoting oxidative stress are mediated by p66Shc regulating the release of ROS.

While p66Shc's role in mediating the bovine embryo's response to oxidative stress has been thoroughly investigated, it remains unclear whether p66Shc has an important functional role in development to the blastocyst stage, since its knockdown in GV oocytes ultimately reduces bovine blastocyst development. Based on the roles of p66Shc in other cell types, it may be acting to modulate metabolism or mitogenic signalling through receptor tyrosine kinases. Furthermore, blastocysts produced by p66Shc knockdown embryos were not investigated for the correct allocation of the trophectoderm and inner cell mass and were not tested for developmental competence by embryo transfer or by *in vitro* outgrowth assays. P66Shc is expressed in mouse and human embryonic stem cells (Papadimou et al., 2009; Shimizu et al., 2012; Smith et al., 2016), and thus may be important early in development to specify the pluripotent cell population in the blastocyst.

1.4.4 P66Shc in mouse preimplantation embryos

The role of p66Shc during mouse preimplantation development is less well studied than in the bovine model. Studies so far have focused on its role in mediating the embryo's response to arsenic exposure. P66Shc protein abundance increases 48 hours after arsenic exposure *in vitro*, which can be reduced if the embryos are incubated in medium supplemented with the antioxidant N-acetyl cysteine (Zhang et al., 2010). An increase in p66Shc expression correlates with an increase in ROS production, an increase in apoptosis, and a decrease in embryonic development, suggesting that p66Shc may mediate the release of ROS in the embryo in response to arsenic (Zhang et al., 2010). Embryos injected with siRNA targeting all Shc1 isoforms and then subsequently exposed to arsenic did not develop to the blastocyst stage but were able to form morulae and had lower levels of ROS as measured by DCF fluorescence (Ren et al., 2014). Together, these results suggest that p66Shc expression is regulated by ROS after arsenic exposure, and

increased expression of p66Shc may result in a further increase in ROS that is ultimately detrimental to preimplantation development.

Interestingly, pronuclear injection of 20 μ M Shc1 siRNA in mouse zygotes resulted in a decrease in development to the blastocyst stage and an increase in arrest at the 2-cell and morula stages, suggesting that p66Shc may have an important role in progression through preimplantation development (Ren et al., 2014). However, this study did not address this and used a lower concentration of siRNA (2 μ M) instead to observe effects of knockdown to the embryo's response to arsenic. Another limitation is that the siRNA employed targeted all three Shc1 isoforms, and thus decreased p52/p46Shc expression may also negatively affect early embryo development. Due to species-specific differences between bovine and murine preimplantation development and the level of optimization of culture systems, the biological function of p66Shc in normal blastocyst development may be better elucidated in a mouse model.

1.4.5 P66Shc in embryonic stem cells

As a component of a mitogenic cell signalling pathway, studies are emerging on the role of Shc proteins in embryonic stem cell function. Papadimou *et al.* observed that all three Shc1 isoforms are upregulated in the early stages of directed neuronal differentiation of mouse embryonic stem cells, and that overexpressing p66Shc accelerated directed neural differentiation and the loss of OCT4 expression. Overexpression of p66Shc did not affect self-renewal by alkaline phosphatase staining, though notably, p66Shc overexpression altered cell morphology to produce smaller and more compact colonies, characteristic of naïve pluripotency (Papadimou et al., 2009). Overexpressing p66Shc in human embryonic stem cells produced a similar morphological phenotype. Additionally, overexpression of p66Shc during neural differentiation increased β -catenin signalling through increased phosphorylation of GSK-3 β , without affecting phosphorylated ERK1/2 (Papadimou et al., 2009). Interestingly, other studies suggest that p66Shc can modulate Wnt/ β -catenin signalling through production of ROS (Vikram et al., 2014). Shc1 proteins have also been implicated in mESC differentiation through modulating the cellular response to substrate stiffness downstream of Src, transduced through ERK1/2 signalling (Shimizu et al., 2012).

ShcD, the most recent family of Shc proteins to be discovered, has also been studied in the context of embryonic stem cells. ShcD is detectable by in situ hybridization in the epiblast of E4.5 mouse blastocysts and is highly expressed in mouse epiblast stem cell lines (Turco et al., 2012). Turco et al. generated ShcD knockout mESCs and observed that during the ESC to EpiSC transition, loss of ShcD accelerated the decline in OCT4 expression and significantly increased the number of apoptotic cells. Differentiating cells also displayed higher phosphorylated ERK1/2 levels than controls, suggesting that ShcD may regulate ERK1/2 signalling downstream of receptor tyrosine kinase activation (Turco et al., 2012).

Thus, our insight into the roles of Shc proteins in embryonic stem cells so far suggests that they regulate cell signalling pathways during differentiation with potential cross talk between pathways, particularly, RTK/MAPK and Wnt/ β -Catenin.

1.5 Rationale and study aims

Both cow and mouse preimplantation embryo development are effective animal models of human preimplantation development. While bovine embryos better recapitulate certain aspects of human reproduction and development such as oocyte maturation, fertilization, and timing of the embryonic cell cycle, mouse embryos are the most frequently used model for embryo micromanipulation and quality control testing of reagents for human embryo culture (Ménézo and Héribel, 2002; Quinn and Horstman, 1998). Furthermore, morphological and developmental events such as cleavage, compaction, and formation of the blastocyst cavity in the mouse embryo closely resembles these events in the human embryo (Quinn and Horstman, 1998). Thus, for my thesis work, I used mouse preimplantation development to assay the entire preimplantation period *in vivo*, to use embryo micromanipulation, and to use embryo culture to determine the role of p66Shc in mouse blastocyst development. Additionally, I used mESCs for their ease of genome editing and the ability to clearly distinguish the naïve and primed pluripotent states in order to understand the role of p66Shc in ESC function and biology.

P66Shc promotes apoptosis and senescence in many cell types, including early embryos (Favetta et al., 2007a). P66Shc is expressed throughout preimplantation development

including at the blastocyst stage (Ren et al., 2014), and knockdown of p66Shc appears to negatively impact bovine blastocyst development (Favetta et al., 2007a). Furthermore, increased p66Shc expression appears to promote embryonic stem cell pluripotency (Papadimou et al., 2009). Given these observations, I predict that p66Shc is required for normal mouse blastocyst development and mouse embryonic stem cell function. Thus, the overall hypothesis of my thesis is that *loss of p66Shc expression in the mouse preimplantation embryo will dysregulate blastocyst development and mouse embryonic stem cell pluripotency*. First, I will determine the expression and localization of p66Shc during mouse preimplantation development, and if oxygen tension and/or medium glucose concentrations alter p66Shc expression (Chapter 2). Secondly, I aim to determine the effects of p66Shc knockdown on mouse blastocyst development and blastocyst cell lineage specification (Chapter 3). Lastly, I aim to determine if genetic knockout of p66Shc in mouse embryonic stem cells alters pluripotency and biases spontaneous differentiation of embryonic stem cells into germ layer derivatives (Chapter 4). Taken together, my work will advance our knowledge of p66Shc function during mammalian development and contribute to a greater understanding of how pluripotency and cell fate are established in the mouse preimplantation embryo.

1.6 References

- Acin-Perez, R., Hoyos, B., Gong, J., Vinogradov, V., Fischman, D. A., Leitges, M., Borhan, B., Starkov, A., Manfredi, G. and Hammerling, U.** (2010). Regulation of intermediary metabolism by the PKCdelta signalosome in mitochondria. *FASEB J* **24**, 5033-5042.
- Anani, S., Bhat, S., Honma-Yamanaka, N., Krawchuk, D. and Yamanaka, Y.** (2014). Initiation of Hippo signaling is linked to polarity rather than to cell position in the pre-implantation mouse embryo. *Development* **141**, 2813-2824.
- Bain, N. T., Madan, P. and Betts, D. H.** (2013). Elevated p66Shc is associated with intracellular redox imbalance in developmentally compromised bovine embryos. *Mol Reprod Dev* **80**, 22-34.
- Baltz, J. M., Smith, S. S., Biggers, J. D. and Lechene, C.** (1997). Intracellular ion concentrations and their maintenance by Na⁺/K⁺ -ATPase in preimplantation mouse embryos. *Zygote* **5**, 1-9.

- Barcroft, L. C., Offenberg, H., Thomsen, P. and Watson, A. J.** (2003). Aquaporin proteins in murine trophoblasts mediate transepithelial water movements during cavitation. *Dev Biol* **256**, 342-354.
- Betts, D. H., Bain, N. T. and Madan, P.** (2014). The p66(Shc) adaptor protein controls oxidative stress response in early bovine embryos. *PLoS One* **9**, e86978.
- Betts, D. H. and Madan, P.** (2008). Permanent embryo arrest: molecular and cellular concepts. *Mol Hum Reprod* **14**, 445-453.
- Brice, E. C., Wu, J.-X., Muraro, R., Adamson, E. D. and Wiley, L. M.** (1993). Modulation of mouse preimplantation development by epidermal growth factor receptor antibodies, antisense RNA, and deoxyoligonucleotides. *Developmental Genetics* **14**, 174-184.
- Brons, I. G., Smithers, L. E., Trotter, M. W., Rugg-Gunn, P., Sun, B., Chuva de Sousa Lopes, S. M., Howlett, S. K., Clarkson, A., Ahrlund-Richter, L., Pedersen, R. A., et al.** (2007). Derivation of pluripotent epiblast stem cells from mammalian embryos. *Nature* **448**, 191-195.
- Brook, F. A. and Gardner, R. L.** (1997). The origin and efficient derivation of embryonic stem cells in the mouse. *Proc Natl Acad Sci U S A* **94**, 5709-5712.
- Chan, Y. S., Goke, J., Ng, J. H., Lu, X., Gonzales, K. A., Tan, C. P., Tng, W. Q., Hong, Z. Z., Lim, Y. S. and Ng, H. H.** (2013). Induction of a human pluripotent state with distinct regulatory circuitry that resembles preimplantation epiblast. *Cell Stem Cell* **13**, 663-675.
- Chazaud, C. and Yamanaka, Y.** (2016). Lineage specification in the mouse preimplantation embryo. *Development* **143**, 1063-1074.
- Chazaud, C., Yamanaka, Y., Pawson, T. and Rossant, J.** (2006). Early lineage segregation between epiblast and primitive endoderm in mouse blastocysts through the Grb2-MAPK pathway. *Dev Cell* **10**, 615-624.
- Chen, Y. and Lai, D.** (2015). Pluripotent states of human embryonic stem cells. *Cell Reprogram* **17**, 1-6.
- Cheng, A. M., Saxton, T. M., Sakai, R., Kulkarni, S., Mbamalu, G., Vogel, W., Tortorice, C. G., Cardiff, R. D., Cross, J. C., Muller, W. J., et al.** (1998). Mammalian Grb2 regulates multiple steps in embryonic development and malignant transformation. *Cell* **95**, 793-803.
- Cockburn, K., Biechele, S., Garner, J. and Rossant, J.** (2013). The Hippo pathway member Nf2 is required for inner cell mass specification. *Curr Biol* **23**, 1195-1201.

- Cockburn, K. and Rossant, J.** (2010). Making the blastocyst: lessons from the mouse. *J Clin Invest* **120**, 995-1003.
- Doetschman, T. C., Eistetter, H., Katz, M., Schmidt, W. and Kemler, R.** (1985). The in vitro development of blastocyst-derived embryonic stem cell lines: formation of visceral yolk sac, blood islands and myocardium. *J Embryol Exp Morphol* **87**, 27-45.
- Evans, M. J. and Kaufman, M. H.** (1981). Establishment in culture of pluripotential cells from mouse embryos. *Nature* **292**, 154-156.
- Favetta, L. A., Madan, P., Mastromonaco, G. F., St John, E. J., King, W. A. and Betts, D. H.** (2007a). The oxidative stress adaptor p66Shc is required for permanent embryo arrest in vitro. *BMC Dev Biol* **7**, 132.
- Favetta, L. A., Robert, C., St John, E. J., Betts, D. H. and King, W. A.** (2004). p66shc, but not p53, is involved in early arrest of in vitro-produced bovine embryos. *Mol Hum Reprod* **10**, 383-392.
- Favetta, L. A., St John, E. J., King, W. A. and Betts, D. H.** (2007b). High levels of p66shc and intracellular ROS in permanently arrested early embryos. *Free Radic Biol Med* **42**, 1201-1210.
- Fleming, T. P., Sheth, B. and Fesenko, I.** (2001). Cell adhesion in the preimplantation mammalian embryo and its role in trophoblast differentiation and blastocyst morphogenesis. *Front Biosci* **6**, D1000-1007.
- Fogarty, N. M. E., McCarthy, A., Snijders, K. E., Powell, B. E., Kubikova, N., Blakeley, P., Lea, R., Elder, K., Wamaitha, S. E., Kim, D., et al.** (2017). Genome editing reveals a role for OCT4 in human embryogenesis. *Nature* **550**, 67-73.
- Frum, T., Halbisen, M. A., Wang, C., Amiri, H., Robson, P. and Ralston, A.** (2013). Oct4 cell-autonomously promotes primitive endoderm development in the mouse blastocyst. *Dev Cell* **25**, 610-622.
- Galimov, E. R.** (2010). The role of p66shc in oxidative stress and apoptosis. *Acta Naturae* **2**, 44-51.
- Garg, V., Morgani, S. and Hadjantonakis, A. K.** (2016). Capturing identity and fate ex vivo: stem cells from the mouse blastocyst. *Curr Top Dev Biol* **120**, 361-400.
- Gerbe, F., Cox, B., Rossant, J. and Chazaud, C.** (2008). Dynamic expression of Lrp2 pathway members reveals progressive epithelial differentiation of primitive endoderm in mouse blastocyst. *Dev Biol* **313**, 594-602.
- Giorgio, M., Berry, A., Berniakovich, I., Poletaeva, I., Trinei, M., Stendardo, M., Hagopian, K., Ramsey, J. J., Cortopassi, G., Migliaccio, E., et al.** (2012). The

p66Shc knocked out mice are short lived under natural condition. *Aging Cell* **11**, 162-168.

- Giorgio, M., Migliaccio, E., Orsini, F., Paolucci, D., Moroni, M., Contursi, C., Pelliccia, G., Luzi, L., Minucci, S., Marcaccio, M., et al.** (2005). Electron transfer between cytochrome c and p66Shc generates reactive oxygen species that trigger mitochondrial apoptosis. *Cell* **122**, 221-233.
- Grabarek, J. B., Zyzynska, K., Saiz, N., Piliszek, A., Frankenberg, S., Nichols, J., Hadjantonakis, A. K. and Plusa, B.** (2012). Differential plasticity of epiblast and primitive endoderm precursors within the ICM of the early mouse embryo. *Development* **139**, 129-139.
- Guo, G., Huss, M., Tong, G. Q., Wang, C., Li Sun, L., Clarke, N. D. and Robson, P.** (2010). Resolution of cell fate decisions revealed by single-cell gene expression analysis from zygote to blastocyst. *Dev Cell* **18**, 675-685.
- Guo, G., Yang, J., Nichols, J., Hall, J. S., Eyres, I., Mansfield, W. and Smith, A.** (2009). Klf4 reverts developmentally programmed restriction of ground state pluripotency. *Development* **136**, 1063-1069.
- Hamatani, T., Carter, M. G., Sharov, A. A. and Ko, M. S.** (2004). Dynamics of global gene expression changes during mouse preimplantation development. *Dev Cell* **6**, 117-131.
- Handyside, A. H., Lesko, J. G., Tarin, J. J., Winston, R. M. and Hughes, M. R.** (1992). Birth of a normal girl after in vitro fertilization and preimplantation diagnostic testing for cystic fibrosis. *N Engl J Med* **327**, 905-909.
- Hanna, J., Cheng, A. W., Saha, K., Kim, J., Lengner, C. J., Soldner, F., Cassady, J. P., Muffat, J., Carey, B. W. and Jaenisch, R.** (2010). Human embryonic stem cells with biological and epigenetic characteristics similar to those of mouse ESCs. *Proc Natl Acad Sci U S A* **107**, 9222-9227.
- Hardy, K., Martin, K. L., Leese, H. J., Winston, R. M. L. and Handyside, A. H.** (1990). Human preimplantation development in vitro is not adversely affected by biopsy at the 8-cell stage. *Hum Reprod* **5**, 708-714.
- Hassani, S. N., Totonchi, M., Gourabi, H., Scholer, H. R. and Baharvand, H.** (2014). Signaling roadmap modulating naive and primed pluripotency. *Stem Cells Dev* **23**, 193-208.
- Hirate, Y., Cockburn, K., Rossant, J. and Sasaki, H.** (2012). Tead4 is constitutively nuclear, while nuclear vs. cytoplasmic Yap distribution is regulated in preimplantation mouse embryos. *Proc Natl Acad Sci U S A* **109**, E3389-3390; author reply E3391-3382.

- Hirate, Y., Hirahara, S., Inoue, K., Suzuki, A., Alarcon, V. B., Akimoto, K., Hirai, T., Hara, T., Adachi, M., Chida, K., et al.** (2013). Polarity-dependent distribution of angiominin localizes Hippo signaling in preimplantation embryos. *Curr Biol* **23**, 1181-1194.
- Houliston, E., Pickering, S. J. and Maro, B.** (1989). Alternative routes for the establishment of surface polarity during compaction of the mouse embryo. *Dev Biol* **134**, 342-350.
- Hoyos, B., Acin-Perez, R., Fischman, D. A., Manfredi, G. and Hammerling, U.** (2012). Hiding in plain sight: uncovering a new function of vitamin A in redox signaling. *Biochim Biophys Acta* **1821**, 241-247.
- Jones, N., Hardy, W. R., Friese, M. B., Jorgensen, C., Smith, M. J., Woody, N. M., Burden, S. J. and Pawson, T.** (2007). Analysis of a Shc family adaptor protein, ShcD/Shc4, that associates with muscle-specific kinase. *Molecular and Cellular Biology* **27**, 4759-4773.
- Kang, M., Garg, V. and Hadjantonakis, A. K.** (2017). Lineage establishment and progression within the inner cell mass of the mouse blastocyst requires FGFR1 and FGFR2. *Dev Cell* **41**, 496-510 e495.
- Kang, M., Piliszek, A., Artus, J. and Hadjantonakis, A. K.** (2013). FGF4 is required for lineage restriction and salt-and-pepper distribution of primitive endoderm factors but not their initial expression in the mouse. *Development* **140**, 267-279.
- Keller, G.** (2005). Embryonic stem cell differentiation: emergence of a new era in biology and medicine. *Genes & Development* **19**, 1129-1155.
- Kidder, G. M. and McLachlin, J. R.** (1985). Timing of transcription and protein synthesis underlying morphogenesis in preimplantation mouse embryos. *Dev Biol* **112**, 265-275.
- Korotkevich, E., Niwayama, R., Courtois, A., Friese, S., Berger, N., Buchholz, F. and Hiiragi, T.** (2017). The apical domain is required and sufficient for the first lineage segregation in the mouse embryo. *Dev Cell* **40**, 235-247 e237.
- Krawchuk, D., Honma-Yamanaka, N., Anani, S. and Yamanaka, Y.** (2013). FGF4 is a limiting factor controlling the proportions of primitive endoderm and epiblast in the ICM of the mouse blastocyst. *Dev Biol* **384**, 65-71.
- Kuijk, E. W., van Tol, L. T., Van de Velde, H., Wubbolts, R., Welling, M., Geijsen, N. and Roelen, B. A.** (2012). The roles of FGF and MAP kinase signaling in the segregation of the epiblast and hypoblast cell lineages in bovine and human embryos. *Development* **139**, 871-882.
- Kunath, T., Arnaud, D., Uy, G. D., Okamoto, I., Chureau, C., Yamanaka, Y., Heard, E., Gardner, R. L., Avner, P. and Rossant, J.** (2005). Imprinted X-inactivation

in extra-embryonic endoderm cell lines from mouse blastocysts. *Development* **132**, 1649-1661.

Laflamme, M. A., Chen, K. Y., Naumova, A. V., Muskheli, V., Fugate, J. A., Dupras, S. K., Reinecke, H., Xu, C., Hassanipour, M., Police, S., et al. (2007).

Cardiomyocytes derived from human embryonic stem cells in pro-survival factors enhance function of infarcted rat hearts. *Nat Biotechnol* **25**, 1015-1024.

Lai, K. M. and Pawson, T. (2000). The ShcA phosphotyrosine docking protein sensitizes cardiovascular signaling in the mouse embryo. *Genes Dev* **14**, 1132-1145.

Le Bin, G. C., Munoz-Descalzo, S., Kurowski, A., Leitch, H., Lou, X., Mansfield, W., Etienne-Dumeau, C., Grabole, N., Mulas, C., Niwa, H., et al. (2014). Oct4 is required for lineage priming in the developing inner cell mass of the mouse blastocyst. *Development* **141**, 1001-1010.

Lee, D. R., Lee, J. E., Yoon, H. S., Roh, S. I. and Kim, M. K. (2001). Compaction in preimplantation mouse embryos is regulated by a cytoplasmic regulatory factor that alters between 1- and 2-cell stages in a concentration-dependent manner. *Journal of Experimental Zoology* **290**, 61-71.

Lemmon, M. A. and Schlessinger, J. (2010). Cell Signaling by Receptor Tyrosine Kinases. *Cell* **141**, 1117-1134.

Leung, C. Y. and Zernicka-Goetz, M. (2013). Angiomotin prevents pluripotent lineage differentiation in mouse embryos via Hippo pathway-dependent and -independent mechanisms. *Nat Commun* **4**, 2251.

Leung, C. Y., Zhu, M. and Zernicka-Goetz, M. (2016). Polarity in cell-fate acquisition in the early mouse embryo. *Curr Top Dev Biol* **120**, 203-234.

Lokken, A. A. and Ralston, A. (2016). The Genetic Regulation of Cell Fate During Preimplantation Mouse Development. *Curr Top Dev Biol* **120**, 173-202.

Madan, P., Rose, K. and Watson, A. J. (2007). Na/K-ATPase beta1 subunit expression is required for blastocyst formation and normal assembly of trophectoderm tight junction-associated proteins. *J Biol Chem* **282**, 12127-12134.

Martin, G. R. (1981). Isolation of a pluripotent cell line from early mouse embryos cultured in medium conditioned by teratocarcinoma stem cells. *Proc Natl Acad Sci USA* **78**, 7634-7638.

Martin, G. R. and Evans, M. J. (1975). Differentiation of clonal lines of teratocarcinoma cells: formation of embryoid bodies in vitro. *Proc Natl Acad Sci USA* **72**, 1441-1445.

- Meilhac, S. M., Adams, R. J., Morris, S. A., Danckaert, A., Le Garrec, J. F. and Zernicka-Goetz, M.** (2009). Active cell movements coupled to positional induction are involved in lineage segregation in the mouse blastocyst. *Dev Biol* **331**, 210-221.
- Ménézo, Y. J. R. and Hérubel, F.** (2002). Mouse and bovine models for human IVF. *Reprod Biomed Online* **4**, 170-175.
- Migliaccio, E., Giorgio, M., Mele, S., Pelicci, G., Reboldi, P., Pandolfi, P. P., Lanfrancone, L. and Pelicci, P. G.** (1999). The p66shc adaptor protein controls oxidative stress response and life span in mammals. *Nature* **402**, 309-313.
- Migliaccio, E., Mele, S., Salcini, A. E., Pelicci, G., Lai, K. M., Superti-Furga, G., Pawson, T., Di Fiore, P. P., Lanfrancone, L. and Pelicci, P. G.** (1997). Opposite effects of the p52shc/p46shc and p66shc splicing isoforms on the EGF receptor-MAP kinase-*fos* signalling pathway. *EMBO J* **16**, 706-716.
- Molotkov, A., Mazot, P., Brewer, J. R., Cinalli, R. M. and Soriano, P.** (2017). Distinct requirements for FGFR1 and FGFR2 in primitive endoderm development and exit from pluripotency. *Dev Cell* **41**, 511-526 e514.
- Morris, S. A., Graham, S. J., Jedrusik, A. and Zernicka-Goetz, M.** (2013). The differential response to Fgf signalling in cells internalized at different times influences lineage segregation in preimplantation mouse embryos. *Open Biol* **3**, 130104.
- Morris, S. A., Teo, R. T., Li, H., Robson, P., Glover, D. M. and Zernicka-Goetz, M.** (2010). Origin and formation of the first two distinct cell types of the inner cell mass in the mouse embryo. *Proc Natl Acad Sci U S A* **107**, 6364-6369.
- Murry, C. E. and Keller, G.** (2008). Differentiation of embryonic stem cells to clinically relevant populations: lessons from embryonic development. *Cell* **132**, 661-680.
- Naito, A. T., Shiojima, I., Akazawa, H., Hidaka, K., Morisaki, T., Kikuchi, A. and Komuro, I.** (2006). Developmental stage-specific biphasic roles of Wnt/beta-catenin signaling in cardiomyogenesis and hematopoiesis. *Proc Natl Acad Sci U S A* **103**, 19812-19817.
- Nakano, T., Kodama, H. and Honjo, T.** (1994). Generation of lymphohematopoietic cells from embryonic stem cells in culture. *Science* **265**, 1098-1101.
- Nemoto, S., Combs, C. A., French, S., Ahn, B. H., Fergusson, M. M., Balaban, R. S. and Finkel, T.** (2006). The mammalian longevity-associated gene product p66shc regulates mitochondrial metabolism. *J Biol Chem* **281**, 10555-10560.

- Niakan, K. K. and Eggan, K.** (2013). Analysis of human embryos from zygote to blastocyst reveals distinct gene expression patterns relative to the mouse. *Dev Biol* **375**, 54-64.
- Niakan, K. K., Schrode, N., Cho, L. T. and Hadjantonakis, A. K.** (2013). Derivation of extraembryonic endoderm stem (XEN) cells from mouse embryos and embryonic stem cells. *Nat Protoc* **8**, 1028-1041.
- Nichols, J., Silva, J., Roode, M. and Smith, A.** (2009). Suppression of Erk signalling promotes ground state pluripotency in the mouse embryo. *Development* **136**, 3215-3222.
- Nichols, J. and Smith, A.** (2009). Naive and primed pluripotent states. *Cell Stem Cell* **4**, 487-492.
- Nichols, J., Zevnik, B., Anastassiadis, K., Niwa, H., Klewe-Nebenius, D., Chambers, I., Scholer, H. and Smith, A.** (1998). Formation of pluripotent stem cells in the mammalian embryo depends on the POU transcription factor Oct4. *Cell* **95**, 379-391.
- Nishikawa, S., Nishikawa, S., Hirashima, M., Matsuyoshi, N. and Kodama, H.** (1998). Progressive lineage analysis by cell sorting and culture identifies FLK1(+)VE-cadherin(+) cells at a diverging point of endothelial and hemopoietic lineages. *Development* **125**, 1747-1757.
- Nishioka, N., Inoue, K., Adachi, K., Kiyonari, H., Ota, M., Ralston, A., Yabuta, N., Hirahara, S., Stephenson, R. O., Ogonuki, N., et al.** (2009). The Hippo signaling pathway components Lats and Yap pattern Tead4 activity to distinguish mouse trophectoderm from inner cell mass. *Dev Cell* **16**, 398-410.
- Nishioka, N., Yamamoto, S., Kiyonari, H., Sato, H., Sawada, A., Ota, M., Nakao, K. and Sasaki, H.** (2008). Tead4 is required for specification of trophectoderm in pre-implantation mouse embryos. *Mech Dev* **125**, 270-283.
- Offenberg, H., Barcroft, L. C., Caveney, A., Viuff, D., Thomsen, P. D. and Watson, A. J.** (2000). mRNAs encoding aquaporins are present during murine preimplantation development. *Molecular Reproduction and Development* **57**, 323-330.
- Okada, S., Kao, A. W., Ceresa, B. P., Blaikie, P., Margolis, B. and Pessin, J. E.** (1997). The 66-kDa Shc isoform Is a negative regulator of the epidermal growth factor-stimulated mitogen-activated protein kinase pathway. *Journal of Biological Chemistry* **272**, 28042-28049.
- Orsini, F., Migliaccio, E., Moroni, M., Contursi, C., Raker, V. A., Piccini, D., Martin-Padura, I., Pelliccia, G., Trinei, M., Bono, M., et al.** (2004). The life span determinant p66Shc localizes to mitochondria where it associates with

mitochondrial heat shock protein 70 and regulates trans-membrane potential. *J Biol Chem* **279**, 25689-25695.

- Papadimou, E., Moiana, A., Goffredo, D., Koch, P., Bertuzzi, S., Brustle, O., Cattaneo, E. and Conti, L.** (2009). p66(ShcA) adaptor molecule accelerates ES cell neural induction. *Mol Cell Neurosci* **41**, 74-84.
- Pey, R., Vial, C., Schatten, G. and Hafner, M.** (1998). Increase of intracellular Ca²⁺ and relocation of E-cadherin during experimental decompaction of mouse embryos. *Proc Natl Acad Sci U S A* **95**, 12977-12982.
- Pinton, P., Rimessi, A., Marchi, S., Orsini, F., Migliaccio, E., Giorgio, M., Contursi, C., Minucci, S., Mantovani, F., Wieckowski, M. R., et al.** (2007). Protein kinase C beta and prolyl isomerase 1 regulate mitochondrial effects of the life-span determinant p66Shc. *Science* **315**, 659-663.
- Piotrowska-Nitsche, K., Perea-Gomez, A., Haraguchi, S. and Zernicka-Goetz, M.** (2005). Four-cell stage mouse blastomeres have different developmental properties. *Development* **132**, 479-490.
- Plusa, B., Piliszek, A., Frankenberg, S., Artus, J. and Hadjantonakis, A. K.** (2008). Distinct sequential cell behaviours direct primitive endoderm formation in the mouse blastocyst. *Development* **135**, 3081-3091.
- Quinn, P. and Horstman, F. C.** (1998). Is the mouse a good model for the human with respect to the development of the preimplantation embryo in vitro? *Hum Reprod* **13**, 173-183.
- Ramsey, J. J., Tran, D., Giorgio, M., Griffey, S. M., Koehne, A., Laing, S. T., Taylor, S. L., Kim, K., Cortopassi, G. A., Lloyd, K. C., et al.** (2014). The influence of Shc proteins on life span in mice. *J Gerontol A Biol Sci Med Sci* **69**, 1177-1185.
- Rayon, T., Menchero, S., Nieto, A., Xenopoulos, P., Crespo, M., Cockburn, K., Canon, S., Sasaki, H., Hadjantonakis, A. K., de la Pompa, J. L., et al.** (2014). Notch and hippo converge on Cdx2 to specify the trophoctoderm lineage in the mouse blastocyst. *Dev Cell* **30**, 410-422.
- Rea, S. and Johnson, T. E.** (2003). A metabolic model for life span determination in *Caenorhabditis elegans*. *Developmental Cell* **5**, 197-203.
- Ren, K., Li, X., Yan, J., Huang, G., Zhou, S., Yang, B., Ma, X. and Lu, C.** (2014). Knockdown of p66Shc by siRNA injection rescues arsenite-induced developmental retardation in mouse preimplantation embryos. *Reprod Toxicol* **43**, 8-18.
- Saiz, N., Grabarek, J. B., Sabherwal, N., Papalopulu, N. and Plusa, B.** (2013). Atypical protein kinase C couples cell sorting with primitive endoderm maturation in the mouse blastocyst. *Development* **140**, 4311-4322.

- Schrode, N., Saiz, N., Di Talia, S. and Hadjantonakis, A. K.** (2014). GATA6 levels modulate primitive endoderm cell fate choice and timing in the mouse blastocyst. *Dev Cell* **29**, 454-467.
- Shimizu, T., Ueda, J., Ho, J. C., Iwasaki, K., Poellinger, L., Harada, I. and Sawada, Y.** (2012). Dual inhibition of Src and GSK3 maintains mouse embryonic stem cells, whose differentiation is mechanically regulated by Src signaling. *Stem Cells* **30**, 1394-1404.
- Slack, J. M. W.** (2006). *Essential developmental biology* (2nd edn): Blackwell Publishing Ltd.
- Smith, S. M., Bajpai, R. and Minoo, P.** (2016). The p66Shc Adapter Protein Is Necessary to Maintain Pluripotency. In *B52. NEONATAL LUNG DISEASE: FROM BENCH TO BABIES*, pp. A3857-A3857.
- Soliman, M. A., Abdel Rahman, A. M., Lamming, D. W., Birsoy, K., Pawling, J., Frigolet, M. E., Lu, H., Fantus, I. G., Pasculescu, A., Zheng, Y., et al.** (2014). The adaptor protein p66Shc inhibits mTOR-dependent anabolic metabolism. *Sci Signal* **7**, ra17.
- Strumpf, D., Mao, C. A., Yamanaka, Y., Ralston, A., Chawengsaksophak, K., Beck, F. and Rossant, J.** (2005). Cdx2 is required for correct cell fate specification and differentiation of trophoblast in the mouse blastocyst. *Development* **132**, 2093-2102.
- Suwinska, A., Czolowska, R., Ozdzenski, W. and Tarkowski, A. K.** (2008). Blastomeres of the mouse embryo lose totipotency after the fifth cleavage division: expression of Cdx2 and Oct4 and developmental potential of inner and outer blastomeres of 16- and 32-cell embryos. *Dev Biol* **322**, 133-144.
- Tabansky, I., Lenarcic, A., Draft, R. W., Loulier, K., Keskin, D. B., Rosains, J., Rivera-Feliciano, J., Lichtman, J. W., Livet, J., Stern, J. N., et al.** (2013). Developmental bias in cleavage-stage mouse blastomeres. *Curr Biol* **23**, 21-31.
- Tada, S., Era, T., Furusawa, C., Sakurai, H., Nishikawa, S., Kinoshita, M., Nakao, K., Chiba, T. and Nishikawa, S.** (2005). Characterization of mesendoderm: a diverging point of the definitive endoderm and mesoderm in embryonic stem cell differentiation culture. *Development* **132**, 4363-4374.
- Takahashi, K. and Yamanaka, S.** (2006). Induction of pluripotent stem cells from mouse embryonic and adult fibroblast cultures by defined factors. *Cell* **126**, 663-676.
- Tanaka, S., Kunath, T., Hadjantonakis, A.-K., Nagy, A. and Rossant, J.** (1998). Promotion of trophoblast stem cell proliferation by FGF4. *Science* **282**, 2072-2075.

- Tarkowski, A. K., Suwinska, A., Czolowska, R. and Ozdzanski, W.** (2010). Individual blastomeres of 16- and 32-cell mouse embryos are able to develop into fetuses and mice. *Dev Biol* **348**, 190-198.
- Tesar, P. J., Chenoweth, J. G., Brook, F. A., Davies, T. J., Evans, E. P., Mack, D. L., Gardner, R. L. and McKay, R. D.** (2007). New cell lines from mouse epiblast share defining features with human embryonic stem cells. *Nature* **448**, 196-199.
- Theunissen, T. W., Powell, B. E., Wang, H., Mitalipova, M., Faddah, D. A., Reddy, J., Fan, Z. P., Maetzel, D., Ganz, K., Shi, L., et al.** (2014). Systematic identification of culture conditions for induction and maintenance of naive human pluripotency. *Cell Stem Cell* **15**, 471-487.
- Thomson, J. A., Itskovitz-Eldor, J., Shapiro, S. S., Waknitz, M. A., Swiergiel, J. J., Marshall, V. S. and Jones, J. M.** (1998). Embryonic stem cell lines derived from human blastocysts. *Science* **282**, 1145-1147.
- Tomilov, A. A., Ramsey, J. J., Hagopian, K., Giorgio, M., Kim, K. M., Lam, A., Migliaccio, E., Lloyd, K. C., Berniakovich, I., Prolla, T. A., et al.** (2011). The Shc locus regulates insulin signaling and adiposity in mammals. *Aging Cell* **10**, 55-65.
- Torres-Padilla, M. E., Parfitt, D. E., Kouzarides, T. and Zernicka-Goetz, M.** (2007). Histone arginine methylation regulates pluripotency in the early mouse embryo. *Nature* **445**, 214-218.
- Tramont, P., Zhang, L. and Ravichandran, K. S.** (2006). ShcA mediates the dominant pathway to extracellular signal-regulated kinase activation during early thymic development. *Mol Cell Biol* **26**, 9035-9044.
- Turco, M. Y., Furia, L., Dietze, A., Fernandez Diaz, L., Ronzoni, S., Sciallo, A., Simeone, A., Constam, D., Faretta, M. and Lanfrancone, L.** (2012). Cellular heterogeneity during embryonic stem cell differentiation to epiblast stem cells is revealed by the ShcD/RaLP adaptor protein. *Stem Cells* **30**, 2423-2436.
- van den Brink, S. C., Baillie-Johnson, P., Balayo, T., Hadjantonakis, A. K., Nowotschin, S., Turner, D. A. and Martinez Arias, A.** (2014). Symmetry breaking, germ layer specification and axial organisation in aggregates of mouse embryonic stem cells. *Development* **141**, 4231-4242.
- Ventura, A., Luzi, L., Pacini, S., Baldari, C. T. and Pelicci, P. G.** (2002). The p66Shc longevity gene is silenced through epigenetic modifications of an alternative promoter. *J Biol Chem* **277**, 22370-22376.
- Vikram, A., Kim, Y. R., Kumar, S., Naqvi, A., Hoffman, T. A., Kumar, A., Miller, F. J., Jr., Kim, C. S. and Irani, K.** (2014). Canonical Wnt Signaling Induces Vascular Endothelial Dysfunction via p66Shc-Regulated Reactive Oxygen Species. *Arterioscler Thromb Vasc Biol*.

- Vodyanik, M. A., Bork, J. A., Thomson, J. A. and Slukvin, II** (2005). Human embryonic stem cell-derived CD34+ cells: efficient production in the coculture with OP9 stromal cells and analysis of lymphohematopoietic potential. *Blood* **105**, 617-626.
- Warmflash, A., Sorre, B., Etoc, F., Siggia, E. D. and Brivanlou, A. H.** (2014). A method to recapitulate early embryonic spatial patterning in human embryonic stem cells. *Nat Methods* **11**, 847-854.
- White, M. D., Bissiere, S., Alvarez, Y. D. and Plachta, N.** (2016). Mouse embryo compaction. *Curr Top Dev Biol* **120**, 235-258.
- Wicklow, E., Blij, S., Frum, T., Hirate, Y., Lang, R. A., Sasaki, H. and Ralston, A.** (2014). HIPPO pathway members restrict SOX2 to the inner cell mass where it promotes ICM fates in the mouse blastocyst. *PLoS Genet* **10**, e1004618.
- Wills, Melanie K. B. and Jones, N.** (2012). Teaching an old dogma new tricks: twenty years of Shc adaptor signalling. *Biochemical Journal* **447**, 1-16.
- Winkel, G. K., Ferguson, J. E., Takeichi, M. and Nuccitelli, R.** (1990). Activation of protein kinase C triggers premature compaction in the four-cell stage mouse embryo. *Dev Biol* **138**, 1-15.
- Yagi, R., Kohn, M. J., Karavanova, I., Kaneko, K. J., Vullhorst, D., DePamphilis, M. L. and Buonanno, A.** (2007). Transcription factor TEAD4 specifies the trophoblast lineage at the beginning of mammalian development. *Development* **134**, 3827-3836.
- Yamanaka, Y., Lanner, F. and Rossant, J.** (2010). FGF signal-dependent segregation of primitive endoderm and epiblast in the mouse blastocyst. *Development* **137**, 715-724.
- Yamanaka, Y., Ralston, A., Stephenson, R. O. and Rossant, J.** (2006). Cell and molecular regulation of the mouse blastocyst. *Dev Dyn* **235**, 2301-2314.
- Ying, Q. L., Stavridis, M., Griffiths, D., Li, M. and Smith, A.** (2003). Conversion of embryonic stem cells into neuroectodermal precursors in adherent monoculture. *Nat Biotechnol* **21**, 183-186.
- Zhang, C., Liu, C., Li, D., Yao, N., Yuan, X., Yu, A., Lu, C. and Ma, X.** (2010). Intracellular redox imbalance and extracellular amino acid metabolic abnormality contribute to arsenic-induced developmental retardation in mouse preimplantation embryos. *J Cell Physiol* **222**, 444-455.
- Zhang, L., Camerini, V., Bender, T. P. and Ravichandran, K. S.** (2002). A nonredundant role for the adapter protein Shc in thymic T cell development. *Nat Immunol* **3**, 749-755.

Chapter 2

2 P66Shc is expressed in mouse preimplantation embryos and is dysregulated by mouse embryo culture

A version of this chapter has been published:

Edwards, N.A., Watson, A.J., Betts, D.H. (2016) P66Shc, a key regulator of metabolism and mitochondrial ROS production, is dysregulated by mouse embryo culture. *Molecular Human Reproduction*. 22(9): 634-647.

Reproduced here with permission from Oxford University Press.

2.1 Introduction

In assisted reproductive technologies (ART), embryo culture routinely follows *in vitro* fertilization (IVF) to permit growth to the blastocyst stage. Despite improvements in culture medium formulations and the use of physiological oxygen environments, the rate of successful pregnancy after embryo culture remains low. In 2014, the average live birth rate per IVF cycle for women in Canada was 23% (CFAS, 2015). Low success rates may be due to exposure of the preimplantation embryo to stresses introduced by the artificial culture environment (Feuer and Rinaudo, 2012; Wale and Gardner, 2016). The mammalian preimplantation embryo may adapt to these adverse culture conditions. However, these stress induced responses can result in major changes to gene expression, epigenetic modifications, and cellular metabolism (de Waal et al., 2014; Rinaudo and Schultz, 2004; Wale and Gardner, 2012). These changes are currently undetectable according to non-invasive morphological assessment methods, and thus embryos selected by morphology for transfer may still not be the most developmentally competent. This is a particular concern in current efforts to reduce multiple pregnancies by performing single embryo transfer (Grady et al., 2012).

To further advance embryo culture and optimize culture parameters, it is important to understand the biological mechanisms of the preimplantation embryo and its interactions with the reproductive tract environment *in vivo* and the culture environment *in vitro*. Metabolism has emerged as an important research avenue in efforts to understand how culture conditions affect the developmental competence of early embryos (Gardner et al., 2001; Seli et al., 2010; Wale and Gardner, 2013). Modulating oxygen tension during embryo culture alters glucose metabolism, demonstrating that the culture atmosphere can dramatically influence embryo metabolism and subsequent viability (Wale and Gardner, 2012). This may affect the later stages of development in particular, as the trophoctoderm must generate ATP to power the Na^+/K^+ ATPases and form the blastocoele cavity (Betts et al., 1998; Houghton et al., 2003). The adaptor protein p66Shc is responsive to oxygen tension and is involved in the bovine embryo's oxidative stress response by promoting permanent embryo arrest and apoptosis under adverse environmental conditions (Betts et al., 2014; Favetta et al., 2007a). P66Shc is a member of the Shc1 family of adaptor

proteins with functions in growth factor receptor signalling, reactive oxygen species (ROS) production, and oxidative phosphorylation metabolism (Acin-Perez et al., 2010; Migliaccio et al., 1999; Migliaccio et al., 1997; Nemoto et al., 2006). Loss-of-function studies in mouse embryonic fibroblasts (MEFs) and more recently in HeLa cells provide evidence that p66Shc is involved in ATP production by oxidative phosphorylation (Nemoto et al., 2006; Soliman et al., 2014). Dysregulated p66Shc function in the mammalian embryo may therefore not only negatively impact development through high ROS production inducing embryo arrest or apoptosis (Betts et al., 2014; Favetta et al., 2007a; Favetta et al., 2007b), but also may affect cellular metabolism (Favetta et al., 2007a).

To define a new metabolic route through which preimplantation embryo culture may affect early embryonic development, the objective of our study was to determine if p66Shc expression changes in cultured embryos compared to *in vivo* derived embryos, and if altered p66Shc expression is a marker of altered embryo metabolism. In the following study, we use a well-defined preimplantation mouse embryo culture model to modulate atmospheric conditions (oxygen) and culture media (glucose concentration) to determine their effects on p66Shc expression and readouts of oxidative phosphorylation metabolism. Our results demonstrate that preimplantation developmental variations in p66Shc expression observed *in vivo* are further exacerbated by culture and correlate with aberrant mitochondrial ATP and ROS production.

2.2 Materials and Methods

2.2.1 Animal Source and Ethical Approval

Experimental protocols were approved by the Canadian Council of Animal Care and the University of Western Ontario Animal Care and Veterinary Services (Watson #2010-021). Female and male CD1 mice were obtained from Charles River Canada (St-Constant, Quebec, Canada). Mice were housed in the conventional manner, with a 12h light/dark cycle and access to food and water *ad libitum*. For all experiments, mice were euthanized by CO₂ asphyxiation.

2.2.2 Embryo Collection and Culture

Three-to-four-week-old female mice were injected i.p. with 7.5 IU pregnant mare's serum gonadotrophin (Merck Animal Health, Canada) followed by injection of 7.5 IU hCG (Merck Animal Health, Canada) 48 hours later. Female mice were then placed with males for mating. Confirmation of mating was determined by checking for the presence of a vaginal plug the next morning; presence of a vaginal plug indicated embryonic day 0.5 (E0.5). Embryos were flushed with M2 medium (Sigma Aldrich, Canada) from the oviducts and/or uteri of female mice according to the number of hours post injection (hpi): zygotes (18 hpi), 2-cell embryos (44 hpi), 8-cell embryos (68 hpi) and blastocysts (90 hpi). Zygotes were briefly incubated in M2 medium containing 1% hyaluronidase (Sigma Aldrich, Canada) to remove cumulus cells. Embryos were washed twice in M2, then transferred to Extraction Buffer or radioimmunoprecipitation assay buffer (RIPA buffer, 150 mM NaCl, 1% Triton X-100, 0.5% sodium deoxycholate, 0.1% SDS, 50 mM Tris) until analysis, or to pre-equilibrated KSOMaa (potassium simplex optimized media with amino acids) Evolve medium supplemented with 1% bovine serum albumin (Zenith Biotech, USA). Embryos were cultured under low (5% O₂) or high (in air: ~20%) oxygen tensions in a 5% CO₂, 37°C incubator. For glucose experiments, D- or L-glucose (Sigma Aldrich, Canada) was added to KSOMaa Evolve to the desired concentration and embryos were cultured under low oxygen. For transcriptional inhibition experiments, 10 mg/ml α -amanitin (Sigma Aldrich, Canada) in water was diluted to 10 μ g/ml in KSOMaa Evolve.

2.2.3 Real time RT-qPCR

Pools of twenty embryos collected from 1-3 mice were stored in Extraction Buffer (Life Technologies, USA) at -80°C until use. Total RNA was extracted using the PicoPure RNA isolation kit (Life Technologies, USA) according to the manufacturer's guidelines. For glucose treatment experiments, 0.5 μ g of exogenous luciferase mRNA (Promega, USA) was added to the extract prior to ethanol precipitation. Eluted RNA was reverse transcribed to cDNA using SuperScript III (Life Technologies, USA) according to manufacturer's instructions, with final concentrations of 150 ng random hexamers (Life Technologies, USA) and 2 pmol p66Shc-specific reverse primer (Table 2-1). Real time

quantitative RT-PCR (qRT-PCR) was performed in a CFX384 thermocycler (BioRad, Canada) with each reaction containing 7 μ l PerfeCTa SYBR Green 2X SuperMix (Quanta BioSciences, USA), 200 nM each of forward and reverse primers (see Table 2-1 for all primer sequences) and 4 μ l cDNA (equivalent to 0.25 embryo per reaction). PCR conditions are as follows: 95°C for 3 minutes, followed by 45 cycles of 95°C for 15 seconds, 59°C for 15 seconds, and 72°C for 30 seconds. Relative transcript abundance was determined using the delta-delta CT method using expression of *Ppia* (peptidylprolyl isomerase A) and *H2afz* (H2A Histone Family, Member Z), or luciferase, for normalization (Mamo et al., 2007). To determine amplification specificity after PCR amplification of p66Shc in blastocyst cDNA, PCR products were purified using the PureLink Quick Gel Extraction and PCR Purification Kit (Life Technologies, USA) according to manufacturer's instructions. PCR products were sequenced by the Robarts Research Institute DNA Sequencing Facility (London, Ontario, Canada). Amplified p66Shc PCR products displayed 96% sequence identity to *Mus musculus* src homology 2 domain-containing transforming protein C1 (Shc1), transcript variant 1 (NM_001113331.2) after BLAST analysis (NCBI database), indicating specific amplification of the p66Shc isoform.

2.2.4 Western Blot Analysis

Pools of 30-50 embryos collected from 2-4 mice were stored in RIPA buffer containing protease and phosphatase inhibitor cocktails (Millipore, USA) at -80°C until use. Total protein lysates were resolved on a 4-12% Bis-Tris gel (Life Technologies) and transferred to a polyvinylidene difluoride membrane (PVDF: Millipore, USA). Membranes were blocked in 5% skim milk or 5% bovine serum albumin in TBS with 0.1% Tween-20 (TBST, Sigma Aldrich) for 1 hour at room temperature, followed by overnight incubation in primary antibody at the indicated concentration at 4°C. Primary antibodies used were: anti NT-Shc (Acris Antibodies, USA, 1:100), anti-(phospho S36) p66Shc (Abcam, USA, 1:100), anti-(phospho Y239/Y240) p66Shc (Cell Signaling Technologies, USA, 1:500), and horse-radish peroxidase (HRP)-conjugated anti β -actin (Sigma Aldrich, Canada, 1:20,000). Membranes were then incubated in HRP-conjugated secondary antibody (Jackson Laboratories, USA). Membranes were visualized by detection of Forte enhanced

Table 2-1. Oligonucleotide primer sequences.

Gene	Sequence	Product size
p66Shc R (reverse transcription)	5'-GGTGGATTCCTGAGATACTGTTT-3'	N/A
p66Shc (qPCR)	F: 5'-CCGACTACCCTGTGTTCCTTCTT-3' R: 5'-CCCATCTTCAGCAGCCTTCC-3'	111 bp
<i>Ppia</i>	F: 5'-GTCCTGGCATCTTGTCCATG-3' R: 5'-TGCCTTCTTTCACCTTCCCA-3'	126 bp
<i>H2afz</i>	F: 5'-CGCAGAGGTACTTGAGTTGG-3' R: 5'-TCTTCCCGATCAGCGATTTG-3'	176 bp
Luciferase	F: 5'-TTGACAAGGATGGATGGCTAC-3' R: 5'-TTCGGTACTTCGTCCACCAAAC-3'	336 bp

chemiluminescence (Millipore, USA). Densitometry analysis was performed in Image Lab 4.0 (BioRad, USA).

2.2.5 HT-22 culture and transfection

The HT-22 cell line (immortalized mouse hippocampal cells) and human p66Shc-HA expression plasmid were obtained from Dr. Robert Cumming (University of Western Ontario, London, Canada). Cells were cultured in DMEM supplemented with 10% fetal bovine serum and 1% penicillin/streptomycin (Life Technologies, USA), at 37°C and 5% CO₂ in air. Cells were transfected with the p66Shc-HA expression plasmid using Lipofectamine 3000 according to the manufacturer's protocol (Life Technologies, USA), fixed in 4% paraformaldehyde in PBS and processed for immunofluorescence and confocal microscopy.

2.2.6 Immunofluorescence and Confocal Microscopy

Embryos were fixed in 2% paraformaldehyde in PBS and permeabilized in 0.1% Triton X-100 in PBS (Sigma Aldrich, Canada) for 30 minutes. Fixed cells were blocked in 5% normal goat serum (Sigma Aldrich, Canada) for 1 hour at room temperature, followed by overnight incubation in primary antibody at the indicated concentration at 4°C. Primary antibodies used were: anti NT-Shc (Acris Antibodies, 1:100), anti phospho-S36-p66Shc (Abcam, 1:100), anti CDX2 (Abcam, 1:100), anti HA-Alexa 647 (Santa Cruz, USA, 1:50). Embryos were incubated in rabbit-anti-mouse Alexa 488 (Life Technologies) for 30 minutes, followed by incubation in goat-anti-rabbit Alexa 488 (Life Technologies) for signal amplification. For caudal type homeobox 2 (CDX2) immunoreactivity, embryos were incubated in goat-anti-rabbit Alexa 547 (Life Technologies). Cells were counterstained with 0.5 µg/ml DAPI (Sigma Aldrich, Canada) and mounted on a glass microscope slide in VectaShield antifade medium (Vector Laboratories, USA). Cells were imaged with a laser scanning confocal microscope (Zeiss LSM510). Laser settings were unchanged when detecting the same primary antibody.

2.2.7 ATP content assay

Pools of 5 blastocysts collected from individual mice after treatment under each oxygen tension group were transferred to 96-well plates containing KSOMaa Evolve. ATP content was measured using the Luminescent ATP Detection Assay Kit (Abcam, USA) according to manufacturer's guidelines. Luminescence was quantified using an eight-point ATP standard curve (0.78 pmol to 100 pmol) and normalized to blastocyst cell number.

2.2.8 MitoSOX superoxide staining

Blastocysts from each oxygen tension group were transferred to KSOMaa Evolve containing 5 μ M MitoSOX red mitochondrial superoxide indicator (Life Technologies, USA) and incubated for 1 hour at 37°C, 5% CO₂, 5% O₂ (*in vivo* and low oxygen groups) or in air (high oxygen groups). Blastocysts were transferred to a drop of PBS covered by embryo culture grade mineral oil (Zenith Biotech, USA) for imaging. Blastocysts were imaged using laser scanning confocal microscopy (Zeiss LSM510). Relative fluorescence was quantified by measuring the mean gray value in Image J (National Institutes of Health). Only blastocyst images with visible inner cell mass were quantified for fluorescence and compared between groups.

2.2.9 Blastocyst Cell Counts

Blastocysts were fixed in 4% paraformaldehyde in PBS, permeabilized in 0.2% Triton X-100 in PBS, and stained with DAPI for 1 hour at room temperature. Stained blastocysts were imaged using laser scanning confocal microscopy, with three z-stacks taken per embryo. DAPI-positive nuclei from three stacks were counted using ImageJ.

2.2.10 Statistical Analyses

Experiments were performed a minimum of three times using independent replicates with the indicated sample sizes. Statistical analyses were performed in Graph Pad Prism (6.0) for Student's t-test (unpaired, two-tailed, equal variance) or one-way analysis of variance (ANOVA) followed by Tukey's honestly significant difference (HSD) test to correct for multiple comparisons. Values presented in figures are the mean \pm the standard error of

the mean (SEM). Probability values less than 0.05 ($p < 0.05$) were considered statistically significant.

2.3 Results

2.3.1 P66Shc expression increases in blastocysts during mouse preimplantation development

P66Shc mRNA and protein have been previously detected in bovine (Favetta et al., 2004) and murine embryos (Ren et al., 2014), but an analysis of expression during the progression of mouse preimplantation development *in vivo* has not been carried out. To determine the expression profile of p66Shc during preimplantation development, we performed real time qRT-PCR and immunoblotting on pools of embryos from four developmental stages. P66Shc mRNA transcript and protein were detectable in all stages observed. We observed a significant increase in both transcript and protein abundance from the 8-cell to blastocyst stages. P66Shc mRNA or protein did not significantly change between the zygote and 8-cell stages (Fig. 2-1A, B; for uncropped immunoblot, see Fig. 2-2A). To determine the cellular localization of p66Shc during preimplantation development, we performed whole mount immunofluorescence followed by confocal microscopy using a p66Shc-specific antibody on embryos from six developmental stages. We observed p66Shc immunoreactivity throughout the cytoplasm of pre-compaction stage embryos (Fig. 2-3A-D), with restriction to the apical cell periphery of compacted 16 cell morulae (Fig. 2-3E). To determine if p66Shc localization is restricted to the trophectoderm lineage, we co-stained blastocysts with CDX2. Of all blastocysts observed, p66Shc showed detectable cell periphery localization in only CDX2 positive cells (Fig. 2-3F). P66Shc immunoreactivity was undetectable in CDX2 negative cells (Fig. 2-3F). These results indicate that p66Shc expression is normally upregulated in the blastocyst and may be restricted primarily to the trophectoderm of *in vivo* produced blastocysts.

2.3.2 Validation of NT-Shc antibody specificity

To verify that the antibodies used to detect p66Shc and phosphorylated (S36) p66Shc only recognized the 66-kDa Shc isoform by immunofluorescence confocal microscopy,

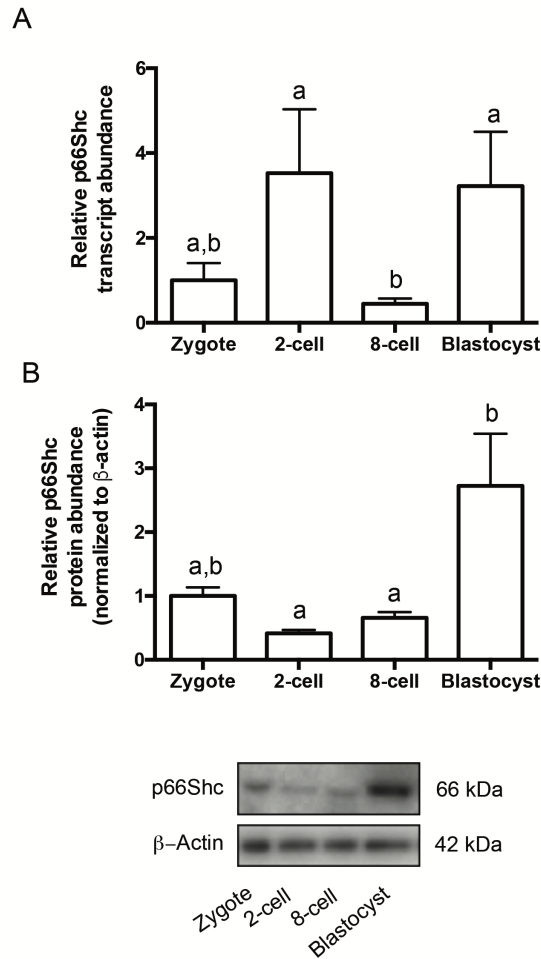


Figure 2-1. p66Shc expression increases during mouse preimplantation development *in vivo*.

A) Quantitative real time RT-PCR (qRT-PCR) for p66Shc relative transcript abundance was performed on three replicates of pools of 20 embryos per stage. P66Shc relative transcript abundance significantly increases from eight cell to blastocyst-stage embryos ($n=3$, mean \pm SEM, $p=0.0476$ 1W-ANOVA). (B) Immunoblotting for total p66Shc protein abundance was performed on three replicates of pools of 30-50 embryos per stage. P66Shc relative protein abundance increases from eight cell to blastocyst-stage embryos ($n=3$, mean \pm SEM, $p=0.0331$ one way-ANOVA). A representative blot is shown (for uncropped immunoblot, see Figure 2-2).

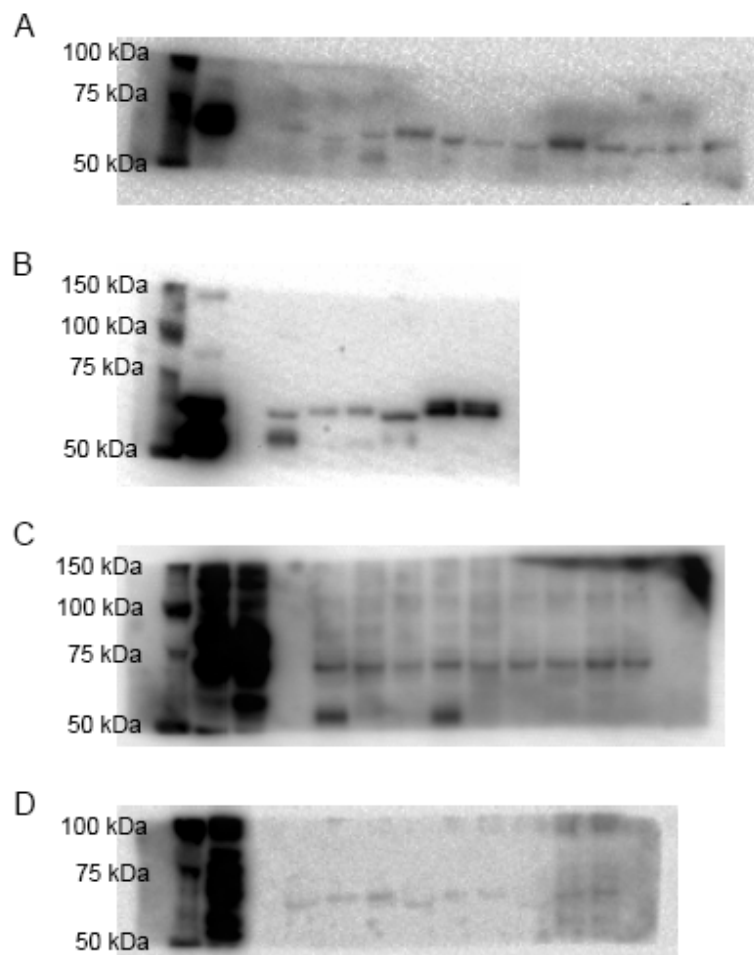


Figure 2-2. Full Western blots for anti-NT-Shc, anti-pSer36-p66Shc, and anti-pY239/Y240-Shc.

Positive control samples of 10 μ g whole mouse embryonic stem cell lysate were loaded right of the protein marker lane in all blots shown. Images shown are merged enhanced chemiluminescence (ECL) and protein marker (Cy5 fluorescence) performed in Image Lab. (A) Full immunoblot corresponding to the representative blot in Figure 1B between 50 and 100 kDa using anti-NT-Shc. (B) Full immunoblot corresponding to the representative blot in Figure 4A between 50 and 150 kDa using anti-NT-Shc. (C) Full immunoblot corresponding to the representative blot in Figure 4B between 50 and 150 kDa using anti-pSer36-p66Shc. (D) Full immunoblot corresponding to the representative blot in Figure 4C between 50 and 150 kDa using anti-pY239/Y240-Shc.

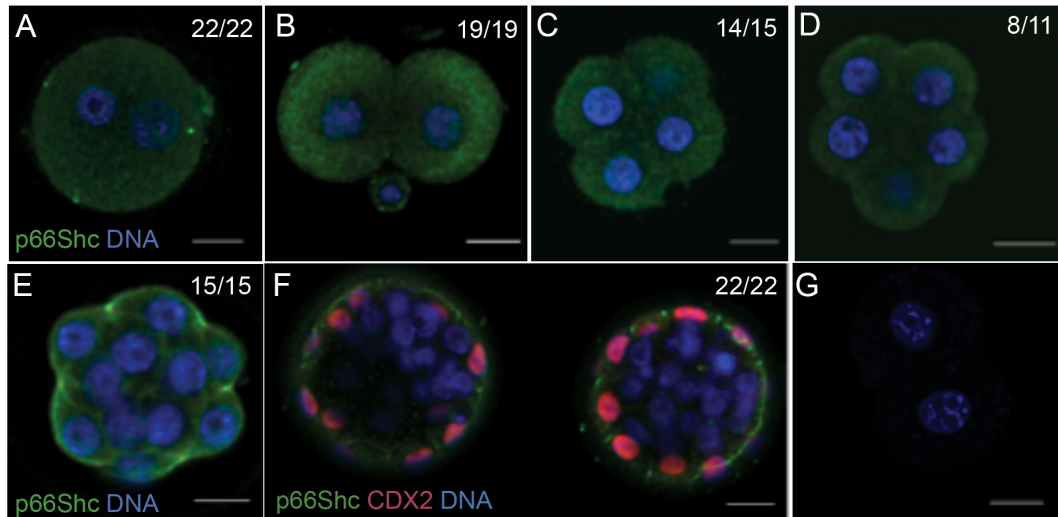


Figure 2-3. p66Shc progressively localizes to the cell periphery during mouse preimplantation development.

Immunofluorescence and confocal microscopy for p66Shc was performed on 10-20 embryos per stage. Representative confocal images are shown: (A) Zygote (B) 2-cell embryo (C) 4-cell embryo (D) 8-cell non-compacted embryo (E) 8-16 cell compacted morula (F) Blastocyst, counterstained for caudal type homeobox 2 (CDX2) (G) Primary antibody omitted. Green = p66Shc, Red = CDX2, Blue = DAPI. Scale bar = 20 μ m.

we cultured mature neurons known to have undetectable basal p66Shc expression (Ventura et al., 2002). We performed immunofluorescence using both antibodies on the mouse HT-22 hippocampal cell line. HT-22 cells transfected with a HA-tagged p66Shc DNA construct showed p66Shc and HA immunoreactivity, while non-transfected cells showed no detectable p66Shc or HA immunoreactivity (Fig. 2-4A). Transfected HT-22 cells also displayed phosphorylated S36 p66Shc and HA immunoreactivity compared to undetectable levels in non-transfected cells Fig. 2-4B). These results validate the use of these antibodies for immunofluorescent detection of p66Shc and S36-phosphorylated p66Shc cell localization in mouse preimplantation embryos.

2.3.3 P66Shc expression is sensitive to oxygen tension, but not glucose concentration, during embryo culture

Under *in vivo* conditions, p66Shc expression levels may be fine-tuned to prevent adverse developmental events. Given our observations within *in vivo* derived mouse embryos, we then aimed to determine whether certain embryo culture conditions induce aberrant changes in embryonic p66Shc expression levels. Mouse zygotes were cultured to the blastocyst stage under low oxygen tension (5% O₂) or high oxygen tension (21% O₂). Embryos cultured in low or high oxygen tensions in KSOMaa Evolve show comparable rates of blastocyst formation (Fig. 2-5A). However, blastocysts cultured in low oxygen have significantly increased cell numbers compared to flushed *in vivo*-derived blastocysts (Fig. 2-5B). Real time qRT-PCR was performed on pools of embryos to determine changes in p66Shc transcript abundance. Blastocysts examined after 96 hours of culture showed increasing p66Shc transcript abundance with increasing oxygen tension (Figure 2-6A). This increase was dependent on *de novo* transcription of p66Shc, as the increase in p66Shc abundance was abolished in blastocysts cultured at high oxygen tension in the presence of the transcriptional inhibitor α -amanitin (Figure 2-6B). It is interesting to note that some p66Shc transcripts were still detectable in treated blastocysts, suggesting that maternally stored p66Shc may still be present at the blastocyst stage (Figure 2-6B). Overall, these observations suggest that p66Shc is actively transcribed by the embryo under atmospheric oxygen conditions.

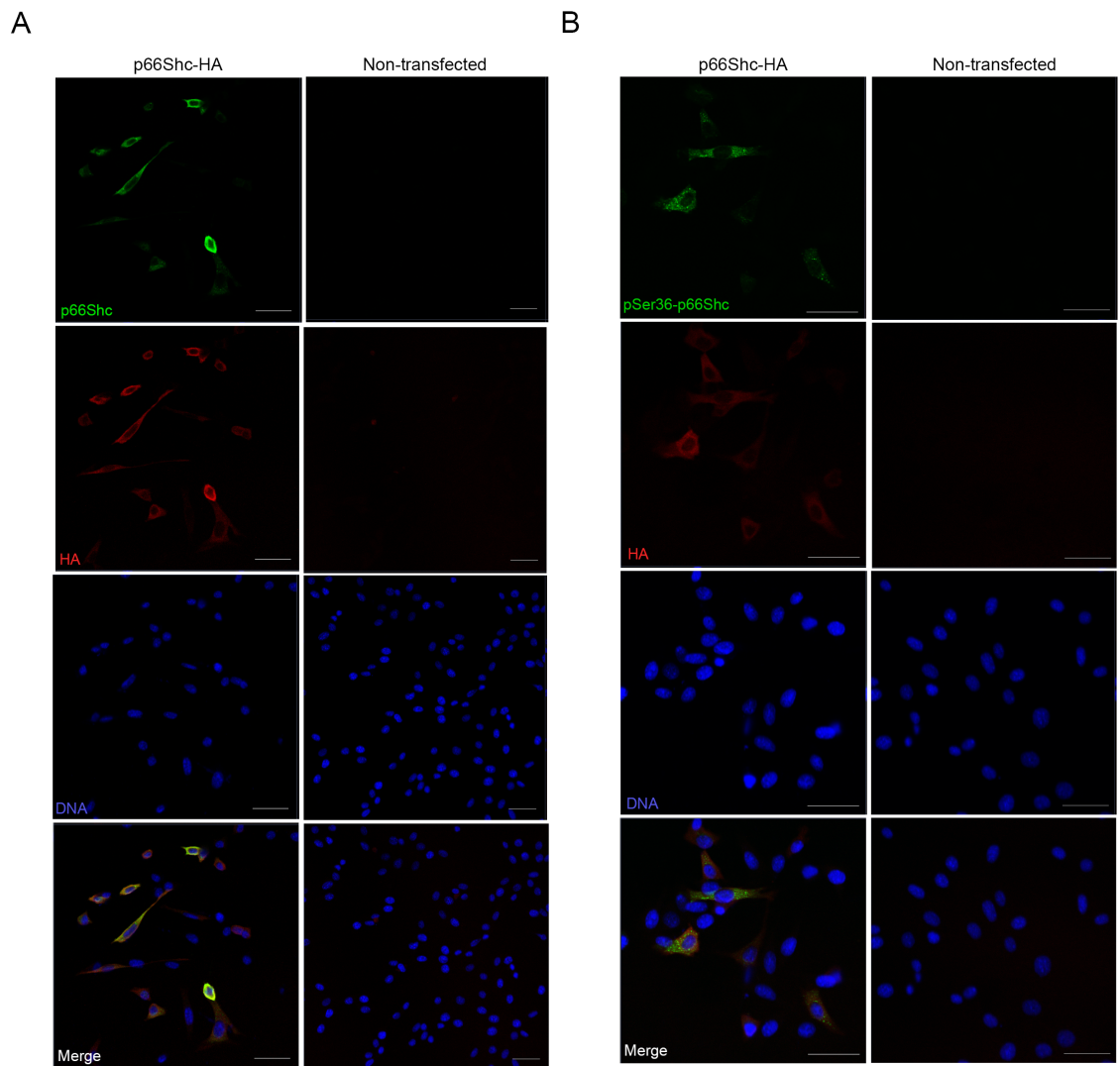


Figure 2-4. NT-Shc and phosphorylated S36 p66Shc antibody validation for immunofluorescence and confocal microscopy.

(A) Immunofluorescence and confocal microscopy images of p66Shc-HA transfected HT-22 cells (left) and non-transfected cells (right). Green = total p66Shc, Red = HA, Blue = DAPI. Scale bar = 50 μm . (B) Images of p66Shc-HA transfected HT-22 cells (left) and non-transfected cells (right). Green = pSer36-p66Shc, Red = HA, Blue = DAPI. Scale bar = 50 μm .

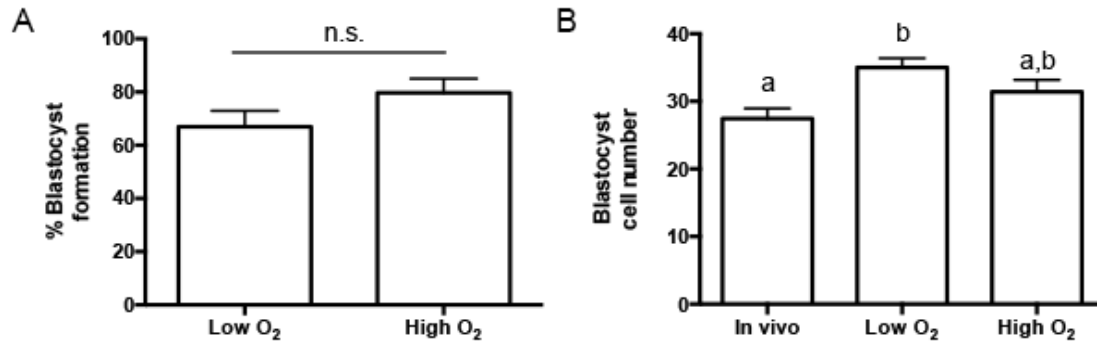


Figure 2-5. Developmental outcomes of embryos cultured in KSOMaa Evolve under low and high oxygen tensions.

(A) Percent blastocyst formation from the zygote stage does not significantly change between embryos cultured under low or high oxygen tension ($n=3$, mean \pm SEM, $p=0.1867$ Student's t-test). (B) Blastocyst cell number significantly increases in embryos cultured at low oxygen tension ($n=46$ in vivo, $n=31$ low oxygen, $n=30$ high oxygen, mean \pm SEM, $p=0.0022$ 1W-ANOVA).

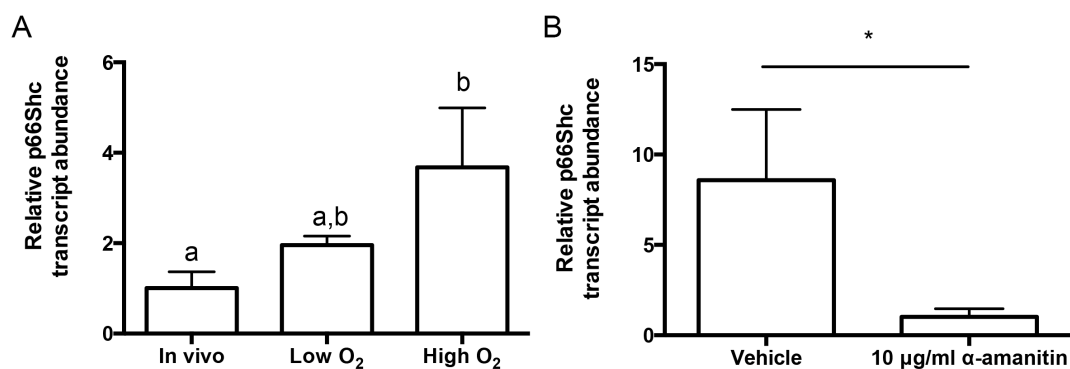


Figure 2-6. Culture and high oxygen tension increases the relative p66Shc mRNA abundance in mouse blastocysts.

(A) RT-qPCR for p66Shc was performed on four replicates of pools of 20 blastocysts. There is a significant increase in p66Shc mRNA abundance in blastocysts cultured at high oxygen tension compared to in vivo controls ($n=4$, mean \pm SEM, $p=0.0305$ one way-ANOVA). (B) Blastocysts cultured for 24h in 10 µg/ml α -amanitin showed significantly decreased p66Shc transcript abundance compared to controls ($n=3$, mean \pm SEM, $p=0.0477$ Student's t-test).

We next aimed to determine if p66Shc protein abundance also increased with increasing oxygen tension. Immunoblotting for total p66Shc on pools of embryos showed a significant increase in p66Shc protein abundance in cultured blastocysts compared to *in vivo* derived blastocysts (Fig. 2-7A). This induction of p66Shc expression was unique to the blastocyst stage, as p66Shc transcript abundance decreased and protein abundance was unchanged in cultured 2-cell and 8-cell embryos (Fig. 2-8A and B). We then saw that culture in both low and high oxygen tensions significantly decreased the ratio of phosphorylated S36 p66Shc to total p66Shc in blastocysts, suggesting a possible change in the mitochondrial fraction of p66Shc in cultured blastocysts (Fig. 2-7B) as serine-36 phosphorylation of p66Shc promotes Pin-1, isomerization, and ultimately p66Shc translocation to the mitochondria (Pinton et al., 2007). Oxygen tension did not alter the ratio of phosphorylated Y239/Y240 p66Shc to total p66Shc (Fig. 2-7C). These are two residues on Shc1 proteins that are known to be phosphorylated after interaction with receptor tyrosine kinases (Gotoh et al., 1997). This result suggests that the shift in the 66-kDa band seen in cultured blastocysts may be due to an alternative (e.g. Ser138, Y317) or novel post-translational modification induced by culture.

To determine if p66Shc cellular localization changed with embryo culture, cultured blastocysts were stained for p66Shc immunoreactivity and were compared to freshly flushed, *in vivo* derived blastocysts. Blastocysts cultured in high oxygen conditions showed an increase in p66Shc fluorescence intensity and detectable diffuse p66Shc staining in inner cells, compared to that of *in vivo* and low oxygen cultured blastocysts (Fig. 2-9A-C). As we did not co-stain for lineage markers, we cannot definitively identify these inner cells as the inner cell mass. However, p66Shc fluorescence is undetectable in inner cells of *in vivo* derived and low oxygen blastocysts in culture, suggesting that high oxygen may induce abnormal p66Shc expression in the inner cell mass. To determine the localization of phosphorylated S36 p66Shc, cultured blastocysts were stained for phosphorylated S36 p66Shc immunoreactivity and compared to *in vivo* controls. Consistent with the immunoblotting results, neither the fluorescence levels of phosphorylated S36 p66Shc nor its localization appeared to change between treatment groups. However, phosphorylated S36 p66Shc did show a distinct cellular localization pattern compared to total p66Shc, showing cytoplasmic and nuclear immunoreactivity in

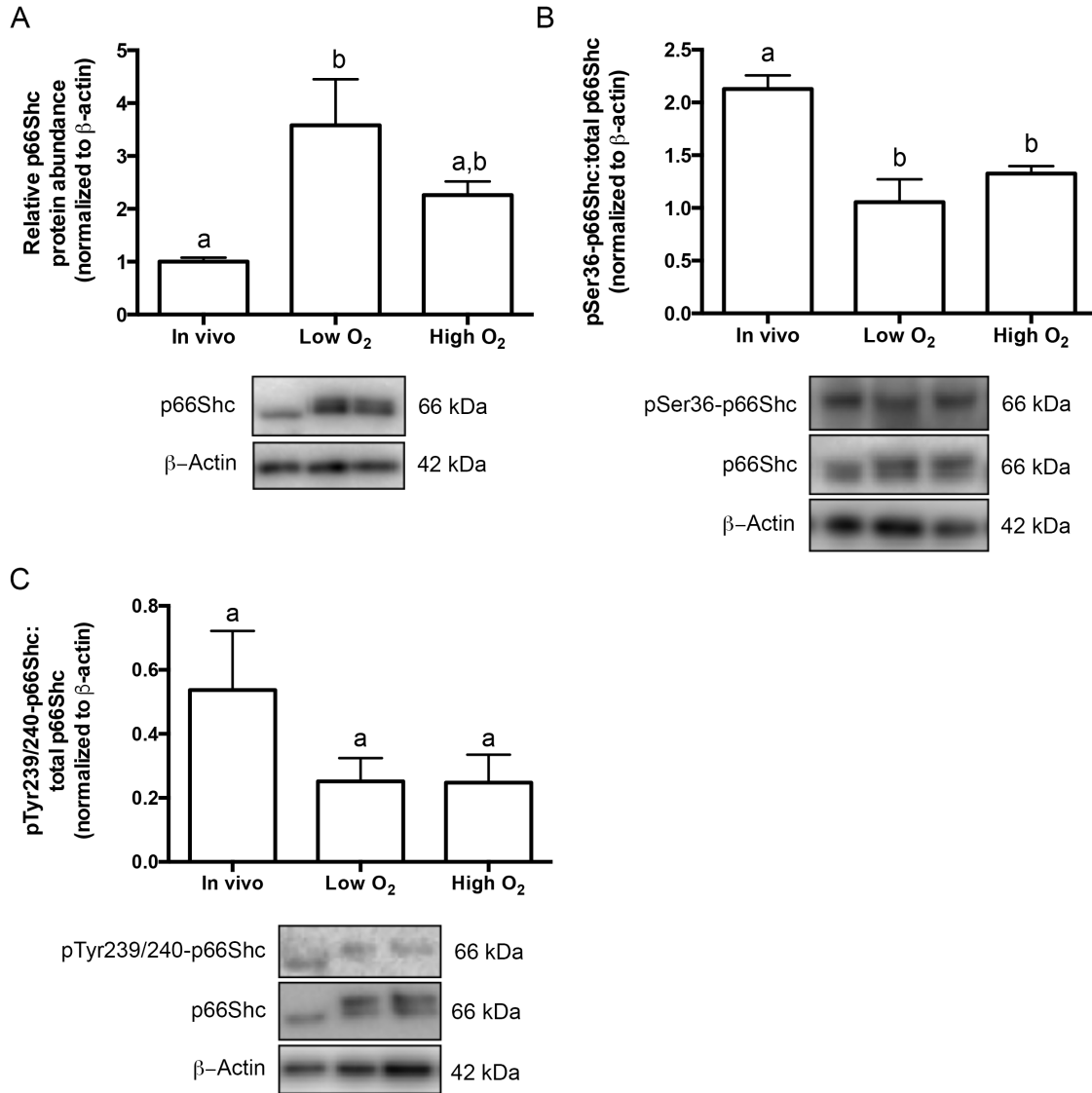


Figure 2-7. Culture and high oxygen tension increases the relative p66Shc protein abundance in mouse blastocysts.

(A) Immunoblotting for p66Shc was performed on four replicates of pools of 50 blastocysts. P66Shc protein abundance significantly increases in blastocysts cultured at low oxygen tension compared to *in vivo* controls (n=4, mean \pm SEM, p=0.0306 one way-ANOVA). A representative blot is shown (for uncropped immunoblot, see Supplementary Figure 1B). (B) Immunoblotting for phosphorylated p66Shc on serine 36 (S36) and total p66Shc was performed on three replicates of pools of 40-50 blastocysts. The ratio of phosphorylated serine 36 (S36)-p66Shc to total p66Shc significantly decreases in blastocysts cultured in low and high oxygen tensions compared to controls (n=3, mean \pm SEM, p=0.0057 for low O₂; p=0.0219 for high O₂ one way-ANOVA). A representative blot is shown (for uncropped immunoblot, see Supplementary Figure 1C). (C) Immunoblotting for phosphorylated tyrosine 239/240 (Y239/Y240)-p66Shc and total p66Shc was performed on three replicates of pools of 20-30 blastocysts. The ratio of phospho Y239/Y240-p66Shc to total p66Shc does not significantly in cultured blastocysts compared to controls (n=3, mean \pm SEM, p=0.5043, one way-ANOVA). A representative blot is shown (for uncropped immunoblot, see Supplementary Figure 1D).

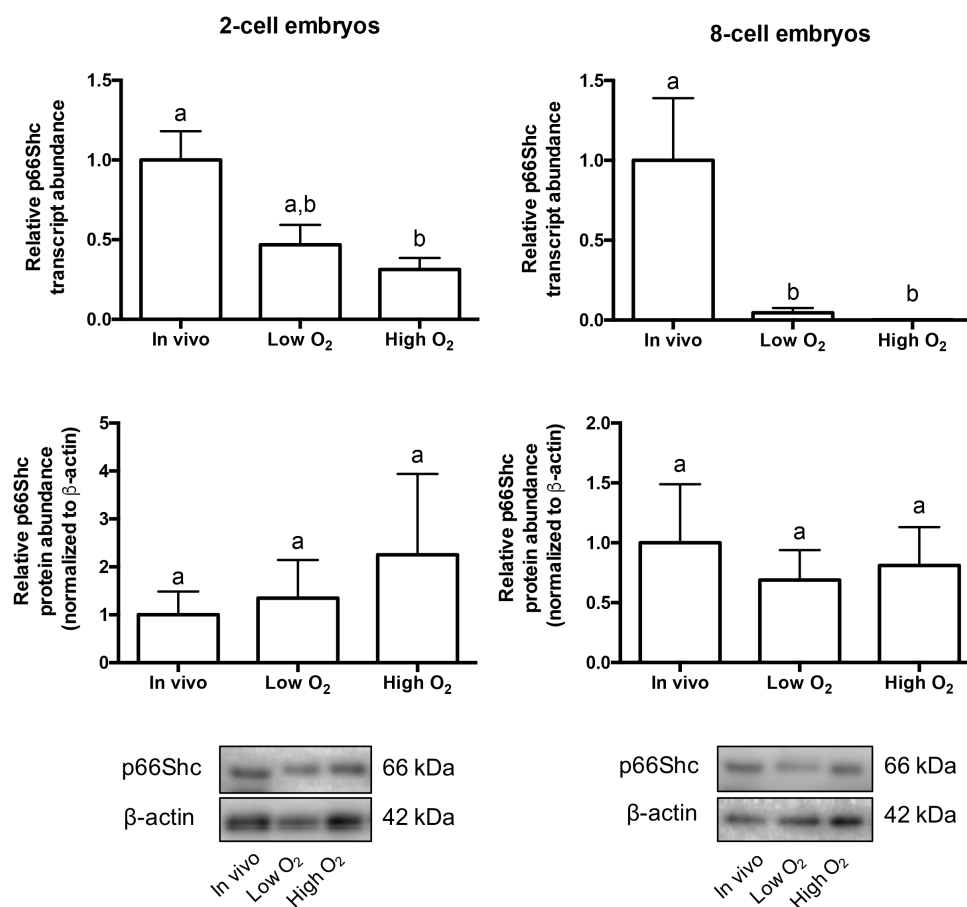


Figure 2-8. Relative p66Shc mRNA and protein abundance in cultured 2-cell and 8-cell embryos.

(A) qRT-PCR was performed on pools of 20 2-cell embryos for p66Shc relative transcript abundance. P66Shc transcript abundance significantly decreases with culture and increasing oxygen tension ($n=4$, mean \pm SEM, $p=0.0310$ 1W-ANOVA). Immunoblotting was performed on pools of 50 2-cell embryos for p66Shc relative protein abundance. A representative blot is shown ($n=3$, mean \pm SEM, $p=0.7256$ 1W-ANOVA).

(B) qRT-PCR was performed on pools of 20 8-cell embryos for p66Shc relative transcript abundance, which significantly decreases with culture and increasing oxygen tension ($n=4$, mean \pm SEM, $p=0.0004$ 1W-ANOVA). Immunoblotting was performed on pools of 50 8-cell embryos for p66Shc relative protein abundance. A representative blot is shown ($n=4$, mean \pm SEM, $p=0.8375$ 1W-ANOVA).

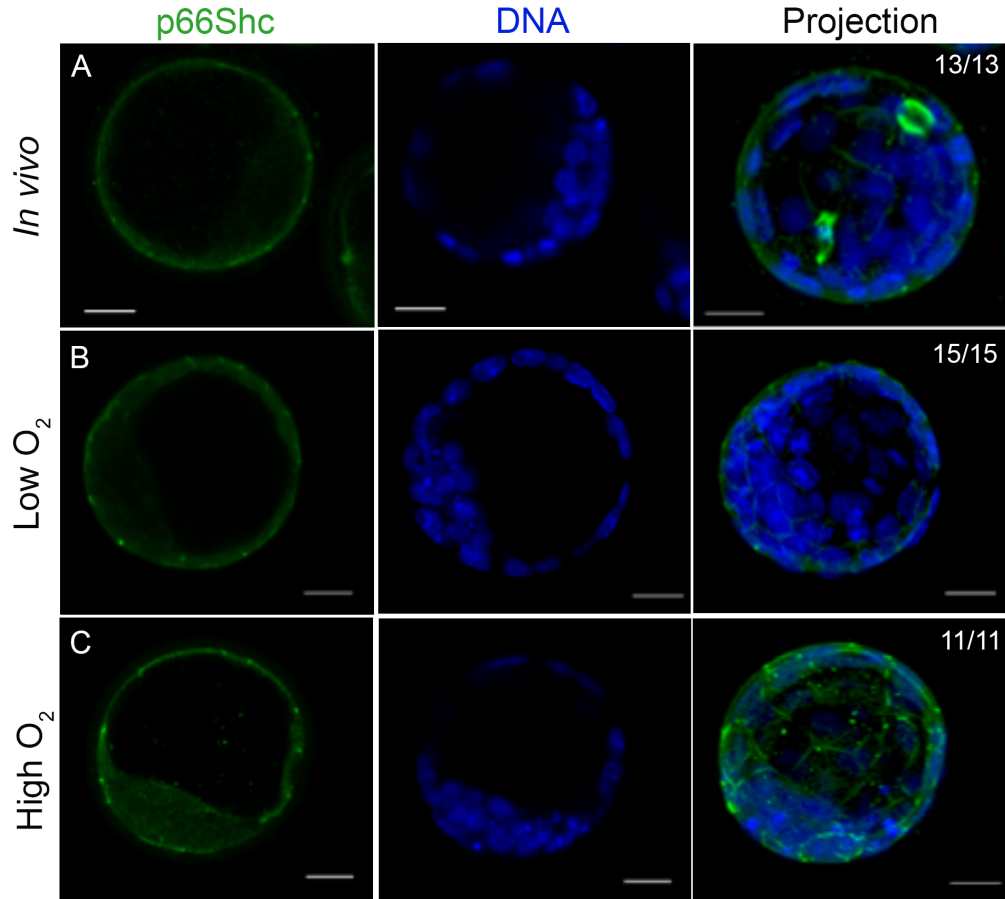


Figure 2-9. Total p66Shc becomes detectable in the inner cells of mouse blastocysts cultured under atmospheric oxygen tension.

Representative immunofluorescence and confocal microscopy images for total p66Shc in pools of 10-15 blastocysts per treatment group. (A) *In vivo* flushed blastocysts. (B) Blastocysts after 96 h culture under low oxygen tension. (C) Blastocysts after 96 h culture under high oxygen tension. Green = p66Shc, Blue = DAPI. Scale bar = 20 μm .

the outer and inner cells of the blastocyst (Fig. 2-10A-C). In addition, phosphorylated S36 p66Shc was also detectable in inner cells of the *in vivo* produced blastocyst while total p66Shc was not. We observed similar cytoplasmic staining of both total p66Shc and pSer36-p66Shc in HT-22 cells, suggesting that the NT-Shc (total p66Shc) antibody can detect phosphorylated p66Shc. However, we overexpressed p66Shc in these cells, whereas we assessed basal p66Shc expression in mouse blastocysts. Overexpression of the protein and differences in antibody sensitivities may explain why total p66Shc fluorescence appears to differ from pSer36-p66Shc fluorescence in blastocysts. (Figs. 2-9A and 2-10A). The localization pattern may also suggest that the phosphorylated S36 p66Shc fraction in blastocysts produced *in vivo* or in culture may be localized to a distinct compartment in the cytoplasm or nucleus compared to non-phosphorylated, or p66Shc phosphorylated at a different residue.

In addition to its role in mediating the oxidative stress response, several studies have implicated p66Shc in regulating cellular glucose uptake through growth factor receptor signalling, actin cytoskeleton regulation, or modulation of anaerobic respiration (Natalicchio et al., 2009; Soliman et al., 2014). Thus, we next aimed to determine if p66Shc expression is sensitive to culture medium glucose concentration, a component often modified in embryo culture to simulate *in vivo* microenvironmental conditions. We cultured flushed 8-cell stage embryos for 24 hours in KSOM varying in glucose concentrations under low oxygen tension: 0.2 mM (standard KSOM), 3.4 mM (equivalent to normal mouse oviductal glucose levels, (Gardner and Leese, 1990)), 30 mM D-glucose (hyperglycemia, (Moley et al., 1998)) and 30 mM L-glucose to control for increased osmolarity. We observed that embryos cultured in 30 mM D-glucose have decreased rates of blastocyst cavitation (Fig. 2-11A). The embryos did not fail to cavitate due to glucose toxicity, as 18 hours culture in 0.2 mM D-glucose rescued cavitation (Fig. 2-11B). Furthermore, cell number in non-cavitated embryos did not significantly change with high glucose culture compared to control, suggesting that these embryos were not developing slower than the controls (Fig. 2-11C).

To determine if p66Shc expression changed during culture in high glucose, we performed qRT-PCR and immunoblotting for p66Shc in pools of blastocysts cultured in the four

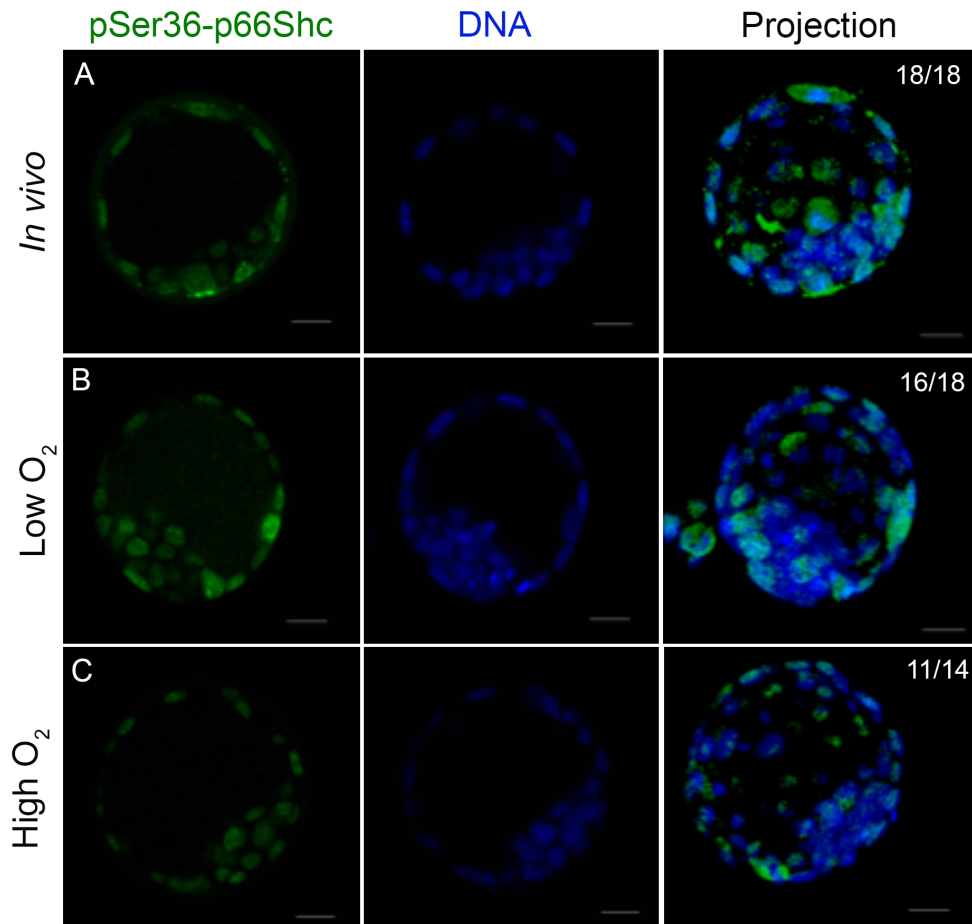


Figure 2-10. Phosphorylated S36 p66Shc localization does not change in cultured mouse blastocysts.

Representative immunofluorescence and confocal microscopy images for phosphorylated (S36) p66Shc in pools of 15-20 blastocysts per treatment group. (A) *In vivo* flushed blastocysts. (B) Blastocysts after 96 h culture under low oxygen tension. (C) Blastocysts after 96 h culture under high oxygen tension. Green = p66Shc, Blue = DAPI. Scale bar = 20 μ m.

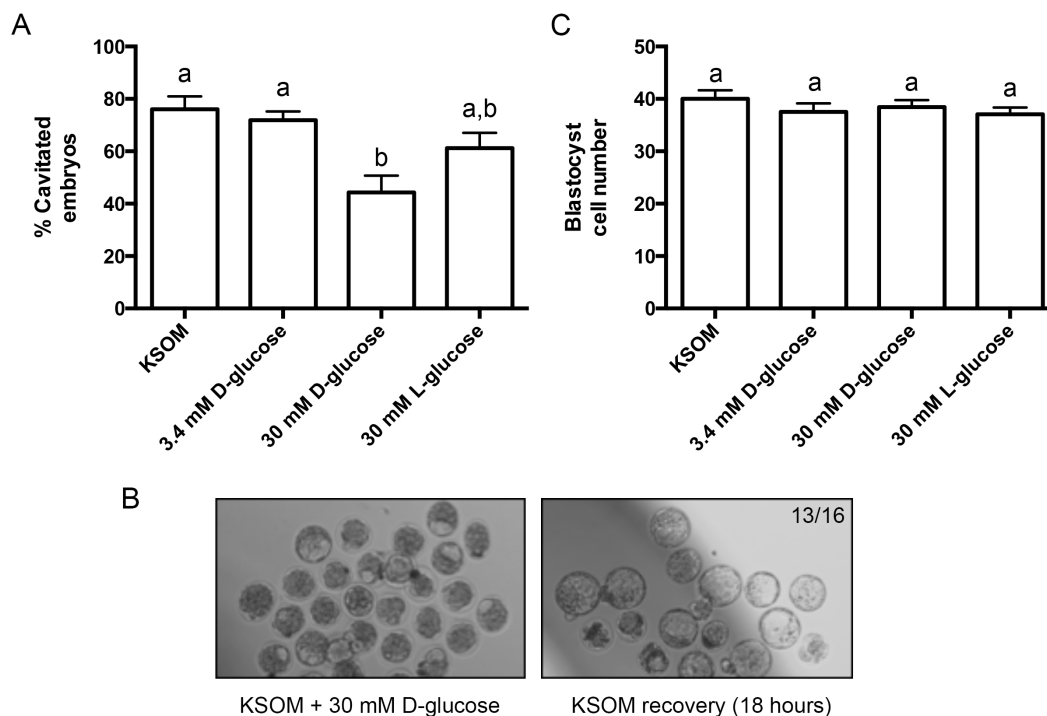


Figure 2-11. High glucose media concentrations reversibly inhibit mouse embryo cavitation.

(A) Percent cavitation of blastocysts after 24h culture in each treatment group, indicated by the formation of any cavity in the embryo ($n=4$, mean \pm SEM, $p=0.0052$ 1W-ANOVA). (B) Bright field microscopy images of embryos after 24h treatment in 30 mM D-glucose, followed by recovery in low glucose potassium simplex optimized media (KSOM) for 18 hours. Arrows in the left panel indicate examples of embryos classified as non-cavitated. Thirteen of sixteen non-cavitated embryos after high glucose treatment cavitated after 18 hours of recovery. (C) Blastocyst cell number after 24h culture in each treatment group ($n=19-21$ per group, mean \pm SEM, $p=0.5099$ one way-ANOVA).

glucose concentrations. Neither transcript levels nor protein abundance significantly changed in embryos cultured in varying glucose conditions (Fig. 2-12A-B), suggesting that p66Shc expression levels are not sensitive to increased glucose in embryo culture media. To determine if p66Shc cellular localization changed with glucose concentration, embryos cultured in 30 mM D-glucose were stained for p66Shc immunoreactivity and compared to embryos cultured in KSOM. We saw comparable peripheral and cytoplasmic p66Shc immunoreactivity in non-cavitated embryos after high glucose culture compared to controls, suggesting that p66Shc cellular localization is not impacted by media glucose concentrations (Fig. 2-12C).

2.3.4 Changes to p66Shc expression in culture correlate with altered embryo metabolism

To determine if increased p66Shc expression levels in cultured embryos could be a marker of altered embryo metabolism, we performed two metabolic assays on blastocysts derived *in vivo* and after culture under low and high oxygen. We first assessed total ATP content of blastocysts from each group and observed that ATP levels per cell significantly decreased in blastocysts cultured under low oxygen compared to *in vivo* blastocysts (Fig. 2-13A). As oxidative phosphorylation in the trophectoderm is the major source of cellular ATP in the blastocyst (Houghton, 2006), we then assayed for production of superoxide in the same treatment groups. Superoxide is a free radical produced as a by-product of oxidative phosphorylation that is normally present at low levels and is readily scavenged by superoxide dismutase. Blastocysts were incubated in MitoSOX red superoxide indicator and imaged using confocal microscopy. We observed that blastocysts cultured under low and high oxygen showed significantly higher MitoSOX fluorescence compared to *in vivo* controls, suggesting increased superoxide production or decreased antioxidant scavenging in these culture conditions (Fig. 2-13B). Our results suggest that even under low oxygen conditions, cultured blastocysts contain less ATP and increased superoxide levels, correlating with increased mRNA and protein abundance of p66Shc.

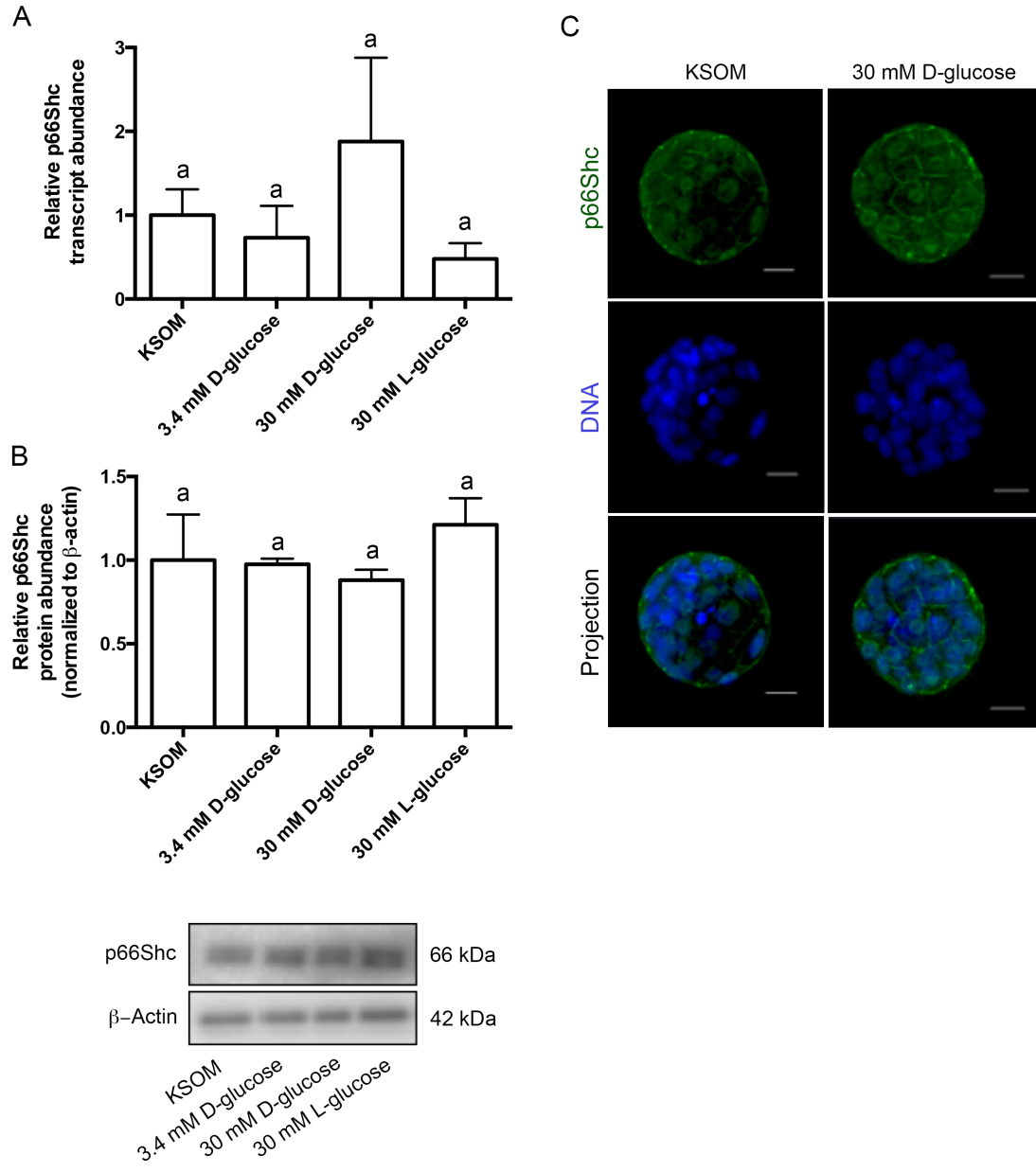


Figure 2-12. High glucose media concentrations do not significantly change relative p66Shc mRNA and protein abundance in mouse blastocysts.

(A) qRT-PCR was performed on pools of 10 blastocysts for relative p66Shc transcript abundance, normalized to levels of exogenously added luciferase (n=3, mean \pm SEM, p=0.3783 one way-ANOVA). (B) Immunoblotting was performed on pools of 30 blastocysts per treatment group for total p66Shc protein abundance, normalized to levels of β -actin. A representative blot is shown (n=3, mean \pm SEM, p=0.5549 one way-ANOVA). (C) Representative immunofluorescence and confocal microscopy images of blastocysts cultured in 30 mM D-glucose (right panel) and KSOM only (left panel) for total p66Shc reactivity. Green = p66Shc, Blue =DNA. Scale bar = 20 μ m.

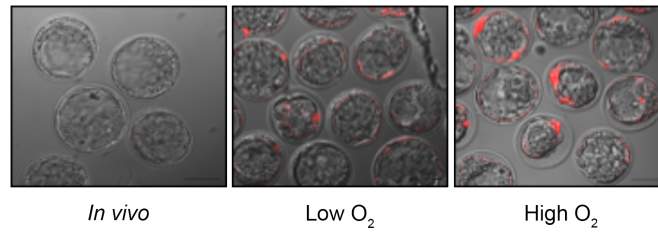
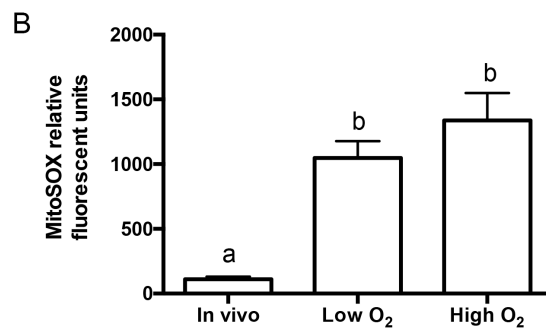
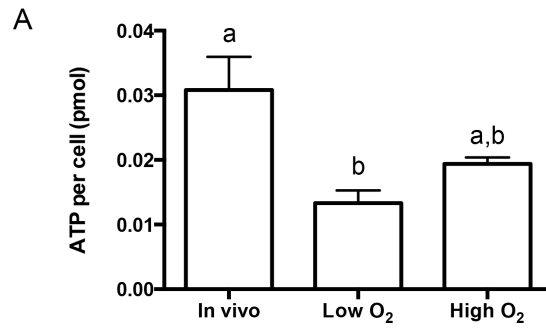


Figure 2-13. Increased p66Shc expression correlates with decreased ATP and increased superoxide in cultured mouse blastocysts.

(A) Total ATP content was quantified from pools of 5 blastocysts in each treatment group and normalized to blastocyst cell number. ATP content per cell significantly decreases in blastocysts cultured in low oxygen for 96h compared to in vivo controls (n=3, mean \pm SEM, $p=0.0199$ one way-ANOVA). Mean cell numbers for each treatment group are: in vivo = 27.43 ± 10.31 (n=46), low oxygen = 35.03 ± 7.36 (n=31), high oxygen = 31.41 ± 9.49 (n=30). (B) MitoSOX relative fluorescence was quantified in blastocysts in each treatment group. MitoSOX fluorescence significantly increases in blastocysts cultured under low or high oxygen compared to in vivo controls (in vivo n=28, low oxygen n=26, high oxygen n=23, mean \pm SEM, $p<0.0001$ 1W-ANOVA). Representative images of MitoSOX staining are shown in the three panels.

2.4 Discussion

Here we demonstrate that p66Shc is basally expressed in mouse preimplantation embryos and its expression is altered by embryo culture. We also show that dysregulated p66Shc expression coincides with metabolic changes in culture that may negatively affect embryo developmental viability. Our results suggest that p66Shc mRNA is stored in the oocyte and degraded during the maternal-to-embryonic transition. P66Shc mRNA is later upregulated by the blastocyst stage, and predominately located at the cell periphery of trophoblast cells. Blastocysts grown *in vitro* show increasing p66Shc mRNA and protein abundance with increasing oxygen tension, coupled with alterations to phosphorylated residues that have implications for the protein's cellular compartmentalization and function. These changes appear to be oxygen-sensitive, while changing media glucose concentrations did not significantly affect p66Shc expression levels in the blastocyst. Lastly, we are the first to correlate these changes in culture and high oxygen tension to dysregulated ATP and superoxide production within *in vitro* produced blastocysts.

Our expression analysis of p66Shc during *in vivo* blastocyst development suggests that p66Shc is normally upregulated during the eight-cell embryo to blastocyst transition. This basal level of expression during *in vivo* development implies that despite promoting apoptosis, p66Shc expression may be necessary for survival and prevents blastocysts from being selected against during development. One possible biological function of p66Shc during preimplantation development may be the promotion of oxidative phosphorylation. Basal oxygen consumption in p66Shc-null MEFs decreases by 30-50% with no change in mitochondrial or cytochrome c content, with a compensatory increase in ATP production by anaerobic respiration (Nemoto et al., 2006). There is also evidence suggesting that in MEFs, p66Shc forms a complex with cytochrome c in the inner mitochondrial membrane to regulate pyruvate dehydrogenase kinase, ultimately regulating the activity of pyruvate dehydrogenase) depending on the redox state of cytochrome c (Acin-Perez et al., 2010). In the mouse blastocyst, the trophoblast produces ATP through oxidative phosphorylation to support development, but the inner cell mass is relatively metabolically quiescent (Houghton, 2006). Metabolic differences

between the two embryonic lineages could account for our immunolocalization results, as p66Shc appears to localize predominately to the trophectoderm *in vivo* and under low oxygen conditions, suggesting that p66Shc could be involved in trophectoderm metabolism. Although our study did not directly test the role of p66Shc in oxidative phosphorylation, we have correlated increasing p66Shc transcript and protein abundances after embryo culture with alterations to ATP and superoxide production, suggesting that dysregulated p66Shc levels in the embryo may have a negative impact on embryo metabolism.

Studies of p66Shc in mammalian embryos have thus far focused primarily on the apoptosis- and senescence-promoting functions of p66Shc, basally or in stress-inducing culture conditions. In bovine preattachment embryos, siRNA-mediated knockdown of p66Shc reduces levels of intracellular ROS, DNA damage, and apoptosis in untreated and oxidant-treated culture conditions (Betts et al., 2014). Early bovine embryos exhibit high levels of developmental arrest (>50%) in culture (Leidenfrost et al., 2011), likely due to suboptimal culture conditions, which could result in increased p66Shc transcript levels, leading to senescence (permanent embryo arrest) and apoptosis. Due to species-specific differences in early development, or better optimized conditions, mouse preimplantation embryos from inbred strains exhibit high developmental rates with >75% of zygotes reaching the blastocyst stage in optimized media and low oxygen conditions (Karagenc et al., 2004). It is possible that p66Shc expression is carefully regulated during preimplantation development, such that both abnormally high and low p66Shc expression levels are detrimental to the embryo.

Consistent with our findings in our mouse embryo culture model, there is strong evidence associating p66Shc induction with negative developmental outcomes under adverse bovine and murine embryo culture conditions. Bovine embryos grown in oviductal epithelial cell co-culture, considered a suboptimal culture environment, show a significantly increased p66Shc transcript abundance compared to culture under chemically defined synthetic oviductal fluid media at lower oxygen tension. This increase was associated with increased markers of oxidative stress (intracellular ROS, DNA damage) and embryo arrest (Favetta et al., 2007b). Mouse embryos cultured in media

containing arsenic show significantly decreased blastocyst development and increased p66Shc immunofluorescence intensity, suggesting that p66Shc may mediate a stress response to arsenic. Treatment with the antioxidant N-acetyl cysteine rescued apoptosis and p66Shc expression levels observed in arsenic-treated embryos, suggesting that arsenic-induced ROS increases p66Shc expression, which may in turn further increase ROS and lead to apoptosis (Zhang et al., 2010). Preimplantation development under both cases improved when p66Shc was knocked down by RNA interference (Betts et al., 2014; Favetta et al., 2007a; Ren et al., 2014). Previous RNA-interference experiments may have normalized an adverse environment-induced “spike” in p66Shc expression, but not completely deplete the embryo of maternal- or zygotic-derived p66Shc, thus masking any loss-of-function phenotype. Maternally-derived p66Shc function may be important to preimplantation development, as embryo cleavage and blastocyst development is impaired when p66Shc is knocked down in immature bovine oocytes (Favetta et al., 2007a). We are the first to show that p66Shc transcript and protein expression is upregulated at the blastocyst stage during mouse *in vivo* development, indicating that p66Shc may also have an important physiological function other than promoting apoptosis and embryo arrest.

We found that the induction of p66Shc transcription in cultured blastocysts appears to be specific to oxygen, as increasing media glucose concentrations did not significantly change p66Shc transcript abundance compared to controls. Oxygen-sensitive induction in our results is consistent with findings that p66Shc transcription can be regulated by the Nrf2-antioxidant response element (ARE) pathway under stress-inducing conditions. Chromatin immunoprecipitation assays performed in hemin-treated human erythroleukemic cells demonstrated that Nrf2 binds to an ARE enhancer upstream of the transcriptional start site of p66Shc and that Nrf2 induction of expression is isoform-specific (Miyazawa and Tsuji, 2014). This could be the upstream mechanism in our model of p66Shc transcriptional upregulation in blastocysts cultured under high oxygen. High glucose concentrations in the culture media did not significantly change p66Shc expression in blastocysts but did affect cavitation. This is consistent with previous reports of hyperglycemic conditions negatively affecting blastocyst development (Fraser et al., 2007). Thus, it is unlikely that the cell’s response to high glucose regulates the

transcription of p66Shc, but instead may affect other genes known to be involved in cavitation (e.g. ATPase Na⁺/K⁺ transporting subunit beta 1, aquaporin 3, aquaporin 9, cadherin 1). Furthermore, it is not known whether p66Shc is important for the regulation of glucose uptake in preimplantation embryos or if this function is dependent on mammalian target of rapamycin (mTOR) or growth factor receptor signalling pathways (Natalicchio et al., 2009; Soliman et al., 2014). It is possible that p66Shc could mediate a response to high glucose levels in embryos independent of an increase in its transcript or protein abundance, through phosphorylation of certain residues.

It is possible that culture conditions increase p66Shc expression to promote its apoptotic functions, removing it from its metabolic function in the mitochondria. Our results suggest that culture-mediated changes to phosphorylated residues on p66Shc may impact its cellular compartmentalization and may ultimately be a key factor in its cellular function. Subcellular fractionation of untreated MEF lysates showed that p66Shc is detectable in the soluble, mitochondrial, and endoplasmic reticulum fractions (Orsini et al., 2004). Phosphorylation of the serine-36 residue, which is unique to the 66 kDa isoform of the Shc1 family, has been implicated in its cellular localization. Serine-36 phosphorylation of p66Shc under oxidizing conditions increases its association with the prolyl isomerase Pin-1, ultimately resulting in p66Shc translocation to the mitochondria. Fibroblasts lacking Pin-1 have a decreased mitochondrial fraction of p66Shc after H₂O₂ treatment compared to wild type fibroblasts, linking the modification of this residue to the protein's mitochondrial localization (Pinton et al., 2007). In our study, blastocysts cultured under low or high oxygen conditions show decreased ratios of phosphorylated 36 to total p66Shc, suggesting that these conditions may decrease the mitochondrial fraction of p66Shc despite an increase in total p66Shc protein abundance. This alteration in cellular localization may affect the functions of p66Shc in the mitochondria, which our results of altered embryo metabolism may reflect.

Despite using optimal culture conditions, both p66Shc expression and the metabolic parameters measured were significantly altered in blastocysts grown under low oxygen tension. No significant difference between increased superoxide production in blastocysts after culture in low or high oxygen tension suggests that oxidative phosphorylation

metabolism may be adversely affected regardless of oxygen tension, or that there is another parameter in the microenvironment that must be further optimized to limit metabolic alterations in cultured embryos. Levels of p66Shc may therefore be an indicator of altered blastocyst metabolism, particularly of the trophoctoderm, which is responsible for generating nearly all of the blastocyst's ATP content (Houghton, 2006). Altered expression levels and/or p66Shc function in culture may lead to adverse trophoctoderm development through increases in ROS-mediated apoptosis or decreases in ATP production, which may impact implantation and placentation.

Our study did not follow up on peri- and post-implantation stage embryos and p66Shc expression levels, but we suspect that p66Shc expression is likely altered in the trophoblast or post-implantation trophoblast-derived tissues after embryo culture. Supporting this is evidence that p66Shc CpG promoter methylation is decreased in human placental tissue of intrauterine growth restricted neonates compared to neonates appropriate and small for gestational age (Tzschoppe et al., 2013). This is also consistent with the finding that most culture-induced embryo abnormalities affect the trophoblast and placenta, and to a lesser extent the fetal tissues (de Waal et al., 2014; Fauque et al., 2010). Post-implantation development is affected by oxygen tension, as transferred blastocysts cultured at 20% oxygen show a significant increase in the number of uterine resorption sites and a decrease in living fetuses compared to blastocysts cultured at 5% oxygen (Karagenc et al., 2004). Additionally, transferred blastocysts cultured in both oxygen tensions resulted in decreased fetal weights compared to freshly flushed blastocysts, suggesting that some component of culture aside from oxygen tension impacts fetal development (M Harlow and Quinn, 1979). These studies used different culture medium conditions from ours, which may be critical to the developmental outcomes observed. Culture effects observed in our study may impact fetal development through abnormal increases in p66Shc expression and/or altered oxidative phosphorylation metabolism.

Our study correlated increased p66Shc expression levels with altered oxidative phosphorylation metabolism, however, we did not directly implicate a mechanism for p66Shc involvement in dysregulated metabolism. Further work must be performed to

determine the mechanism of p66Shc function during preimplantation development and its implications for post-implantation development. Additionally, we used one formulation of embryo culture medium that differs from media used in other mouse model studies and from clinical media used to support human blastocyst development. Our findings may be limited to this media or may be a species-specific phenomenon. However, as increases in p66Shc expression due to culture are observed in another large animal model (bovine) (Favetta et al., 2007b), it would be interesting to explore whether cultured human embryos exhibit varying p66Shc levels and if this correlates with developmental outcome. For clinical applications, using increased p66Shc expression as a molecular marker of altered metabolism may impact on which blastocyst may be the most developmentally competent for embryo transfer.

2.5 References

- Acin-Perez, R., Hoyos, B., Gong, J., Vinogradov, V., Fischman, D. A., Leitges, M., Borhan, B., Starkov, A., Manfredi, G. and Hammerling, U.** (2010). Regulation of intermediary metabolism by the PKCdelta signalosome in mitochondria. *FASEB J* **24**, 5033-5042.
- Betts, D. H., Bain, N. T. and Madan, P.** (2014). The p66(Shc) adaptor protein controls oxidative stress response in early bovine embryos. *PLoS One* **9**, e86978.
- Betts, D. H., Barcroft, L. C. and Watson, A. J.** (1998). Na/K-ATPase-mediated 86Rb⁺ uptake and asymmetrical trophectoderm localization of alpha1 and alpha3 Na/K-ATPase isoforms during bovine preattachment development. *Dev Biol* **197**, 77-92.
- CFAS (2015). Human Assisted Reproduction 2015 Live Birth Rates for Canada.
- de Waal, E., Mak, W., Calhoun, S., Stein, P., Ord, T., Krapp, C., Coutifaris, C., Schultz, R. M. and Bartolomei, M. S.** (2014). In vitro culture increases the frequency of stochastic epigenetic errors at imprinted genes in placental tissues from mouse concepti produced through assisted reproductive technologies. *Biol Reprod* **90**, 22.
- Fauque, P., Mondon, F., Letourneur, F., Ripoche, M.-A., Journot, L., Barbaux, S., Dandolo, L., Patrat, C., Wolf, J.-P., Jouannet, P., et al.** (2010). In vitro fertilization and embryo culture strongly impact the placental transcriptome in the mouse model. *PLoS One* **5**, e9218.
- Favetta, L. A., Madan, P., Mastromonaco, G. F., St John, E. J., King, W. A. and Betts, D. H.** (2007a). The oxidative stress adaptor p66Shc is required for permanent embryo arrest in vitro. *BMC Dev Biol* **7**, 132.

- Favetta, L. A., Robert, C., St John, E. J., Betts, D. H. and King, W. A.** (2004). p66shc, but not p53, is involved in early arrest of in vitro-produced bovine embryos. *Mol Hum Reprod* **10**, 383-392.
- Favetta, L. A., St John, E. J., King, W. A. and Betts, D. H.** (2007b). High levels of p66shc and intracellular ROS in permanently arrested early embryos. *Free Radic Biol Med* **42**, 1201-1210.
- Feuer, S. and Rinaudo, P.** (2012). Preimplantation stress and development. *Birth Defects Res C Embryo Today* **96**, 299-314.
- Fraser, R. B., Waite, S. L., Wood, K. A. and Martin, K. L.** (2007). Impact of hyperglycemia on early embryo development and embryopathy: in vitro experiments using a mouse model. *Hum Reprod* **22**, 3059-3068.
- Gardner, D. K., Lane, M., Stevens, J. and Schoolcraft, W. B.** (2001). Noninvasive assessment of human embryo nutrient consumption as a measure of developmental potential. *Fertil Steril* **76**, 1175-1180.
- Gardner, D. K. and Leese, H. J.** (1990). Concentrations of nutrients in mouse oviduct fluid and their effects on embryo development and metabolism in vitro. *Journal of reproduction and fertility* **88**, 361-368.
- Gotoh, N., Toyoda, M. and Shibuya, M.** (1997). Tyrosine phosphorylation sites at amino acids 239 and 240 of Shc are involved in epidermal growth factor-induced mitogenic signaling that is distinct from Ras/mitogen-activated protein kinase activation. *Molecular and Cellular Biology* **17**, 1824-1831.
- Grady, R., Alavi, N., Vale, R., Khandwala, M. and McDonald, S. D.** (2012). Elective single embryo transfer and perinatal outcomes: A systematic review and meta-analysis. *Fertil Steril* **97**, 324-331.
- Houghton, F. D.** (2006). Energy metabolism of the inner cell mass and trophectoderm of the mouse blastocyst. *Differentiation* **74**, 11-18.
- Houghton, F. D., Humpherson, P. G., Hawkhead, J. A., Hall, C. J. and Leese, H. J.** (2003). Na⁺, K⁺, ATPase activity in the human and bovine preimplantation embryo. *Dev Biol* **263**, 360-366.
- Karagenc, L., Sertkaya, Z., Ciray, N., Ulug, U. and Bahçeci, M.** (2004). Impact of oxygen concentration on embryonic development of mouse zygotes. *Reprod Biomed Online* **9**, 409-417.
- Leidenfrost, S., Boelhaue, M., Reichenbach, M., Güngör, T., Reichenbach, H. D., Sinowatz, F., Wolf, E. and Habermann, F. A.** (2011). Cell arrest and cell death in mammalian preimplantation development: Lessons from the bovine model. *PLoS One* **6**.

- M Harlow, G. and Quinn, P.** (1979). Foetal and placental growth in the mouse after pre-implantation development in vitro under oxygen concentrations of 5 and 20%. *Australian Journal of Biological Sciences* **32**, 363-370.
- Mamo, S., Gal, A. B., Bodo, S. and Dinnyes, A.** (2007). Quantitative evaluation and selection of reference genes in mouse oocytes and embryos cultured in vivo and in vitro. *BMC Dev Biol* **7**, 14.
- Migliaccio, E., Giorgio, M., Mele, S., Pelicci, G., Reboldi, P., Pandolfi, P. P., Lanfrancone, L. and Pelicci, P. G.** (1999). The p66shc adaptor protein controls oxidative stress response and life span in mammals. *Nature* **402**, 309-313.
- Migliaccio, E., Mele, S., Salcini, A. E., Pelicci, G., Lai, K. M., Superti-Furga, G., Pawson, T., Di Fiore, P. P., Lanfrancone, L. and Pelicci, P. G.** (1997). Opposite effects of the p52shc/p46shc and p66shc splicing isoforms on the EGF receptor-MAP kinase-fos signalling pathway. *EMBO J* **16**, 706-716.
- Miyazawa, M. and Tsuji, Y.** (2014). Evidence for a novel antioxidant function and isoform-specific regulation of the human p66Shc gene. *Mol Biol Cell* **25**, 2116-2127.
- Moley, K. H., Chi, M. M., Knudson, C. M., Korsmeyer, S. J. and Mueckler, M. M.** (1998). Hyperglycemia induces apoptosis in pre-implantation embryos through cell death effector pathways. *Nature Medicine* **4**, 1421-1424.
- Natalicchio, A., De Stefano, F., Perrini, S., Laviola, L., Cignarelli, A., Caccioppoli, C., Quagliari, A., Melchiorre, M., Leonardini, A., Conserva, A., et al.** (2009). Involvement of the p66Shc protein in glucose transport regulation in skeletal muscle myoblasts. *American Journal of Physiology. Endocrinology and Metabolism* **296**, E228-E237.
- Nemoto, S., Combs, C. A., French, S., Ahn, B. H., Fergusson, M. M., Balaban, R. S. and Finkel, T.** (2006). The mammalian longevity-associated gene product p66shc regulates mitochondrial metabolism. *J Biol Chem* **281**, 10555-10560.
- Orsini, F., Migliaccio, E., Moroni, M., Contursi, C., Raker, V. A., Piccini, D., Martin-Padura, I., Pelliccia, G., Trinei, M., Bono, M., et al.** (2004). The life span determinant p66Shc localizes to mitochondria where it associates with mitochondrial heat shock protein 70 and regulates trans-membrane potential. *J Biol Chem* **279**, 25689-25695.
- Pinton, P., Rimessi, A., Marchi, S., Orsini, F., Migliaccio, E., Giorgio, M., Contursi, C., Minucci, S., Mantovani, F., Wieckowski, M. R., et al.** (2007). Protein kinase C beta and prolyl isomerase 1 regulate mitochondrial effects of the life-span determinant p66Shc. *Science* **315**, 659-663.
- Ren, K., Li, X., Yan, J., Huang, G., Zhou, S., Yang, B., Ma, X. and Lu, C.** (2014). Knockdown of p66Shc by siRNA injection rescues arsenite-induced

developmental retardation in mouse preimplantation embryos. *Reprod Toxicol* **43**, 8-18.

Rinaudo, P. and Schultz, R. M. (2004). Effects of embryo culture on global pattern of gene expression in preimplantation mouse embryos. *Reproduction* **128**, 301-311.

Seli, E., Vergouw, C. G., Morita, H., Botros, L., Roos, P., Lambalk, C. B., Yamashita, N., Kato, O. and Sakkas, D. (2010). Noninvasive metabolomic profiling as an adjunct to morphology for noninvasive embryo assessment in women undergoing single embryo transfer. *Fertil Steril* **94**, 535-542.

Soliman, M. A., Abdel Rahman, A. M., Lamming, D. W., Birsoy, K., Pawling, J., Frigolet, M. E., Lu, H., Fantus, I. G., Pasculescu, A., Zheng, Y., et al. (2014). The adaptor protein p66Shc inhibits mTOR-dependent anabolic metabolism. *Sci Signal* **7**, ra17.

Tzschoppe, A., Doerr, H., Rascher, W., Goecke, T., Beckmann, M., Schild, R., Struwe, E., Geisel, J., Jung, H. and Dötsch, J. (2013). DNA methylation of the p66Shc promoter is decreased in placental tissue from women delivering intrauterine growth restricted neonates. *Prenatal Diagnosis* **33**, 484-491.

Ventura, A., Luzi, L., Pacini, S., Baldari, C. T. and Pelicci, P. G. (2002). The p66Shc longevity gene is silenced through epigenetic modifications of an alternative promoter. *J Biol Chem* **277**, 22370-22376.

Wale, P. L. and Gardner, D. K. (2012). Oxygen regulates amino acid turnover and carbohydrate uptake during the preimplantation period of mouse embryo development. *Biol Reprod* **87**, 24-24.

Wale, P. L. and Gardner, D. K. (2013). Oxygen affects the ability of mouse blastocysts to regulate ammonium. *Biol Reprod* **89**, 75.

Wale, P. L. and Gardner, D. K. (2016). The effects of chemical and physical factors on mammalian embryo culture and their importance for the practice of assisted human reproduction. *Hum Reprod Update* **22**, 2-22.

Zhang, C., Liu, C., Li, D., Yao, N., Yuan, X., Yu, A., Lu, C. and Ma, X. (2010). Intracellular redox imbalance and extracellular amino acid metabolic abnormality contribute to arsenic-induced developmental retardation in mouse preimplantation embryos. *J Cell Physiol* **222**, 444-455.

Chapter 3

3 Loss of p66Shc accelerates primitive endoderm identity in the inner cell mass of mouse blastocysts

A version of this chapter has been submitted for publication, entitled:

Edwards, N.A., Watson, A.J., Betts, D.H. (2018) Knockdown of p66Shc alters lineage-associated transcription factor expression in mouse blastocysts.

3.1 Introduction

Mouse preimplantation embryo development results in the formation of a blastocyst containing three distinct cell types: the trophoctoderm (TE), the primitive endoderm (PrE), and the epiblast (EPI). Post-implantation, the TE and PrE form extraembryonic structures, while the EPI will contribute to the fetal germ layers and germ cells. Proper specification of these three cell lineages requires spatiotemporal activation of signalling pathways that promote the expression of lineage-specific markers, some of which are required to maintain cell fate and identity. In the 8-16 cell embryo, the HIPPO signalling pathway is the main signalling pathway critical to establishing TE versus inner cell mass (ICM) cell identity (Cockburn et al., 2013; Hirate et al., 2013; Nishioka et al., 2009). In the blastocyst, differential fibroblast growth factor 4 (FGF4)/mitogen-activated protein kinase (MAPK) signalling drives the acquisition of an EPI or PrE fate in the ICM (Frankenberg et al., 2011; Krawchuk et al., 2013; Yamanaka et al., 2010). Disrupting components of either signalling pathway results in aberrant cell fate specification and failure to maintain embryonic development post-implantation, or failure to generate lineage-specific stem cells (Cockburn et al., 2013; Hirate et al., 2013; Krawchuk et al., 2013; Lorthongpanich et al., 2013).

Of these signalling pathway components, receptor tyrosine kinase (RTK) signalling in response to FGF4 binding is required for PrE cell fate determination. Growth factor receptor-bound protein 2 (GRB2) is an adaptor protein linking activated RTKs to Ras/MAPK signalling. *Grb2* knockout (KO) embryos have ICMs containing no PrE cells as identified by the absence of *Gata6* expression. Instead, all cells of *Grb2* KO blastocyst ICMs are Nanog positive, an EPI cell marker (Chazaud et al., 2006). These results therefore demonstrate that MAPK signalling downstream of RTK activation is required for PrE specification. Similarly, embryos treated with the extracellular signal-regulated kinase (ERK) inhibitor PD0325901 from the 8-cell to the blastocyst stage generate ICMs containing all EPI cells (Yamanaka et al., 2010). However, this phenotype is partially reversible if the inhibitor is removed by embryonic day 3.75 (E3.75), indicating that ICM cells maintain plasticity until E4.0-E4.5. Similarly, cell aggregation experiments showed that ICM cells lose plasticity by E4.5 (Grabarek et al., 2012). Thus, MAPK signalling is

important for stabilizing PrE specification in the blastocyst until commitment occurs just prior to implantation.

Another RTK signalling pathway component expressed in many cell types is the family of SHC1 adaptor proteins. P66Shc is an isoform of the Shc1 gene that, unlike the p52Shc isoform, negatively regulates RTK/MAPK signalling. P66Shc contains a phosphotyrosine binding domain that associates with activated RTKs but does not activate downstream Ras-MAPK signalling (Migliaccio et al., 1997; Okada et al., 1997). Under conditions of oxidative stress, p66Shc is phosphorylated, translocates to the mitochondria, and promotes the release of reactive oxygen species (ROS), leading to apoptosis. We have demonstrated that p66Shc is expressed in mouse preimplantation embryos, is upregulated at the blastocyst stage, and that its expression is modulated by the culture environment (Edwards et al., 2016). Loss of function studies using RNA interference (RNAi) showed that p66Shc promotes apoptosis and senescence associated with an increase in ROS in cow and mouse embryos exposed to stress-inducing environmental conditions (Betts et al., 2014; Favetta et al., 2007; Ren et al., 2014). However, whether p66Shc has a biological function that is required to ensure proper preimplantation development remains unknown.

Due to its role in RTK/MAPK signalling in other cell types, we hypothesize that p66Shc might act as a regulatory component in the pathways underlying blastocyst cell lineage specification. Thus, the objective of our study was to determine the role of p66Shc in mouse blastocyst development using short interfering RNA (siRNA) knockdown in mouse preimplantation embryos. Interestingly, our results show that mouse embryos with decreased p66Shc levels formed blastocysts with faster restriction of OCT4 to the inner cells, had an earlier onset of GATA4 expression, and had earlier sorting of PrE cells to the PrE layer. P66Shc knockdown ICMs contained significantly more PrE cells than EPI cells most likely mediated through altered regulation of ERK signalling. Thus, we have uncovered a novel role for p66Shc associated with the timing and expression of lineage-associated transcription factors in the inner cell mass of mouse blastocysts.

3.2 Materials and Methods

3.2.1 Animal source and ethical approval

Female and male wild type CD1 mice were obtained from Charles River Canada (St-Constant, Quebec, Canada). Mice were housed with a 12h light/dark cycle and access to food and water ad libitum. All experimental protocols were approved by the University of Western Ontario Animal Care and Veterinary Services and the Canadian Council of Animal Care (protocol Watson #2010-021). For all experiments, mice were euthanized by CO₂ asphyxiation.

3.2.2 Mouse zygote collection and culture

Three- to four-week old female CD1 mice were superovulated by intraperitoneal (i.p.) injection of pregnant mare serum gonadotropin (Merck Animal Health, Canada) followed by i.p. injection of human chorionic gonadotropin (Merck Animal Health, Canada) 48 hours later. Female mice were then singly housed with male mice for mating. The following morning, female mice were checked for the presence of a vaginal plug. Females with vaginal plugs were euthanized and oviducts were dissected. Zygotes were collected by flushing the oviducts with M2 medium (Sigma-Aldrich, Canada). To remove cumulus cells, zygotes were briefly incubated in M2 medium containing hyaluronidase (Zenith Biotech, USA). Zygotes were washed through drops of M2 medium, followed by washes in embryo culture medium (potassium simplex optimized media with amino acids, KSOMaa, Zenith Biotech, USA). Embryos were cultured in KSOMaa in a 5% O₂, 5% CO₂, 90% N, 37°C humidified incubator. Zygotes underwent a recovery period for a minimum of one hour after collection prior to microinjection. Post injection, mouse embryos were cultured for up to 110 hours post siRNA injection in KSOMaa in a 5% O₂, 5% CO₂, 90% N, 37°C humidified incubator. For MEK inhibitor experiments, embryos were incubated in KSOMaa containing 1 μM PD0325901 (Selleck Chemicals, USA) or DMSO (vehicle control; Sigma Aldrich, Canada) for 24 hours. For the *in vitro* blastocyst outgrowth assay, the zona pellucida was removed by briefly incubating blastocysts in Acidic Tyrode's Solution (Sigma Aldrich, Canada). One to three blastocysts were transferred to one well of an 8-well chamber slide (Ibidi, USA) on a feeder layer of

irradiated mouse embryonic fibroblasts (ATCC, Canada). Embryos were cultured for four days in Knockout DMEM/F12 containing 20% Knockout Serum Replacement (Life Technologies, Canada), 1% GlutaMAX (Life Technologies, Canada), non-essential amino acids, 55 μM β -mercaptoethanol, and 1000 U/ml mouse LIF (Sigma Aldrich, Canada).

3.2.3 Cytoplasmic microinjection of siRNA

Short interfering RNA (siRNA) oligonucleotide sequences targeting the mouse p66Shc transcript and scrambled control targets used in previous studies (Betts et al., 2014; Nemoto et al., 2006) (*see* Table 3-1 for sequences), were synthesized by Thermo Fisher Scientific (Silencer Select siRNA, Canada). siRNA were stored at -20°C as a 100 μM stock and diluted in nuclease-free water. Diluted siRNA solutions were back filled into Femtotips (outside diameter 1 μM , Eppendorf, Germany). Mouse zygotes were held in M2 medium overlaid with embryo culture grade oil (Zenith Biotech, USA) during injection periods. The cytoplasm of mouse zygotes was injected with 10 μl of 50 μM of either p66Shc-specific or scrambled sequence siRNA using a FemtoJet Microinjector (Eppendorf, Germany) at the following settings: injection pressure 75 hPa, injection time 0.1s, constant pressure 15 hPa (Betts et al., 2014). After injection, mouse zygotes were placed into KSOMaa and any embryos that had lysed were immediately removed from culture. Twenty zygotes were injected at a time, then moved to a 5% CO_2 , 37°C humidified incubator until all injections were completed.

3.2.4 Mouse embryonic stem cell transfection

R1 mouse embryonic stem cells (Sick Kids, Toronto, Canada) were cultured without mouse embryonic fibroblast feeders on 0.1% gelatin in Knockout DMEM/F12/Neurobasal media (Life Technologies, Canada) supplemented with 1% N2, 2% B27 (Life Technologies, Canada), 1000 U/ml mouse LIF (Esgro, Millipore, USA), 3 μM CHIR99021 (Selleck Chemicals, USA), and 1 μM PD0325901 (Selleck Chemicals, USA). Cells were transfected with 60 pmol of siRNA with Lipofectamine 3000 (Thermo Fisher Scientific, Canada) according to manufacturer's protocols. Twenty-four hours post

Table 3-1. siRNA sequences.

p66Shc siRNA #1	Sense: UGAGUCUCUGUCAUCGCUGtt Antisense: CAGCGAUGACAGAGACUCAtt
Scrambled siRNA #1	Sense: AUGCGUCGCGAUUAUAUCUtt Antisense: AGAUAAUAAUCGCGACGCAUgc
p66Shc siRNA #2	Sense: ACAACCCACUUCGGAAUGAtt Antisense: UCAUUCCGAAGUGGGUUGUac
Scrambled siRNA #2	Sense: AGCCGUCAAUCACUACAGUtt Antisense: ACUGUAGUGAUUGACGGCUUc

siRNA transfection, cells were lysed in radioimmunoprecipitation assay (RIPA, 150 mM NaCl, 1% Triton X-100, 0.5% sodium deoxycholate, 0.1% SDS, 50 mM Tris) buffer for immunoblotting.

3.2.5 Quantitative real time RT-PCR

RNA was extracted from pools of 20 cleavage stage embryos or 10 blastocysts using the PicoPure RNA Isolation Kit (Thermo Fisher Scientific, Canada) according to manufacturer's instructions. During extraction, RNA was incubated with RNase-Free DNase I (Qiagen, Canada) to digest genomic DNA from the samples. RNA was reverse transcribed to cDNA using SuperScript III (Thermo Fisher Scientific, Canada) according to manufacturer's instructions with the following modifications: priming was done with random hexamers (Thermo Fisher Scientific, Canada) and a gene specific reverse primer (Edwards et al., 2016). Quantitative real time qPCR was performed on a CFX384 thermal cycler (BioRad, Canada) using SensiFAST SYBR (FroggaBio, Canada) and a final concentration of 400 nM primers with the following cycling conditions: 95°C for 2 mins, 39 cycles of 95° for 5 seconds, 60°C for 10 seconds, 72°C for 20 seconds. Ct values were obtained from Bio-Rad CFX Manager 3.1 (BioRad, Canada). Relative transcript abundance was determined by using the delta-delta Ct method using the geometric mean of Ct values of *Ppia* and *Hprt* for normalization. Primer sequences are in Table 3-2.

3.2.6 Immunoblotting

Cells and embryos were lysed in RIPA buffer containing protease and phosphatase inhibitors (Millipore, USA) and stored at -80°C until processing. Total protein lysates were resolved on a 4-12% Bis-Tris polyacrylamide gel (Thermo Fisher Scientific, Canada) and transferred to a PVDF membrane (Millipore, USA). Membranes were blocked in 5% skim milk in TBST for one hour at room temperature. Membranes were then incubated in primary antibody diluted in 5% skim milk in TBST overnight at 4°C at the following dilutions: mouse anti-Shc (BD Biosciences 610879, 1:500), rabbit anti-CDX2 (Abcam ab76541, 1:500), rabbit anti-EOMES (Abcam ab23345, 1:1000). Membranes were then incubated in HRP-conjugated secondary antibody (Jackson Labs, 1:2000) diluted in 5% skim milk in TBST for one hour at room temperature prior

Table 3-2. Oligonucleotide primer sequences.

Gene	Sequences	Expected RT-PCR product size
p66Shc	F: 5'- CCGACTACCCTGTGTTTCCTTCTT-3' R: 5'- CCCATCTTCAGCAGCCTTTCC-3'	111 bp
<i>Cdkn1a</i>	F: 5'- TCCAGACATTCAGAGCCACAGG-3' R: 5'- ACGGGACCGAAGAGACAACG-3'	97 bp
<i>Rbl</i>	F: 5'- CTTGCATGGCTTTCAGATTCACCT-3' R: 5'- ATGGTTACCCTGGAGAGGCAG-3'	117 bp
<i>Trp53</i>	F: 5'- GGACCATCCTGGCTGTAGGT-3' R: 5'- GGCAGTCATCCAGTCTTCGG-3'	113 bp
<i>Gadd45a</i>	F: 5'- TGCTGGTGACGAACCCACAT-3' R: 5'- CATGTAGCGACTTTCCTCCGGC-3'	86 bp
<i>Dusp4</i>	F: 5'- AAAGTGGGTGCCGTTTCAGAT-3' R: 5'- AACACCCAATGTATCCGCGA-3'	116bp
<i>Ppia</i>	F: 5'- GTCCTGGCATCTTGTCCATG-3' R: 5'- TGCCTTCTTTCACCTTCCCA-3'	126 bp
<i>Hprt</i>	F: 5'- GCTTACCTCACTGCTTTCCTG-3' R: 5'- ATCATCGCTAATCACGACGC-3'	128 bp

to ECL detection (Luminata Forte, Millipore, USA). Western blot images were taken with a ChemiDoc Imaging System (BioRad, Canada) and densitometry analysis of band intensity was performed in ImageLab 4.0 (BioRad, Canada). Membranes were stripped for 20 minutes using Antibody Stripping Buffer (FroggaBio, Canada), then blocked and probed with mouse anti- β -actin-HRP (Sigma A3854, 1:10,000).

3.2.7 Immunofluorescence and confocal microscopy

Embryos were fixed in 2% paraformaldehyde in PBS for 30 minutes at room temperature. Embryos were then permeabilized in 0.25% Triton X-100 in PBS for 30 minutes, blocked in 5% normal goat serum in PBS, and incubated overnight at 4°C in the following primary antibodies: mouse anti-NT-Shc (Acris AM00143PU-N, 1:100, validated in Edwards et al., 2016), mouse anti-OCT3/4 (C-10, Santa Cruz Biotech sc-5279, 1:50), goat anti-GATA4 (Santa Cruz Biotech sc-1237, 1:200), rabbit anti-cleaved caspase-3 (R&D Systems AF835, 1:50), rabbit anti-CDX2 (Abcam, 1:100), rabbit anti-Nanog (ReproCell, RCAB001P, 1:200), rabbit anti-DUSP4 (Abcam ab216576, 1:200). Embryos were then incubated at room temperature for 1 hour in either Alexa Fluor 488 or 594 conjugated secondary antibodies (Thermo Fisher Scientific, Canada), then mounted in VectaShield antifade solution (Vector Labs, USA) on a glass microscopy slide. Confocal microscopy was performed with a Zeiss LSM510 laser scanning confocal microscope with ten z-sections taken through each blastocyst. Laser settings were unchanged when detecting the same primary antibody between treatment groups. Nuclei with detectable antibody staining were manually counted in duplicate in ImageJ (National Institutes of Health). For fluorescence intensity quantification, 3D z-stack projections were created in ZEN Black (Zeiss, Germany) exported as TIFF files and opened in ImageJ. Images were converted to grayscale and LUT inverted. The mean grey value was measured, and the average mean grey value of three images of embryos with no primary antibody was subtracted to control for background fluorescence.

3.2.8 BrdU incorporation assay

Embryos were incubated in KSOMaa containing 10 μ M of bromodeoxyuridine (BrdU, Acros Organics, USA) for 45 minutes before fixation with 2% paraformaldehyde.

Embryos were then processed for immunofluorescence as described above with the following additions: after permeabilization, embryos were incubated in 300 ug/ml DNase for 30 minutes at 37°C (Xie et al., 2006). Embryos were incubated overnight at 4°C in mouse anti-BrdU antibody (G3G4, Developmental Studies Hybridoma Bank deposited by Kaufman, S.J., 1:100), then incubated at room temperature for 1 hour in goat-anti-mouse Alexa Fluor 488 (1:400). Confocal microscopy was performed as described above.

3.2.9 Statistical Analyses

Statistical tests were performed using Prism 6 (GraphPad Inc.) for Students' t-test (unpaired, two-tailed with equal variance) or Fisher's exact test (two-tailed). At least three independent replicates were performed for each experiment.

3.3 Results

3.3.1 Specific knockdown of p66Shc in mouse preimplantation embryos

To target p66Shc for knockdown by RNAi, two siRNA sequences were designed to recognize the unique N-terminal exon of the p66Shc transcript variant of mouse Shc1 (sequences in Table 3-1). 50 μ M of each sequence, designated #1 and #2, and its associated control (scrambled nucleotide) sequence was microinjected into the cytoplasm of zygotes. Pools of embryos were then collected at different time points post siRNA injection to assess knockdown efficiency by quantitative real time RT-PCR. We were unable to detect a statistically significant decrease in p66Shc transcript abundance 24 hours post siRNA #1 injection due to the high variability of p66Shc transcript levels in control 2-cell embryos (Edwards et al., 2016) (Fig. 3-1A). However, p66Shc transcript abundance significantly decreased to 33% of control levels in embryos injected with p66Shc siRNA #1 48 hours post injection ($p < 0.05$, Fig. 3-1A). By 72 and 96 hours post injection p66Shc transcript abundance levels in embryos injected with p66Shc siRNA became comparable to controls (Fig. 3-1A). P66Shc sequence #2 also significantly knocked down p66Shc transcript abundance 48 hours post siRNA injection (Fig. 3-2A). Due to the higher knockdown efficiency at 48 hours post injection, the remaining

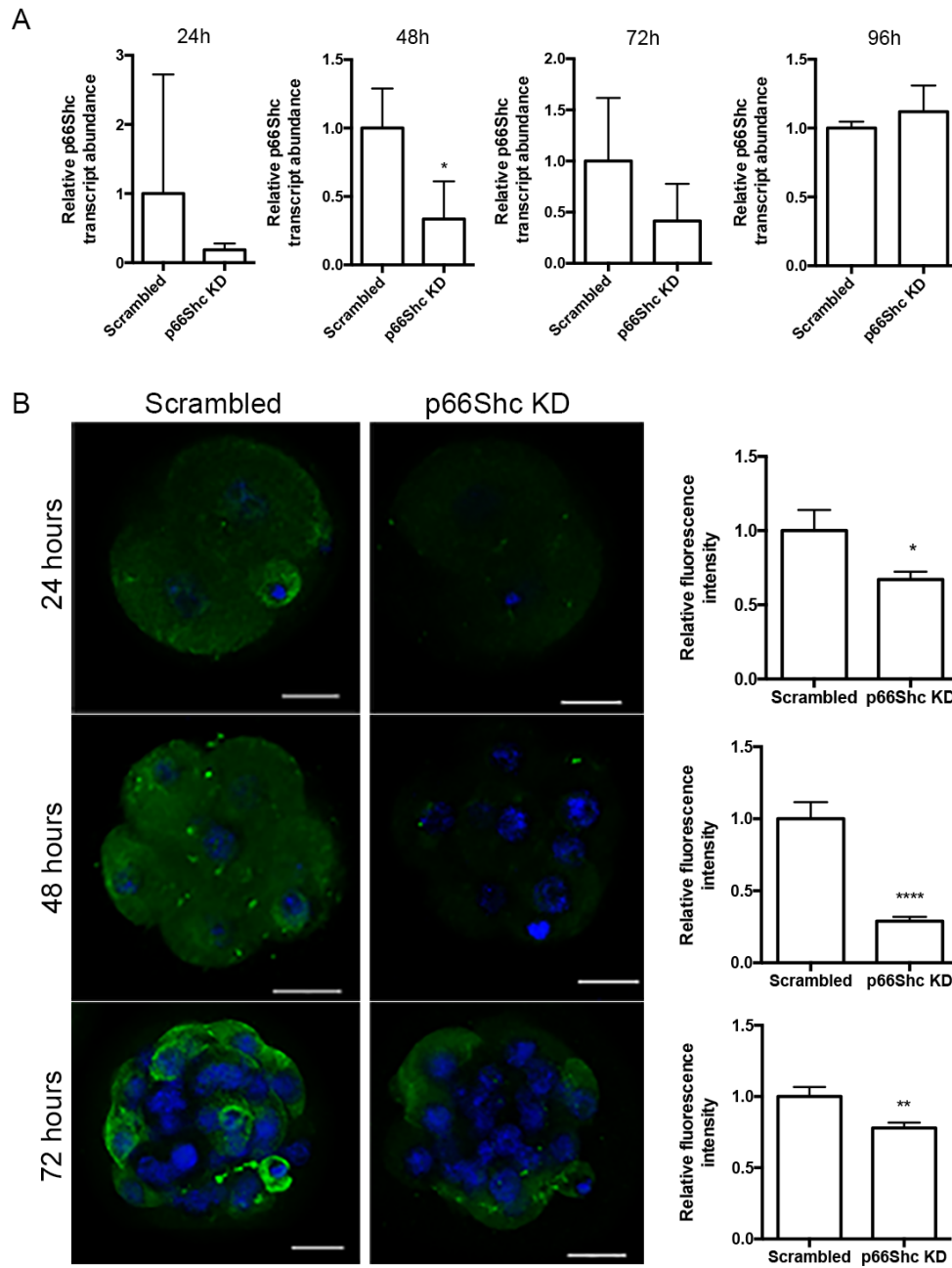


Figure 3-1. p66Shc siRNA reduces p66Shc transcript and protein abundance in mouse preimplantation embryos.

(A) RT-qPCR was performed on pools of 20 embryos or 10 blastocysts at four-time points post injection of 50 μ M siRNA (24h N=5 pools of embryos, 48h N=4, 72h N=4, 96h N=3). P66Shc transcript abundance is significantly reduced at 48 hours post siRNA injection (mean \pm SD, * $p < 0.05$, Student's t-test). (B) Immunofluorescence and confocal microscopy for p66Shc protein was performed on embryos taken at three-time points post siRNA injection. The relative fluorescence intensities of z-stack projections were quantified. P66Shc fluorescence intensity was significantly decreased at 24 (n=15 embryos), 48 (n=17), and 72 hours (n=14) post p66Shc-siRNA injection compared to controls (mean \pm SEM, * $p < 0.05$, ** $p < 0.01$, **** $p < 0.00001$, Student's t-test). Scale bars are 20 μ m.

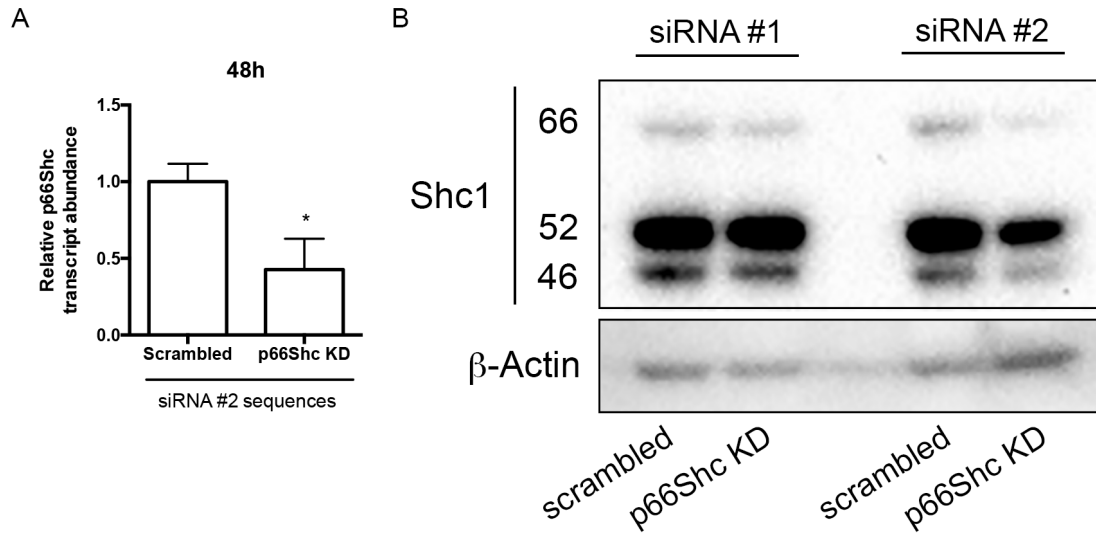


Figure 3-2. Efficiency of p66Shc knockdown by siRNA.

(A) P66Shc is significantly knocked down in mouse embryos by p66Shc siRNA sequence #2 48 hours post injection (n=3 pools of 20 embryos, mean \pm SD, * $p < 0.05$, Student's t-test). (B) p66Shc is knocked down in mouse embryonic stem cells by both p66Shc siRNA sequences 24 hours post transfection. A representative immunoblot of three independent experiments is shown.

experiments were performed with sequence #1. Some experiments were replicated by injection of sequence #2 to confirm gene-specific phenotypes.

To confirm knockdown at the protein level, zygotes were injected with siRNA #1 sequences, fixed 24, 48, and 72 hours post injection, and stained for p66Shc immunofluorescence. Significant decreases in p66Shc fluorescence intensity were detected at all three time points post siRNA injection, with the greatest reduction in fluorescence intensity observed at 48 hours post siRNA injection (29% of control levels, $p < 0.0001$, Fig. 3-1B, additional microscopy pictures in Fig. 3-3). Thus, our results demonstrate that 50 μ M of p66Shc-specific siRNA significantly reduces p66Shc transcript and protein levels during mouse preimplantation development. Knockdown specificity and efficiency were confirmed in R1 mouse embryonic stem cells (Fig. 3-2B).

3.3.2 P66Shc knockdown embryos form blastocysts containing more cells than controls

We next aimed to determine if embryos receiving p66Shc siRNA could form blastocysts. Blastocyst formation did not significantly change in embryos receiving p66Shc siRNA compared to controls with frequencies of blastocyst development observed between 60-70% (Fig. 3-4A). Blastocysts formed by embryos that received p66Shc siRNA were morphologically identical to scrambled siRNA injected controls (Fig. 3-4B). However, p66Shc knockdown blastocysts contained, on average, 12 more cells than scrambled controls at 96 hours post injection (Fig. 3-4C, middle panel). Interestingly, p66Shc knockdown embryos at 72 hours post injection contained significantly fewer cells than scrambled controls, while p66Shc knockdown embryos at 110 hours post injection contained cell numbers comparable to controls (Fig. 3-4C). This suggests that although embryos receiving p66Shc siRNA can form blastocysts, they produce blastocysts with more total cells than controls four days after p66Shc siRNA introduction.

We next investigated the effects of p66Shc knockdown on cell apoptosis and proliferation at 96 hours. There was no difference in the percentage of cleaved caspase-3 positive cells in p66Shc knockdown blastocysts compared to controls, suggesting that apoptosis is not contributing to the change in total cell number (Fig. 3-5A). However, p66Shc knockdown

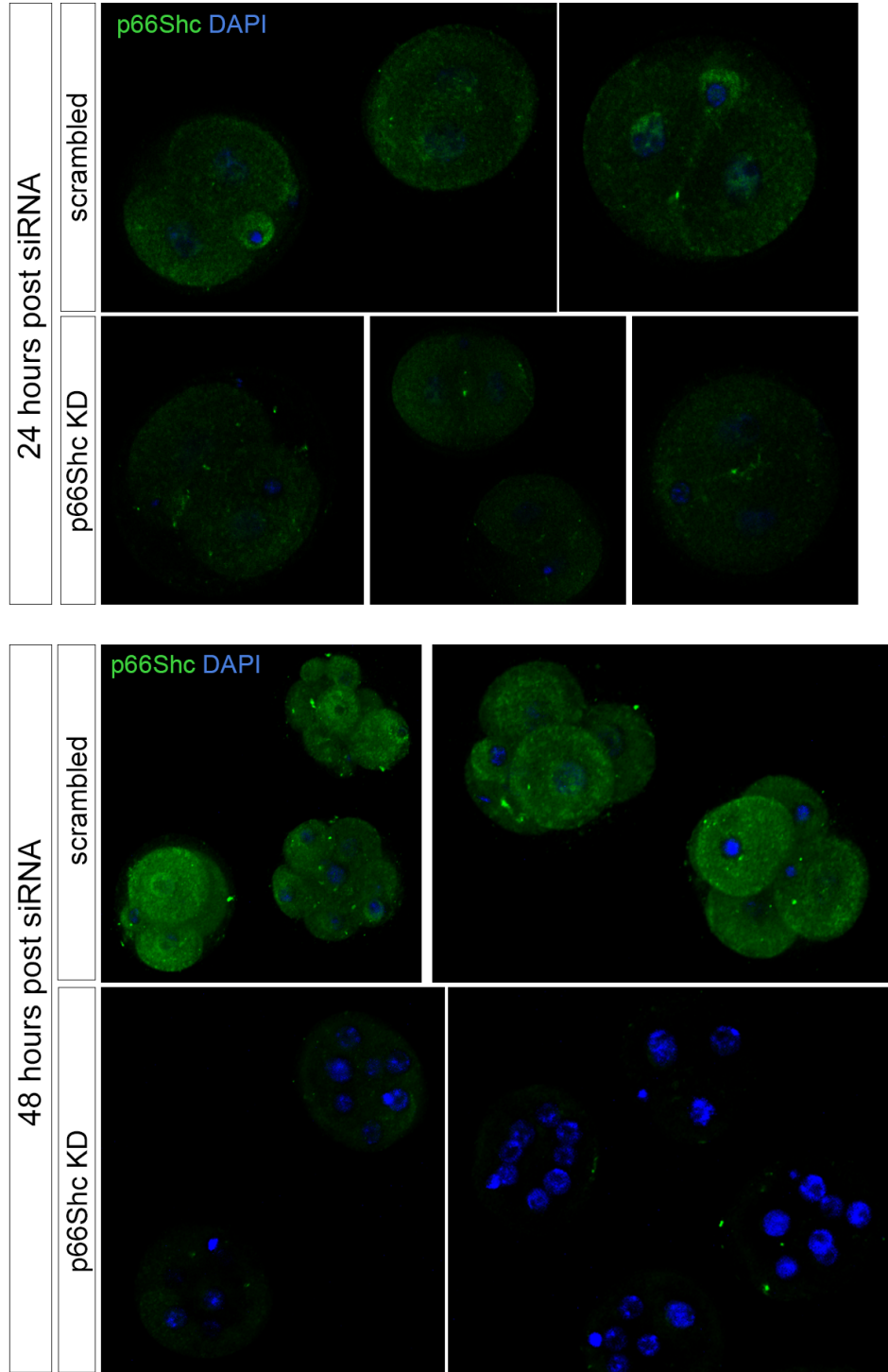


Figure 3-3. P66Shc protein knockdown confirmed post siRNA injection in mouse embryos.

Panels show additional immunofluorescent confocal microscopy images at 24 (upper panel) and 48 hours (lower panel) post siRNA injection.

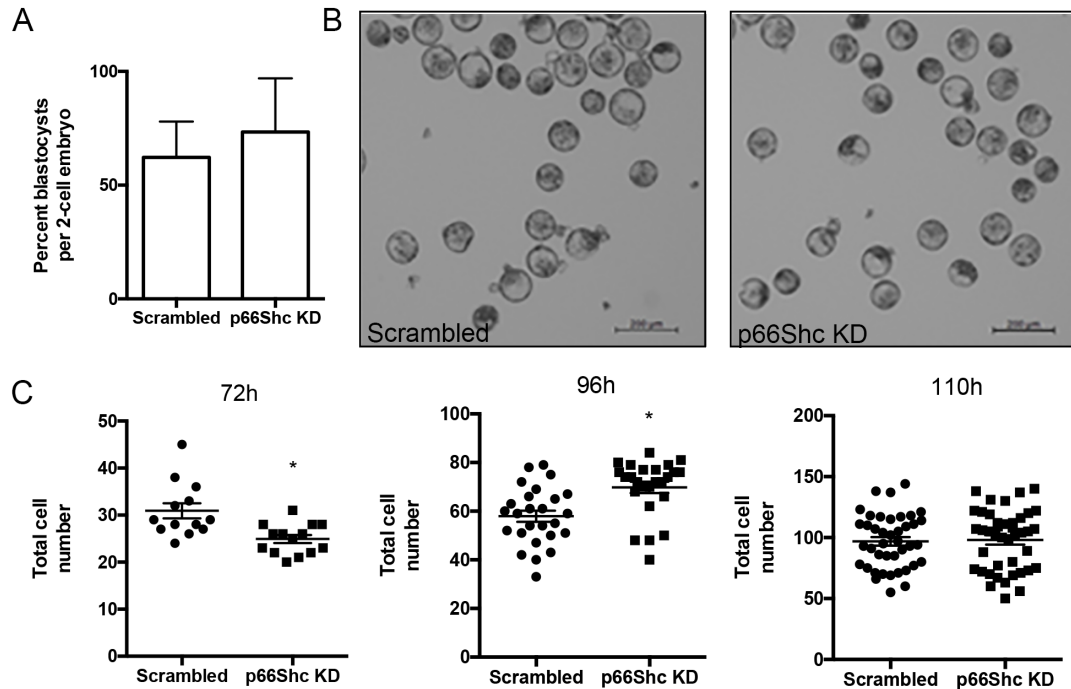


Figure 3-4. p66Shc knockdown embryos form blastocysts containing more cells than controls.

(A) Embryos receiving p66Shc siRNA form blastocysts at equivalent rates to scrambled controls (N=3 experimental replicates, mean \pm SD). (B) p66Shc knockdown embryos form morphologically similar blastocysts compared to scrambled controls (scale bars = 200 μ m). (C) Total cell number in p66Shc knockdown embryos is significantly lower than controls at 72 hours post siRNA injection (n=15 per group, *p<0.05, Student's t-test), significantly higher than controls at 96 hours post siRNA injection (n=25 per group, *p<0.05, Student's t-test) and not significantly different at 110 hours post siRNA injection (n=41 per group). Graphs are the mean \pm SEM.

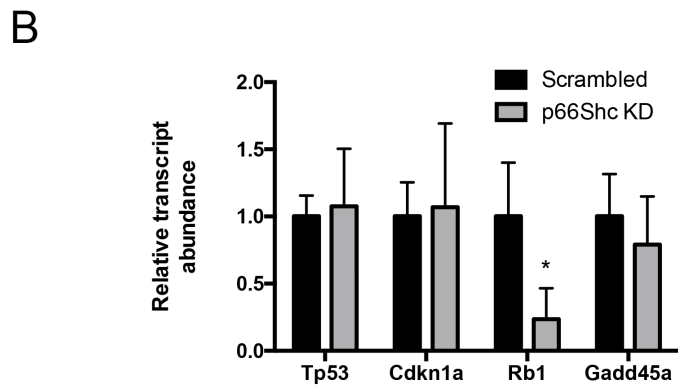
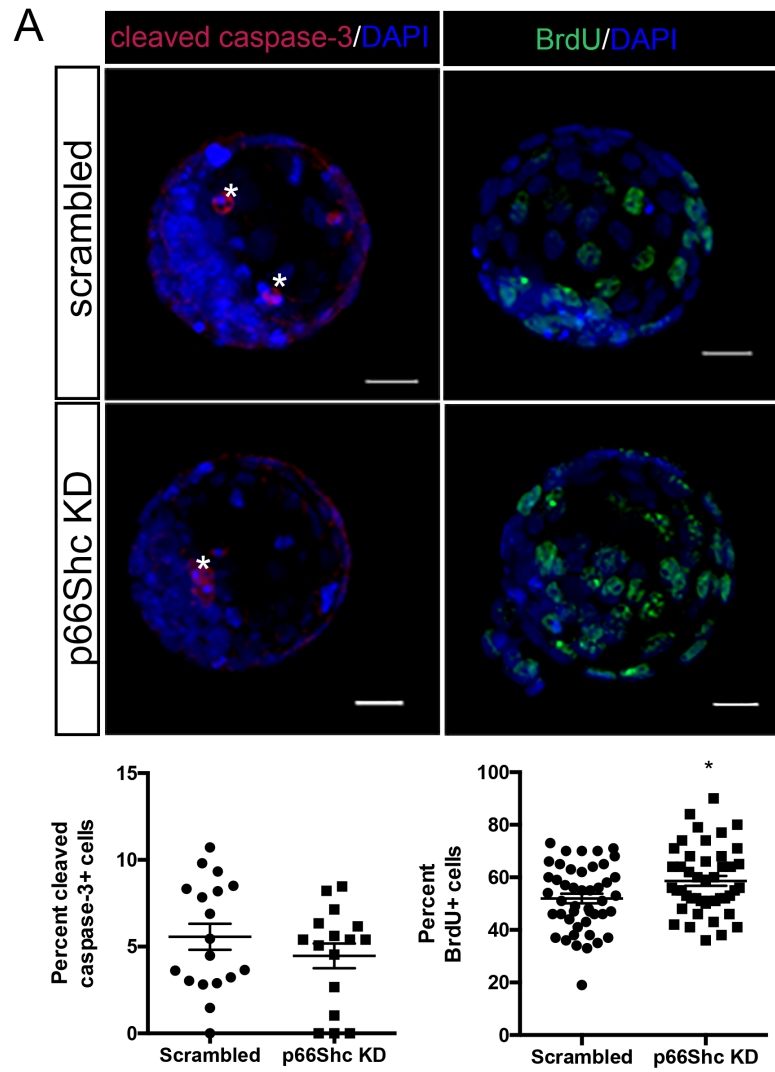


Figure 3-5. Altered proliferation in p66Shc knockdown blastocysts.

(A) p66Shc knockdown blastocysts have similar levels of cleaved caspase-3 cells compared to controls (n=16, mean \pm SEM, white asterisks indicate cells positive for cleaved caspase-3). However, p66Shc knockdown blastocysts have a significantly increased percentage of cells positive for BrdU incorporation after 45 minutes of incubation compared to controls (n=46, *p<0.05, mean \pm SEM, Student's t-test). (B) RT-qPCR was performed on pools of 10 blastocysts for transcript abundance of cell cycle markers. P66Shc knockdown blastocysts have significantly lower *Rb1* transcript abundance compared to controls (N=3 pools of 10 embryos, *p<0.05, mean \pm SD, Student's t-test).

embryos at 96 hours displayed significantly increased BrdU incorporation, which reflects the increased total cell number observed (Fig. 3-5A). Interestingly, p66Shc knockdown blastocysts had significantly reduced *Rb1* transcript abundance compared to controls, suggesting that the G1/S checkpoint was altered in these embryos (Fig. 3-5B).

3.3.3 P66Shc knockdown accelerates the onset of primitive endoderm identity in mouse blastocysts

Though p66Shc knockdown embryos formed blastocysts at the same frequency and appeared morphologically like controls, we hypothesized that loss of p66Shc might produce differences in cell allocation of the TE and ICM. To investigate this directly, we processed blastocysts 96 hours post siRNA injection for immunofluorescence and confocal microscopy for CDX2 and OCT3/4, markers of the TE and ICM respectively. Two patterns of OCT3/4 staining were observed in both scrambled control and p66Shc knockdown blastocysts. Sixty percent of p66Shc knockdown blastocysts showed OCT3/4 restriction to the inner cells compared to 25% of scrambled control blastocysts when fixed at 96 hours post siRNA injection (Fig. 3-6). Total protein abundance of CDX2 and EOMES was unaffected by p66Shc knockdown, suggesting that p66Shc knockdown does not affect the expression of TE markers in the blastocyst (Fig. 3-7A).

To further quantify the differences in OCT3/4 staining, nuclei were counted for detectable OCT3/4 and CDX2 staining. To analyze blastocysts at approximately the same developmental time point, we determined the total cell number and categorized embryos from both groups into blastocysts containing 32-64 cells or blastocysts containing 64-128 cells. In 32-64 cell blastocysts, p66Shc knockdown blastocysts contained approximately the same percentage of double positive (OCT3/4+ and CDX2+) nuclei. However, at the 64-128 cell stage, p66Shc knockdown embryos contained a significantly lower percentage of double positive nuclei, supporting the observation that OCT3/4 expression is restricted earlier in p66Shc knockdown blastocysts compared to controls (Fig. 3-6).

Since OCT3/4 is restricted earlier to the inner cells in p66Shc knockdown blastocysts, we hypothesized that the ICMs in these embryos might be developmentally advanced in regard to their differentiation program and may be specifying EPI versus PrE fate earlier

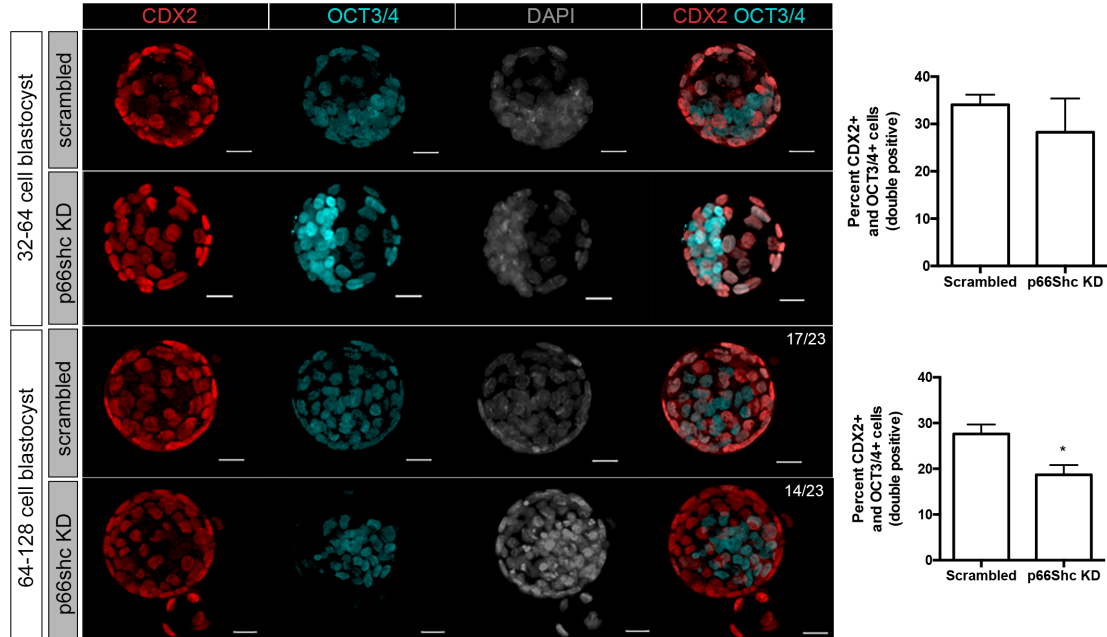


Figure 3-6. Earlier restriction of OCT3/4 to the inner cells in p66Shc knockdown blastocysts.

Embryos were categorized according to cell number before analysis (32-64 cells or 64-128 cells). Sixty percent of p66Shc knockdown blastocysts showed restricted OCT3/4 immunofluorescent staining to the inner cells of the blastocyst compared to 25% of scrambled control blastocysts (n=23). Numbers in the image panels indicate how many embryos had the displayed staining pattern. P66Shc knockdown blastocysts had similar CDX2+/OCT3/4+ nuclei compared to scrambled controls in 32-64 cell blastocysts, but significantly fewer CDX2+/OCT3/4+ nuclei in 64-128 cell blastocyst (n=23, *p<0.05, mean \pm SEM). Scale bars are 20 μ m.

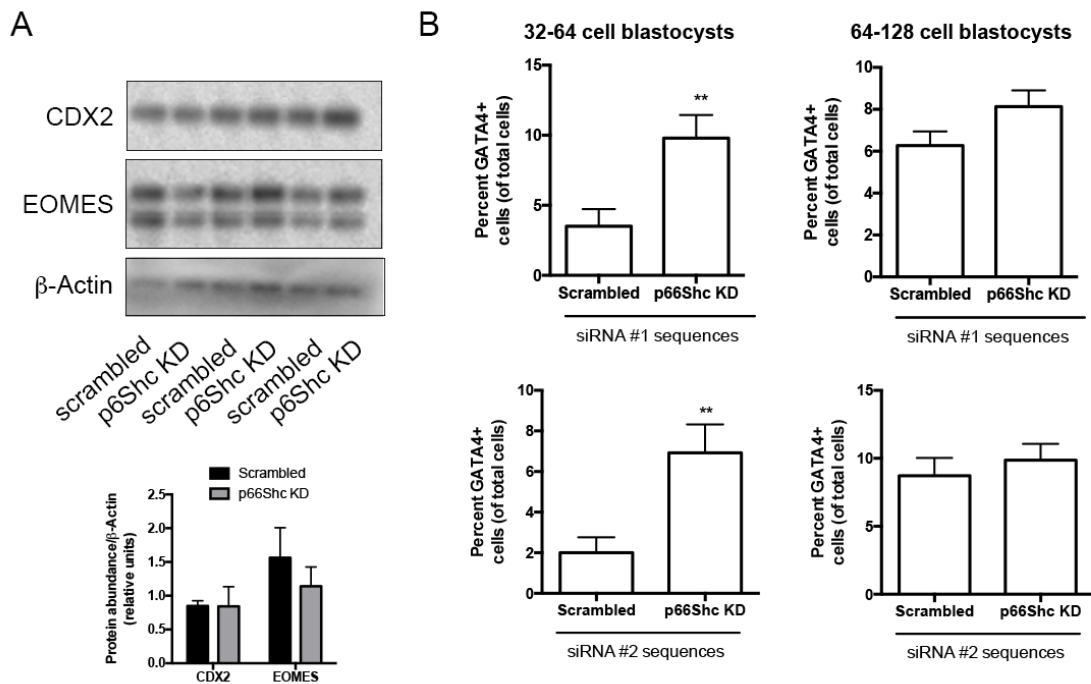


Figure 3-7. P66Shc knockdown increases percent GATA4-positive cells of total cells in blastocysts but does not affect expression of TE markers.

(A) CDX2 and EOMES protein abundance in blastocysts 96 hours post siRNA injection are not significantly changed by p66Shc knockdown. Immunoblots show results from three independent microinjection experiments and the graph below is the densitometry values of the immunoblot (n=3 pools of 25 blastocysts). (B) The percent GATA4+ cells of total cells in p66Shc knockdown blastocysts (32-64 cells) is significantly higher than control embryos using both p66Shc siRNA sequence #1 and #2 (n=16 per group, mean \pm SEM, ** p < 0.01, Student's t-test). The percentage of GATA4+ cells of total cells in 64-128 cell blastocysts is not significantly different than controls (n=47, mean \pm SEM, Student's t-test).

than controls. To investigate this, blastocysts were fixed and processed for immunofluorescence for GATA4 and Nanog, markers of the PrE and EPI fates respectively. In 32-64 cell p66Shc knockdown blastocysts, we observed that the percentage of total cells and inner cells expressing GATA4 was significantly higher than that for scrambled controls (Fig. 3-8, Fig. 3-7B). This increase in the GATA4 positive cell proportion of inner cells was at the expense of Nanog positive cells, and not due to selective proliferation of GATA positive cells, as the total number of inner cells was unchanged between knockdown and control blastocysts (Fig. 3-8). The percentage of GATA4 positive cells of total cells was also significantly increased in embryos receiving the second p66Shc siRNA sequence (Fig. 3-7B).

As ICM cells are not committed until E4.0, we aimed to determine whether the shift to PrE fate in p66Shc knockdown blastocysts persisted in late blastocysts. Blastocysts were cultured to 110 hours post siRNA injection, then fixed and processed for GATA4 and Nanog immunofluorescence. We observed a significant increase in the percentage of GATA4 positive cells of total inner cells and a decreased percentage of Nanog positive cells in p66Shc knockdown blastocysts, though this difference was not as extensive as was observed in 32-64 cell blastocysts (Fig. 3-9A). The total number of inner cells did not significantly change between groups, nor did it significantly increase from 32-64 cell blastocysts, indicating that some GATA4 positive cells altered their fate to become Nanog positive. Additionally, when blastocysts were categorized based on their GATA4 and Nanog staining pattern to determine the extent of primitive endoderm sorting (Plusa et al., 2008), 36% of p66Shc knockdown blastocysts contained GATA4 positive cells categorized as sorted, versus only 14% of the control blastocyst population containing sorted GATA4 positive cells (Fig. 3-9B). Together, our results suggest that not only does the EPI/PrE imbalance in p66Shc knockdown blastocysts persist until E4.5, but these blastocysts also show much earlier sorting to the PrE layer.

We next aimed to determine if the changes to the composition of the ICM in p66Shc knockdown blastocysts affect post-implantation development. Blastocysts were plated for an *in vitro* outgrowth assay under conditions promoting pluripotency for four days and

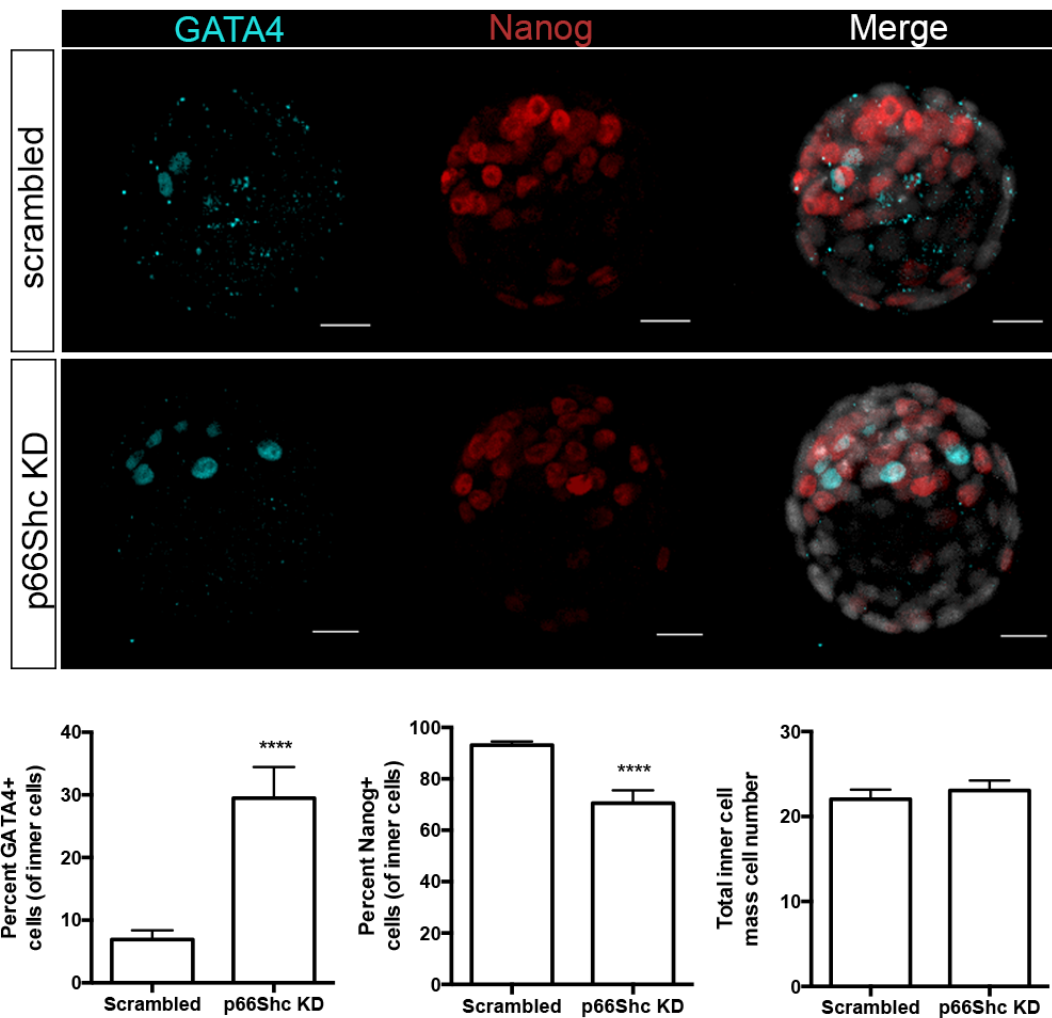


Figure 3-8. Loss of p66Shc promotes primitive endoderm fate in the inner cell mass at E3.5.

Blastocysts were fixed and processed for immunofluorescence and confocal microscopy 96 hours post siRNA injection. p66Shc knockdown blastocysts have significantly increased percentage of inner cells positive for GATA4 and significantly decreased percentage positive for Nanog ($n=19$ per group, mean \pm SEM, **** $p<0.0001$, Student's t-test). The total cell number of the inner cell mass was not significantly different between p66Shc knockdown embryos and controls ($n=19$ per group, mean \pm SEM, Student's t-test). Scale bars are 20 μm .

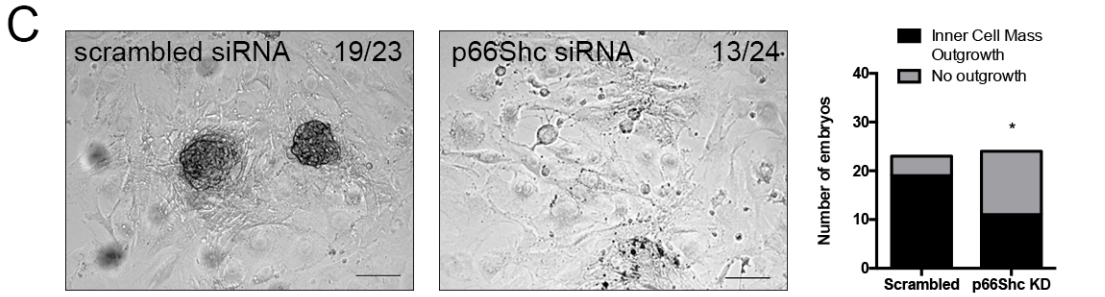
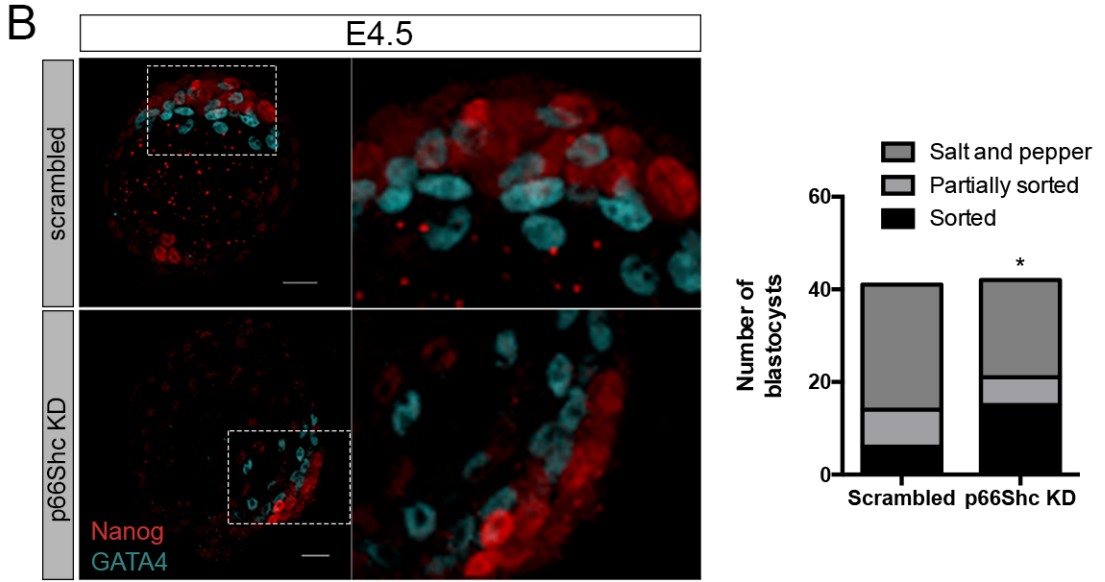
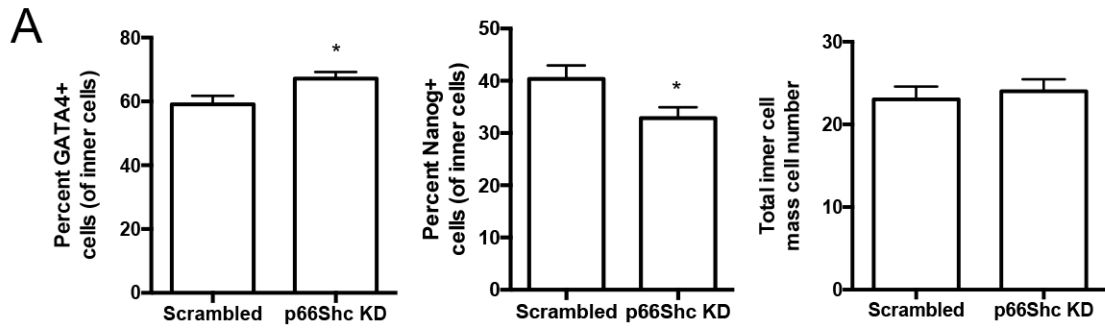


Figure 3-9. Loss of p66Shc accelerates sorting of the primitive endoderm in 64-128 cell blastocysts.

(A) Blastocysts were processed for immunofluorescence and confocal microscopy 110 hours post siRNA injection. p66Shc knockdown late blastocysts had a significant increase in the percentage of inner cells positive for GATA4 and a significant decrease in cells positive for NANOG (n=41 blastocysts, mean \pm SEM, *p<0.05, Student's t-test). (B) At E4.5, p66Shc knockdown blastocysts also had a significantly higher proportion of embryos displaying sorted primitive endoderm staining compared to scrambled controls (n=41 blastocysts per group, *p<0.05, Fisher's exact test). Scale bars are 20 μ m. (C) Bright field microscopy of in vitro blastocyst outgrowths. A significantly lower proportion of p66Shc knockdown blastocysts formed inner cell mass-derived outgrowths compared to scrambled controls (n=23 and 24 outgrowths per group, *p<0.05, Fisher's exact test). Numbers in the image panels indicate the number of outgrowths resembling the displayed morphology. Scale bars are 100 μ m.

then assessed for the presence of an inner cell mass-derived outgrowth (Figure 3-9C). Eighty-two percent of scrambled siRNA-injected blastocysts formed inner cell mass-derived outgrowths (n=19 of 23), while only 46% of p66Shc siRNA-injected blastocysts formed inner cell mass outgrowths (n=11 of 24). We observed formation of trophoblast giant cells in all plated blastocysts, suggesting that p66Shc knockdown does not affect the survival of the trophectoderm *in vitro*. Instead our results suggest that p66Shc knockdown in preimplantation embryos significantly affects the formation of inner cell mass-derived lineages *in vitro*.

3.3.4 P66Shc knockdown increases the number of DUSP4-positive cells in the blastocyst

As the allocation of EPI and PrE cells in the inner cell mass is dependent on FGF4-MAPK signalling (Yamanaka et al., 2010), we next determined if decreased p66Shc levels resulted in a greater number of PrE cells to emerge due to increased or inappropriate MAPK signalling. Like previous studies, we were unable to detect phosphorylated-ERK1/2 in ICM cells by immunofluorescence (Frankenberg et al., 2011). Although we attempted localization of total-ERK1/2 to detect nuclear translocation of ERK1/2, we encountered high background staining by immunofluorescence microscopy (Fig. 3-10A). To overcome the challenge of reliably detecting ERK1/2 activation, we proceeded to define DUSP4 localization, (a transcriptional target of FGF4-MAPK signalling), specific to ICM cells committing to the PrE fate (Kang et al., 2017). Accordingly, we observed DUSP4 co-localization with GATA4 in blastocysts (Fig. 3-11A). We did not observe a significant change in DUSP4 positive cells or *Dusp4* transcript abundance in embryos 72 hours post siRNA injection (Fig. 3-10B). However, p66Shc knockdown blastocysts at 96 hours post siRNA injection contained a significantly higher percentage of DUSP4 positive cells compared to scrambled controls, suggesting that these blastocysts have more cells with active ERK1/2 compared to controls (Fig. 3-11A). The imbalance between EPI and PrE allocation in the inner cell mass of p66Shc knockdown blastocysts was reversed by ERK1/2 inhibition, as treatment for 24 hours with 1 μ M PD0325901 resulted in all inner cells of p66Shc knockdown blastocysts to become Nanog positive 96 hours post siRNA injection (Fig. 3-11B).

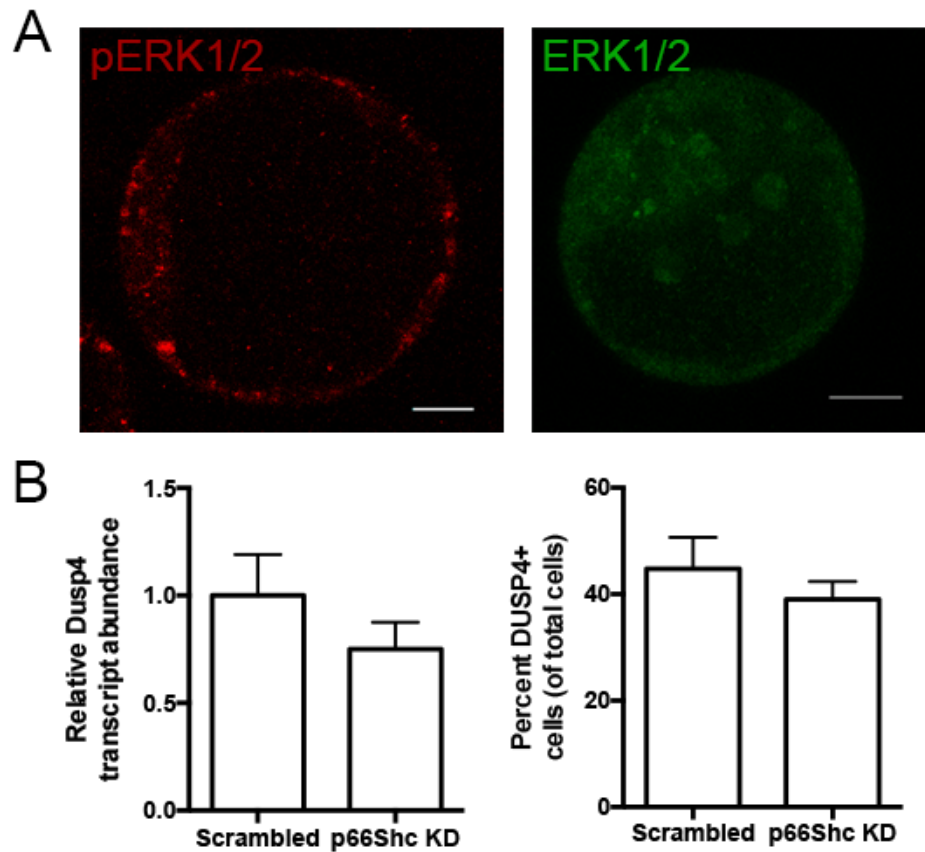


Figure 3-10. High background after immunofluorescent staining of total and phosphorylated ERK1/2.

(A) Representative confocal microscopy images of blastocysts stained for phosphorylated ERK1/2 (left panel) and total ERK1/2 (right panel). High background staining was observed using both antibodies. (B) P66Shc knockdown does not significantly change Dusp4 transcript abundance or the percentage of DUSP4-positive cells in embryos 72 hours post siRNA injection. Graphs represent the mean \pm SEM, n=4 pools of 20 embryos (left), n=10 embryos (right), Student's t-test.

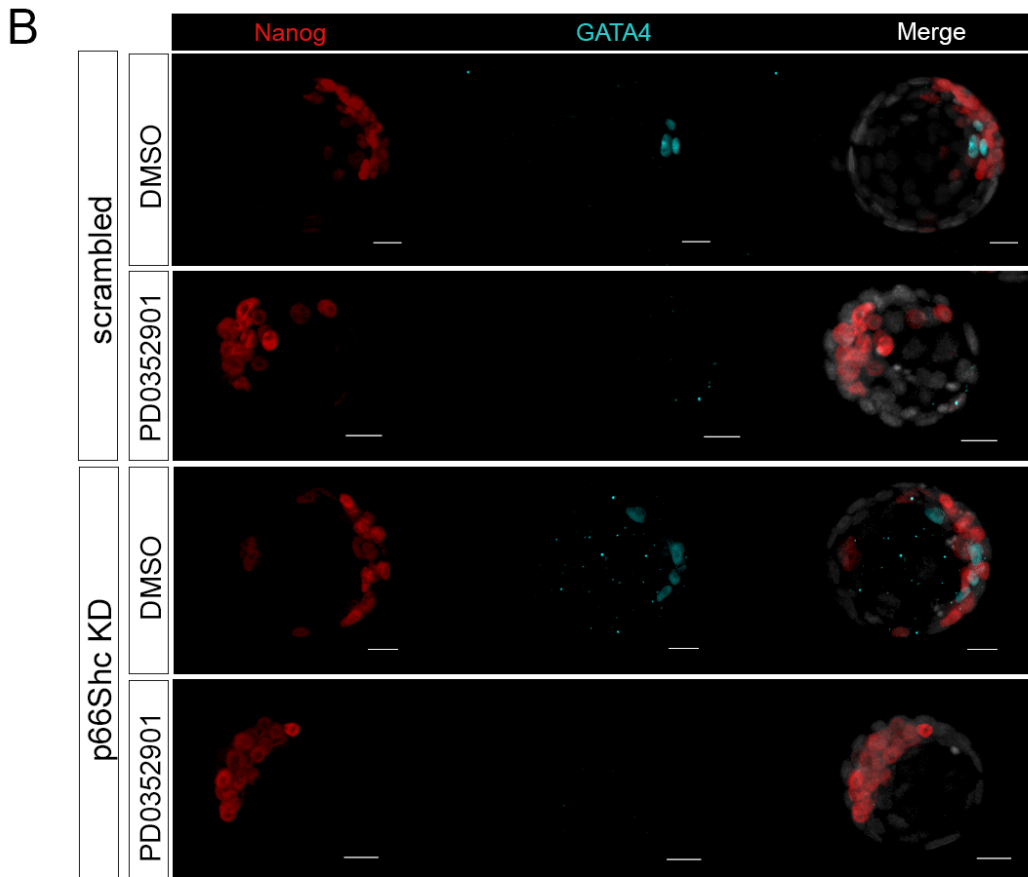
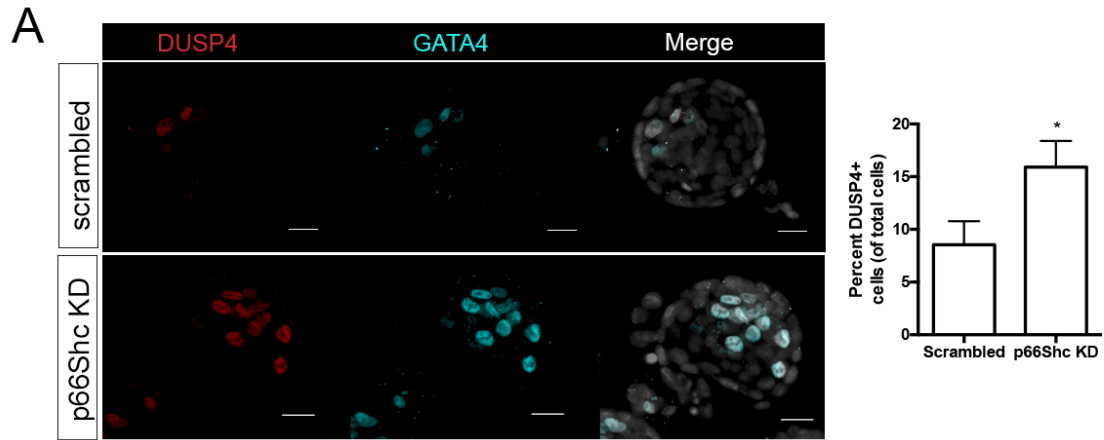


Figure 3-11. p66Shc knockdown blastocysts displayed altered ERK1/2 activity.

(A) p66Shc knockdown blastocysts had a significant increase in cells positive for DUSP4, an ERK1/2 transcriptional target downstream of FGF/MAPK signalling, compared to controls (n=13 blastocysts, mean \pm SEM, *p<0.05). (B) When treated with 1 μ M PD0325901, all cells of the ICM of p66Shc knockdown blastocysts were Nanog⁺ (n=17 blastocysts per group). Scale bars are 20 μ m.

Together, our results suggest that decreased expression of p66Shc leads to increased cells in the blastocyst with active ERK1/2, and that the increase in GATA4 positive cells in the inner cell mass is reversible by MEK1/2 inhibition.

3.4 Discussion

Here we show a novel role for p66Shc during mouse preimplantation development, demonstrating that p66Shc is mechanistically linked to the expression dynamics of blastocyst lineage-associated transcription factors. Our results demonstrate that knockdown of p66Shc during preimplantation embryo development affects the balance of EPI to PrE cells in blastocysts. Knockdown of p66Shc in mouse embryos leads to blastocysts with more PrE cells than EPI cells in the ICM compared to controls. This imbalance is partially resolved by the late blastocyst stage, but PrE cells appear to sort to the PrE layer earlier in knockdown blastocysts compared to controls. When explanted *in vitro*, p66Shc knockdown blastocysts have a decreased ability to generate inner cell mass-derived outgrowths compared to controls. Furthermore, decreased p66Shc expression leads to increased cells expressing DUSP4, and the increased proportion of PrE cells is rescued by ERK1/2 inhibition. Our study also suggests a possible novel role for p66Shc in regulating the cell signaling pathways that lead to cell commitment to extraembryonic endoderm.

Regulation of cell fate is a novel proposed function for p66Shc, as the protein has thus far been shown to negatively regulate embryo development by promoting apoptosis and senescence (embryo arrest). However, many of these effects were stimulated by stressful environmental conditions including treatment with H₂O₂ (Favetta et al., 2007) and arsenic (Ren et al., 2014). In these cases, p66Shc may act to ensure that embryos that cannot adapt to stress do not continue to develop by increasing mitochondrial ROS and promoting apoptosis or senescence. In our study, mouse embryos were cultured under low oxygen conditions and medium supplemented with amino acids to minimize exposure to environmental stress following siRNA injection thus potentially minimizing the stress response function of p66Shc. In contrast to studies with bovine embryos, we did not observe a significant increase in the number of embryos developing into blastocysts after p66Shc knockdown compared to controls, suggesting that knockdown of

p66Shc in our experimental model did not improve blastocyst formation *in vitro* (Betts et al., 2014). Interestingly, our results also suggest that p66Shc knockdown blastocysts may be more developmentally advanced than controls, which suggests that they are following the developmental timeline of embryos developing *in vivo*. It is well known that late blastocyst development is delayed in embryos cultured *in vitro* relative to their *in vivo* counterpart (Dietrich and Hiiragi, 2007). However, culture does not appear to significantly alter the timing of lineage-specific marker patterning, as *in vivo* derived blastocysts also show initial OCT3/4 expression in the TE until the late blastocyst stage (Dietrich and Hiiragi, 2007). This apparent developmental advancement in p66Shc knockdown embryos may be due to enhanced stress resistance to the culture environment conferred by reduced p66Shc expression.

Our results instead point to a critical cell fate specification role for p66Shc during the late morula to early blastocyst stages during mouse preimplantation development, when p66Shc is typically upregulated *in vivo* (Edwards et al., 2016). This function is potentially through its function as RTK adaptor, binding phosphotyrosine sites on the activated receptor and negatively regulating downstream ERK1/2 signalling. These results provide insight into the biological role of p66Shc and some explanation as to why the gene has not been selected against, despite its deletion having several beneficial effects in adult mice (Berniakovich et al., 2008; Giorgio et al., 2012; Migliaccio et al., 1999; Tomilov et al., 2011). It would be interesting to see the effects of culturing knockdown blastocysts in atmospheric (20% oxygen) conditions as we have observed increases in p66Shc expression correlated with altered metabolic function in embryos (Edwards et al., 2016).

We were unable to detect differences in MAPK signaling between p66Shc knockdown and control embryos at 72 hours post siRNA injection, when p66Shc protein expression is still significantly decreased by RNAi. Instead, we observed phenotypic differences at the blastocyst stage, when the knockdown effect is no longer present at the transcriptional level. RNA interference using siRNAs is a limitation of our study as knockdown effects did not persist at the transcript level to the blastocyst stage (Betts et al., 2014; Edwards et al., 2016). However, due to protein turnover and stability, the timing of maximal phenotypic effects does not necessarily correspond to maximal knockdown effects.

Several studies using siRNA to knockdown p66Shc in preimplantation embryos also observe restoration of p66Shc transcript levels to wild type levels at the blastocyst stage, but the transient knockdown of p66Shc during preimplantation development significantly affected the ability of blastocysts to develop under basal and stress-inducing culture conditions (Betts et al., 2014; Favetta et al., 2007; Ren et al., 2014). Our results suggest that transient knockdown of p66Shc up to 72 hours of development has an effect on cell-lineage transcription factor expression at the blastocyst stage. This could be through affecting earlier events in PE specification such as differences in FGF4/FGFR2 signaling that first occurs in the early ICM (Guo et al., 2010), or through regulating the levels of OCT3/4 in morulae that in turn would affect FGF4 levels (Dietrich and Hiiragi, 2007; Nichols et al., 1998). Additionally, there may be effects of p66Shc on other signaling pathways that have not yet been identified but are independently required for the onset of *Gata6* expression (Frankenberg et al., 2011). Our future experiments are being directed towards producing maternal and embryonic genetic knockout models of p66Shc in preimplantation embryos and the production of these lines will determine the extent of p66Shc regulation of OCT3/4 expression during preimplantation development, its requirement for establishing cell fate in the ICM, and the consequences of its loss on fetal and postpartum development.

Knockdown of p66Shc during mouse preimplantation development resulted in morphologically normal blastocysts. However, we detected an increased total cell number in p66Shc knockdown blastocysts compared to controls, and attribute this increase to altered proliferation. P66Shc has not been extensively linked with cell cycle regulation in other studies, but it could indirectly affect cell proliferation through regulating epidermal growth factor receptor (EGFR) signalling activity (Migliaccio et al., 1997). The time frame for altered proliferation is short, as knockdown embryos 72 hours post siRNA injection contained fewer total cells, and knockdown embryos 110 hours post injection did not significantly differ in cell number than controls. Though we only observed changes in *Rbl* transcript abundance, the effects of p66Shc knockdown to other key cell cycle genes (*Ccnd1*, *Ccne1*) would be useful and could provide insight into the role of p66Shc in cell cycle regulation in the mouse blastocyst. Other studies with EPI/PrE imbalance phenotypes also have altered proliferation, suggesting that the cell cycle may

be linked to cell fate specification in the mouse blastocyst (Azami et al., 2017; Chen and Yu, 2012).

Our results suggest that the effects of p66Shc on mouse blastocyst cell fate are mediated through ERK1/2 signalling. However, we did not directly confirm that these effects were downstream or upstream of FGF4 and cannot conclude that p66Shc regulates this specific pathway. No other signalling pathway aside from FGF4/MAPK has been identified as being critical for EPI/PrE specification, however, and thus we speculate that in the blastocyst p66Shc is acting as a canonical adaptor protein to negatively regulate ERK1/2 activity downstream of FGF4/RTK activation. It is possible that p66Shc could be acting through another RTK, such as EGFR, and ERK1/2 activity is regulated through pathway cross talk. For example, p66Shc overexpression is associated with increased β -Catenin activity in mouse embryonic stem cells undergoing directed neural differentiation, which may be regulated through p66Shc-mediated generation of reactive oxygen species (Papadimou et al., 2009). Though its interactions with the EGFR are the most well-studied, there is evidence that Shc proteins are recruited to and phosphorylated by FGFR1,3, and 4, and indirectly associate with FGFR2 *in vivo* (Schuller et al., 2008). It is also possible that FGFR1 versus FGFR2 expression is altered downstream of p66Shc knockdown, which would affect the EPI/PrE balance in the ICM (Kang et al., 2017). Determining how p66Shc fits into the hierarchy and regulation of cell fate signalling in the blastocyst ICM would provide insight into how it may affect EPI establishment and ultimately the pluripotency of mouse embryonic stem cells. Our work outlines an additional novel role of p66Shc in mouse blastocyst development associated with the onset and relative abundance of lineage-associated transcription factors.

3.5 References

Azami, T., Waku, T., Matsumoto, K., Jeon, H., Muratani, M., Kawashima, A., Yanagisawa, J., Manabe, I., Nagai, R., Kunath, T., et al. (2017). Klf5 maintains the balance of primitive endoderm versus epiblast specification during mouse embryonic development by suppression of Fgf4. *Development* **144**, 3706-3718.

- Berniakovich, I., Trinei, M., Stendardo, M., Migliaccio, E., Minucci, S., Bernardi, P., Pelicci, P. G. and Giorgio, M.** (2008). p66Shc-generated oxidative signal promotes fat accumulation. *J Biol Chem* **283**, 34283-34293.
- Betts, D. H., Bain, N. T. and Madan, P.** (2014). The p66(Shc) adaptor protein controls oxidative stress response in early bovine embryos. *PLoS One* **9**, e86978.
- Chazaud, C., Yamanaka, Y., Pawson, T. and Rossant, J.** (2006). Early lineage segregation between epiblast and primitive endoderm in mouse blastocysts through the Grb2-MAPK pathway. *Dev Cell* **10**, 615-624.
- Chen, Y. H. and Yu, J.** (2012). Ectopic expression of Fgf3 leads to aberrant lineage segregation in the mouse parthenote preimplantation embryos. *Dev Dyn* **241**, 1651-1664.
- Cockburn, K., Biechele, S., Garner, J. and Rossant, J.** (2013). The Hippo pathway member Nf2 is required for inner cell mass specification. *Curr Biol* **23**, 1195-1201.
- Dietrich, J. E. and Hiiragi, T.** (2007). Stochastic patterning in the mouse pre-implantation embryo. *Development* **134**, 4219-4231.
- Edwards, N. A., Watson, A. J. and Betts, D. H.** (2016). P66Shc, a key regulator of metabolism and mitochondrial ROS production, is dysregulated by mouse embryo culture. *Mol Hum Reprod* **22**, 634-647.
- Favetta, L. A., Madan, P., Mastro Monaco, G. F., St John, E. J., King, W. A. and Betts, D. H.** (2007). The oxidative stress adaptor p66Shc is required for permanent embryo arrest in vitro. *BMC Dev Biol* **7**, 132.
- Frankenberg, S., Gerbe, F., Bessonard, S., Belville, C., Pouchin, P., Bardot, O. and Chazaud, C.** (2011). Primitive endoderm differentiates via a three-step mechanism involving Nanog and RTK signaling. *Dev Cell* **21**, 1005-1013.
- Giorgio, M., Berry, A., Berniakovich, I., Poletaeva, I., Trinei, M., Stendardo, M., Hagopian, K., Ramsey, J. J., Cortopassi, G., Migliaccio, E., et al.** (2012). The p66Shc knocked out mice are short lived under natural condition. *Aging Cell* **11**, 162-168.
- Grabarek, J. B., Zyzynska, K., Saiz, N., Piliszek, A., Frankenberg, S., Nichols, J., Hadjantonakis, A. K. and Plusa, B.** (2012). Differential plasticity of epiblast and primitive endoderm precursors within the ICM of the early mouse embryo. *Development* **139**, 129-139.
- Guo, G., Huss, M., Tong, G. Q., Wang, C., Li Sun, L., Clarke, N. D. and Robson, P.** (2010). Resolution of cell fate decisions revealed by single-cell gene expression analysis from zygote to blastocyst. *Dev Cell* **18**, 675-685.

- Hirate, Y., Hirahara, S., Inoue, K., Suzuki, A., Alarcon, V. B., Akimoto, K., Hirai, T., Hara, T., Adachi, M., Chida, K., et al.** (2013). Polarity-dependent distribution of angiominin localizes Hippo signaling in preimplantation embryos. *Curr Biol* **23**, 1181-1194.
- Kang, M., Garg, V. and Hadjantonakis, A. K.** (2017). Lineage establishment and progression within the inner cell mass of the mouse blastocyst requires FGFR1 and FGFR2. *Dev Cell* **41**, 496-510 e495.
- Krawchuk, D., Honma-Yamanaka, N., Anani, S. and Yamanaka, Y.** (2013). FGF4 is a limiting factor controlling the proportions of primitive endoderm and epiblast in the ICM of the mouse blastocyst. *Dev Biol* **384**, 65-71.
- Lorthongpanich, C., Messerschmidt, D. M., Chan, S. W., Hong, W., Knowles, B. B. and Solter, D.** (2013). Temporal reduction of LATS kinases in the early preimplantation embryo prevents ICM lineage differentiation. *Genes Dev* **27**, 1441-1446.
- Migliaccio, E., Giorgio, M., Mele, S., Pelicci, G., Reboldi, P., Pandolfi, P. P., Lanfrancone, L. and Pelicci, P. G.** (1999). The p66shc adaptor protein controls oxidative stress response and life span in mammals. *Nature* **402**, 309-313.
- Migliaccio, E., Mele, S., Salcini, A. E., Pelicci, G., Lai, K. M., Superti-Furga, G., Pawson, T., Di Fiore, P. P., Lanfrancone, L. and Pelicci, P. G.** (1997). Opposite effects of the p52shc/p46shc and p66shc splicing isoforms on the EGF receptor-MAP kinase-fos signalling pathway. *EMBO J* **16**, 706-716.
- Nemoto, S., Combs, C. A., French, S., Ahn, B. H., Fergusson, M. M., Balaban, R. S. and Finkel, T.** (2006). The mammalian longevity-associated gene product p66shc regulates mitochondrial metabolism. *J Biol Chem* **281**, 10555-10560.
- Nichols, J., Zevnik, B., Anastassiadis, K., Niwa, H., Klewe-Nebenius, D., Chambers, I., Scholer, H. and Smith, A.** (1998). Formation of pluripotent stem cells in the mammalian embryo depends on the POU transcription factor Oct4. *Cell* **95**, 379-391.
- Nishioka, N., Inoue, K., Adachi, K., Kiyonari, H., Ota, M., Ralston, A., Yabuta, N., Hirahara, S., Stephenson, R. O., Ogonuki, N., et al.** (2009). The Hippo signaling pathway components Lats and Yap pattern Tead4 activity to distinguish mouse trophectoderm from inner cell mass. *Dev Cell* **16**, 398-410.
- Okada, S., Kao, A. W., Ceresa, B. P., Blaikie, P., Margolis, B. and Pessin, J. E.** (1997). The 66-kDa Shc isoform Is a negative regulator of the epidermal growth factor-stimulated mitogen-activated protein kinase pathway. *Journal of Biological Chemistry* **272**, 28042-28049.

- Papadimou, E., Moiana, A., Goffredo, D., Koch, P., Bertuzzi, S., Brustle, O., Cattaneo, E. and Conti, L.** (2009). p66(ShcA) adaptor molecule accelerates ES cell neural induction. *Mol Cell Neurosci* **41**, 74-84.
- Plusa, B., Piliszek, A., Frankenberg, S., Artus, J. and Hadjantonakis, A. K.** (2008). Distinct sequential cell behaviours direct primitive endoderm formation in the mouse blastocyst. *Development* **135**, 3081-3091.
- Ren, K., Li, X., Yan, J., Huang, G., Zhou, S., Yang, B., Ma, X. and Lu, C.** (2014). Knockdown of p66Shc by siRNA injection rescues arsenite-induced developmental retardation in mouse preimplantation embryos. *Reprod Toxicol* **43**, 8-18.
- Schuller, A. C., Ahmed, Z., Levitt, J. A., Suen, K. M., Suhling, K. and Ladbury, J. E.** (2008). Indirect recruitment of the signalling adaptor Shc to the fibroblast growth factor receptor 2 (FGFR2). *Biochem J* **416**, 189-199.
- Tomilov, A. A., Ramsey, J. J., Hagopian, K., Giorgio, M., Kim, K. M., Lam, A., Migliaccio, E., Lloyd, K. C., Berniakovich, I., Prolla, T. A., et al.** (2011). The Shc locus regulates insulin signaling and adiposity in mammals. *Aging Cell* **10**, 55-65.
- Xie, Y., Puscheck, E. E. and Rappolee, D. A.** (2006). Effects of SAPK/JNK inhibitors on preimplantation mouse embryo development are influenced greatly by the amount of stress induced by the media. *Mol Hum Reprod* **12**, 217-224.
- Yamanaka, Y., Lanner, F. and Rossant, J.** (2010). FGF signal-dependent segregation of primitive endoderm and epiblast in the mouse blastocyst. *Development* **137**, 715-724.

Chapter 4

4 Knockout of p66Shc alters pluripotency-associated transcription factor expression in mouse embryonic stem cells

This chapter is a version of a manuscript under preparation entitled, “Knockout of p66Shc alters pluripotency-associated transcription factor expression in mouse embryonic stem cells”.

4.1 Introduction

Embryonic stem cells (ESCs) are derivatives of the inner cell mass (ICM) of the preimplantation blastocyst that can be maintained in culture indefinitely (Evans and Kaufman, 1981). ESCs are self-renewing and pluripotent, as they can differentiate into lineages representing the three embryonic germ layers (endoderm, mesoderm, ectoderm) (Murry and Keller, 2008). ESCs can be isolated from both mouse and human blastocysts (Evans and Kaufman, 1981; Martin, 1981; Thomson et al., 1998). However, key characteristics of ESCs derived from human blastocysts differ from ESCs derived from mouse blastocysts. Human ESCs resemble stem cells derived from the mouse post-implantation epiblast (Tesar et al., 2007). Thus, ESC pluripotency exists in more than one state, and two metastable pluripotent states are defined as naïve and primed pluripotency (Nichols and Smith, 2009). Naïve ESCs (mouse ESCs) represent the ground state of pluripotency and can reincorporate into the ICM of a blastocyst when introduced into the preimplantation embryo (Nichols and Smith, 2009). Primed ESCs (human ESCs and mouse epiblast stem cells) cannot reincorporate into the blastocyst but are capable of generating teratocarcinomas (teratomas) with tissues representative of the three embryonic germ layers. ESCs derived from many species can be interconverted between these two states through genetic and/or environmental manipulation (Manor et al., 2015).

Pluripotency is maintained in ESCs by a network of transcription factors including OCT4, KLF4, NANOG, and SOX2 that promote self-renewal and prevent differentiation (Niwa, 2007). Expression of these transcription factors (along with c-MYC) can induce pluripotency in terminally differentiated cells (e.g. mouse embryonic or adult fibroblasts) to create induced pluripotent stem cells (iPSCs) with characteristics of naïve pluripotent stem cells (Takahashi and Yamanaka, 2006). Naïve pluripotency can be stabilized in ESCs by providing exogenous factors. LIF/STAT3 signalling is required for self-renewal and pluripotency in mESCs, but naïve pluripotency can be maintained if mESCs are cultured in a combination of MEK, FGFR3, and GSK-3 β inhibitors without LIF supplementation (Manor et al., 2015). The combination of MEK and GSK-3 β inhibition with LIF supplementation (“2i/LIF”) has thus far represented the optimal conditions to

capture and stabilize naïve pluripotency in non-permissive mouse strains (Hanna et al., 2009). Conversely, MEK signalling stabilizes the primed pluripotent state (Nichols et al., 2009). The contrasting effects of MEK signalling on naïve and primed pluripotency states, suggests that it is a key pathway involved in the interconversion between these two pluripotent states.

The Shc1 (also known as ShcA) family of adaptor proteins are key components of receptor tyrosine kinase (RTK)-MEK-ERK signalling. These RTK adaptors sensitize cells to low levels of growth factors present in the environment (Lai and Pawson, 2000). Three isoforms are expressed from the Shc1 locus and differ in their protein domain composition and cellular functions. P46Shc/p52Shc promote Ras/MAPK signalling downstream of RTK activation, while p66Shc does not. Additionally, p66Shc promotes mitochondrial reactive oxygen species (ROS) release under stress-inducing conditions. We have demonstrated that knock down of p66Shc, the largest isoform of Shc1, in mouse preimplantation embryos results in a higher proportion of primitive endoderm cells and a lower proportion of epiblast cells in the mouse blastocyst ICM (Chapter 3, Edwards et al., under review). P66Shc knockdown blastocysts form fewer ICM-derived outgrowths when explanted *in vitro* (Chapter 3, Edwards et al., under review). This suggests that p66Shc plays a role in the establishment and/or maintenance of the pluripotent cell population in the mouse preimplantation embryo. Interestingly, p66Shc overexpression in mouse and human ESCs changed colony morphology to a more compact and rounded appearance, characteristic of naïve pluripotent stem cells (Papadimou et al., 2009). Furthermore, preliminary p66Shc knockdown experiments in human ESCs resulted in decreased expression of pluripotent markers and an increase in neural differentiation markers (Smith et al., 2016).

Together, these observations suggest that p66Shc functions to promote pluripotency in ESCs. Thus, the objective of the present study was to determine the effects of p66Shc genetic knockout to mouse ESC pluripotency. We show that targeted CRISPR-Cas9 deletion of p66Shc in mESCs results in altered expression of pluripotent markers, notably, a consistent reduction in NANOG expression detected by immunofluorescence. Furthermore, we show that p66Shc knockout mESCs downregulate neuroectoderm

transcriptional markers and upregulate mesoderm transcriptional markers during spontaneous embryoid body differentiation. Our results suggest that p66Shc may be required to maintain naïve pluripotency and to maintain the complete ability to spontaneously differentiate into the three embryonic germ layers *in vitro*.

4.2 Materials and Methods

4.2.1 Generation of p66Shc knockout mESCs with CRISPR-Cas9

Two pairs of guide (g)RNA sequences were designed in-house (<http://crispr.mit.edu>) to target the intronic region where the p66Shc-specific promoter is located and the 5' region of coding exon 2 and synthesized by Life Technologies. Pair 1: 5'-TCGGGGTCTACCCCTCCGG-3' and 5'-ATATATCTGTAGGTCCGAG-3'; Pair 2: 5'-TAGTCGGACTATCGTCCCCC-3' and 5'-AATATATCTGTAGGTCCGAG-3' (Fig. 4-1A). Guide RNA sequences were cloned into the pSpCas9(BB)-2A-Puro (PX459) plasmid (Feng Zhang, deposited in Addgene #48139, (Ran et al., 2013)) by *BbsI* restriction enzyme digest. Cloned plasmids were transfected into R1 mouse embryonic stem cells with Lipofectamine 3000 (Life Technologies) according to manufacturer's guidelines. Cells were selected for transfection of the plasmid by puromycin. Surviving colonies were mechanically picked, trypsin digested to single cells, then plated at a density of 1 cell/well of a 96-well plate on MEFs to generate clonal lines. Clonal lines were then expanded under both feeder-free conditions (MEF-conditioned DMEM containing 2i/LIF) for genotyping and on MEFs for maintenance. For experimental analyses, p66Shc knockout lines were compared to isogenic unedited R1 mESCs.

Genomic (g)DNA was isolated using the GenElute Mammalian Genomic DNA Miniprep Kit (Sigma) according to manufacturer's guidelines. Genomic DNA from eighty-nine clonal lines was then genotyped by PCR for deletions using LA Taq DNA polymerase (Takara Bio, USA) according to manufacturer's protocol and using the primer sequences in Table 4-1. PCR products were visualized by agarose gel electrophoresis. Twenty-six out of the eighty-nine screened identified as compound heterozygous deletions after genomic DNA PCR screening were screened for deletion of p66Shc protein by

Table 4-1. Oligonucleotide primer sequences.

Gene	Primer Sequences	Expected product size
p66Shc (gDNA)	F: 5'-CTGTGGCAGGAAACTGTGGGCAA-3' R: 5'-GCCAGCCTCGTGTGGGCTTAT-3'	1689 bp
<i>T</i> (<i>Brachyury</i>)	F: 5'-GCTTCAAGGAGCTAACTAACGAG-3' R: 5'-CCAGCAAGAAAGAGTACATGGC-3'	117 bp
<i>Thy1</i>	F: 5'-TGCTCTCAGTCTTGCAGGTG-3' R: 5'-TGGATGGAGTTATCCTTGGTGTT-3'	121 bp
<i>Tagln</i>	F: 5'-CAACAAGGGTCCATCCTACGG-3' R: 5'-ATCTGGGCGGCCTACATCA-3'	133 bp
<i>Eng</i>	F: 5'-AGGGGTGAGGTGACGTTTAC-3' R: 5'-GTGCCATTTTGTCTGGATGC-3'	155 bp
<i>Fgf2</i>	F: 5'-GCGACCCACACGTCAAATA-3' R: 5'-TCCCTTGATAGACACAACCTCCTC-3'	62 bp
<i>Gapdh</i>	F: 5'-TGACGTGCCGCCTGGAGAAA-3' R: 5'-AGTGTAGCCCAAGATGCCCTTCAG-3'	98 bp
<i>Pax6</i>	F: 5'-TACCAGTGTCTACCAGCCAAT-3' R: 5'-TGCACGAGTATGAGGAGGTCT-3'	194 bp
<i>Gfap</i>	F: 5'-CCCTGGCTCGTGTGGATTT-3' R: 5'-GACCGATACTCCTCTGTC-3'	238 bp
<i>Scn1a</i>	F: 5'-TCAGAGGGAAGCACAGTAGAC-3' R: 5'-TTCCACGCTGATTTGACAGCA-3'	138 bp
<i>Isl1</i>	F: 5'-ATGATGGTGGTTTACAGGCTAAC-3' R: 5'-TCGATGCTACTTCACTGCCAG-3'	174 bp
<i>Meis1</i>	F: 5'-GCCCATGATAGACCAGTCCAA-3' R: 5'-ACCGTCCATTACAAAACCTCC-3'	91 bp
<i>Sox3</i>	F: 5'-TTGGGACGCCTTGCTGTTTA-3' R: 5'-CGGCTCTAGCAAGTCCCATT-3'	147 bp
<i>Dppa5a</i>	F: 5'-ATGATGGTGACCCTCGTGAC-3' R: 5'-CCTGCTCGATGTGAGACATTC-3'	151 bp
<i>Sox2</i>	F: 5'-GGAAAGGGTTCTTGCTGGGT-3' R: 5'-ACGAAAACGGTCTTGCCAGT-3'	148 bp

<i>Pou5f1</i>	F: 5'-GGCGTTCTCTTTGGAAAGGTGTTC-3' R: 5'-CTCGAACCACATCCTTCTCT-3'	313 bp
<i>Otx2</i>	F: 5'-AACTTGCCAGAATCCAGGGT-3' R: 5'-GCCTCACTTTGTTCTGACC-3'	148 bp
<i>Fgf5</i>	F: 5'-CCAGTGTGTTAAGCCAAATTTACG-3' R: 5'-CCACTCTCGGCCTGTCTTTT-3'	117 bp
<i>Rex1</i>	F: 5'-AGAAGAAAGCAGGATCGCCT-3' R: 5'-TATGACTCACTTCCAGGGGG-3'	108 bp
<i>Zic2</i>	F: 5'-GGTGACCCACGTCTCTGTG-3' R: 5'-CGGATGTGGTTGACCAGTTT-3'	126 bp
<i>Nr5a2</i>	F: 5'-TTGAGTGGGCCAGGAGTAGT-3' R: 5'-TCAAGAGCTCACTCCAGCAG-3'	90 bp
<i>Dppa3</i>	F: 5'-AAAGTCGACCCAATGAAGGA-3' R: 5'-CGGGGTTTAGGGTTAGCTTT-3'	127 bp
<i>Ppia</i>	F: 5'-GTCCTGGCATCTTGTCCATG-3' R: 5'-TGCCTTCTTTCACCTTCCCA-3'	126 bp

immunoblotting. Densitometry was performed to determine which lines had p52Shc/p46Shc protein abundance not significantly different from wild type R1 controls. Two lines were chosen for experimental analysis: 4D (gRNA pair 1) and 10D (gRNA pair 2). Genomic PCR products from 8A, 4D (gRNA pair 1), 10D and 10D² (gRNA pair 2) were gel extracted, purified, and sequenced at the London Regional Genomics Center (Robarts Research Institute, London, Canada). Deleted sequences were determined by comparing sequenced DNA to mouse genomic DNA using NCBI BLAST and UCSC Genome Browser Basic Local Alignment Tool (BLAT). Off-target predictions were generated using the Wellcome Trust Sanger Institute Genome Editing website (<http://www.sanger.ac.uk/htgt/wge/>) (Table 4-2) (Hodgkins et al., 2015).

4.2.2 Embryonic stem cell culture

R1 mouse embryonic stem cells (Sick Kids, Toronto, Canada, (Nagy et al., 1993) and p66Shc knockout clonal lines were maintained on a mouse embryonic fibroblast (MEF) feeder layer and in DMEM containing 15% embryonic stem cell-qualified FBS (Life Technologies) and 1000 U/ml mouse leukemia inhibitory factor (mLIF, Esgro, Millipore Sigma). To reintroduce p66Shc expression, cells were transfected with a human p66Shc-HA expression plasmid (obtained from Dr. Robert Cumming, University of Western Ontario) using Lipofectamine 3000 according to manufacturer's protocol.

4.2.3 Immunofluorescence and confocal microscopy

Cells and EBs grown on glass coverslips were fixed with 4% paraformaldehyde for 30 minutes, then stored in PBS at 4°C until processing. Coverslips were permeabilized for 30 minutes in 0.25% Triton X-100 in PBS, then blocked in 5% donkey serum in PBS. Coverslips were incubated overnight at 4°C in primary antibody in the indicated concentrations in Table 4-3. Coverslips were incubated in donkey anti-mouse Alexa Fluor-488 or donkey anti-goat Alexa Fluor-488, and/or donkey anti-rabbit Alexa Fluor-568 (Life Technologies) for 45 minutes at room temperature. Coverslips were stained for 5 minutes with DAPI (NucBlue Fixed Cell ReadyProbes Reagent, Life Technologies)

Table 4-2. Summary of predicted Cas9-gRNA off-target effects.

gRNA sequence	Off target sequence	Details
TTCGGGGTCTACCCCTCCGG AGG	CCTGGGGGCTACCCCTCAGG TGG	Exonic – Adrbk1
	GTCGGTGTCTACACCGCCGG CGG	Exonic – Stox2
AATATATCTGTAGGTCCGAG GGG	AATAGATCTGTGGGTCAAGAG AGG	Intronic – Entpd4
	TATATTTCAC TAGGTCCGAG AGG	Exonic – Plch2
	AATATTTCTGTAGGCTCCAG GGG	Exonic – Pydc3
GTAGTCGGACTATCGTCCCC CGG	GAAGTGGGTCTATCTTCCCC AGG	Intronic – Adgrg4
	GGAGTAGGACTATTTCCCC TGG	Intronic – Slc44a5
	GTAGTCAGAGCATCGTTCCC AGG	Intronic – Slit3
CAATATATCTGTAGGTCCGA GGG	No data available	

Table 4-3. Primary antibody information.

Antibody	Species	Application	Catalog number
SHC1	Rabbit	WB; 1:1000	BD Biosciences 610879
OCT4	Mouse	IF; 1:100	Santa Cruz sc-5279
SOX2	Mouse	IF; 1:100	Santa Cruz sc-365823
NANOG	Rabbit	IF; 1:200	ReproCell RCAB001P
T/Brachyury	Goat	IF; 1:100	R&D Systems AF2085
OTX2	Rabbit	IF; 1:250	EMD Millipore AB9566
PAX6	Rabbit	IF; 1:100	Invitrogen A24340
HA-AF647	Rabbit	IF; 1:50	Santa Cruz sc-805

then mounted onto glass microscopy slides in VectaShield antifade mounting medium (Vector Labs). Images were obtained using an LSM 510 laser-scanning confocal microscope (Zeiss). Laser settings were unchanged when imaging the same primary antibodies across cell lines.

4.2.4 Immunoblotting

Cells prepared for immunoblotting were cultured in feeder-free conditions with 2i/mLIF. Cells were scraped into radioimmunoprecipitation assay (RIPA) buffer and stored at -80°C until processing. 10 µg of total protein lysate was resolved on a 4-12% gradient polyacrylamide gel (NuPage, Life Technologies) and transferred to a PVDF membrane (Millipore). Membranes were blocked with 5% milk in PBST and incubated overnight at 4°C with anti-total Shc1 (BD Biosciences, 1:1000), which recognizes all three Shc isoforms (p46Shc, p52Shc and p66Shc). Membranes were then incubated in HRP-conjugated secondary antibody for 45 minutes at room temperature. Membranes were visualized using enhanced chemiluminescence (Forte ECL, Millipore) and imaged using a ChemiDoc MP Imaging system (BioRad). Densitometry was performed in ImageLab 4.0 (BioRad).

4.2.5 Embryoid body formation and differentiation

Wild type and p66Shc KO mESCs were trypsinized and removed from MEF feeders by incubating for 45 minutes at 37°C in DMEM containing 10% fetal bovine serum. Cells were plated into AggreWell 400 6-well plates (STEMCELL Technologies) at 9.5×10^5 cells per well to generate EBs composed of approximately 500-1000 cells. EBs were formed in EB medium (KnockOut DMEM/F12 supplemented with 15% KnockOut Serum Replacement, non-essential amino acids and GlutaMAX (Life Technologies)). EBs were formed over 72 hours with a 50% medium change every day. EBs were harvested from the AggreWell plates, counted, and seeded at 1000 EBs per well onto 0.1% gelatin-coated 6-well plate and 200 EBs per gelatinized coverslip, and allowed to adhere for 24 hours in EB medium containing 10% FBS. Adhered EBs were then cultured for up to 14 days in EB medium, with a complete medium change every 24 hours.

4.2.6 RNA extraction, RT² Profiler PCR array and quantitative real time (qRT)-PCR

Cells and EBs were scraped into TRIzol reagent (Thermo Fisher Scientific) and stored at -20°C until RNA extraction. RNA was extracted with chloroform and purified using the RNeasy Mini Kit (Qiagen) according to manufacturer's instructions. Genomic DNA digestion was performed using the RNase-free DNase Set (Qiagen). For the RT² Profiler PCR array, 400 ng of RNA was reverse transcribed to cDNA using the RT² First Strand Kit (Qiagen). For validating targets using qRT-PCR, 400 ng of RNA was reverse transcribed using qScript XLT cDNA SuperMix (Quanta Biosciences) according to manufacturer's protocol. Quantitative real time PCR was performed using the Mouse Embryonic Stem Cells RT² Profiler PCR Array (Qiagen) according to manufacturer's guidelines. Data generated from the PCR Array was analyzed using the Qiagen Data Analysis Center (www.SABiosciences.com/pcrarraydataanalysis.php). Genes identified by Qiagen software that were either upregulated or downregulated by 5-fold between p66Shc KO (clone 4D) and wild type cells were validated by qRT-PCR using SensiFast SYBR (FroggaBio) using a CFX384 thermal cycler (BioRad) at the following cycling conditions: 95°C for 2 minutes, then 30 cycles of 95°C for 5 seconds, 60°C for 10 seconds, 72°C for 30 seconds. Relative transcript abundance was determined by the delta-delta Ct method normalizing to Ct values for *Gapdh* or *Ppia*. Primer sequences are in Table 4-1.

4.2.7 Statistical analyses

Statistical tests were performed in Prism 6 (GraphPad Inc.) using Student's t-test (equal variance, unpaired, two-tailed) and one-way ANOVA followed by Tukey's honestly significant difference test to correct for multiple comparisons. Experiments were performed a minimum of three times using independent replicates unless otherwise indicated in the figure legends.

4.3 Results

4.3.1 Generation of p66Shc-specific knockout mESCs

We hypothesized that deletion of the p66Shc-specific promoter and transcriptional start site would specifically target p66Shc for knockout without affecting the expression of p42Shc/p52Shc. To delete the p66Shc-specific promoter, transcriptional start site, 5' untranslated region (UTR) and part of coding exon 2, pairs of two gRNAs were designed to induce two Cas9-mediated double stranded DNA breaks and subsequently delete approximately 1kb in the mouse *Shc1* locus (Fig. 4-1A). The first gRNA for both pair 1 and pair 2 overlap in 19 of 20 nucleotides in the sequence. The second gRNA for pair 1 targets amino acids 26 through 32 of p66Shc, while the second gRNA targets amino acids 50 through 57. Both pairs of gRNAs resulted in deletions detectable by PCR amplification of genomic DNA in transfected mESCs (Fig. 4-1B). P66Shc deletion was verified by immunoblotting (Fig. 4-1C). PCR products generated by genomic DNA amplification were then sequenced to determine the precise deletions produced by each pair of gRNAs. Clone 4D (gRNA pair 1) has deleted genomic sequences from upstream of the p66Shc promoter up to amino acid 30 in coding exon 2, while clone 10D (gRNA pair 2) is missing genomic sequences from upstream of the promoter up to amino acid 71 in coding exon 2 (Fig. 4-1D). Deleted sequences were similar between clones using the same pairs of guide RNAs with the exception of clone 10D². Clone 10D² retained approximately 30bp of genomic sequence upstream of the deletion in clone 10D. However, a 66-kDa band is undetectable in protein lysates from clone 10D², demonstrating that p66Shc is not translated in this clonal line. Predicted off-target effects of the gRNAs used show that at least 3 nucleotide mismatches with off target genomic DNA sequences is required for gRNAs to bind and to produce off-target Cas9 editing (Table 4-3). Our genotyping results thus demonstrate that we have successfully generated several p66Shc-specific knockout mESC lines with our targeting strategy.

4.3.2 Altered pluripotency marker expression in p66Shc knockout mESCs

P66Shc knockout did not alter mESC colony morphology or cause mESCs to spontaneously differentiate at a higher frequency than controls when maintained in

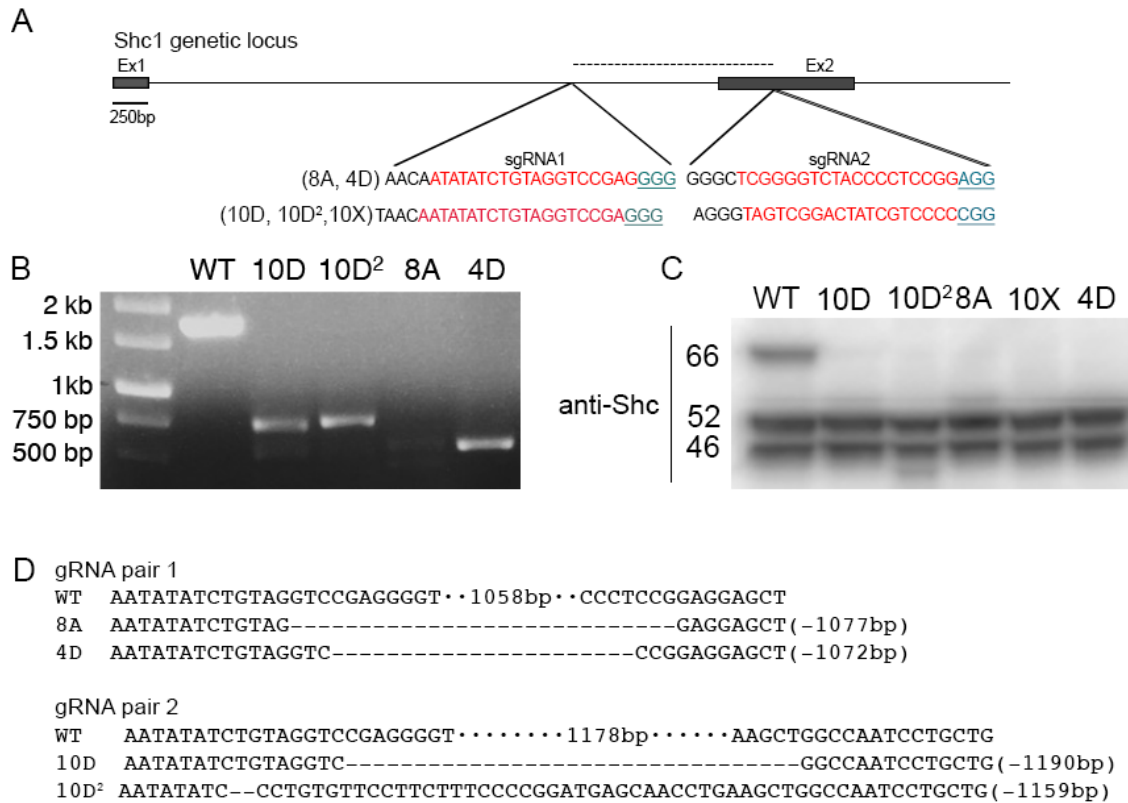


Figure 4-1. CRISPR-Cas9 knockout of p66Shc in mESCs.

(A) Structure of wild type Shc1 indicating the targeting sequences of the gRNA pairs. PAM sequences are blue and underlined, while the gRNA sequences are red. The predicted deleted region between the gRNA pairs is indicated with the dashed line between the gRNAs. (B) Gel electrophoresis of genomic DNA PCR amplification to detect Cas9-induced deletions (WT = wild type R1 mESCs; 10D, 10D², 8A, 4D = p66Shc knockout mESC clonal lines). (C) Immunoblotting for total Shc to detect p66Shc knockout. (D) Sequencing of deleted regions from each gRNA pair. Dashed lines indicate deleted sequences. Size of deleted sequences are in parentheses.

serum/LIF medium and on a MEF feeder layer (Fig. 4-2). To determine if p66Shc knockout mESCs maintained pluripotency, we investigated the expression of pluripotency-associated markers in knockout mESCs by immunofluorescence and confocal microscopy, and by qRT-PCR. Knockout lines 4D, 10D, and 10D² all had detectable OCT4 immunostaining comparable to wild type mESCs (Fig. 4-3). SOX2 was detectable in p66Shc knockout mESCs but restricted to the edge of cell colonies in knockout clonal 4D and 10D cell lines. Similarly, NANOG expression was detected at the edge of mESC colonies in knockout line 10D, while wild type mESCs had detectable NANOG expression throughout most of the cell colonies. NANOG expression was undetectable in knockout line 4D and reduced in knockout line 10D². Preliminary experiments (n=1) demonstrate that NANOG fluorescence intensity is restored in knockout line 4D transfected with a p66Shc-HA expression plasmid, supporting that the loss of NANOG expression is due to p66Shc knockout and not due to off-target effects of CRISPR-Cas9 (Fig. 4-4). P66Shc knockout lines had significant differences in the relative abundance of naïve (*Rex1*, *Nanog*, *Dppa3*, *Nr5a2*, Fig. 4-5A) and primed (*Fgf5*, *Otx2*, *Zic2*, *Brachyury*, Fig. 4-4B) transcriptional markers compared to wild type mESCs. Knockout line 4D had significantly decreased transcript abundance of *Rex1*, but significantly increased *Nanog* transcript abundance (p<0.05, Fig. 4-5), and no significant changes in transcriptional abundance of primed markers compared to wild type mESCs. Knockout line 10D had significantly decreased transcript abundance of *Dppa3* and significantly increased transcript abundance of the primed markers *Fgf5* and *Otx2* compared to wild type mESCs (p<0.05, Fig. 4-5). Our results thus suggest that knockout of p66Shc alters the expression of pluripotency-associated markers compared to unedited controls.

4.3.3 p66Shc knockout upregulates markers of mesoderm-derivatives during spontaneous embryoid body differentiation

We next determined if the changes observed to the pluripotent state of p66Shc knockout mESCs affected their differentiation capacity. To test this, we performed an EB differentiation assay and investigated which lineages emerged spontaneously during differentiation. After a 72-hour period of EB aggregation, EBs were plated on gelatin

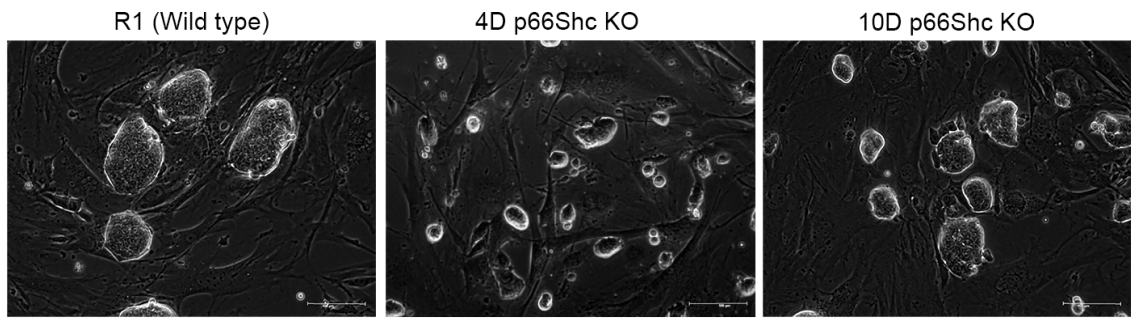


Figure 4-2. p66Shc knockout does not change morphology of mESCs cultured on MEFs in serum/LIF conditions.

Phase contrast images of unedited (R1 wild type) and two p66Shc knockout lines (4D and 10D). ESC colonies are shown grown on a MEF feeder layer. Scale bars are 100 μm .

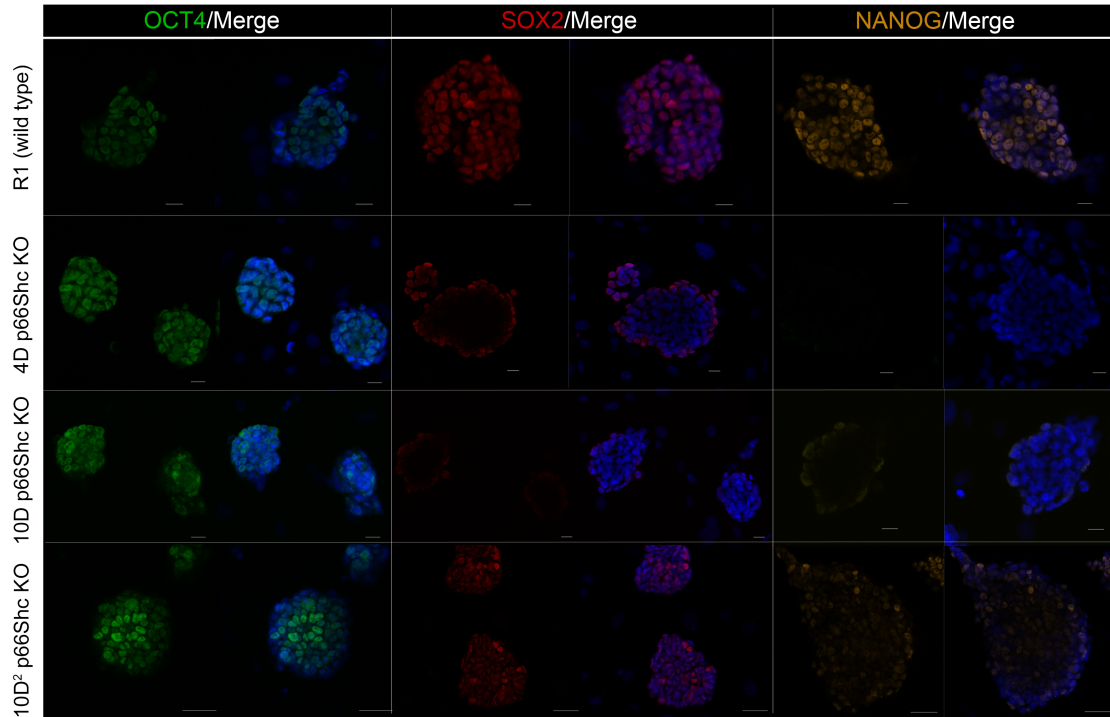


Figure 4-3. Reduced SOX2 and NANOG expression in p66Shc knockout mESCs.

Representative confocal microscopy images of mESC colonies stained for OCT4 (green), SOX2 (red), and NANOG (yellow). DAPI (blue) co-stains nuclei. Scale bars are 50 μm .

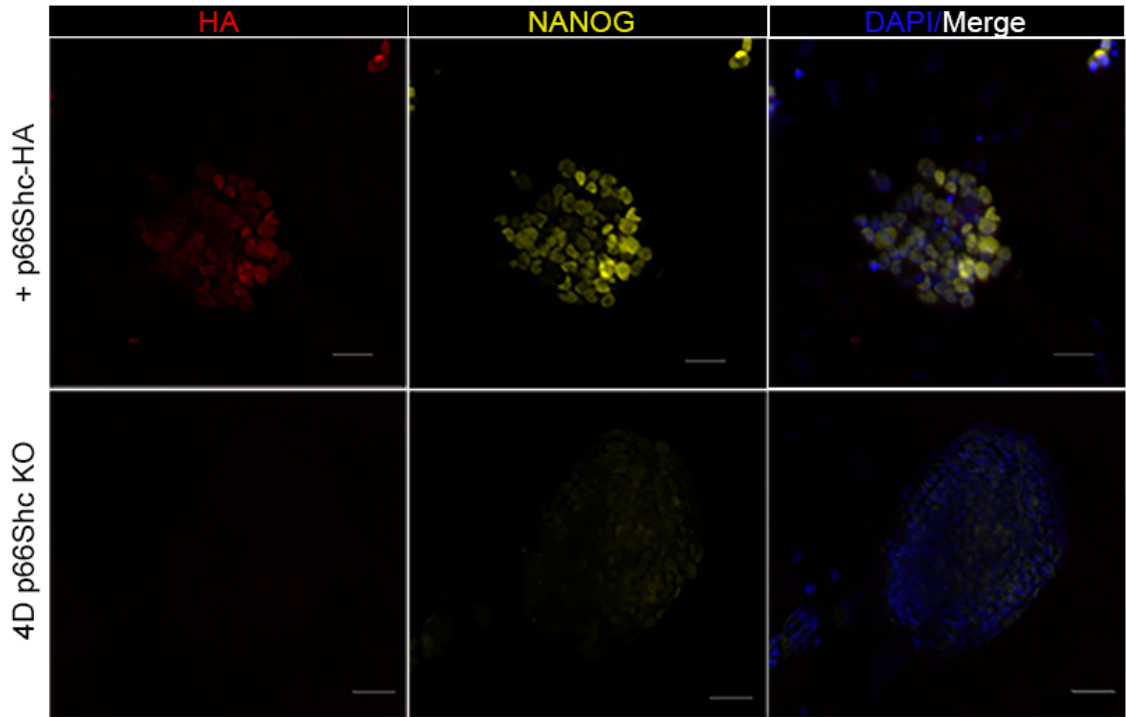


Figure 4-4. Reintroduction of p66Shc expression rescues NANOG fluorescence intensity in 4D p66Shc knockout mESCs.

Representative confocal microscopy images of mESC colonies stained for HA (red) and NANOG (yellow). DAPI (blue) co-stains nuclei. Upper panels (+ p66Shc-HA) are 4D p66Shc knockout mESCs transiently transfected with 3 μ g of p66Shc-HA expression plasmid, lower panels are non-transfected controls. Scale bars are 50 μ m.

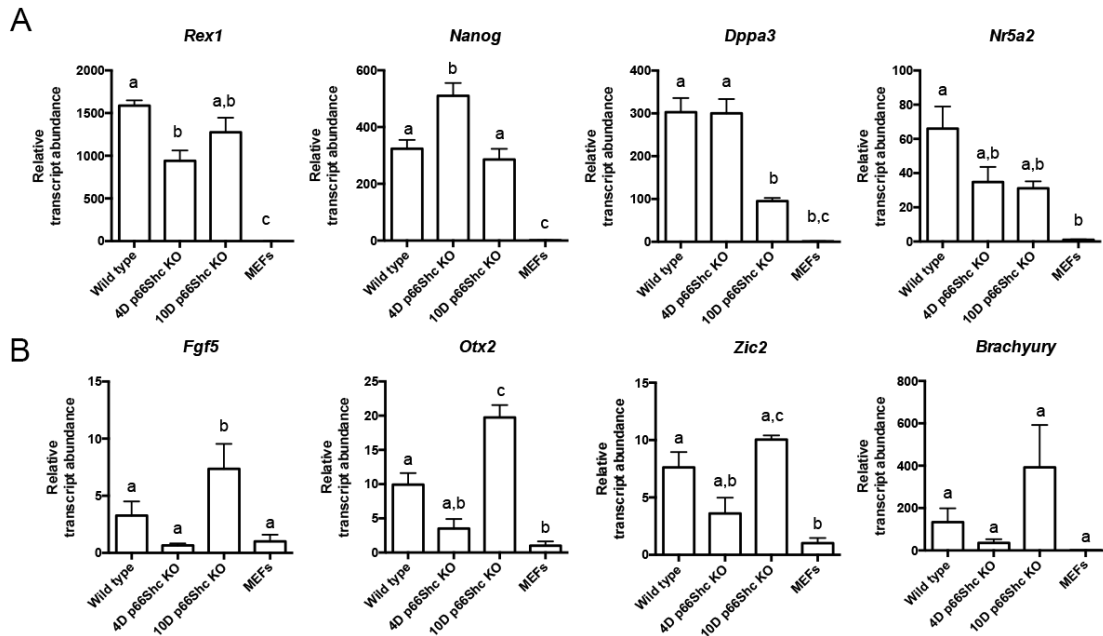


Figure 4-5. Altered expression of naïve and primed pluripotent markers in p66Shc knockout mESCs.

(A) p66Shc knockout mESCs have significantly altered transcript abundance of the naïve pluripotent markers *Rex1*, *Nanog*, and *Dppa3* compared to wild type mESCs (n=3 biological replicates, mean \pm SEM, 1W-ANOVA, different letters indicate statistically significant ($p < 0.05$) groups). (B) p66Shc knockout line 10D has significantly increased transcript abundance of the primed markers *Fgf5* and *Otx2* compared to wild type mESCs (n=3 biological replicates, mean \pm SEM, 1W-ANOVA, different letters indicate statistically significant ($p < 0.05$) groups). MEFs (mouse embryonic fibroblasts) samples were included to control for MEF contamination during separation of mESCs from the feeder layer.

and differentiated for up to 14 days in medium without specific inductive signals. PCR array analysis for markers of mESC pluripotency and differentiation demonstrated that relative to wild type-derived EBs, p66Shc knockout (4D)-derived embryoid bodies upregulated transcriptional markers of mesoderm-derived lineages (*T*, *Thy1*, *Tagln*, *Eng*, *Fgf2*) and downregulated transcriptional markers of neuroectoderm-derived lineages (*Pax6*, *Gfap*, *Scn1a*, *Sox2*, *Sox3*) after 14 days of spontaneous differentiation (Fig. 4-6A). Transcripts displaying at least a 5-fold up- or down-regulation in the p66Shc knockout-derived embryoid bodies were validated by qRT-PCR. *Tagln* and *Fgf2* were significantly upregulated in p66Shc knockout-derived embryoid bodies, while *Scn1a*, *Gfap*, and *Pax6* were significantly downregulated relative to wild type-derived embryoid bodies after 14 days of spontaneous differentiation (Fig. 4-6B). At 7 days post differentiation, *Fgf2* was also significantly upregulated in p66Shc knockout-derived EBs relative to wild type controls, while *Pax6* and *Sox2* were significantly downregulated (Fig. 4-7A). Twenty-four hours post adhering to gelatin (Day 0 of differentiation), there was no significant differences in analyzed transcripts between p66Shc knockout-derived EBs compared to wild type-derived EBs (Fig. 4-7B).

To verify our characterization of cell lineages emerging from p66Shc knockout derived-EB after spontaneous differentiation, we performed immunofluorescence and confocal microscopy using markers of mesoderm (T/Brachyury) and neuroectoderm (OTX2, PAX6, SOX2) at day 14, day 7, and day 0 of differentiation. At day 14 of differentiation, PAX6/Brachyury-positive projections emerged from wild type EBs that were not present in p66Shc knockout EBs. In contrast, structures that emerged from p66Shc knockout EBs had colonies of PAX6/Brachyury positive cells surrounded by Brachyury positive outgrowths (Fig. 4-8). At day 7 of differentiation, OTX2/Brachyury immunofluorescence appeared to increase in p66Shc knockout EBs, while OTX2 and Brachyury were restricted to the edges of the EB aggregate (Fig. 4-9). Furthermore, elongated PAX6/SOX2 positive cells emerged from wild type EBs, while PAX6/SOX2 positive cells were small and remained in compacted colonies in p66Shc knockout EBs (Fig. 4-10). At day 0 of differentiation, both OTX2 and Brachyury were detectable in EBs formed from p66Shc knockout and wild type cells.

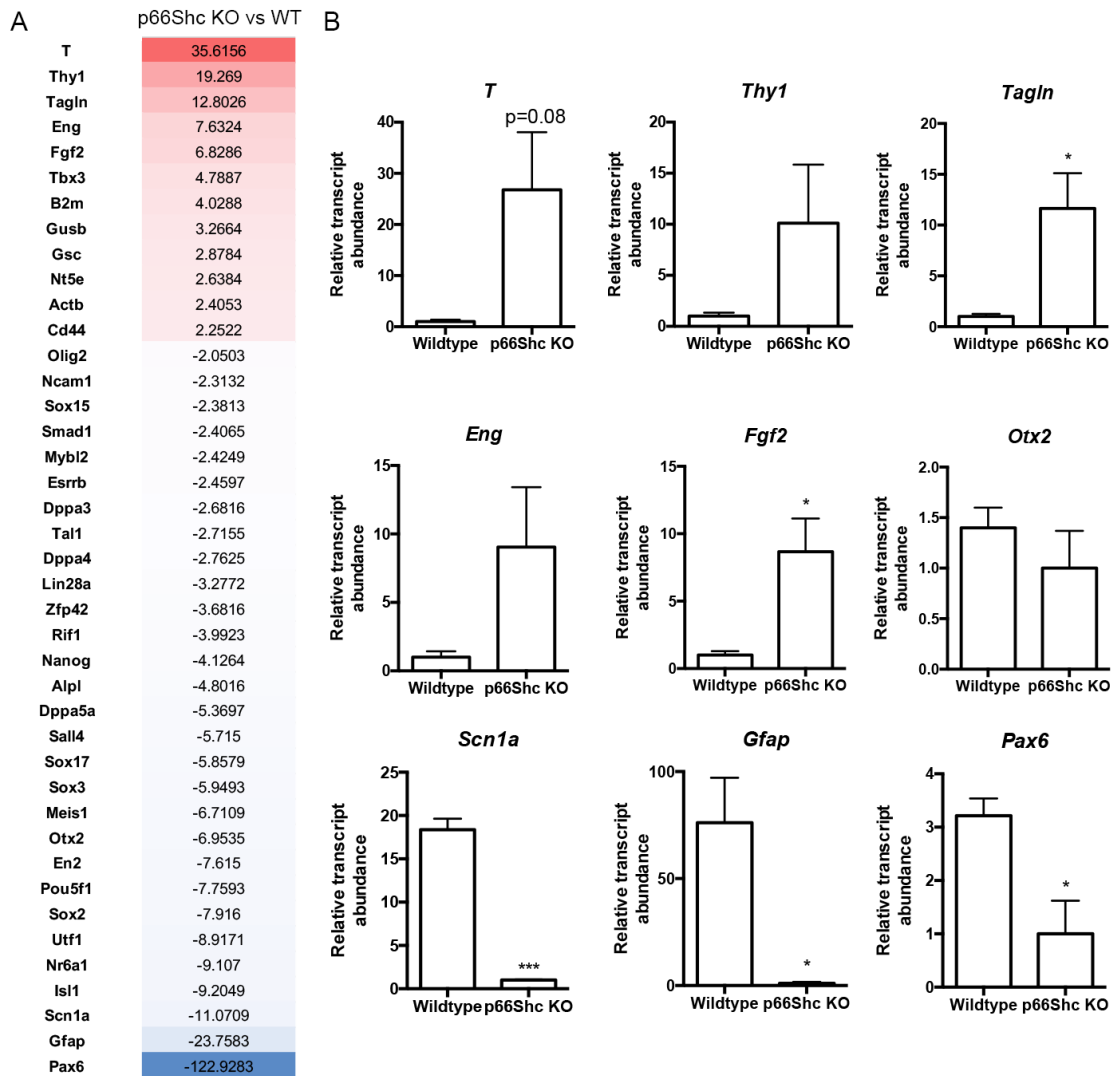


Figure 4-6. Embryoid bodies derived from p66Shc knockout mESCs upregulate markers of mesoderm derivatives and downregulate markers of neuroectoderm after 14 days of spontaneous differentiation.

(A) Heat map displaying relative fold regulation of transcripts in p66Shc knockout EBs (4D) from day 14 of differentiation compared to wild type EBs at day 14. Transcripts are displayed from greatest fold upregulation (top, red) to greatest fold downregulation (bottom, blue) (n=1 biological replicate). (B) Validation of select genes showing greater than five-fold upregulation or downregulation from the RT² qPCR array by RT-qPCR (n=3 biological replicates, mean \pm SEM, * p < 0.05, *** p < 0.001 Student's t-test).

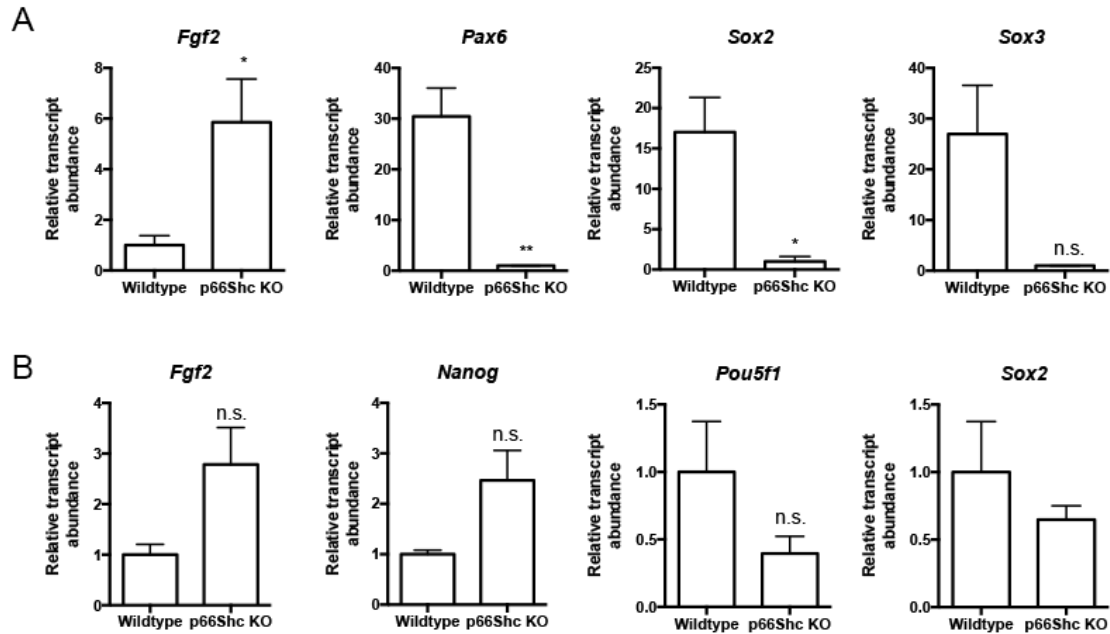


Figure 4-7. Embryoid bodies derived from p66Shc knockout mESCs upregulate *Fgf2* and downregulate neuroectoderm markers at day 7 of spontaneous differentiation.

(A) Relative transcript abundance of *Fgf2* and select neuroectoderm markers (*Pax6*, *Sox2*, *Sox3*) in wild type and p66Shc knockout (4D)-derived EBs at day 7 of spontaneous differentiation (n=3 biological replicates, mean \pm SEM, *p<0.05, **p<0.01, n.s.: non-significant, Student's t-test). (B) Relative transcript abundance of *Fgf2* and select pluripotency markers (*Nanog*, *Pou5f1*, *Sox2*) in wild type and p66Shc knockout-derived EBs at day 0 of spontaneous differentiation (n=3 biological replicates, mean \pm SEM, Student's t-test).

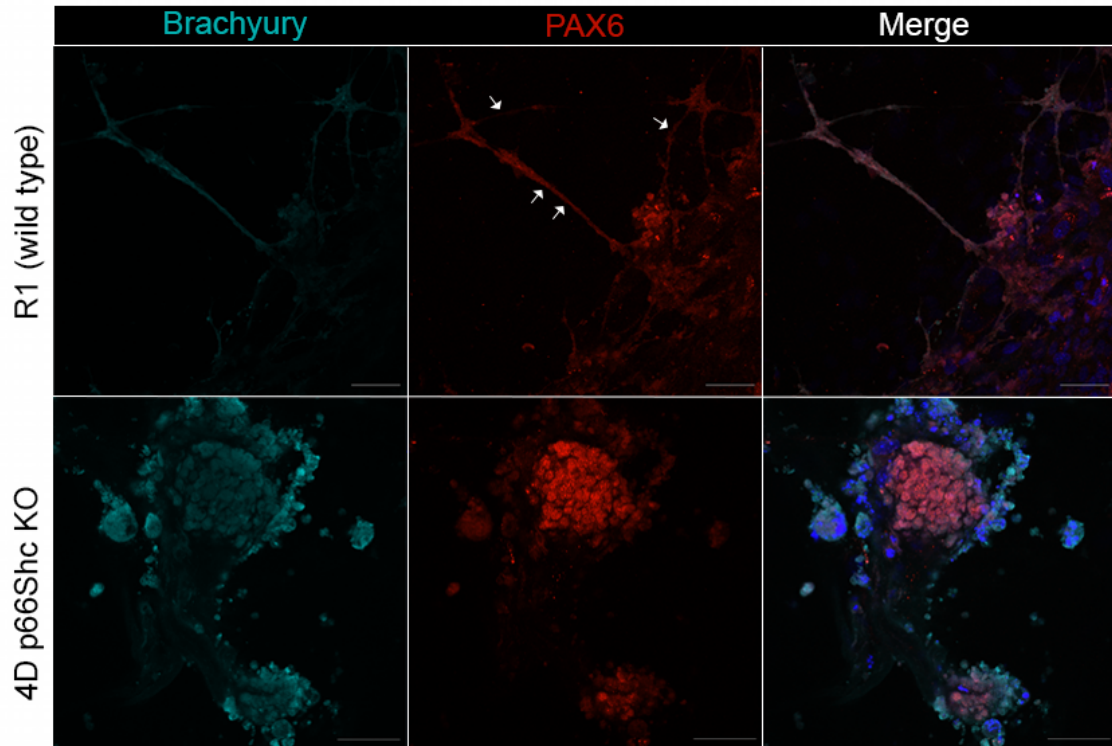


Figure 4-8. PAX6/Brachyury-positive projections emerge from wild type EBs and are absent in p66Shc knockout EBs after 14 days of spontaneous differentiation.

Representative confocal microscopy images of wild type and p66Shc knockout (4D) EBs stained for PAX6 (red) and Brachyury (cyan). DAPI (blue) co-stains nuclei. White arrows indicate examples of Brachyury/PAX6-positive projections present in wild type EBs. Scale bars are 50 μm .

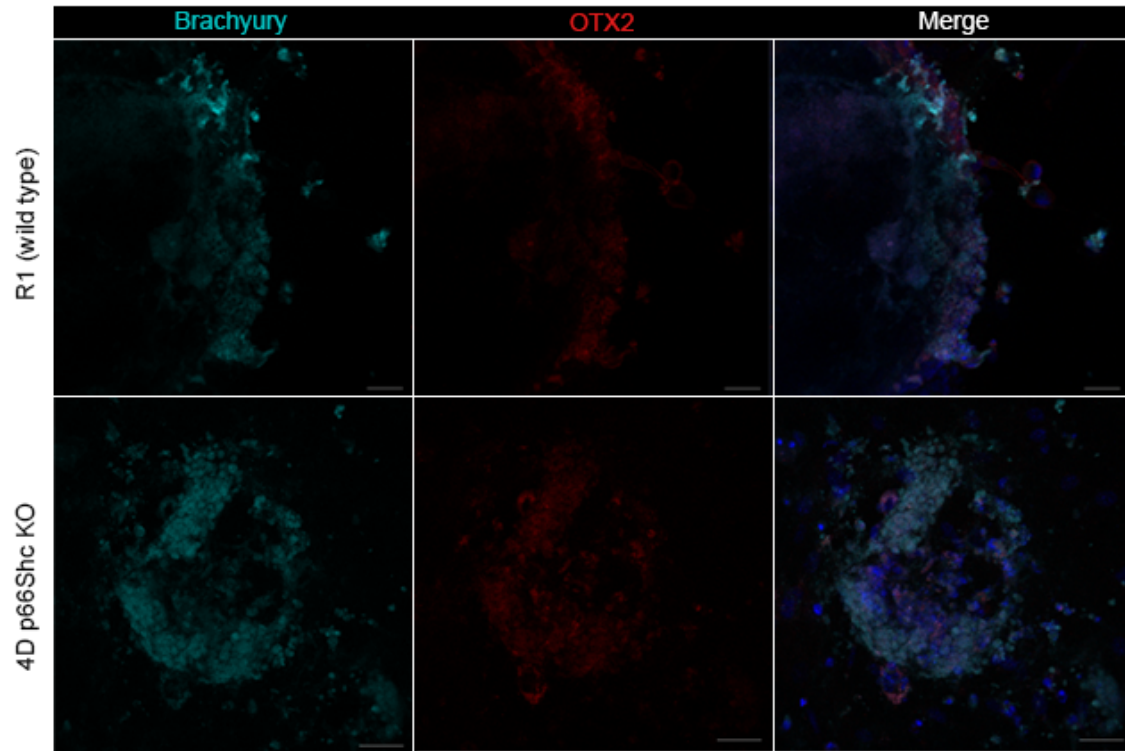


Figure 4-9. Brachyury and OTX2 is detectable in wild type and p66Shc knockout EBs after 7 days of spontaneous differentiation.

Representative confocal microscopy images of EBs stained for Brachyury (cyan) and OTX2 (red). DAPI (blue) co-stains nuclei. Scale bars are 50 μm .

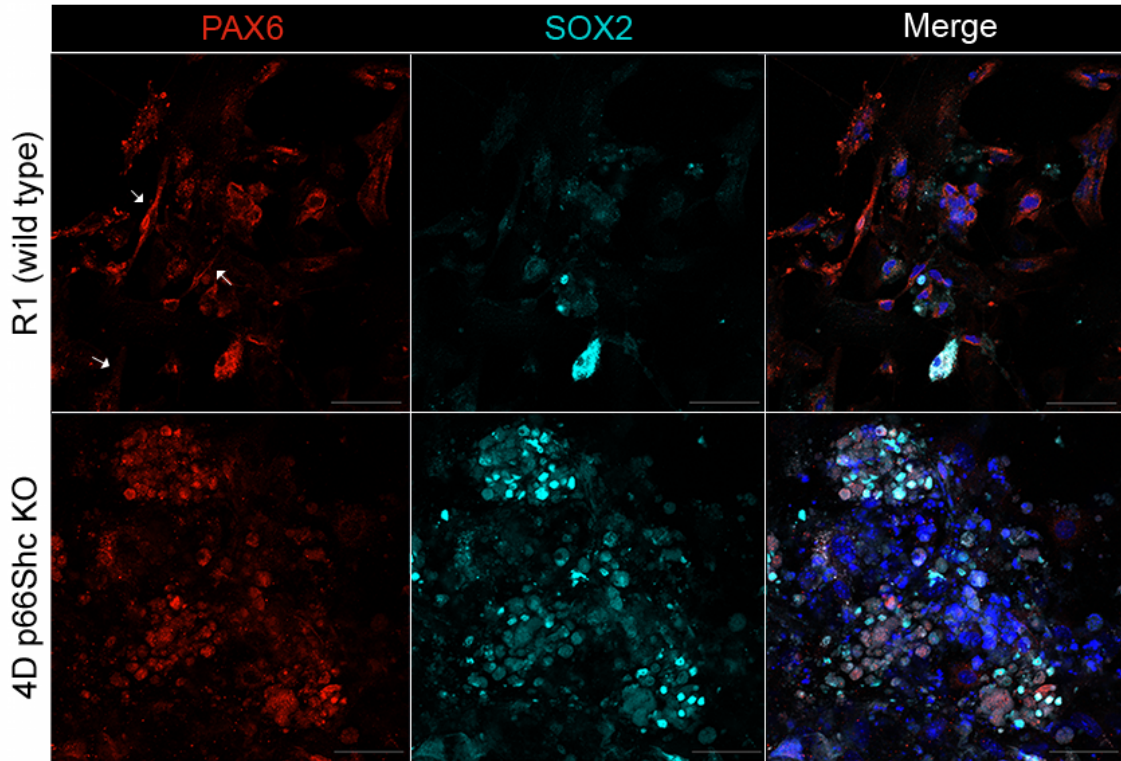


Figure 4-10. PAX6/SOX2-positive cells present in wild type and p66Shc knockout EBs after 7 days of spontaneous differentiation.

Representative confocal microscopy images of EBs stained for PAX6 (red) and SOX2 (cyan). DAPI (blue) co-stains nuclei. White arrows indicate examples of elongated PAX6-positive cells emerging from wild type EBs. Scale bars are 50 μm.

However, OTX2 fluorescence intensity was visibly decreased in p66Shc knockout EBs compared to controls (Fig. 4-11). Our immunofluorescence and confocal microscopy results suggest that morphologically different cell types emerge from p66Shc knockout EBs compared to wild type-derived EBs, while the analysis of lineage-associated transcripts suggests that p66Shc knockout EBs upregulate markers of mesoderm derivatives and downregulate markers of neuroectoderm derivatives relative to wildtype EBs.

4.4 Discussion

Here, we demonstrate that genetic knockout of p66Shc significantly alters the expression of pluripotency-associated markers. Specific deletion of p66Shc by CRISPR-Cas9 does not change morphology of mESC colonies but causes a consistent downregulation of NANOG expression detected by immunofluorescence that is rescued by reintroduction of p66Shc expression. Additionally, p66Shc knockout results in an upregulation of mesoderm-associated markers and a downregulation of neuroectoderm-associated markers relative to wild type controls during spontaneous differentiation of EBs. Our results suggest that p66Shc may be important for promoting the naïve pluripotent state observed in unedited mESCs, and the ability to differentiate into derivatives of all three germ layers in an unbiased manner.

Three isoforms are transcribed from the *Shc1* loci with shared sequences, and thus it is challenging to specifically target a *Shc* genetic knockout to one isoform. The only difference between the coding sequences of p66Shc compared to p52Shc/p46Shc is an N-terminal extension to exon 2 (Migliaccio et al., 1999). However, the transcription of p52Shc/p46Shc and p66Shc is under regulation of two different promoters (Ventura et al., 2002). We are the first to use a genetic knockout strategy that targets the known promoter region of p66Shc and its transcriptional start site. Other studies have targeted p66Shc in mice by deleting the unique N-terminal CH2 domain (Migliaccio et al., 1999). However, this strategy has been shown to affect the expression levels of p52Shc/p46Shc in certain tissues, precluding investigation into the specific role of p66Shc (Tomilov et al., 2011). We selected knockout clonal lines that had unaffected levels of p52Shc/p46Shc protein relative to wild type controls to ensure that the observed

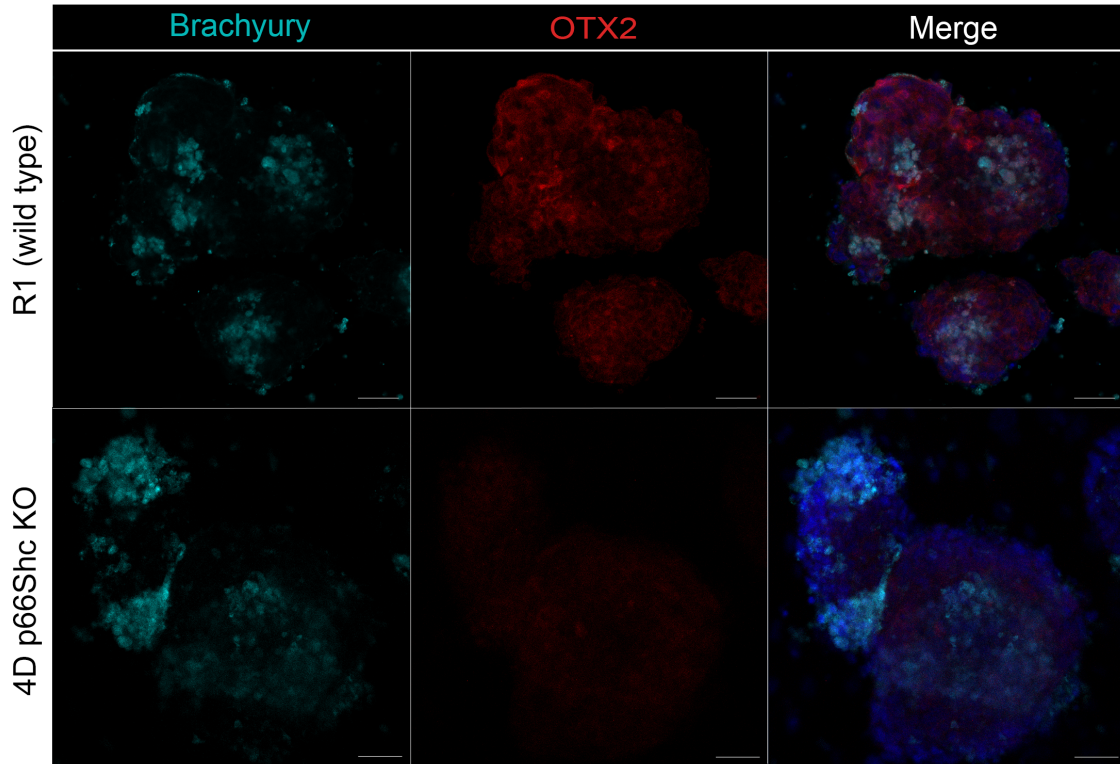


Figure 4-11. Reduced OTX2 fluorescence in p66Shc knockout EBs after 24 hours (Day 0) of spontaneous differentiation.

Representative confocal microscopy images of EBs stained for Brachyury (cyan) and OTX2 (red). DAPI (blue) co-stains nuclei. Scale bars are 50 μm .

phenotype was due to the loss of p66Shc expression specifically. Supporting this, transient reintroduction of p66Shc expression restored NANOG expression in the 4D knockout line, an overlapping phenotype observed in knockout lines generated from both gRNA pairs. Our specific knockout of p66Shc in mESCs validates the targeting strategy our group is using to generate a transgenic p66Shc-loxP mouse model by flanking the promoter and transcriptional start site with loxP sites. Furthermore, CRISPR-Cas9 knockout mESCs could be used to create full p66Shc knockout mice by blastocyst injection and chimera generation.

P66Shc knockout mESCs remained capable of self-renewal as they maintained a pluripotent colony morphology with no overt tendency to differentiate over six passages when cultured on a MEF-feeder layer in serum/LIF medium, comparable to wild type mESCs cultured in parallel. However, the transcriptional abundance of selected naïve and primed pluripotency markers was variably and significantly altered in different p66Shc knockout mESC clonal lines compared to wild type controls. Interestingly, knockout line 4D had significantly increased *Nanog* transcript abundance levels, which contradicts the reduced NANOG protein expression seen by immunofluorescence and confocal microscopy. Furthermore, *Rex1* (*Zfp42*) is a known transcriptional target of *Nanog* and its expression should be maintained if *Nanog* expression is elevated (Shi et al., 2006). Interestingly, increased transcript abundance of *Fgf5* and *Otx2* in knockout line 10D suggests that it has a more primed pluripotent phenotype. However, it is known that mESCs cultured in serum/LIF conditions have dynamic expression of pluripotency markers and likely have a mix of naïve and primed characteristics (Manor et al., 2015). Variability in the changes in pluripotent markers could also be due to off-target effects of the CRISPR-Cas9 editing. Reintroducing p66Shc expression and determining if these transcripts return to wild type levels will confirm a gene-specific phenotype and elucidate any off-target effects. Our results suggest that p66Shc knockout mESCs may have exited naïve pluripotency and may have entered an intermediate stage between naïve and primed (e.g. formative pluripotency) (Smith, 2017). More stringent tests of pluripotency such as teratoma formation or chimera contribution should be used to determine the extent of alterations in pluripotency observed in p66Shc knockout mESCs. Additionally, we did not culture p66Shc knockout mESCs in 2i/LIF medium, which promotes and stabilizes a

more homogeneous naïve phenotype. It would be interesting to compare p66Shc knockout mESCs cultured in 2i/LIF compared to mESCs cultured in serum/LIF conditions to determine if the pluripotency markers assessed become comparable to wild type mESCs.

A common, overlapping phenotype observed between three p66Shc knockout mESC lines is the reduced or undetectable expression of NANOG by immunofluorescence and confocal microscopy. The relative importance of NANOG for maintaining mESC pluripotency is controversial and appears to depend on the culture conditions. NANOG expression is dynamic in mESCs, as it is undetectable in a population of OCT4 positive cells, and isolated NANOG negative cells can regenerate colonies that become NANOG positive (Abranches et al., 2013; Chambers et al., 2007). NANOG knockout mESCs can self-renew but are more prone to spontaneous differentiation into primitive endoderm-like cells (Chambers et al., 2007). NANOG is likely not required for pluripotency as iPSCs can be generated from NANOG^{-/-} MEFs with characteristics of naïve pluripotency, particularly if the reprogramming medium is supplemented with ascorbic acid (Carter et al., 2014; Schwarz et al., 2014). NANOG blocks neural differentiation and can reverse mesoderm differentiation by repressing the expression of T/Brachyury (Suzuki et al., 2006). Thus, we speculate that the bias towards mesoderm differentiation observed in spontaneous EB differentiation of p66Shc knockout mESCs may be due to decreased NANOG repression of mesoderm specification. However, we do not observe significant changes in T/Brachyury expression at our selected time points, and thus future studies will investigate if there is a relationship between decreased NANOG expression and the bias in spontaneous differentiation towards mesoderm derivatives seen in p66Shc knockout mESCs.

Additionally, we observed that relative to EBs derived from wild type mESCs, EBs derived from p66Shc knockout line 4D had significantly lower expression of neuroectoderm markers (*Pax6*, *Scn1a*, *Gfap*, *Sox2*). Our results thus suggest that knockout of p66Shc biases spontaneous differentiation of EBs away from neuroectoderm lineages. Directed differentiation of p66Shc knockout mESCs will determine if p66Shc is required for neuroectoderm differentiation. Overexpression of p66Shc accelerates ESC

neural differentiation under neural-promoting conditions (Papadimou et al., 2009; Ying et al., 2003). However, it is not sufficient to cause spontaneous neural differentiation, as overexpression of p66Shc in pluripotency-maintaining conditions causes mESCs to adopt a colony morphology characteristic of naïve cells (Papadimou et al., 2009). This dual role of p66Shc may be due to regulation of signalling pathways important for both maintaining pluripotency and promoting differentiation, such as the MEK/ERK and Wnt/ β -Catenin pathways. Maintaining active Wnt/ β -catenin signalling through inhibition of GSK-3 β promotes pluripotency and inhibits ectoderm differentiation. Overexpression of p66Shc in self-renewal conditions increases phosphorylated GSK-3 β , causing its inactivation and the promotion of β -catenin signalling, which would further promote ESC pluripotency (Papadimou et al., 2009). Notably, phosphorylated ERK1/2 did not change with p66Shc overexpression in self-renewal conditions (Papadimou et al., 2009). One limitation of our study is that we did not investigate changes to signalling pathways in p66Shc knockout mESCs to determine the mechanism of p66Shc knockout in affecting mESC pluripotency and differentiation. Future studies will investigate whether the reverse, e.g., reduced phosphorylated GSK-3 β and destabilization of β -catenin, occurs in p66Shc knockout mESCs, which would reduce their ability to differentiate towards neural lineages under the same culture conditions used by Papadimou *et al.* Interestingly, *Fgf2* is upregulated at later stages of spontaneous differentiation (e.g. day 7 and day 14) in p66Shc knockout EBs, and therefore changes to FGF/MAPK/ERK signalling should also be investigated in differentiating p66Shc knockout EBs. Ultimately, these differentiation experiments must be repeated in additional p66Shc knockout mESCs to determine reproducibility and the extent of the effects of p66Shc knockout to mESC function.

4.5 References

- Abranches, E., Bekman, E. and Henrique, D.** (2013). Generation and characterization of a novel mouse embryonic stem cell line with a dynamic reporter of Nanog expression. *PLoS One* **8**, e59928.
- Carter, A. C., Davis-Dusenbery, B. N., Koszka, K., Ichida, J. K. and Eggan, K.** (2014). Nanog-independent reprogramming to iPSCs with canonical factors. *Stem Cell Reports* **2**, 119-126.

- Chambers, I., Silva, J., Colby, D., Nichols, J., Nijmeijer, B., Robertson, M., Vrana, J., Jones, K., Grotewold, L. and Smith, A.** (2007). Nanog safeguards pluripotency and mediates germline development. *Nature* **450**, 1230-1234.
- Evans, M. J. and Kaufman, M. H.** (1981). Establishment in culture of pluripotential cells from mouse embryos. *Nature* **292**, 154-156.
- Hanna, J., Markoulaki, S., Mitalipova, M., Cheng, A. W., Cassady, J. P., Staerk, J., Carey, B. W., Lengner, C. J., Foreman, R., Love, J., et al.** (2009). Metastable pluripotent states in NOD-mouse-derived ESCs. *Cell Stem Cell* **4**, 513-524.
- Hodgkins, A., Farne, A., Perera, S., Grego, T., Parry-Smith, D. J., Skarnes, W. C. and Iyer, V.** (2015). WGE: a CRISPR database for genome engineering. *Bioinformatics* **31**, 3078-3080.
- Lai, K. M. and Pawson, T.** (2000). The ShcA phosphotyrosine docking protein sensitizes cardiovascular signaling in the mouse embryo. *Genes Dev* **14**, 1132-1145.
- Manor, Y. S., Massarwa, R. and Hanna, J. H.** (2015). Establishing the human naive pluripotent state. *Curr Opin Genet Dev* **34**, 35-45.
- Martin, G. R.** (1981). Isolation of a pluripotent cell line from early mouse embryos cultured in medium conditioned by teratocarcinoma stem cells. *Proc Natl Acad Sci U S A* **78**, 7634-7638.
- Migliaccio, E., Giorgio, M., Mele, S., Pelicci, G., Reboldi, P., Pandolfi, P. P., Lanfrancone, L. and Pelicci, P. G.** (1999). The p66shc adaptor protein controls oxidative stress response and life span in mammals. *Nature* **402**, 309-313.
- Murry, C. E. and Keller, G.** (2008). Differentiation of embryonic stem cells to clinically relevant populations: lessons from embryonic development. *Cell* **132**, 661-680.
- Nagy, A., Rossant, J., Nagy, R., Abramow-Newerly, W. and Roder, J. C.** (1993). Derivation of completely cell culture-derived mice from early-passage embryonic stem cells. *Proc Natl Acad Sci U S A* **90**, 8424-8428.
- Nichols, J., Silva, J., Roode, M. and Smith, A.** (2009). Suppression of Erk signalling promotes ground state pluripotency in the mouse embryo. *Development* **136**, 3215-3222.
- Nichols, J. and Smith, A.** (2009). Naive and primed pluripotent states. *Cell Stem Cell* **4**, 487-492.
- Niwa, H.** (2007). How is pluripotency determined and maintained? *Development* **134**, 635-646.

- Papadimou, E., Moiana, A., Goffredo, D., Koch, P., Bertuzzi, S., Brustle, O., Cattaneo, E. and Conti, L.** (2009). p66(ShcA) adaptor molecule accelerates ES cell neural induction. *Mol Cell Neurosci* **41**, 74-84.
- Ran, F. A., Hsu, P. D., Wright, J., Agarwala, V., Scott, D. A. and Zhang, F.** (2013). Genome engineering using the CRISPR-Cas9 system. *Nat Protoc* **8**, 2281-2308.
- Schwarz, B. A., Bar-Nur, O., Silva, J. C. and Hochedlinger, K.** (2014). Nanog is dispensable for the generation of induced pluripotent stem cells. *Curr Biol* **24**, 347-350.
- Shi, W., Wang, H., Pan, G., Geng, Y., Guo, Y. and Pei, D.** (2006). Regulation of the pluripotency marker Rex-1 by Nanog and Sox2. *J Biol Chem* **281**, 23319-23325.
- Smith, A.** (2017). Formative pluripotency: the executive phase in a developmental continuum. *Development* **144**, 365-373.
- Smith, S. M., Bajpai, R. and Minoo, P.** (2016). The p66Shc Adapter Protein Is Necessary to Maintain Pluripotency. In *B52. NEONATAL LUNG DISEASE: FROM BENCH TO BABIES*, pp. A3857-A3857.
- Suzuki, A., Raya, A., Kawakami, Y., Morita, M., Matsui, T., Nakashima, K., Gage, F. H., Rodriguez-Esteban, C. and Izpisua Belmonte, J. C.** (2006). Maintenance of embryonic stem cell pluripotency by Nanog-mediated reversal of mesoderm specification. *Nat Clin Pract Cardiovasc Med* **3 Suppl 1**, S114-122.
- Takahashi, K. and Yamanaka, S.** (2006). Induction of pluripotent stem cells from mouse embryonic and adult fibroblast cultures by defined factors. *Cell* **126**, 663-676.
- Tesar, P. J., Chenoweth, J. G., Brook, F. A., Davies, T. J., Evans, E. P., Mack, D. L., Gardner, R. L. and McKay, R. D.** (2007). New cell lines from mouse epiblast share defining features with human embryonic stem cells. *Nature* **448**, 196-199.
- Thomson, J. A., Itskovitz-Eldor, J., Shapiro, S. S., Waknitz, M. A., Swiergiel, J. J., Marshall, V. S. and Jones, J. M.** (1998). Embryonic stem cell lines derived from human blastocysts. *Science* **282**, 1145-1147.
- Ventura, A., Luzi, L., Pacini, S., Baldari, C. T. and Pelicci, P. G.** (2002). The p66Shc longevity gene is silenced through epigenetic modifications of an alternative promoter. *J Biol Chem* **277**, 22370-22376.
- Ying, Q. L., Stavridis, M., Griffiths, D., Li, M. and Smith, A.** (2003). Conversion of embryonic stem cells into neuroectodermal precursors in adherent monoculture. *Nat Biotechnol* **21**, 183-186.

Chapter 5

5 General Discussion and Conclusions

5.1 Discussion and Significance of Research

In addition to promoting apoptosis and senescence in embryos exposed to stress-inducing culture conditions or agents, p66Shc is expressed throughout mammalian preimplantation development, suggesting an additional important physiological role in regulating early development. The overall hypothesis of my thesis is that loss of p66Shc expression in the mouse preimplantation embryo will dysregulate blastocyst development and mouse embryonic stem cell pluripotency. With my thesis work, I have advanced our understanding of p66Shc function both in mouse blastocyst development and the regulation of pluripotency by discovering a novel role for p66Shc in cell fate specification. The main findings that support my hypothesis and advance this knowledge are that:

- (1) P66Shc expression likely needs to be maintained at a level which promotes normal blastocyst physiology and cell fate specification.
- (2) P66Shc promotes the expression of pluripotency-associated markers in mouse embryonic stem cells.

I have provided insight into the possible mechanisms by which p66Shc regulates blastocyst physiology in response to external stimuli (culture, oxygen tension), possibly through the generation of ROS which may in turn modulate cell signalling pathways such as the Wnt/ β -catenin pathway. On the other hand, p66Shc may be acting as an adaptor protein in RTK/MAPK signalling, negatively regulating ERK1/2 activation and promoting a pluripotent or epiblast fate (Figure 5-1).

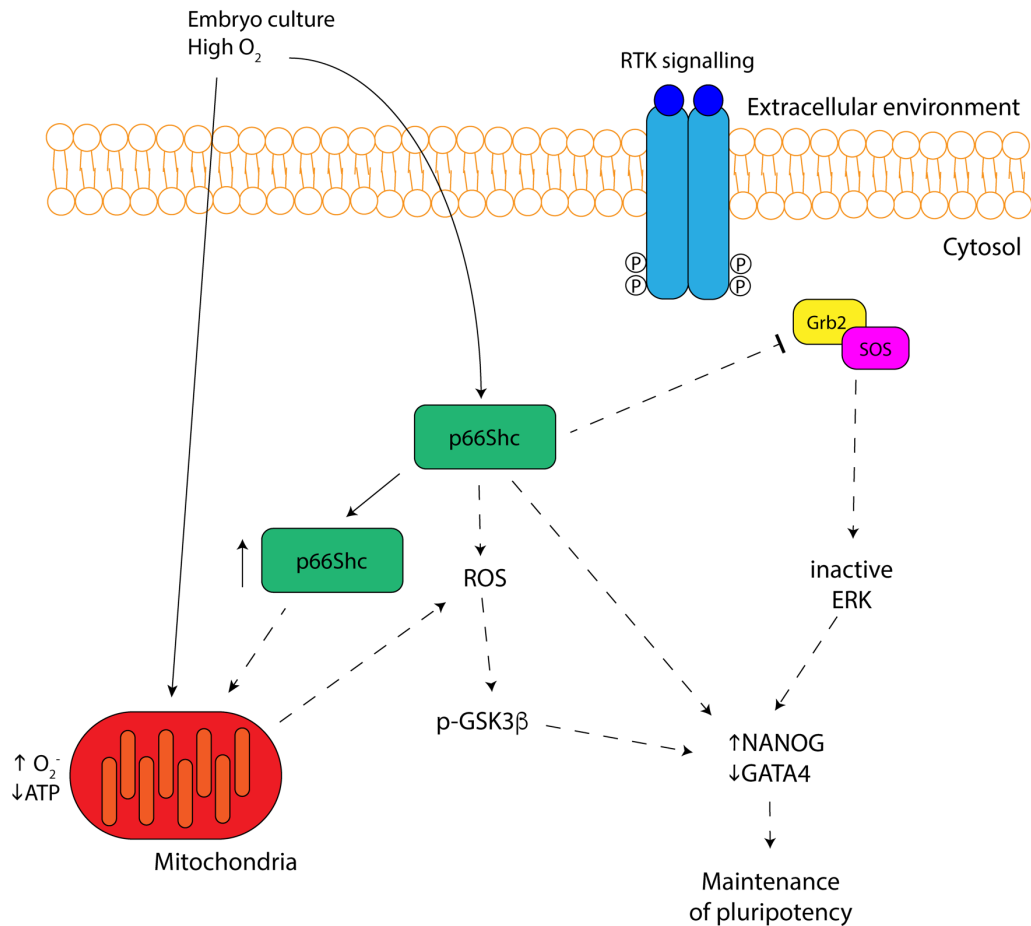


Figure 5-1. Summary of p66Shc functions and potential mechanisms in the mouse preimplantation embryo and mouse embryonic stem cells.

Embryo culture and high oxygen tension cause an increase in p66Shc (green) expression in the mouse blastocyst, which correlates with increased superoxide (O_2^-) and decreased ATP production under the same experimental conditions. P66Shc may indirectly regulate the expression of lineage-associated markers through its role as an adaptor protein for receptor tyrosine kinase (RTK) signalling, leading to reduced activation of ERK and thus reducing GATA4 expression in the blastocyst inner cell mass. Another potential mechanism by which p66Shc may promote pluripotency is through ROS-mediated regulation of GSK3 β activity, which in turn may promote nuclear β -catenin and the maintenance of pluripotency. Solid lines represent known effects, dashed lines represent putative mechanisms.

5.1.1 P66Shc expression likely needs to be maintained at a level which promotes normal blastocyst development

I propose a model in which p66Shc expression must be maintained at a level that promotes normal preimplantation development. Aberrant increases in p66Shc transcript and protein abundance induced by embryo culture disrupt physiological processes such as metabolism (Chapter 2), and RNAi-mediated decreases in p66Shc disrupt lineage allocation in the blastocyst ICM (Chapter 3) (Figure 5-2).

Quantification of p66Shc transcript and protein abundance during *in vivo* mouse preimplantation development demonstrated that p66Shc is normally upregulated at the blastocyst stage (Chapter 2). This was confirmed by the reemergence of p66Shc expression 96 hours after siRNA knockdown in the zygote (Chapter 3). Increasing atmospheric oxygen tension during embryo culture caused additional, *de novo* transcription of p66Shc in blastocysts, correlated with increased superoxide production and decreased ATP levels compared to *in vivo* controls. This is consistent with previous work demonstrating that bovine embryos with poor developmental outcomes (e.g. late cleaving) had increased p66Shc expression levels compared to embryos with good developmental outcomes (e.g. early cleaving) (Favetta et al., 2004). In bovine embryos, p66Shc levels are a cause rather than an effect of developmental competency, as siRNA-mediated knockdown reduces permanent embryo arrest at the 2-4 cell stage (Betts et al., 2014; Favetta et al., 2007). In contrast, I did not observe significant changes in mouse blastocyst development between oxygen treatment groups in this study or with siRNA knockdown of p66Shc (Chapter 3). Instead, my results suggest that culture-induced increases in p66Shc transcript and protein abundance coincide with altered metabolism. Altered metabolism is associated with poor developmental competency to the blastocyst stage which likely would also result in poor post-implantation development (Gardner and Harvey, 2015; Gardner et al., 2001; Wale and Gardner, 2012; Wale and Gardner, 2013). Interestingly, overexpression of p66Shc in multiple cell lines, including embryonic stem cells, did not affect cell viability, suggesting that increased p66Shc expression does not

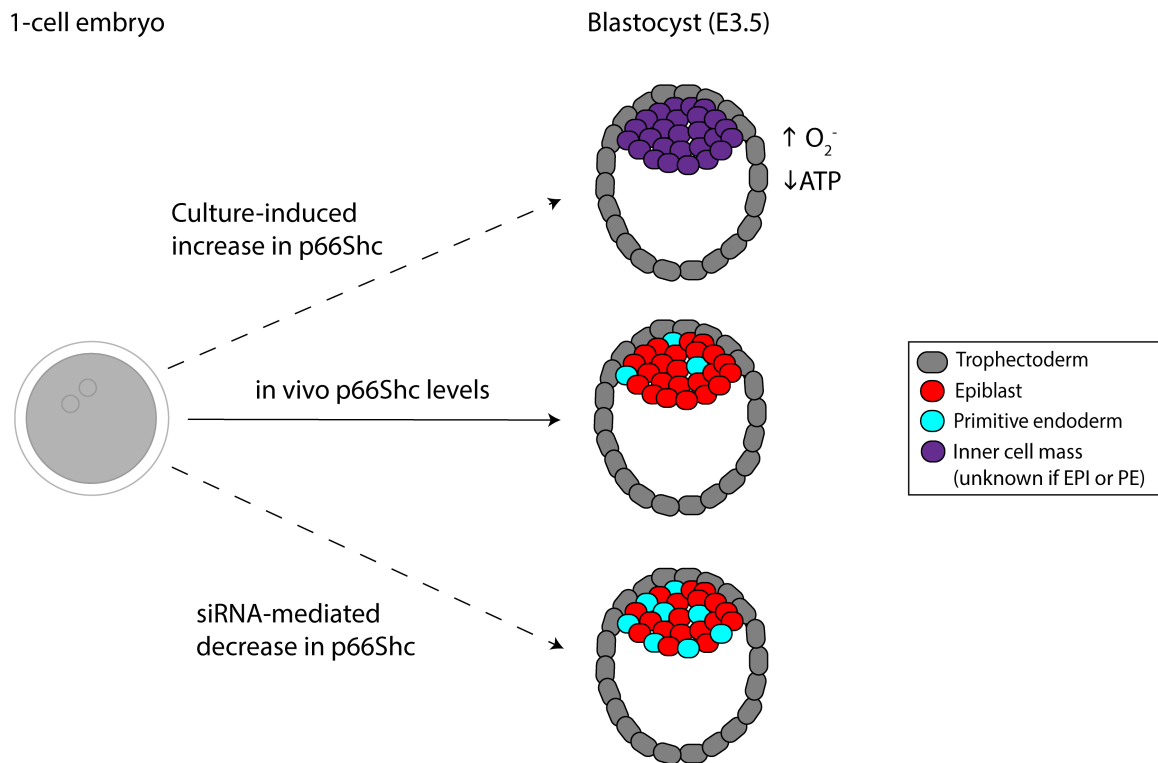


Figure 5-2. P66Shc likely needs to be expressed at a certain level to promote normal mouse preimplantation development.

Mouse preimplantation embryos expressing normal levels of p66Shc (e.g. developing *in vivo*, or scrambled siRNA injected) progress normally through blastocyst development, maintaining physiology and cell fate specification. Aberrant culture-induced increases in p66Shc expression, i.e. increasing oxygen tension *in vitro*, causes altered metabolic physiology in the blastocyst with increased production of superoxide (O_2^-) and decreased total ATP content. However, it is not known if cell specification in the blastocyst ICM significantly altered compared to controls. Knockdown of p66Shc expression causes altered cell fate specification with a significant increase in the proportion of PrE cells and a concomitant decrease in the proportion of EPI cells in the blastocyst ICM compared to controls. Thus, both elevated and low levels of p66Shc dysregulate blastocyst development.

promote apoptosis in non-stress inducing conditions (Migliaccio et al., 1997; Okada et al., 1997; Papadimou et al., 2009). Thus, increased p66Shc expression due to environmental insults, rather than experimentally overexpressing p66Shc, negatively affects embryo physiology and viability, and most interestingly the embryo is able to alter its response depending upon the insult and conditions it is placed under.

Reducing p66Shc levels in mouse preimplantation embryos by siRNA-mediated knockdown affected blastocyst development by altering cell fate specification. These results significantly advance our understanding of p66Shc function in mammalian preimplantation development and reveal a novel role of p66Shc in cell fate regulation. Similar observations have been made with knockdown or knockout of genes involved in signalling pathways controlling cell fate specification in the ICM, such as FGF4/FGFR2 (Kang et al., 2017; Krawchuk et al., 2013) GRB2 (Chazaud et al., 2006) and KLF5 (Azami et al., 2017). Thus, it is likely that p66Shc regulates MEK-ERK signalling downstream of FGF4 in the inner cell mass to regulate the proportions of EPI and PrE cells. Accordingly, I observed a significant increase in cells expressing DUSP4, a specific transcriptional target of FGF4/MAPK, in p66Shc knockdown blastocysts compared to controls, suggesting inappropriate activation of MEK-ERK signalling in cells that were committed to the EPI fate. When p66Shc binds RTKs, ERK is not activated (Migliaccio et al., 1997; Okada et al., 1997), thus I would predict that a reduction in p66Shc in ICM cells allows for increased ERK activation leading to the adoption of PrE fate. However, I did not determine the level at which p66Shc acts in this pathway, or whether p66Shc could also influence the activation of other developmental signalling pathways that could cross-talk with the FGF4/MAPK pathway (e.g. through ROS signalling) (Lee and Esselman, 2002). Additionally, p66Shc knockdown embryos were cultured under optimal (e.g. 5% oxygen atmosphere) culture conditions. To potentially link the stress-related functions of p66Shc to blastocyst cell fate specification, it would be interesting to assess blastocyst lineage specification in embryos cultured at high (~20%) oxygen tension, which I have associated with aberrantly increased p66Shc expression. Embryos cultured at low (5%) oxygen contain a significantly increased percentage of ICM cells of total cells in the blastocyst compared to embryos cultured at high (~20%) oxygen and *in vivo* controls determined by differential propidium iodide staining (Karagenc et al., 2004;

Rinaudo et al., 2006), but no study to date has determined the proportions of EPI vs PrE cells in these ICMs.

Taken together, my results demonstrate that p66Shc is normally expressed in controlled, stage-specific levels throughout *in vivo* embryonic development, but aberrant increases above these levels due to exposure to the culture environment impacts blastocyst physiology or experimentally-induced decreases affects cell fate specification.

5.1.2 P66Shc promotes the expression of pluripotency-associated markers

A significant decrease in the proportion of Nanog-expressing cells in the ICM of p66Shc knockdown blastocysts suggests that p66Shc is critical for proper establishment and/or maintenance of pluripotency during blastocyst cell lineage specification. However, it is not fully understood at which point in cell specification p66Shc may be acting on the pluripotent cell population in the ICM. Expression of the pluripotency markers OCT4 and SOX2 in the ICM are unaffected by p66Shc knockdown, suggesting that EPI identity is initially established in these embryos. OCT4 is linked to the promotion of PrE fate, and OCT4 levels must be carefully regulated in order to promote EPI cell identity and pluripotency in embryonic stem cells (Frum et al., 2013; Le Bin et al., 2014; Niwa et al., 2000). The high levels of OCT4 fluorescence observed in p66Shc knockdown blastocyst ICMs suggests that elevated OCT4 expression promotes a PrE fate. P66Shc expression in the ICM thus is likely necessary for **maintaining** EPI identity and in preventing aberrant conversion to the PrE fate. A partial rescue of the Nanog-expressing population in the ICM of 64-128 cell blastocysts supports this, as some GATA4-positive cells became Nanog-positive as p66Shc knockdown blastocysts advanced their development. However, there must be a critical number of Nanog-positive cells required to promote ICM-derived outgrowth expansion *in vitro*, representing a threshold that is not met by a significant proportion of p66Shc knockdown blastocysts. To determine if p66Shc is required for the **establishment** of pluripotency, iPSC generation must be attempted in differentiated cells (e.g. MEFs) with a genetic knockout of p66Shc.

A limitation of the experiments performed in Chapter 3 is that p66Shc expression was transiently knocked down by siRNA, and expression was regained at the blastocyst stage. Thus, the full extent of p66Shc requirement for EPI fate cannot be elucidated with this study. Genetic knockout of p66Shc in preimplantation embryos will overcome this limitation (details in Future Studies section below). Furthermore, the complementary experiment, e.g. overexpressing p66Shc in mouse preimplantation embryos, should be performed to determine if the proportion of Nanog-positive cells significantly increases over GATA4-positive cells in the ICM. However, based on results from Chapter 2, the culture system currently used may require further optimization to prevent environmentally induced increases in p66Shc expression that may become additive with experimentally induced p66Shc overexpression, leading to increased embryo apoptosis/arrest and decreased development to the blastocyst stage.

By using mouse embryonic stem cells as a cell model of the EPI, I determined the importance of p66Shc in maintaining pluripotency. In serum/LIF culture conditions, mESCs with a genetic knockout of p66Shc have consistently decreased or undetectable NANOG fluorescence compared to wild type mESCs that is rescued by reintroduction of a p66Shc expression plasmid. Together with significant changes to naïve and primed transcriptional markers, p66Shc knockout mESCs are evidently different than naïve pluripotent, wild type controls. However, they do not fully meet the criteria of primed pluripotency with regards to colony morphology, the consistent upregulation of lineage specification markers (e.g. T/Brachyury), and the consistent downregulation of naïve pluripotency markers (e.g. *Rex1*). ESCs cultured in serum/LIF conditions are intermediate on the pluripotency spectrum, i.e., less naïve than ESCs cultured in 2i (Hackett and Surani, 2014). Serum/LIF ESCs can contribute to the germline in chimeras, are *Rex1* positive, but some cells have primed characteristics (e.g. are OCT4-positive but *Rex1*-negative) (Hackett and Surani, 2014). This heterogeneity in serum/LIF is metastable and interchangeable. However, p66Shc knockout mESCs in serum/LIF have properties that suggest they may be less naïve than wild type ESCs in serum/LIF. And thus, if p66Shc knockout mESCs are neither fully naïve nor fully primed, where do they fall on the pluripotency spectrum?

Recently, an intermediate state has been proposed that describes cells resembling the *in vivo* epiblast just after implantation (E5.0-6.25) that are transcriptionally different from naïve and primed ESCs. Termed formative pluripotency, these cells encompass more developmentally advanced ESCs that have acquired lineage competence and can respond to inductive cues faster than naïve ESCs (Mohammed et al., 2017; Mulas et al., 2017; Smith, 2017) (Figure 5-3). Formative cells express the pluripotency markers OCT4 and SOX2, but have low NANOG expression, and express the primed markers FGF5 and OTX2. Notably, formative cells display robust primordial germ cell-like cell (PGCLC) generation in response to BMP4, in contrast to BMP4 maintaining naïve ESC pluripotency and promoting differentiation in primed ESCs. Based on the expression of transcriptional markers, p66Shc knockout mESCs, particularly knockout line 10D, have exited the naïve pluripotent state and may be in the formative state. To confirm this, the transcriptome of p66Shc knockout mESCs should be characterized and compared to the existing naïve, formative, and primed transcriptomes. Formative pluripotent cells can contribute to chimeras and teratomas (Morgani et al., 2017) and therefore I expect p66Shc knockout mESCs to integrate into blastocysts and contribute to the formation of embryonic germ layers. However, the defining characteristic will be how p66Shc knockout mESCs respond to BMP4. If p66Shc knockout mESCs in serum/LIF differentiate into PGCLCs when treated with BMP4, this would provide strong evidence that they have exited naïve pluripotency and are in the formative pluripotent state.

The change in pluripotent characteristics in p66Shc knockout mESCs may be related to the bias in spontaneous differentiation observed during embryoid body (EB) differentiation. Notably, EBs formed from p66Shc knockout mESCs showed a significant reduction in mature neuroectoderm transcriptional markers compared to wild type controls, suggesting that p66Shc may be required for either maintaining a pluripotent state that facilitates robust neural differentiation or is necessary for the early stages of neural differentiation. Supporting this, Papadimou *et al.* observed increasing p66Shc protein abundance in mESCs undergoing directed neural differentiation and that overexpressing p66Shc in mESCs accelerated neural differentiation (Papadimou et al., 2009).

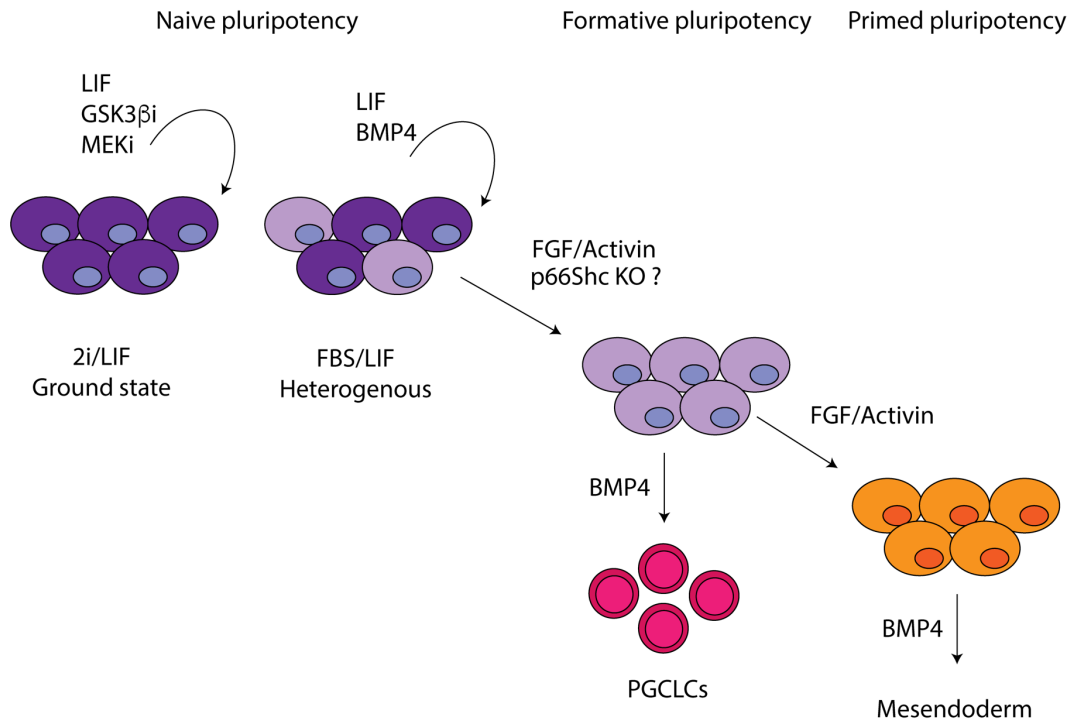


Figure 5-3. p66Shc knockout mESCs are likely in the formative pluripotent state.

Naïve pluripotency encompasses ESCs cultured in 2i/LIF (ground state, or more naïve) and ESCs cultured in fetal bovine serum (FBS) and LIF (heterogeneous, or less naïve). ESCs in 2i/LIF can be maintained without serum in medium containing inhibitors of GSK3beta and MEK. FBS contains BMP4, which maintains self-renewal along with LIF in ESCs cultured in FBS/LIF. If treated with FGF/Activin, ESCs exit the naïve state and enter formative pluripotency, a developmental window that allows primordial germ cell-like cell (PGCLC) differentiation if cells are treated with BMP4. Since p66Shc knockout mESCs in FBS/LIF display altered pluripotency marker expression that is different from wild type mESCs in FBS/LIF, they may instead be in the formative rather than naïve pluripotent state. ESCs then exit formative pluripotency with continued FGF/Activin stimulation into primed pluripotency. Here, treatment of ESCs with BMP4 will promote mesendoderm differentiation.

As BMP, Wnt, and Nodal signaling inhibit ectoderm differentiation, loss of p66Shc may promote these pathways resulting in a bias to mesendoderm over ectoderm differentiation. Furthermore, if p66Shc knockout mESCs are in the formative pluripotent state, they might respond more readily to autocrine and/or paracrine inductive signals promoting mesendoderm differentiation produced by the three-dimensional environment of EBs compared to wild type controls. Future studies include determining the mechanism by which p66Shc regulates Wnt/ β -catenin signalling in mESCs (e.g. through ROS signalling, or cross-talk with RTK/MAPK signalling), and if p66Shc is necessary for directed neural differentiation. A detailed time course of pluripotency and differentiation transcriptional markers, and changes to components of the Wnt/ β -catenin and MAPK/ERK pathways during spontaneous and/or directed differentiation will provide insight into the relative importance of p66Shc to the signalling pathways regulating mESC differentiation. Interestingly, p66Shc is also implicated in the proliferation and differentiation of more restricted cell types such as lung epithelia, skeletal muscle and osteoclasts (D'Agostino et al., 2018; Lee et al., 2014; Qu et al., 2018), also likely through the regulation of signalling pathways critical to the differentiation of these cell types.

Consistent with the proposed model of p66Shc knockout mESCs being more developmentally advanced than wild type mESCs, p66Shc knockdown blastocyst ICMs also appear to be further along their developmental program when compared, at the same time point, to control blastocyst ICMs. OCT4 is initially expressed in all cells of the blastocyst until restricted to the inner cells at E4.5 (blastocysts containing approximately 100 cells) (Dietrich and Hiiragi, 2007). I observed that OCT4 restriction is faster in p66Shc knockdown blastocysts compared to controls. Furthermore, significantly more cells in p66Shc knockdown blastocysts express GATA4, a mature primitive endoderm marker, at the 32-64 cell stage compared to controls. Together with the significant decrease in Nanog-positive cells, it is possible that cells that were once Nanog-positive cannot maintain their EPI fate and instead default towards the PrE fate. Since ICM fate remains plastic until E4.0-4.25, these cells are capable of reverting to the EPI fate before irreversible commitment occurs (Yamanaka et al., 2010). Since I did not pursue the effects of p66Shc knockdown to *in vivo* peri- and post-implantation development by

embryo transfer experiments, it is not known if a more developmentally advanced ICM would necessarily negatively affect later development. However, p66Shc knockdown significantly affects the ability of blastocysts to form an ICM-derived outgrowth, suggesting a similar *in vivo* phenotype would be observed.

Collectively, my results demonstrate that p66Shc regulates the maintenance of naïve pluripotency by maintaining the EPI cell population in the blastocyst ICM and by conserving naïve pluripotent characteristics in mESCs. Nanog expression is significantly affected in both the p66Shc knockdown blastocyst ICM and p66Shc knockout mESCs, and both appear to be more developmentally advanced than their respective controls.

5.2 Future studies: generation of p66Shc-loxP mice

Determining the full extent of p66Shc requirement for the establishing the pluripotent cell population in the blastocyst can be achieved by using knockout mouse models. To this end, I am generating a p66Shc-specific loxP transgenic mouse to use with oocyte-specific Cre-mediated recombination. I employed a similar targeting strategy to the one used to generate p66Shc knockout mouse embryonic stem cells (mESCs) (Figure 5-3A). A targeting vector was designed to insert the 5' loxP site upstream of the known p66Shc promoter region and insert the 3' loxP site in the 5'-untranslated region of the p66Shc coding sequence (*see* Materials and Methods in Appendix A). In collaboration with the London Regional Transgenic and Gene Targeting Facility (LRTGT), homologous recombination was then used to generate mESC clones with one targeted *Shc1* allele verified by Southern blotting (Figure 5-3B). Chromosome counts were performed on clonal cell lines 2A12 and 2F12, which were then injected into blastocysts to form chimeras (Figure 5-4A). Pups born from blastocysts injected with 2F12 are shown in Fig. 5-4B. Final steps in this process include: confirming germline transmission, breeding out of the neomycin selectable marker by Flp recombination, and establishment of a homozygous p66Shc-loxP mouse colony.

Mating with Cre-expressing mouse lines and appropriate breeding schemes will be used to generate preimplantation embryos with maternal- and/or zygotic-knockouts of p66Shc. To generate a body-wide heterozygote knockout of p66Shc, p66Shc-loxP mice can be

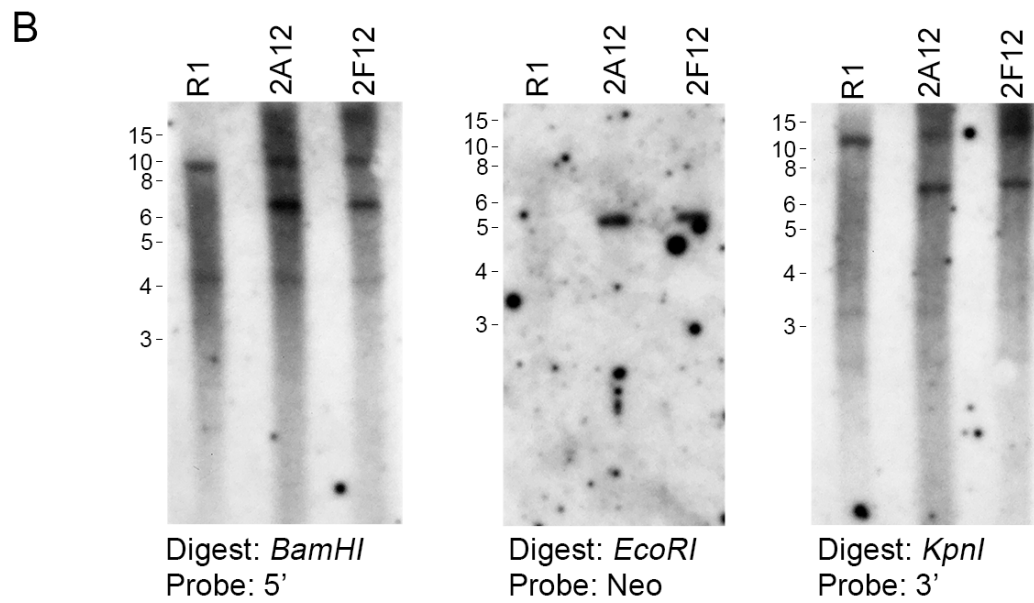
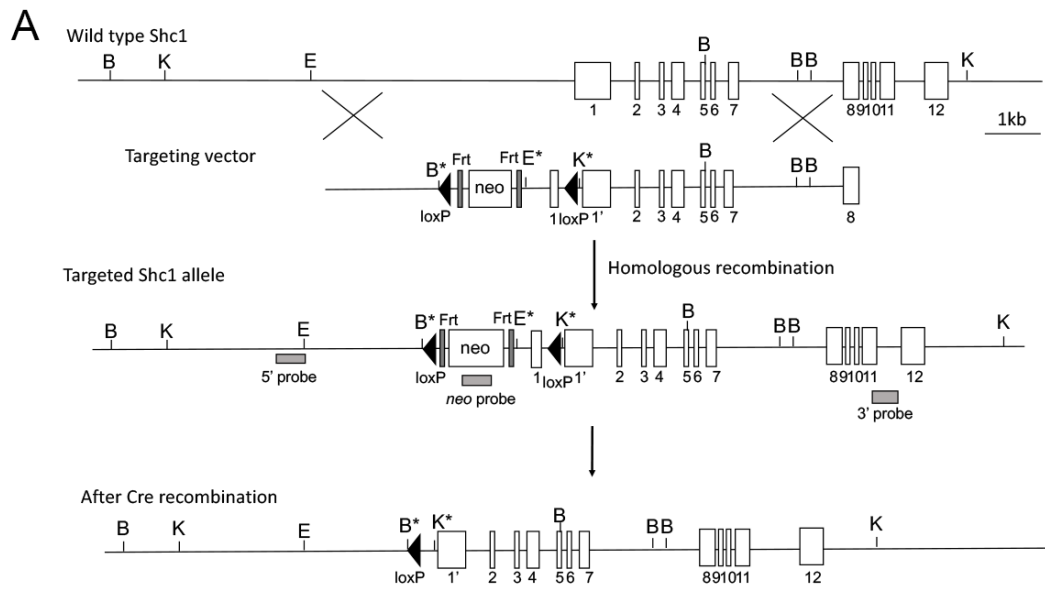


Figure 5-4. Targeting strategy by homologous recombination to generate p66Shc-loxP transgenic mice.

(A) The wild type *Shc1* locus will be replaced by homologous recombination with the targeting vector containing the neomycin selectable marker flanked by Frt sites and the conditional knockout region flanked by loxP sites. Cre recombination will delete the sequences between the two loxP sites, resulting in loss of part of coding exon 1. (B) Southern blots for the 5' recombination end, the presence of a neomycin gene, and the 3' recombination end confirm that 2A12 and 2F12 are correctly targeted mESC clones compared to wild type R1 mESCs.

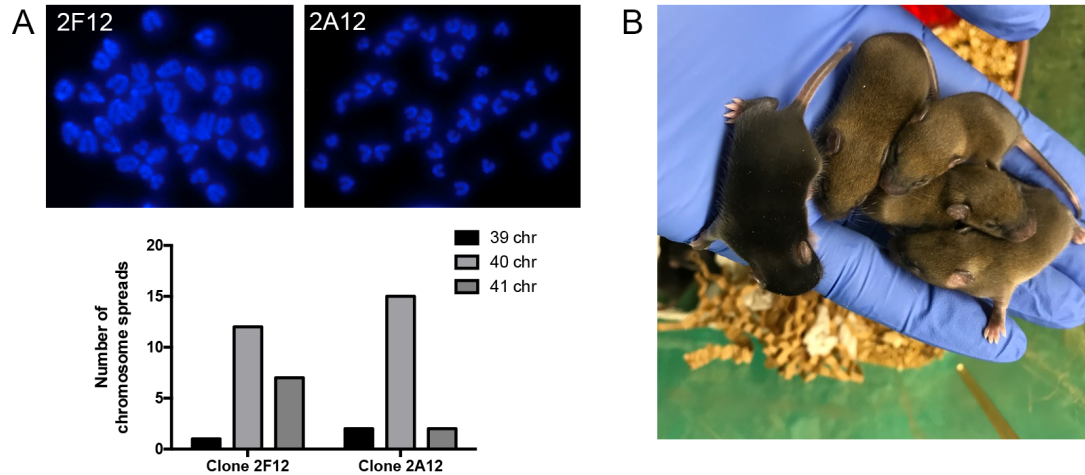


Figure 5-5. Distribution of chromosome counts, and chimeras generated from targeted clones.

(A) Panels are representative images of DAPI-stained chromosome spreads from targeted mESC clones 2F12 and 2A12. The bar graph displays the distribution of chromosome counts from 25 image panels for each clonal line. (B) Chimeric pups born from blastocysts injected with clone 2F12. Four chimeric pups are shown with agouti (brown) fur while a non-chimeric litter mate is shown with black fur.

crossed with mice expressing CMV promoter-driven Cre. P66Shc-loxP mice can also be crossed with ZP3-Cre mice to generate female offspring with an oocyte-specific deletion of p66Shc. These mice can then be mated with p66Shc^{+/-} (heterozygote) males to generate embryos lacking maternal p66Shc (50% m-/z+) or lacking both maternal and zygotic p66Shc (50% m-/z-). These embryos will help determine the contribution of maternally stored p66Shc to mouse preimplantation development. To complement these studies, embryos lacking only zygotic p66Shc (m+/z-) can be generated by crossing two p66Shc^{+/-} mice.

Based on my results using siRNA knockdown I predict that zygotic (m+/z-) and maternal-zygotic (m-/z-) p66Shc knockout embryos will form blastocysts with inner cell masses composed of the majority or all primitive endoderm cells (NANOG-negative, GATA4-positive). This will then result in peri-implantation embryonic lethality. I predict that these blastocysts will also be incapable of deriving embryonic stem cell lines.

5.3 Summary

Cell fate specification and differentiation are integral events that occur in the development of a single cell to the hundreds of specialized cell types in the adult organism. The first two cell differentiation events in development occur in the preimplantation embryo. This ensures that a pluripotent cell population is established as a source of cells that will form the developing fetus. Our knowledge in how this occurs has been advanced through my discovery that a signalling adaptor protein, p66Shc, regulates blastocyst cell lineage specification. Knockdown of p66Shc significantly affects the development of the pluripotent epiblast in the blastocyst inner cell mass, and knockout of p66Shc in mouse embryonic stem cells significantly changes their pluripotent characteristics, resulting in a bias during their spontaneous differentiation. Collectively, this work expands on the diversity of cellular functions attributed to p66Shc and provides an avenue for further study on this adaptor protein in developmental biology.

5.4 References

Azami, T., Waku, T., Matsumoto, K., Jeon, H., Muratani, M., Kawashima, A., Yanagisawa, J., Manabe, I., Nagai, R., Kunath, T., et al. (2017). Klf5

maintains the balance of primitive endoderm versus epiblast specification during mouse embryonic development by suppression of Fgf4. *Development* **144**, 3706-3718.

Betts, D. H., Bain, N. T. and Madan, P. (2014). The p66(Shc) adaptor protein controls oxidative stress response in early bovine embryos. *PLoS One* **9**, e86978.

Chazaud, C., Yamanaka, Y., Pawson, T. and Rossant, J. (2006). Early lineage segregation between epiblast and primitive endoderm in mouse blastocysts through the Grb2-MAPK pathway. *Dev Cell* **10**, 615-624.

D'Agostino, M., Torcinaro, A., Madaro, L., Marchetti, L., Sileno, S., Beji, S., Salis, C., Proietti, D., Imeneo, G., M, C. C., et al. (2018). Role of miR-200c in myogenic differentiation impairment via p66Shc: implication in skeletal muscle regeneration of dystrophic mdx mice. *Oxid Med Cell Longev* **2018**, 4814696.

Dietrich, J. E. and Hiiragi, T. (2007). Stochastic patterning in the mouse pre-implantation embryo. *Development* **134**, 4219-4231.

Favetta, L. A., Madan, P., Mastro Monaco, G. F., St John, E. J., King, W. A. and Betts, D. H. (2007). The oxidative stress adaptor p66Shc is required for permanent embryo arrest in vitro. *BMC Dev Biol* **7**, 132.

Favetta, L. A., Robert, C., St John, E. J., Betts, D. H. and King, W. A. (2004). p66shc, but not p53, is involved in early arrest of in vitro-produced bovine embryos. *Mol Hum Reprod* **10**, 383-392.

Frum, T., Halbisen, M. A., Wang, C., Amiri, H., Robson, P. and Ralston, A. (2013). Oct4 cell-autonomously promotes primitive endoderm development in the mouse blastocyst. *Dev Cell* **25**, 610-622.

Gardner, D. K. and Harvey, A. J. (2015). Blastocyst metabolism. *Reproduction, fertility, and development* **27**, 638-654.

Gardner, D. K., Lane, M., Stevens, J. and Schoolcraft, W. B. (2001). Noninvasive assessment of human embryo nutrient consumption as a measure of developmental potential. *Fertil Steril* **76**, 1175-1180.

Hackett, J. A. and Surani, M. A. (2014). Regulatory principles of pluripotency: from the ground state up. *Cell Stem Cell* **15**, 416-430.

Kang, M., Garg, V. and Hadjantonakis, A. K. (2017). Lineage establishment and progression within the inner cell mass of the mouse blastocyst requires FGFR1 and FGFR2. *Dev Cell* **41**, 496-510 e495.

Karagenc, L., Sertkaya, Z., Ciray, N., Ulug, U. and Bahçeci, M. (2004). Impact of oxygen concentration on embryonic development of mouse zygotes. *Reprod Biomed Online* **9**, 409-417.

- Krawchuk, D., Honma-Yamanaka, N., Anani, S. and Yamanaka, Y.** (2013). FGF4 is a limiting factor controlling the proportions of primitive endoderm and epiblast in the ICM of the mouse blastocyst. *Dev Biol* **384**, 65-71.
- Le Bin, G. C., Munoz-Descalzo, S., Kurowski, A., Leitch, H., Lou, X., Mansfield, W., Etienne-Dumeau, C., Grabole, N., Mulas, C., Niwa, H., et al.** (2014). Oct4 is required for lineage priming in the developing inner cell mass of the mouse blastocyst. *Development* **141**, 1001-1010.
- Lee, K. and Esselman, W. J.** (2002). Inhibition of PTPs by H₂O₂ regulates the activation of distinct MAPK pathways. *Free Radical Biology and Medicine* **33**, 1121-1132.
- Lee, M. K., Smith, S. M., Banerjee, M. M., Li, C., Minoo, P., Volpe, M. V. and Nielsen, H. C.** (2014). The p66Shc adapter protein regulates the morphogenesis and epithelial maturation of fetal mouse lungs. *Am J Physiol Lung Cell Mol Physiol* **306**, L316-325.
- Migliaccio, E., Mele, S., Salcini, A. E., Pelicci, G., Lai, K. M., Superti-Furga, G., Pawson, T., Di Fiore, P. P., Lanfrancone, L. and Pelicci, P. G.** (1997). Opposite effects of the p52shc/p46shc and p66shc splicing isoforms on the EGF receptor-MAP kinase-fos signalling pathway. *EMBO J* **16**, 706-716.
- Mohammed, H., Hernando-Herraez, I., Savino, A., Scialdone, A., Macaulay, I., Mulas, C., Chandra, T., Voet, T., Dean, W., Nichols, J., et al.** (2017). Single-cell landscape of transcriptional heterogeneity and cell fate decisions during mouse early gastrulation. *Cell Rep* **20**, 1215-1228.
- Mulas, C., Kalkan, T. and Smith, A.** (2017). NODAL secures pluripotency upon embryonic stem cell progression from the ground state. *Stem Cell Reports* **9**, 77-91.
- Niwa, H., Miyazaki, J. and Smith, A. G.** (2000). Quantitative expression of Oct-3/4 defines differentiation, dedifferentiation or self-renewal of ES cells. *Nat Genet* **24**, 372-376.
- Okada, S., Kao, A. W., Ceresa, B. P., Blaikie, P., Margolis, B. and Pessin, J. E.** (1997). The 66-kDa Shc isoform Is a negative regulator of the epidermal growth factor-stimulated mitogen-activated protein kinase pathway. *Journal of Biological Chemistry* **272**, 28042-28049.
- Papadimou, E., Moiana, A., Goffredo, D., Koch, P., Bertuzzi, S., Brustle, O., Cattaneo, E. and Conti, L.** (2009). p66(ShcA) adaptor molecule accelerates ES cell neural induction. *Mol Cell Neurosci* **41**, 74-84.
- Qu, B., Gong, K., Yang, H., Li, Y., Jiang, T., Zeng, Z., Cao, Z. and Pan, X.** (2018). SIRT1 suppresses high glucose and palmitate-induced osteoclast differentiation via deacetylating p66Shc. *Mol Cell Endocrinol*.

- Rinaudo, P. F., Giritharan, G., Talbi, S., Dobson, A. T. and Schultz, R. M.** (2006). Effects of oxygen tension on gene expression in preimplantation mouse embryos. *Fertil Steril* **86**, 1252-1265, 1265 e1251-1236.
- Smith, A.** (2017). Formative pluripotency: the executive phase in a developmental continuum. *Development* **144**, 365-373.
- Wale, P. L. and Gardner, D. K.** (2012). Oxygen regulates amino acid turnover and carbohydrate uptake during the preimplantation period of mouse embryo development. *Biol Reprod* **87**, 24-24.
- Wale, P. L. and Gardner, D. K.** (2013). Oxygen affects the ability of mouse blastocysts to regulate ammonium. *Biol Reprod* **89**, 75.
- Yamanaka, Y., Lanner, F. and Rossant, J.** (2010). FGF signal-dependent segregation of primitive endoderm and epiblast in the mouse blastocyst. *Development* **137**, 715-724.

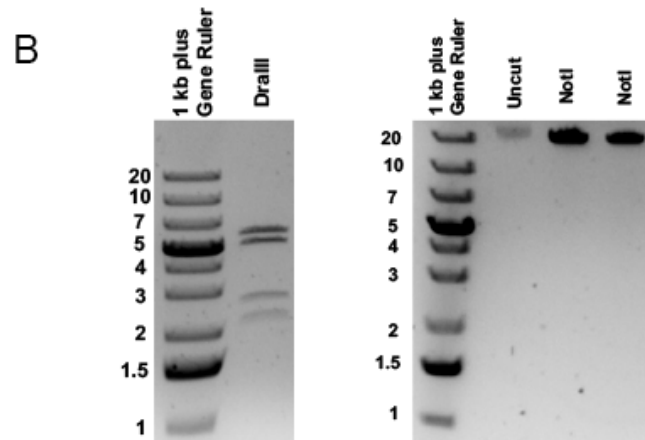
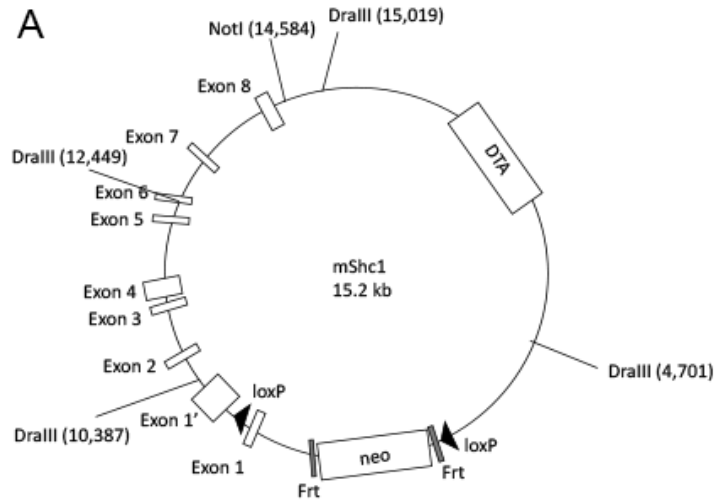
Appendix A: Materials and Methods for generation of p66Shc-loxP mice

Construction of mShc1 targeting vector

The targeting vector was designed and synthesized by Cyagen Biosciences Inc (USA). Briefly, the targeting vector, homology arms, and conditional knockout region was constructed by PCR amplification with high fidelity Taq and BAC clones RP23-137J12 and RP23-64L17 from the C57BL/6J library as templates. Mouse genomic fragments were assembled into the vector with recombination sites and selection markers as shown on the vector map (Figure A-1A). The vector identity was confirmed by *Dra*III digest (Fig A-1B). The targeting vector was linearized by *Not*I digest and electroporated into G4 mouse embryonic stem cells by the London Regional Transgenic and Gene Targeting Facility (University of Western Ontario, London, Ontario, Canada). Electroporated mESCs were selected by neomycin resistance. Genomic DNA obtained from clonally expanded mESCs was then screened by Southern blotting.

Southern blotting

The Southern blotting strategy is outlined in Fig A-2. DNA probes were synthesized by PCR amplification of C57BL/6 mouse genomic DNA, cloned, digested and purified by gel extraction. Probe sequences are in Table A-1. 10 µg of genomic DNA was digested with 100 units of restriction enzyme overnight at 37°C. The following morning, the digestion reaction mixture was spiked with 10-20 additional units of restriction enzyme. Digestion reaction mixtures were resolved by gel electrophoresis on a 0.8% agarose gel overnight at 30 V. The gel was stained with ethidium bromide to visualize DNA digestion and measure migration distances of the DNA ladder. The gel was then washed twice for thirty minutes in Buffer 1 (1.5M NaCl, 0.5M NaOH), rinsed with double distilled water, then washed twice for thirty minutes in Transfer Buffer (1M ammonium acetate, 20 mM NaOH). DNA was transferred overnight onto a nitrocellulose membrane (GE Life Sciences) using a Stratagene Posiblott apparatus. The membrane was dried for one hour, then baked for one hour at 80°C in a vacuum oven. The membrane was



DraIII digest: 5.6 kb + 4.9 kb
+ 2.5 kb + 2.1 kb

Figure A-1. Shc1 targeting vector.

(A) Map of Shc1 targeting vector with *DraIII* digestion sites. (B) Vector identity was confirmed by *DraIII* digestion and linearized with *NotI* digestion.

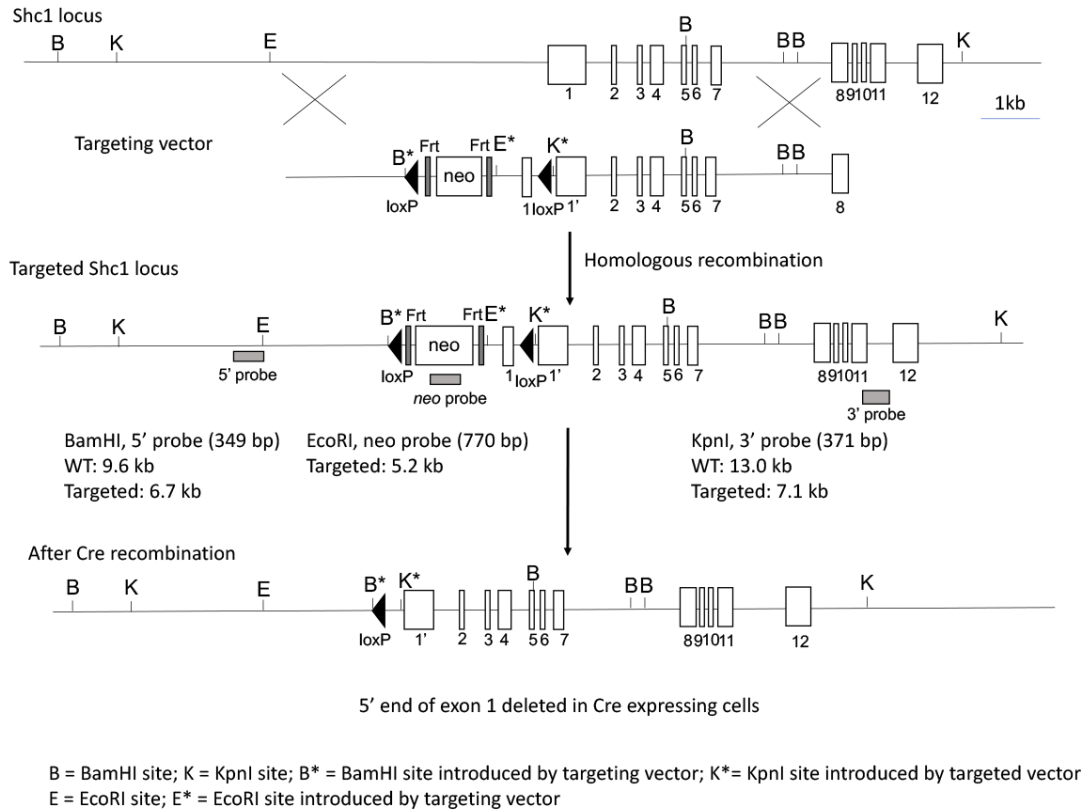


Figure A-2. Southern blot strategy for genotyping targeted clones.

The targeting vector introduces *Bam*HI, *Kpn*I, and *Eco*RI sites into the *Shc1* locus sequence. Digestion and blotting using the indicated probes will result in wild type and targeted bands of different sizes in correctly targeted clones.

Table A-1. Sequences of DNA probes used for Southern blotting.

5' probe	<p>ACCGTACCAGCTTATCTTGCACCTTAACAGAAAACACTTGAAACCTCTA TGCGCGCCATGAATGATCAAGTATTTGAAAGGTATCTACCCACGGCCAC AGTCTTCATGCCACTCCAAGTCCTGTAAAAGCCTATCTAAAACAAGGCT GACAACTACTCATCTTTTTTATAAACTAAAAACCACCAACACTGAGGCT CTCTTAGAACCGTCCTTTCATCAAGAGCATGAACTTTCAGTTCTGCAC GGGCTACCTTCTTCTCCCAGCAGACTTTGAGATTTAGTAACGCGAGC AGTTCCTATTAGGGAAATCGCCACAACAAAGTTGCTTTAGTGATGTGAA TTCCCA</p>
3' probe	<p>CTGAAGGTGTGGTAAGTGTGACAGAGGTGTGGCAGGGGCTGGTGTGGT TTTGCTTTCTAGACTTCCTTTGCCGGAGGCTTCCTGTGGACTCCTTTG CCCTTGCTGGACACTTGCATCCACCTGCAGTGGCTCAGGGTTCTTCC CTGCTGTCCCTCGAGTCTGAGCTGTGTTCTTCTCAGTTCTGACCAGTCC TCACATCCCAGTGAAGCCTGCCAGCCCCAGAGAGTGCTTACTTGATC TTTTGCTAAGTGAGGAAATGACACTGGAAAGGCAGTGGTGCCAGTGT CAGTGGTTAGGGGGTGGAGACCCCAAATTTCTCTTGCAAGAGGAGTC AGGAGCCTCCCTAGCTCCTTAGCTTCAAACCTCAGG</p>

incubated in Hybridization Buffer (4 mM EDTA, 8 mM Tris Base, 600 mM NaCl, 0.2% Ficoll 400, 0.2% polyvinylpyrrolidone, 0.2% bovine serum albumin, 0.1% sodium pyrophosphate, 0.025M Na₃PO₄, 0.2% SDS) for 1 hour at 65°C. Oligonucleotide probes were labelled with ³²P-dCTP using the Prime-It II Random Primer Labeling Kit (Agilent Technologies, USA) according to manufacturer's guidelines. Briefly, 25 ng of probe DNA was mixed with random primers and water, then denatured for 5 minutes at 95°C. ³²P-dCTP and dCTP buffer, and Klenow enzyme were added to the reaction, and incubated at 37°C for 30 minutes. Labelled probe was purified using Sephadex beads and glass wool, and incorporation percentage was approximated using a Geiger counter. The membrane was then incubated in fresh Hybridization Buffer containing 25 ng of labelled probe overnight at 65°C. The membrane was then washed three times in low stringency wash buffer (0.1% SDS, 300 mM NaCl, 30 mM Sodium Citrate pH 7.0) at room temperature, then washed three times in high stringency wash buffer (0.1% SDS, 30 mM NaCl, 3 mM Sodium Citrate pH 7.0) at 65°C. The membrane was then exposed to film for autoradiography for 3 days at -80°C prior to film development.

Chromosome Counting

Targeted mESC clones were incubated in ES cell medium containing 1 ug/ml colcemid (Karyomax, Life Technologies, USA) at 37°C for 1 hour. Cells were then trypsinized, pelleted, resuspended in ice cold 0.56% KCl, then incubated for 6 minutes at room temperature. Cells were pelleted and resuspended by adding fixative solution (3:1 mixture of methanol: glacial acetic acid) drop by drop with continuous mixing. Cells were pelleted, resuspended in 1 ml of fixative, and dropped from a height onto ethanol-cleaned glass microscopy slides. Slides were allowed to dry for 1 hour, mounted in DAPI-containing mounting medium (Vectashield, Vector Laboratories), and examined at 100X magnification. At least twenty-five spreads containing 39 to 41 chromosomes were photographed and counted for each clonal line. The ratio of spreads containing 39, 40, and 41 chromosomes was calculated to determine how likely germline transmission would be achieved after injection into blastocysts.

Appendix B: Copyright Agreement

OXFORD UNIVERSITY PRESS LICENSE TERMS AND CONDITIONS

Apr 17, 2018

This Agreement between Nicole Edwards ("You") and Oxford University Press ("Oxford University Press") consists of your license details and the terms and conditions provided by Oxford University Press and Copyright Clearance Center.

License Number	4331430453426
License date	Apr 17, 2018
Licensed content publisher	Oxford University Press
Licensed content publication	Molecular Human Reproduction
Licensed content title	P66Shc, a key regulator of metabolism and mitochondrial ROS production, is dysregulated by mouse embryo culture
Licensed content author	Edwards, Nicole A.; Watson, Andrew J.
Licensed content date	Sep 6, 2016
Type of Use	Thesis/Dissertation
Institution name	
Title of your work	The role of p66Shc in mouse blastocyst development
Publisher of your work	The University of Western Ontario
Expected publication date	Jun 2018
Permissions cost	0.00 CAD
Value added tax	0.00 CAD
Total	0.00 CAD
Title	The role of p66Shc in mouse blastocyst development
Instructor name	Dr. Dean Betts
Institution name	The University of Western Ontario
Expected presentation date	Jun 2018
Portions	All text, main figures and supplementary figures
Publisher Tax ID	GB125506730

Appendix C: Ethics Approval



2010-021:8:

AUP Number: 2010-021

AUP Title: Mechanisms Controlling Preimplantation Development

Yearly Renewal Date: 08/31/2019

The YEARLY RENEWAL to Animal Use Protocol (AUP) 2010-021 has been approved by the Animal Care Committee (ACC), and will be approved through to the above review date.

Please at this time review your AUP with your research team to ensure full understanding by everyone listed within this AUP.

As per your declaration within this approved AUP, you are obligated to ensure that:

1) Animals used in this research project will be cared for in alignment with:

a) Western's Senate MAPPs 7.12, 7.10, and 7.15

http://www.uwo.ca/univsec/policies_procedures/research.html

b) University Council on Animal Care Policies and related Animal Care Committee procedures

http://uwo.ca/research/services/animalethics/animal_care_and_use_policies.html

2) As per UCAC's Animal Use Protocols Policy,

a) this AUP accurately represents intended animal use;

b) external approvals associated with this AUP, including permits and scientific/departmental peer approvals, are complete and accurate;

c) any divergence from this AUP will not be undertaken until the related Protocol

Modification is approved by the ACC; and

d) AUP form submissions - Annual Protocol Renewals and Full AUP Renewals - will be submitted and attended to within timeframes outlined by the ACC.

http://uwo.ca/research/services/animalethics/animal_use_protocols.html

3) As per MAPP 7.10 all individuals listed within this AUP as having any hands-on animal contact will

a) be made familiar with and have direct access to this AUP;

b) complete all required CCAC mandatory training (training@uwo.ca); and

c) be overseen by me to ensure appropriate care and use of animals.

4) As per MAPP 7.15,

a) Practice will align with approved AUP elements;

b) Unrestricted access to all animal areas will be given to ACVS Veterinarians and ACC Leaders;

c) UCAC policies and related ACC procedures will be followed, including but not limited to:

i) Research Animal Procurement

ii) Animal Care and Use Records

iii) Sick Animal Response

iv) Continuing Care Visits

5) As per institutional OH&S policies, all individuals listed within this AUP who will be using or potentially exposed to hazardous materials will have completed in advance the appropriate institutional OH&S training, facility-level training, and reviewed related (M)SDS Sheets, <http://www.uwo.ca/hr/learning/required/index.html>

Submitted by: Copeman, Laura
on behalf of the Animal Care Committee
University Council on Animal Care

Curriculum Vitae

- Name:** Nicole A. Edwards
- Post-secondary Education and Degrees:** McGill University
Montreal, Quebec, Canada
2007-2011 B.Sc.
- McGill University
Montreal, Quebec, Canada
2011-2013 M.Sc.
- The University of Western Ontario
London, Ontario, Canada
2014-2018 Ph.D.
- Honours and Awards:** Province of Ontario Graduate Scholarship
2014-2016
- Gordon J. Mogenson Award for Research Excellence in Physiology
2016
- Natural Sciences and Engineering Research Council Doctoral Canada Graduate Scholarship
2016-2018
- Related Work Experience** Teaching Assistant
McGill University
2011
- Teaching Assistant
The University of Western Ontario
2014-2017
- Publications:**
- Edwards NA**, Watson AJ, Betts DH. Knockdown of p66Shc alters lineage-associated transcription factor expression in mouse blastocysts. *Under review*. 2018.
 - Crocker K, Calder MD, **Edwards NA**, Betts DH, Watson AJ. CD-1 mouse fertility rapidly declines and is accompanied with early pregnancy loss under conventional housing conditions. *Theriogenology*. December 14, 2017.

3. Calder MD, **Edwards NA**, Betts DH, Watson AJ. Treatment with AICAR inhibits blastocyst development, trophoctoderm differentiation and tight junction formation and function. *Mol. Hum. Reprod.* September 28, 2017.
2. **Edwards NA**, Watson AJ, Betts DH. P66Shc, a key regulator of metabolism and mitochondrial ROS production, is dysregulated by mouse embryo culture. *Mol. Hum. Reprod.* July 6, 2016.
1. **Edwards N**, Farookhi R, Clarke HJ. Identification of a {beta}-galactosidase transgene that provides a live-cell marker of transcriptional activity in growing oocytes and embryos. *Mol. Hum. Reprod.* April 16, 2015.